

## CURRENT UNDERSTANDING OF IRON OXIDE ASSOCIATED-ALKALI ALTERED MINERALISED SYSTEMS: PART II - A REVIEW

T. M. (Mike) Porter

*Porter GeoConsultancy Pty Ltd, Adelaide, South Australia*

This second of the two parts of this paper reviews aspects of the lithospheric- to deposit-scale setting, tectonic and structural controls, associated magmatism, temporal distribution, implied crustal scale sources and circulation dynamics of ore-related fluids, and the resultant alteration and mineralisation patterns, for most of the world's provinces hosting significant examples of iron oxide-alkali altered mineralised systems. It forms the basis for the comparison and observations outlined and discussed in the overview of the first part of the paper. It is also intended as a convenient reference, summarising a comprehensive selection of such provinces and deposits worldwide, and includes some not covered elsewhere in these two volumes, as well as additional background on others that are.

An emphasis is placed on those provinces hosting economic IOCG *sensu stricto* deposits that have produced copper±gold ore, as well as those that are expected to be exploited in the foreseeable future, while also providing information on provinces with similar characteristics that host significant iron oxide-alkali altered mineralised systems and deposits, but do not include IOCG *sensu stricto* ores.

### Contents

	Page		Page
Gawler Craton .....	33	Great Bear Magmatic Zone .....	77
Mount Isa Inlier .....	40	Southeast Missouri Iron Province .....	78
Carajás Mineral Province .....	47	Wernecke Breccia .....	80
Central Andean Coastal Belt .....	53	Fennoscandian Shield .....	82
Khetri and Alwar Copper Belts .....	65	Angara-Ilim District .....	84
Lao Cai District .....	67	Bushveld and Palabora Complexes .....	85
Lufilian Arc .....	71	Ossa Moreno Zone .....	89
Tennant Creek Inlier .....	75	Turgai District .....	90

## Gawler Craton

### *Crustal Setting*

The significant IOCG *sensu stricto* deposits on the eastern margin of the preserved Gawler craton define the Olympic IOCG Province (Fig. 4). These include *Olympic Dam* (Hayward and Skirrow, 2010; Reynolds, 2000; Reeve *et al.*, 1990), *Prominent Hill* (Freeman and Tomkinson, 2010; Belperio *et al.*, 2007), *Carrapateena* (Porter, 2010; Vella and Cawood, 2006) and *Hillside* (Conor *et al.*, 2010).

The emplacement of these deposits has been interpreted to be temporally associated with the ~1.59 Ga Hiltaba Suite granitoids (and the co-magmatic bimodal Gawler Range Volcanics - GRV). The Hiltaba Suite are dominantly a highly fractionated granite to granodiorite (>70% SiO<sub>2</sub>), with accompanying minor, but spatially widespread coeval mafic to ultramafic intrusions (Creaser, 1989, 1996; Stewart and Foden, 2003; Hand *et al.*, 2007). Syn-mineralisation mafic dykes within the Olympic Dam deposit are interpreted to belong to the latter, although these may represent a late phase, marginally post-dating the main felsic Hiltaba Suite (Chambefort *et al.*, 2009; McPhie *et al.*, 2010) whereas other post-ore mafic intrusions may belong to the 825 Ma Gairdner Dyke Swarm. One of the largest of the mafic to ultramafic intrusions in the Olympic IOCG Province is the composite White Hill Complex in the Mount Woods domain, a few kilometres north of the Prominent Hill deposits, which comprises layered pyroxenite, norite and

gabbro covering an area of ~200 km<sup>2</sup>, and is apparently coeval with Hiltaba Suite magmatism in that domain (Belperio *et al.*, 2007). Similarly, mafic and ultramafic intrusions are known in the Olympic Dam district (Johnson and Cross, 1995; Jagodzinski, 2005; Skirrow *et al.*, 2007). Gabbroic intrusives of the regional Pine Point Fault structural corridor with which the Hillside deposit is associated, and the gabbro and granitic intrusions within the Hillside ore zone, are assumed to also be of Hiltaba Suite age, on the basis of structural and textural comparison with those dated elsewhere in the district (e.g., the 1589±5 Ma Curramulka Gabbro; Conor *et al.*, 2010; Zang, 2003). The latter is supported by zircons from the deposit that yielded a range of SHRIMP U-Pb ages between ~1580 and ~1560 Ma (Ried *et al.*, 2010).

The GRV commence with a lower 0.5 to 3 km thick sequence of texturally and compositionally varied volcanic units that are gently to moderately dipping (10 to 30°) and best exposed to the west and south. These lower units range in composition from basalt to rhyolite and comprise lavas, ignimbrites and other minor volcanoclastic facies, with tholeiitic basalt and andesite being subordinate (~10 vol.%) to dacite and rhyolite (Allen *et al.*, 2009). However, the lower Gawler Range Volcanics do include locally thick basalt and andesite (Drexel *et al.*, 1993), which are predominantly found to the east of the Elizabeth Creek fault (Fig. 4). In comparison, the upper GRV comprises widespread, very gently dipping (<5°), thick (250 to 300 m), crystal-rich (15 to 40%), rhyolitic and

## Gawler Craton ... cont.

dacitic units considered to be lavas. The GRV have been intruded by porphyritic rhyolitic dykes and granites. Juxtaposition of granites with the GRV suggests that at least 1 km of the GRV and/or associated sedimentary rocks have been eroded (Allen *et al.*, 2009). Creaser and White (1991), and Stewart (1994), showed that the magmas that fed the GRV had a high temperature (900 to 1100°C) and were relatively dry (<2 wt.% H<sub>2</sub>O). Stewart (1994) also recognised that the dissolved volatiles in these magmas included significant halogens, particularly fluorine (up to

1.3 wt.%). This high fluorine content would significantly reduce the normally high viscosity of the felsic lavas, to allow them to erupt effusively and form extensive lava sheets (Allen *et al.*, 2009). Petrogenetic studies suggest that the mafic magmas, though subordinate in volume, were derived from the mantle and that the silicic magmas were generated by fractional crystallisation of the mafic parent, and in some cases, melting and assimilation of Archaean or Palaeoproterozoic crust (Giles, 1988; Stewart, 1994; Creaser, 1995).

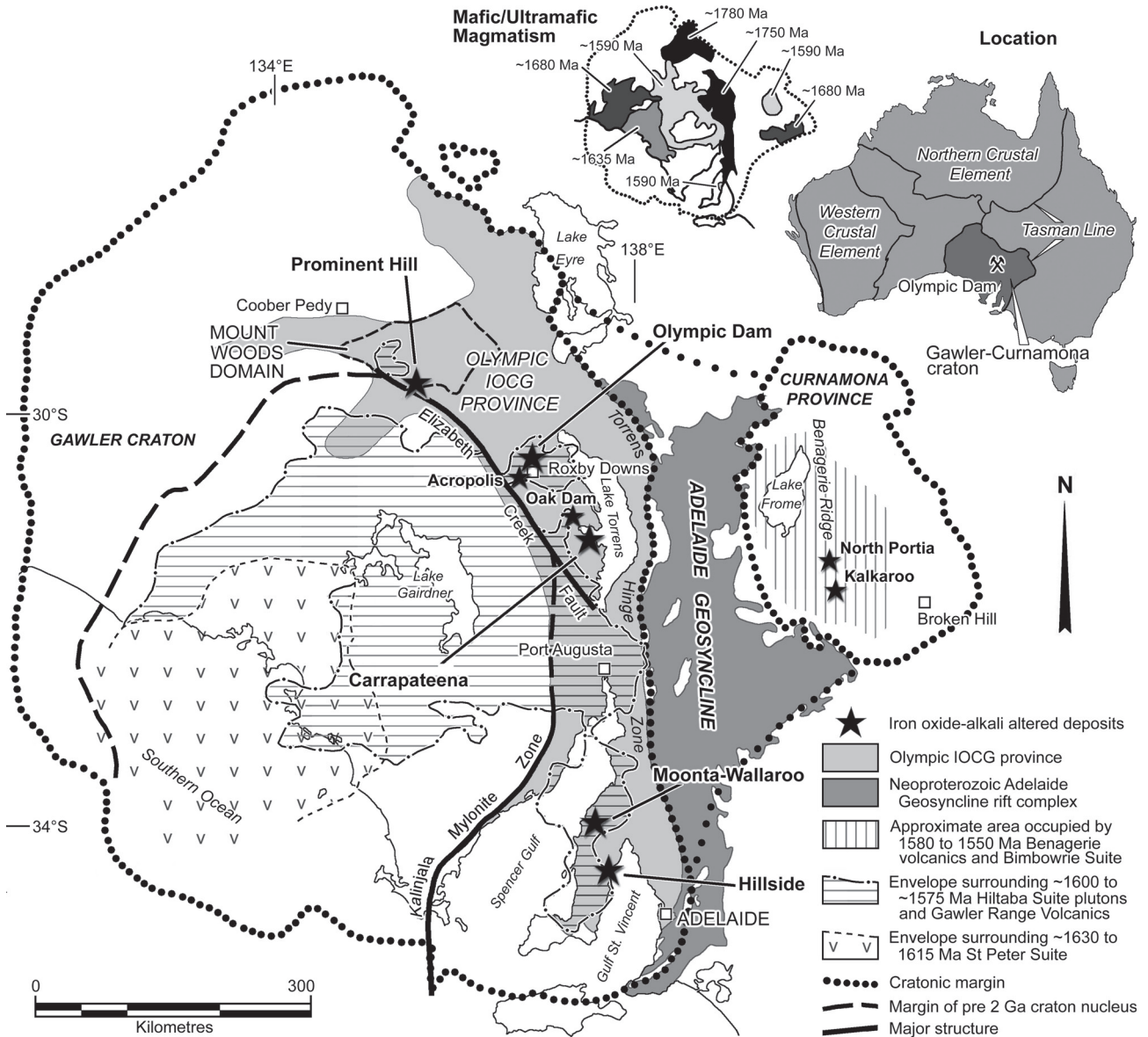


**Figure 4:** The tectonic framework and location of the main iron oxide-alkali altered mineralisation of the combined Mesoproterozoic to Mesoproterozoic Gawler Craton and Curnamona Province of South Australia. Note the central Archaean to Early Palaeoproterozoic nucleus, bounded in part by the Elizabeth Creek Fault and Kalinjala Mylonite Zone. The Neoproterozoic Adelaide Geosyncline rift basin (related to Rodinia break-up extension) masks the mid- to late-Palaeoproterozoic suture between the Gawler craton and Curnamona Province. The northeastern, eastern and southeastern margins of the preserved craton are determined by the Tasman Line, which marks the Rodinia break-up and separation of the eastern sections of the cratonic mass, while the southern margin is the Pangea break-up across which cratonic remnants now in Antarctica were separated. Prior to the break-up of Rodinia, the Gawler craton, Curnamona Provinces, and cratonic elements in North America (?) and Antarctica were all part of the larger Mawson craton. The northern and western margins are collisional with the North Australian (~1560) and Yilgarn crustal elements (~1350 to 1260 and ~1210 to 1140 Ma) respectively. This emphasises the internal location of the Olympic IOCG Province within the Mawson craton at the time of its formation. Note also the temporal progression of magmatism across the interior of the craton from ~1630 to ~1550 Ma, over 300 km from the nearest craton margin to the northwest. The Mafic/Ultramafic Magmatism inset (top-centre), shows the envelopes surrounding regions of mafic to ultramafic dykes, sills, stocks and layered complexes (after Claoué-Long and Hoatson, 2009) that define mafic igneous provinces within the craton. Note that the diachronous progression from the 1630 to 1615 Ma St Peter, to the 1600 to 1575 Ma Hiltaba and 1580 to 1550 Ma Bimbrowie Suites is reflected in mafic igneous province ages. The relationship between the older north-south 1780 to 1750 Ma group (immediately west of the mid Palaeoproterozoic Curnamona-Gawler suture) and the gabbros of the Pine Point structural corridor (assumed to be of the same Hiltaba age as the Curramulka gabbro norite immediately to their west) is of interest. Diagram after Hayward and Skirrow (2010), Conor *et al.* (2010), Claoué-Long and Hoatson (2009) and others quoted therein.

*Gawler Craton ... cont.*

The Hiltaba Suite is composed of both A- and I-type granitoids, with the former dominating in the Olympic IOCG Province (Fig. 4) which hosts all of the major IOCG deposits listed above) in the east, and I-type in the central and western Gawler craton (Skirrow *et al.*, 2007), with more S-type in the Curnamona Province to the east (Skirrow, 2009).

The Olympic IOCG Province spatially coincides with, and overprints, an accreted Palaeoproterozoic terrane of <2000 to 1740 Ma metasedimentary and metavolcanic rocks that is bounded to the west by the Mesoarchaeon to early Palaeoproterozoic nucleus of the Gawler craton (Fig. 4). Its eastern limit is concealed below the north-south trending Neoproterozoic Adelaide Geosyncline intracratonic rift, and corresponds to the suture with the contiguous Curnamona province, which is believed to have docked with the Gawler craton between 1.9 and 1.8 Ga as part of the assembly of the Nuna/Columbia supercontinent (Hayward and Skirrow, 2010; Conor *et al.*, 2010). Subduction related to this collision could have resulted in mantle enrichment in volatiles below what was to become the Olympic IOCG Province within an essentially intracratonic terrane.

The Hiltaba Suite and Gawler Range Volcanics occupy a broadly circular to oval-shaped area with a diameter of ~500 to 600 km, a preserved area of >25 000 km<sup>2</sup> and thickness of up to more than 3 km. It is the central and largest of a progression of three zones of magmatic activity defining a diachronous west-southwest-east-northeast trending corridor of bimodal I-, A- and subordinate S-type intrusions from the western margin of the preserved Gawler craton to the Curnamona Province (Fig. 4), which was by that time amalgamated with, and part of the Gawler craton. These three zones comprise the ~1630 to 1615 Ma Nuyts Volcanics and St Peter Suite bimodal magmas to the west (Fanning *et al.*, 2007), the ~1600 to 1575 Ma intrusive Hiltaba Suite and coeval Gawler Range Volcanics, and the ~1580 to 1550 Ma intrusive Bimbowrie Suite and Benagerie volcanics (Hayward and Skirrow, 2010) to the east of the Adelaide Geosyncline in the Curnamona Province (Fig. 4). Each of these three continental I- and A-type intrusive suites is bimodal, showing evidence for mingling of mantle mafic melts and silicic crustal melts (Stewart, 1994; Skirrow, 2009; Swain *et al.*, 2008). This would result in the magma chemistry varying in accordance with lithospheric composition, heat flow (i.e., temperature and depth of crustal melting), and the degree of involvement of metasomatised sub-crustal lithospheric mantle (Skirrow, 2009).

Numerous separate and collective subduction zones have been proposed to explain this distal continental magmatism, mostly associated with the distant western and northwestern margins of the craton accompanying terrane accretion events during the amalgamation of the North and South Australia cratons between 1690 and 1550 Ma (discussed in Hayward and Skirrow, 2010, in this volume), although none appear to convincingly explain their geometry and composition. The eastern to southeastern and southern limits of the remaining Gawler craton-Curnamona Province are Rodinia and Pangea break-up rift margins respectively, across which cratonic elements now in North America (?) and Antarctica were separated.

The temporal association of IOCG mineralisation in the Olympic IOCG Province with the Hiltaba Suite/GRV is largely based on relationships at the Olympic Dam deposit, where the Olympic Dam Breccia Complex (ODBC), which hosts the ore deposit, cuts the Roxby Downs Granite (RDG) of the Hiltaba Suite. Reeve *et al.* (1990) proposed that ore

formed within multiple mafic maar-diatreme volcanoes, now represented by mafic dykes, and bedded facies considered to represent phreatomagmatic ash from a maar lake. In this case, the ODBC would be related to an explosive Lower GRV mafic volcanic diatreme. However, recent drilling has revealed significant additional volumes of mafic/ultramafic derived sedimentary facies, mafic/ultramafic dykes, and isolated occurrences of basaltic lavas in the upper section of the deposit (Ehrig, 2010). Following this drilling, McPhie *et al.* (2010) argued that the RDG intruded into now eroded overlying comagmatic GRV, and that the bedded facies represent sediments from a more extensive basin overlying (or intercalated within) the GRV, deposited prior to the development of the ODBC. This conclusion is based on the following: (1) the downward decrease of heterolithic clasts (including GRV and sediments) in the hematitic breccias of the ODBC; (2) domains with clasts of GRV in the breccias, indicating the presence of GRV above the RDG when the ODBC was formed; (3) sedimentological features, grain composition, mixed volcanic-granitoid provenance and geochemical signatures which suggest the bedded facies are detrital rather than phreatomagmatic, and that they were deposited below wave-base in an intracontinental, fault bounded lacustrine basin prior to the formation of the ODBC. If this is the case, the bedded sedimentary facies cannot be the surficial 'within-crater' deposits of a diatreme. These conclusions question both the maar-diatreme origin of the ODBC, and that it represents a GRV centre of volcanism. The presence of the bedded facies and their character implies the hydrothermal brecciation that produced the ODBC propagated from a deeper site in the RDG, upwards into the GRV and overlying bedded facies sediments, most likely not breaching to the surface (K. Ehrig, *pers. comm.*, 2011). Age determinations for the RDG, GRV and zircons from the bedded facies, all cluster around 1590 Ma (Johnson and Cross, 1995). It would therefore follow that the ODBC was formed after 1590 Ma, although most likely related to late stage hydrothermal activity associated with the same gross mantle induced event that produced the Hiltaba Suite and GRV. Alteration and mineralisation of the intensity and scale of the Olympic IOCG Province require the influence of a major crustal scale magmatic event. If not related to the Hiltaba/GRV event, the next possible major magmatism is inferred by 1169±48 Ma zircon populations, of unknown provenance, found in regional drainages across the craton (Belousova *et al.*, 2009), and the 0.825 Ga Gairdner dyke swam magmatism (e.g., Claoué-Long and Hoatson, 2009). Both of these latter options appear less viable, as at the Oak Dam East prospect, 57 km southeast of Olympic Dam, IOCG-U mineralisation is unconformably overlain across a sharp unconformity by the unmineralised and unaltered, post 1424 Ma Pandurra Formation, which contains numerous rounded boulders and pebbles of massive iron oxide closely resembling that of the deposit (Davidson *et al.*, 2007).

Hayward and Skirrow (2010) note that in deep seismic transect data, the 3D crustal-scale architecture of the Olympic Dam mineralised system comprises a discrete >40 km wide, elliptical, lower- to mid-crustal zone of reduced or transparent seismic reflectivity (with no associated gravity high) that has been interpreted to reflect voluminous Hiltaba-age migmatites and altered felsic batholiths. This zone is localised above a crust-penetrating fault zone at the edge of an inferred mafic underplate (see Figs. 5 and 6, in Hayward and Skirrow, 2010, this volume). This east-dipping, deep fault, which

*Gawler Craton ... cont.*

apparently offsets the Moho with normal displacement of up to 5 km, broadly coincides with the implied eastern margin of the Archaean nucleus of the Gawler craton and may represent the sub-surface extent of the Elizabeth Creek fault (Fig. 4). Inversions of geophysical data suggest that magnetite-rich alteration extends several kilometres beneath the Olympic Dam deposit, to near the top of the interpreted batholiths.

A coincident zone of low resistivity in the mid-crust beneath the deposit, imaged in magnetotelluric data, may be associated with conductive mineral seams, probably graphite, related to this alteration event. Hayward and Skirrow, (2010) note there is little evidence for a mafic underplate in seismic reflection traverses in the Olympic Dam area (Direen and Lyons, 2007), although west of the Elizabeth Creek Fault Zone (the inferred eastern margin of the Archaean nucleus of the Gawler craton; Fig. 4), Huynh *et al.* (2001) used Bouguer gravity data to model a ~3 km thick, ~200 km diameter, high density (~3.0 g/cm<sup>3</sup>) mafic sheet at the base of the crust beneath the Gawler Range Volcanics. This sheet is interpreted to have resulted from decompression melting of ascending mantle that drove the most intense part of the 1600 to 1575 Ma crustal anatexis event that produced the Hiltaba Suite and Gawler Range Volcanics.

A national compilation and analysis of dated mafic and ultramafic magmatism has been undertaken by GeoScience Australia (Claoué-Long and Hoatson, 2009), based on both significant intrusions and areally distributed clusters of sparsely dispersed, small to moderate dykes, sills, stocks and some layered complexes (Fig. 4 inset). This study has defined a broad, east-northeast trending corridor that crosses the Gawler craton/Curnamona Province, composed of a series of overlapping, eastward migrating pulses centred on 1680, 1635 and 1590 Ma respectively. The last two both spatially and temporally overlap, the Nuyts Volcanics/St Peter Suite, Hiltaba Suite/Gawler Range Volcanics, and Bimbowrie Suite/Benagerie volcanics described above, covering similar areas, and are taken to represent a period of progressive underplating below sections of the Gawler craton/Curnamona Province. No significant exposed magmatic event appears to be related to the older 1680 Ma group of mafic intrusives to the west, although the similarly aged block to the east overlaps the Broken Hill lead-zinc-silver district. An older, narrower, linear belt of mafic to ultramafic magmatism follows the eastern margin of the Olympic IOCG province from Wallaroo to the Mount Woods Inlier, with pulses at 1780 and 1750 Ma, generally coincident with A-type magmatism in the Wallaroo Group (Conor *et al.*, 2010) and the 1760 to 1739 Ma Kimban Orogeny. This locus of mafic to ultramafic intrusions is located just to the west of the inferred Mid-Palaeoproterozoic suture between the Curnamona Province and the main Gawler craton.

### **Regional Alteration**

Although the bulk of iron oxide-alkali altered mineralised systems in the Gawler craton are interpreted to have accompanied post-1600 Ma Hiltaba Suite magmatism, the oldest known alteration has been dated at ~1620 Ma, from monazite associated with syn-deformational magnetite-biotite, and from titanite in sodic-calcic assemblages in the Moonta-Wallaroo district (Raymond *et al.*, 2002; Skirrow *et al.*, 2006, 2007).

In the Curnamona Province, regional-scale stratabound sodic (albitic) alteration was formed during diagenesis

at ~1630 Ma (Teale and Fanning, 2000). Magnetite-dominant and minor hematitic IOCG-style mineralisation associated with K-Fe alteration, and high-temperature syn-tectonic gold (copper-molybdenum), developed in the southern Curnamona Province possibly as early as 1630 to 1612 Ma (Skirrow *et al.*, 2000; Williams and Skirrow, 2000), although re-analysis gave a Re-Os age of ~1603 Ma (Skirrow, 2009).

Post-1600 Ma, regional-scale alteration patterns are well developed within the Olympic IOCG Province. The earliest phase recognised is sodic-calcic-iron, characterised by an assemblage of *albite-calc silicate ± magnetite*. Actinolite, clinopyroxene (diopside or salite) with minor titanite and scapolite occur in places (Hayward and Skirrow, 2010). This alteration is well developed in the Mount Woods Inlier to the north, and Moonta-Wallaroo district to the south (Fig. 4), but not generally in the Olympic Dam district (an exception being at the Oak Dam East prospect), although it may be present at depth, where large scale magnetite-alteration is interpreted from geophysical modelling. This interpreted deep alteration corresponds to the elliptical zone of lower-crustal reduced or transparent seismic reflectivity above the Elizabeth Creek Fault Zone described above, interpreted in turn to reflect a zone of anatexis, comprising migmatites and felsic intrusions. For more detail consult Hayward and Skirrow (2010) in this volume.

A second phase of alteration, characterised by *biotite-magnetite*, is well represented in both the Mount Woods Inlier and Moonta-Wallaroo districts, where it shows mutually crosscutting relationships with the Hiltaba Suite, and is clearly imaged in regional aeromagnetic data which shows it to be widespread. Albite is a stable phase during this K-Fe alteration which is often accompanied by local low grade (<0.5% Cu) pyrite, chalcopyrite, pyrrhotite, monazite and titanite (Hayward and Skirrow, 2010).

A third phase, occurring as an assemblage of *magnetite-K feldspar ± actinolite ± carbonate* is important in the Olympic Dam district, but appears to be absent in other parts of the Olympic IOCG Province. It is locally accompanied by minor pyrite, quartz, carbonate, chalcopyrite, apatite and titanite, although these only account for generally low grade (<0.5% Cu) copper ± uranium ± gold mineralisation (Hayward and Skirrow, 2010). The very large, sub-economic magnetite-rich alteration systems at the Acropolis, Wirrda Well and Murdie Murdie prospects are representatives of this assemblage, while relicts of it are observed in many other IOCG systems (e.g., Davidson *et al.*, 2007).

Fluid inclusion data and oxygen isotope geothermometry for the magnetite-bearing assemblages in the Olympic Dam district indicate that fluid temperatures reached ~420 to 540°C (Oreskes and Einaudi, 1992; Bastrakov *et al.*, 2007; Davidson *et al.*, 2007). Based on Br/Cl ratios, and isotope and other data, Hayward and Skirrow (2010) concluded that sulphur in the generally minor sulphides associated with most magnetite-bearing alteration was arguably of magmatic-hydrothermal or leached-igneous rock origin (e.g., Bastrakov *et al.*, 2007).

### **Deposit-scale Alteration and Mineralisation**

Ore grade mineralisation at the Olympic Dam, Prominent Hill and Carrapateena deposits, and the upper section of the Oak Dam East prospect in the Olympic IOCG Province of the Gawler craton, is all associated with an alteration assemblage of *hematite-sericite-chlorite-carbonate*

Gawler Craton ... cont.

(Hayward and Skirrow, 2010). This assemblage, which is also sporadically found in the Moonta-Wallaroo district, basically represents the alteration of earlier magnetite to hematite, biotite to chlorite and plagioclase to sericite (Ehrig, 2010). Hayward and Skirrow (2010) regard this to be a form of H<sub>2</sub>O-CO<sub>2</sub> metasomatism involving oxidation of Fe<sup>2+</sup> to Fe<sup>3+</sup>, and critical to the development of higher-grade copper-gold-uranium mineralisation. In more detail, hematite either replaces magnetite, or is developed separately (e.g., Prominent Hill; Belperio *et al.*, 2007). Igneous, metamorphic or earlier hydrothermal, K-bearing phases such as K feldspar, are replaced by sericite, while chlorite replaces Fe-Mg silicates such as actinolite and biotite. Where no precursor minerals are evident, hematite, sericite, chlorite and carbonate are seen to grow in veins and breccia matrix. Chalcopyrite, pyrite, bornite, chalcocite, gold and uranium-bearing minerals are characteristically associated with hematite, sericite, chlorite and carbonate, although all of these minerals are rarely all present together at any given location. Other phases that may be present locally include: barite, fluorite, native copper and REE phosphate minerals (Reeve *et al.*, 1990; Gow *et al.*, 1994; Bastrakov *et al.*, 2007; Belperio *et al.*, 2007; Davidson *et al.*, 2007; Freeman and Tomkinson, 2010).

The age of this alteration phase has only been dated in a few localities, as most mineralised sites have been subjected to multiple resetting. Sericite associated with weak copper-gold mineralisation in the Torrens prospect yielded a <sup>40</sup>Ar/<sup>39</sup>Ar age of 1575±11 Ma (Skirrow *et al.*, 2007), while in the Moonta-Wallaroo district, Re-Os ages of 1574±6 and 1577±6 Ma were returned by molybdenite in chalcopyrite-bearing veins with chloritic alteration aureoles, possibly related to the hematite-sericite-chlorite-carbonate event. This assemblage is similar to what other authors (e.g., Hitzman *et al.*, 1992; Williams *et al.*, 2005) refer to as 'hydrolytic' alteration. The preceding is paraphrased in part from Hayward and Skirrow (2010).

The **Olympic Dam** ore deposit is hosted by the 50 km<sup>2</sup> Olympic Dam Breccia Complex (ODBC), which is developed within the ~1590 Ma Roxby Downs Granite (RDG), a member of the Hiltaba Suite. Other lithologies within the ODBC comprise a variety of granite- to hematite-rich breccias, sedimentary facies, felsic/mafic/ultramafic dykes, volcanoclastic units, and their altered/mineralised equivalents. Recent drilling has revealed significant additional volumes of mafic/ultramafic derived sedimentary facies, mafic/ultramafic dykes, and isolated occurrences of basaltic lavas in the southern and eastern parts of the ODBC (Ehrig, 2010).

As detailed above, McPhie *et al.* (2010) argue that prior to development of the ODBC, the RDG intruded into overlying comagmatic Gawler Range Volcanics (GRV) and that the bedded facies represent sediments from a widespread basin above (or intercalated within) the GRV, both of which have subsequently been eroded. This implies that the fragmentation that produced the ODBC propagated from a deeper site in the RDG, upwards into the GRV and overlying (or intercalated) bedded facies sediments, most likely not breaching to the surface.

The bulk of the mineralisation within the Olympic Dam deposit is associated with an assemblage of *hematite-sericite-fluorite-barite-chalcopyrite-bornite-chalcocite (djurleite)*, the outer margin of which largely corresponds to the limits of the ODBC, where a deeper *magnetite-carbonate-chlorite-pyrite ±chalcopyrite* zone marks the transition to the more regional *magnetite-K feldspar*

*±actinolite ±carbonate* assemblage previously described (Ehrig, 2010). Within the overall alteration envelope, the distribution of mineralisation and alteration exhibits a downward and outward zonation, while the ODBC and alteration pattern has a general downward tapering conical configuration. The complex has a central core of barren, but intense hematite-quartz-breccia, passing outwards through concentrically zoned breccia types, from the intense alteration of the core, through to heterolithic hematite breccias (dominantly clasts of granite and recycled hematite breccias, with domains where abundant sedimentary, and volcanoclastic rocks dominate locally), to monoclastic granite breccias with a magnetite/hematite matrix, and weak incipient microfracturing of the RDG on the outer margins. This progression represents an outward decrease in the degree of brecciation and intensity of iron metasomatism away from the core of the complex. The quantity of recycled hematite breccia, GRV and sedimentary rock clasts within the heterolithic hematite breccias decreases from shallow to deep levels (Ehrig, 2010; McPhie *et al.*, 2010).

The better mineralisation outside of the barren core corresponds to the best-developed hematite. These various moderate to steeply inward dipping breccia zones of the ODBC are cut by a convoluted, but overall roughly horizontal, ~50 m thick layer of chalcocite and bornite, ~100 to 200 m below the unconformity with the overlying Neoproterozoic cover sequence. Both the upper and lower margins of this zone are mappable. Above the upper margin, sulphides are rare and little copper mineralisation is found in the same hematitic breccias. The lower margin marks a rapid transition to chalcopyrite, which decreases in copper grade downwards, corresponding to an increase in the pyrite:chalcopyrite ratio. While this zone is largely horizontal, as it approaches the central barren core it steepens markedly, but is still evident at depths of more than 1 km below the unconformity (Reeve *et al.*, 1990; Reynolds, 2000; Ehrig, 2010). The geometry of this mineral zonation, strongly suggest interaction between upwelling and downward percolating fluids. For all fluids related to hematite alteration, fluid inclusion homogenisation temperatures are mostly between 150 and 300°C and salinities range from ~1 to ~23% NaCl<sub>equiv.</sub> (Knutson *et al.*, 1992; Oreskes and Einaudi, 1992; Bastrakov *et al.*, 2007).

McPhie *et al.* (2010), note that the hydrothermal activity that produced the zonation in the copper minerals post-dates formation of the breccia complex by an unknown interval, while intrusion of mafic dykes that cut the deposit followed formation of the breccia complex and the zoned ore body, also by an unknown interval.

The **Carrapateena**, deposit, 100 km southsoutheast of Olympic Dam (Fig. 4), is hosted by strongly brecciated granitoids, which have been dated at 1857±6 Ma, and are assigned to the Palaeoproterozoic Donington Suite. Mineralisation is hosted by hematite and hematite-granite breccias of the Carrapateena Breccia Complex, which covers an area of ~800 × 600 m at the unconformity with the overlying Neoproterozoic cover sequence, tapering to a ~300 to 400 m diameter zone at a depth of ~1 km below that surface. The dominant alteration assemblage is *hematite-chlorite-sericite*, with locally abundant quartz and carbonate. High-grade cores of bornite-rich mineralisation within the Carrapateena Breccia Complex are basically vertically distributed in the core of the complex, surrounded by chalcopyrite-dominated mineralisation (Porter, 2010 and references quoted therein; see Figs. 2, 3 and 7, in the same paper, this volume).

The **Oak Dam East** prospect (Fig. 4; ~560 Mt @ 41 to 56% Fe), 57 km southeast of Olympic Dam, comprises a large, sub-horizontal body of hematite and hematite matrix breccia which overlies an areally less extensive magnetite dominated core near the base of the system. The deposit underlies >500 m of cover, and is hosted by altered rocks interpreted to belong to the 1860 to 1845 Ma Donington Suite, basement to the GRV. At Oak Dam East, the GRV were eroded during the early Mesoproterozoic, and by 1424 Ma, the deposit was overlain above a sharp unconformity by unaltered and unmineralised sandstones of the Pandurra Formation (Davidson *et al.*, 2007).

Davidson *et al.* (2007) considered that the Oak Dam East breccia complex was formed at a shallow depth, following regional albite-calc silicate±magnetite alteration caused by hypersaline, 400 to 500°C fluids. Large-scale brecciation was an early feature, with progressive breccia-fill and replacement comprising: (1) hematite and goethite (hematite stage I); (2) magnetite-apatite-quartz±actinolite (magnetite stage); (3) hematite-goethite-quartz-chalcedony-pyrite-chlorite-monazite (hematite stage II); and (4) chalcopryrite-pitchblende-illite-hydromuscovite-florencite-carrollite (Cu-U-[Au] stage). The upper 200 m of the breccia complex contains colloform hematite void fillings, interpreted to have replaced hydrothermal goethite.

The deposit is divided into sulphide free upper, and sulphidic lower zones, the boundary being within the thick hematite rich upper layer. The alteration/mineralisation zoning is composed of (1) an upper sulphide-deficient, hematite-dominated breccia; (2) sulphide-bearing hematite-dominated breccia, which is 60 to 80 m thick and contains the main sub-horizontal, 10 to 70 m thick copper-uranium mineralised sheet, the top surface of which is generally found at the upper contact of the sulphidic zone. The mineralised sheet has an upper, variably developed low-grade transition to an underlying thin >1% Cu layer, passing down in turn into a variable thickness 0.1 to 1% Cu zone. Mineralisation occurs as sulphides in the hematitic breccia matrix; (3) sulphide bearing, magnetite-dominated breccia, forms an irregular, 600 m long tongue that is 30 to 80 m thick, passing down into disseminated hematite (Davidson *et al.*, 2007).

Mineralisation is zoned vertically from pyrite at depth to shallower chalcopryrite. High-grade pitchblende occurs centrally within the chalcopryrite zone (e.g., 10 m of 0.46% Cu and 3.7 kg/t U<sub>3</sub>O<sub>8</sub>), straddling the boundary between a sericite-illite assemblage and underlying iron-magnesium chlorite alteration. Davidson *et al.* (2007) speculate that Oak Dam East represents the outer wing of a much larger breccia complex with a core to the west.

The **Prominent Hill** deposit is located on the southern margin of the Mount Woods Domain (MWD) of the Gawler craton, 150 km northwest of Olympic Dam (Fig. 4). The MWD comprises at least two separate Palaeoproterozoic sedimentary successions that have been subjected to one or more amphibolite to granulite facies metamorphic events in three periods of deformation, to produce gneisses, metamorphosed banded iron formations and calcsilicates. These metamorphics have been intruded by probably three episodes of magmatism. Intrusions include both metamorphosed and undeformed granites and the large (~200 km<sup>2</sup>), undeformed, lopolithic pyroxenite, norite and gabbro White Hill complex. The latter is ~6 km to the northwest of Prominent Hill and has a pronounced, inwardly dipping layering, defined by plagioclase and pyroxene-rich bands, with interleaved disseminated to

massive magnetite-ilmenite layers (Belperio *et al.*, 2007; Freeman and Tomkinson, 2010). Belperio *et al.* (2007) and sources quoted therein, report dates from unmetamorphosed granites within the MWD of 1587±4 and 1584±18 Ma, and from veining cutting gabbro from the White Hill Complex at 1582±5 Ma, all of which are broadly coeval with the Hiltaba Suite/GRV magmatism.

Mineralisation at Prominent Hill is located immediately to the south of a major structure marking the southern limit of the MWD. It is hosted by a Mesoproterozoic sequence of sedimentary and volcanic rocks (dated at 1585±8 Ma; Belperio *et al.*, 2007, and sources quoted therein) interpreted to be equivalents of the Lower GRV. The structural footwall to the deposit comprise lower greenschist facies, relatively undeformed, mafic to felsic volcanic rocks (basalt-andesite-dacite-rhyolite) with intercalated arenitic red-beds, unconformably underlying the immediate host hematite-stable sequence of hematite-cemented quartz conglomerate, greywacke-shale breccia, sandstone, argillite and dolostone. These are in turn structurally overlain, across the major Hangingwall Fault, by chlorite matrix breccia, a thick band of magnetite-“skarn” (massive magnetite with pyrite, actinolite, phlogopite, chlorite, serpentinite, carbonate and talc), quartzite, schist and calc-silicates (Belperio and Freeman 2004; Belperio *et al.*, 2007; Freeman and Tomkinson, 2010). This sequence is interpreted to be overturned (Freeman and Tomkinson, 2010).

The very coarse to fine-grained, laminated, clastic sedimentary rocks that constitute the immediate host to mineralisation have been subjected to later hydrothermal replacement with only minor additional brecciation during metasomatism. Distinctly bedded breccias occur over widths of ~5 to 10 m within more massive, non-layered, poorly sorted hematite-matrix breccia. Individual breccia bodies occur as stratabound, steeply dipping, tabular, east-west trending sheets and westerly plunging shoots over widths of up to 200 m.

Mineralisation is accompanied by intense hematite alteration (hematite-sericite-chlorite-carbonate ±quartz ±barite ±fluorite ±REE phosphates), which is locally texturally destructive, and includes hematite matrix-supported and steely hematite breccias, as well as steely hematite altered basaltic-andesites. The main copper-gold mineralisation is hosted by the hematite matrix-supported breccias, while the steely hematite contains variable gold. Copper mineralisation occurs as fine-grained disseminations of chalcocite, bornite and chalcopryrite in the breccia matrices, and to a lesser extent, in clasts (Freeman and Tomkinson, 2010). The Hangingwall fault separates the hematite-dominated alteration, with associated copper and gold, from barren magnetite-chlorite assemblages immediately to the north (see Figs. 3 and 11, in Freeman and Tomkinson, 2010, this volume). A much broader iron oxide-sericite alteration system overprints all Mesoproterozoic units over an area of at least 2 km<sup>2</sup> around the breccias (Freeman and Tomkinson, 2010).

Freeman and Tomkinson (2010) conclude that on current evidence, the Prominent Hill mineralisation was emplaced through relatively passive infiltration of hydrothermal fluids and metasomatism, localised by porosity, within a sequence of coarse-grained sedimentary breccias, to form stratigraphically controlled tabular orebodies. The amount of brecciation that can be attributed to hydrothermal processes is unclear. Copper and gold are paragenetically very late, and a direct genetic relationship with hematite is yet to be proven. They further conclude that breccias hosting

Gawler Craton ... cont.

mineralisation may not be of hydrothermal "diatreme origin", and that if they are in part or wholly of hydrothermal origin, then the current vertical disposition of their "layering" and "grading" suggests that the deposit has been tilted into its current steep attitude subsequent to hydrothermal activity, and that hydrothermal brecciation alteration took place when the bedding was originally flat lying.

The **Hillside** deposit (~450 km southsoutheast of Olympic Dam; Fig. 4), is hosted by a strongly deformed and altered sequence of ~1750 Ma Wallaroo Group metasediments, within and adjacent to the major, north-south trending Pine Point structural corridor. The metasediments are intruded by Mesoproterozoic igneous rocks which comprise numerous phases of granite, micro-gabbro, porphyritic gabbro and gabbro-diorite that are presumed to be related to the 1590 Ma Hiltaba Suite.

Mineralisation is hosted within at least three discrete, anastomosing, but apparently laterally and vertically continuous, structures with individual copper-mineralised strike lengths of 1.5 km, occurring along, and on either side of contacts between intensely altered metasediments and steep gabbro and A-type felsic intrusives. Copper and gold is focussed in numerous steeply dipping, sub-vertical "skarn" and associated breccia bodies over a vertical interval of >700 m. Primary copper mineralisation is dominantly chalcopyrite, with lesser, but locally significant, bornite and chalcocite. The latter minerals are associated with strongly oxidised domains, where bornite is often accompanied by carbonate and hematite. Pyrite is also locally abundant, but is usually replaced by chalcopyrite during skarn retrogression. There are numerous high to low temperature alteration mineralogies within the deposit. The earliest higher temperature assemblages are dominated by magnetite ± quartz ± pyrite ± garnet and almost monomineralic garnet. This early alteration is replaced by clinopyroxene, K feldspar, epidote, actinolite, allanite and biotite-rich zones. The introduction of copper is associated with highly oxidising fluids with replacement of magnetite by hematite ± chalcopyrite. Late carbonate and silica flooding creates extreme increases in copper grade in many areas and is associated with the development of chlorite + chalcopyrite which replace clinopyroxene, actinolite and garnet (Conor *et al.*, 2010; see Figs. 2, 13 and 16, in the same paper, this volume).

A number of models have been proposed for the formation of the deposits within the Gawler craton. All recognise the importance of a relatively high-temperature hypersaline fluid in equilibrium with paragenetically early magnetite, and the importance of oxidised conditions during overprinting copper-gold (± uranium) mineralisation with hematitic alteration. These models include: (1) progressive mixing involving at least one non-magmatic fluid (Reeve *et al.*, 1990; Haynes *et al.*, 1995; Davidson *et al.*, 2007); (2) sequential (two-stage) processes, involving two or more fluids (Oreskes and Einaudi, 1992; Gow *et al.*, 1994a; Johnson and McCulloch, 1995; Gow, 1996); and (3) single-fluid magmatic-hydrothermal evolution (Reynolds, 2000; Morales *et al.*, 2002).

Hayward and Skirrow (2010) favour a process, that would be consistent with Olympic Dam, involving three stages and two fluids, one deeply-sourced, high temperature, magnetite-stable, hypersaline, magmatic-hydrothermal (A), the second, highly oxidised, sulphate-bearing surface or basinal fluids (B; see Fig. 10 in Hayward and Skirrow, 2010, this volume). The deeply sourced, fluid A, would be

derived from, or be a response of, deep crustal processes, e.g., mantle sourced mafic intrusions (as under/intraplates, reflected by the mafic to ultramafic intrusions in the vicinity of most deposits), anorogenic magmatism (mingled with CO<sub>2</sub>-rich mafic phases), anatectic induced metamorphic, or deeply circulated basinal fluids, driven by these same heat-sources. This fluid is envisaged to have been responsible for the regional, sodic and potassic alteration and scavenging of iron (transported as FeCl<sub>2</sub>) and other metals from the regional sequence, the mafic intrusions or the Hiltaba Suite/GRV.

Where this fluid was structurally focused during the first of the three proposed stages, it might produce extensive magnetite-actinolite bearing alteration zones that are barren or only contain low-grade copper-gold mineralisation (e.g., <0.1% Cu), due to a lack of sulphur, even though the fluid may in places carry hundreds of ppm Cu. As fluid A rose to shallower crustal levels, reduced pressure and temperature conditions along the upflow paths would force it to evolve, and become hematite-stable.

Stage 2 would involve, either erosion and exhumation of the magnetite bearing stage 1 alteration system, or its continued upward propagation to shallower levels. This would result in the high temperature assemblages being exposed to oxidised surface-derived or basinal waters of fluid B (e.g., from a large, lacustrine, possibly evaporite bearing basin as proposed by McPhie *et al.*, 2010) circulated in shallow geothermal systems, driven by very high geothermal gradients associated with regional magmatism of the Hiltaba Suite and GRV. The coincidence of the Olympic IOCG Province and the basaltic facies of the lower GRV suggest the latter may be a potential source of copper, particularly the >450 m thick Roopena Volcanics. The volcanic rocks of this unit have been subjected to extensive and intense hematite-chlorite-carbonate alteration (at 250 to 150°C; by NaCl-CO<sub>2</sub>-rich bittern or evolved magmatic brines; Haynes *et al.*, 1995; Knutson *et al.*, 1992), accompanied by significant copper depletion (commonly from ~127 ppm background to <20 ppm Cu; Creaser, 1989; Knutson *et al.*, 1992). S and Nd isotopic signatures of ore sulphides indicate igneous sources, which can be explained by leaching of basalts, while high U<sub>3</sub>O<sub>8</sub> at Olympic Dam and Oak Dam are interpreted to have been derived from the strongly radiogenic felsic GRV and Hiltaba Suite plutons (Hitzman and Valenta, 2005). To produce ore during stage 2, fluid B is required to have circulated deeply and encountered sufficient fertile source rock and reacted with either fluid A (which would contribute late stage volatiles, CO<sub>2</sub>, SO<sub>2</sub>/H<sub>2</sub>S, F, P ± Fe, or Cu-Au rather than SO<sub>2</sub>/H<sub>2</sub>S) or its products, to oxidise earlier magnetite to hematite and build on low grade copper-gold-uranium. Hayward and Skirrow (2010) suggest the richest deposits may be the product of: (1) progressive mixing, rather than two stage sequential alteration; (2) greater interaction with source mafic volcanic units; (3) interaction with more oxidised and sulphate rich basinal or meteoric brines at higher fluid/rock ratios. They note that the largest IOCG deposits of the province have the most extreme hydrothermal brecciation, and the most extensive hematite replacement of magnetite assemblages. They also conclude that dissolved sulphate carried by fluid B is critical in generating the gigantic mass of sulphide mineralisation in an otherwise relatively low-sulphur iron oxide-dominated hydrothermal system. Downward percolation of an evolved fluid B through ore at a late stage may leach the upper levels and redeposit metals where in equilibrium with fluid A to produce the bornite-chalcocite layer at Olympic Dam and Oak Dam East.

Chambefort, *et al.* (2009) and McPhie *et al.* (2010) point out that the Hiltaba Suite and GRV throughout the Gawler craton, contain anomalously high levels of fluorine (~1.3 wt.% in homogenised melt inclusions in quartz phenocrysts, compared to an average upper crustal abundance of 0.05% wt.% F). Fluorite was crystallised in melt inclusions in the GRV, where it coexists with a range of constituents, as well as occurring as an interstitial phase in Hiltaba Suite granites, indicating the magmas were saturated with fluorine at the time of mineralisation. This implies that at least some fluorine was exsolved into a magmatic-hydrothermal fluid phase that was retained. Further, the exsolution of fluorine from the crystallising melt was accompanied by loss of REE, U, Th, Zr, Cu, Zn and Pb, the elements enriched in the Olympic Dam deposit. In this setting, the Olympic Dam hydrothermal fluid had to be fluorine rich and could have transported the required metals, and reacted with silica to release K<sup>+</sup> and Al<sup>3+</sup> to promote potassic/sericitic alteration, while the extremely corrosive resultant hydrofluoric acid may have acted as an agent to promote permeability and brecciation of the ODBC in the Hayward and Skirrow (2010) fluid A.

### Structural Control and Brecciation

IOCG mineralisation within the Olympic IOCG Province shows evidence of association with major structural corridors in some zones, while in others, significant deposits are found at fault intersections or in shear packages where no particular structure dominates within a network of faulting.

In the south of the Olympic IOCG Province, the Hillside deposit (Conor *et al.*, 2010) is composed of a series of north-south trending tabular, shear controlled bodies that parallel the immediately adjacent major regional Pine Point Fault Zone, while to the north in the Mount Woods Inlier, the Prominent Hill mineralised system also has a tabular form, developed immediately adjacent, and largely parallel, to an east-west terrane boundary structure, at its intersection with northwest trending fault zones (Freeman and Tomkinson, 2010). In the central section of the province however, the Olympic Dam and Carrapateena IOCG *sensu stricto* deposits, and other subeconomic IOCG or barren magnetite occurrences, are found in an area where a network of generally northwest and northeast trending faults dominate. The northwest trending controlling structures at Carrapateena, Olympic Dam and Prominent Hill are parallel to, and 10 to 50 km in the hanging wall of the major Elizabeth Creek fault zone that is believed to mark the eastern boundary of the Archaean nucleus of the Gawler craton (Hayward and Skirrow, 2010). The deposits in this central part of the province appear to have formed during a short-lived (1595 to 1585 Ma) northnorthwest-southsoutheast directed extension episode that coincided with eruption of the Gawler Range Volcanics (~1595 to 1590 Ma), but was preceded and followed by more protracted northwest-southeast to northnorthwest-southsoutheast contraction (Hayward and Skirrow, 2010, and sources quoted therein).

The *Olympic Dam* ore deposit is hosted entirely within the ~50 km<sup>2</sup> Olympic Dam Breccia Complex (ODBC). Although Reeve *et al.* (1990) proposed that the ODBC represented multiple, lower GRV, mafic maar-diatreme volcanoes. However, McPhie *et al.* (2010) present an argument, as detailed above, favouring its formation as an

upwardly propagating zone of hydrothermal brecciation, most likely not breaching to the surface, that postdated an early Mesoproterozoic sedimentary sequence deposited above, or during the waning stages of the Gawler Range Volcanics. Nevertheless, the broader brecciation complex does enclose individual zones of phreatomagmatic brecciation related to mafic dykes.

The *Carrapateena* deposit is hosted by a steep, pipe-like hematite-altered breccia body, as described above, localised at the intersection of two fault trends.

The *Prominent Hill* ore deposit in the Mount Woods Inlier is also hosted by a series of individual breccia bodies, occurring as stratabound, steeply dipping, tabular, east-west trending sheets and westerly plunging shoots, as described above. Belperio *et al.* (2007) interpreted these breccias to have been formed by repetitive hydrothermal brecciation, milling, and explosive venting within a volcanic setting, with high-pressure spalling, chemical corrosion of clasts, and compositional layering within the breccias, representing a diatreme breccia, analogous to that interpreted at Olympic Dam. However, following the exposure of the deposit by mining, subsequent re-evaluation has shown that these breccias most likely originated as a sequence of very coarse to fine-grained, laminated, clastic sedimentary rocks, that have been subjected to later strong, hydrothermal replacement. They appear to have only undergone minor additional brecciation during metasomatism, involving relatively passive infiltration of hydrothermal fluids and metasomatism, localised by porosity, particularly within the coarse grained sedimentary breccias. The amount of brecciation that can be attributed to hydrothermal processes is unclear, and evidence supports the conclusion that hydrothermal activity, and brecciation took place when the tabular, conformable breccia zones were flat lying (Freeman and Tomkinson, 2010).

## Mount Isa Inlier

### Crustal Setting

The *Eastern Fold Belt* (EFB) of the Mount Isa Inlier in northwest Queensland, Australia, hosts a number of significant IOCG deposits, including *Ernest Henry* (Mark *et al.*, 2000; Rusk *et al.*, 2010), *Mount Elliott* (Brown and Porter, 2010), *Starra/Selwyn* (Sleigh, 2002), *Osborne* (Adshead *et al.*, 1998; Gauthier *et al.*, 2001; Fisher and Kendrick, 2008) within the Cloncurry district (Fig. 5; Table 1).

Mineralisation was not synchronous across the EFB, with deposits having formed at different times over a ~100 m.y. period, extending from ~1595 Ma at Osborne (Rubenach *et al.*, 2001), ~1568 Ma at Starra (Duncan *et al.*, 2009; 2011), ~1530 Ma at Ernest Henry (e.g., Rusk *et al.*, 2010), ~1515 Ma at Mount Elliott (Duncan *et al.*, 2011), and 1497 and 1487 Ma at the Mount Dore and Lady Ella deposits respectively, which are located between Mount Elliott and Starra (Duncan *et al.*, 2009; 2011). This interval encompasses Isan orogeny peak metamorphism from 1600 to 1580 Ma, and a period of magmatism from ~1550 to ~1500 Ma, the most extensive phase of which is represented by the Williams and Naraku batholiths. These batholiths are distributed over an area of approximately 200 × 150 km (Fig. 5) and have extremely variable compositions, variously classified as I- or A-type (Wyborn *et al.*, 1988; Page and Sun 1998, Pollard *et al.*, 1998; Wyborn, 1998; Mark, 2001). They resulted from a number of pulses of voluminous mafic and felsic potassic magmatism, and were emplaced as tabular bodies at mid-crustal levels,

Mount Isa Inlier ... cont.

which, while having predominantly A-type geochemical signatures, are syn-tectonic and derived from high temperature crustal melting at pressures not exceeding 1000 MPa (Mark *et al.*, 2005).

Rubenach *et al.* (2008) propose that mafic rocks emplaced into the lower crust below the Mount Isa Inlier, were responsible for the 1600 to 1580 Ma high temperature (670 to 580°C), low pressure (600 to 400 MPa) metamorphism (greenschist to upper amphibolite facies), partial melting at peak metamorphism, and subsequently contributed to the formation of the 1547 to 1545 Ma Maramungee and Blackeye granodiorite-tonalite-trondhjemite suite granitoids and the 1550 to 1500 Ma Williams and Naraku batholiths (Fig. 5). This proposition is supported by their observation that most of the widespread exposed mafic rocks in the Mount Isa Inlier are predominantly high-Fe tholeiites, and therefore are unlikely to be direct mantle melts, but rather magmas that resided and fractionated in the lower crust, and produced a significant lower crustal thermal anomaly over an extended period.

Generation of melt that produced these batholiths is considered to have occurred at a depth of  $\geq 25$  to 30 km in the plagioclase stability field, and are interpreted to have been triggered by the emplacement of mantle melts in a mafic underplate (Page and Williams, 1988; Wyborn *et al.*, 1988; MacCready *et al.*, 1988; Pollard *et al.*, 1998; Mark, 2001). At the current erosional level, the more mafic phases, which are of possible mantle-origin, include hornblende-diopside monzonites and quartz diorites (Wyborn, 1998; Mark, 1999). The dominant felsic phases, which contain 65 to 77 wt.% SiO<sub>2</sub>, and include potassium-rich porphyritic monzodiorite, monzogranite, granodiorite and granite, are considered to have formed by re-melting of multiply reworked Palaeoproterozoic igneous rocks with depleted mantle Sm-Nd model ages of ~2.2 to 2.3 Ga (Wyborn *et al.*, 1988; Page and Sun 1998; Wyborn, 1998; Mark, 2001).

Iron oxide-alkali altered mineralised systems are also found within the Mary Kathleen Fold Belt (MKFB), the western subdivision of the EFB, immediately west of the Cloncurry district (Fig. 5). This includes the northnorthwest-trending *Roseby corridor* deposits of *Blackard* and *Little Eva* (Table 1), also interpreted to be coeval with the Williams and Naraku batholiths exposed immediately to the east. The principal intrusive phase within the MKFB is the 1.7 Ga Wonga batholith which overlaps the Williams-Naraku batholith to the east and is exposed within inliers in the Cloncurry district (Fig. 5).

The EFB is bounded to the west by the 1870 to 1850 Ma felsic volcanics and coeval granitoids of the narrow Kalkadoon-Leichhardt belt (Fig. 5), which separates it from the Western Fold Belt (WFB). Oliver *et al.* (2008) interpret the Kalkadoon-Leichhardt belt to be the remnant of a magmatic arc, part of the Barramundi orogeny. This orogenic event is recognised across the north of Australia, and is related to the assembly of the Nuna/Columbia supercontinent. Oliver *et al.* (2008) suggest, arc magmatism occurred in association with a pre-1840 Ma plate boundary further to the east, and resulted in mantle enrichment in volatiles below the EFB. They consider much of the subsequent history to have involved eastward thinning of the plate and rapid retreat of the boundary in the same direction between 1850 and 1600 Ma, leaving the EFB in an intracratonic setting.

Dating of inherited zircons from intrusive rocks in the sparsely exposed Palaeoproterozoic basement metamorphics which are only exposed in the WFB, to the west of the Kalkadoon-Leichhardt belt, gives Mesoarchean to Palaeoproterozoic ages, suggesting Archaean crust below at least the western Mount Isa Inlier, or alternatively, Palaeoproterozoic sediments that included clastic sediments of Archaean provenance (Bierlein *et al.*, 2008).

The EFB country rock into which these intrusions were emplaced, is composed of two main cover sequences (CS2 and CS3) deposited in rift basins, the depocentres of which moved progressively eastward with time, as did the centres of magmatism, reflected by the Kalkadoon, Wonga and Williams-Naraku batholiths. CS2 and CS3, were deposited between 1790 and 1690 Ma and from 1680 to 1610 Ma respectively. CS2 includes a rift fill succession commencing with predominantly clastic sediments, overlain by both felsic and basaltic volcanics with siltstones, sandstones and quartzites, which are all succeeded by the laterally extensive platformal evaporitic carbonates (with minor volcanic, clastic and jaspilitic rocks) of the Corella and Doherty formations. The latter formations are now dominantly sodic-calcic altered calc-silicates. The lower rift phase members of the CS2 were deposited diachronously from west to east. The sequence was extensively intruded by the 1750 to 1730 Ma Wonga Granite, while the coeval Mount Fort Constantine volcanics separate the Corella and Doherty formations in the north. The first significant deformation to affect CS2 (but not CS3) was the 1750 to 1735 Ma Wonga extensional event. Minor tonalites, granitoids and diorite emplaced between CS2 and 3 have been dated at 1686 to 1660 Ma (including the Ernest Henry Diorite; Blake, 1987; Blenkinsop *et al.*, 2008; Foster and Austin, 2008).

CS3, which extends much further to the east than does CS2, is composed of a thick, extensive succession of quartzites, pelites, volcanic rocks and carbonates. In the Cloncurry District, it is divided into a thick eastern clastic and thinner western sequence characterised by carbonates, separated by a major north-south structure corresponding broadly to the Mount Dore Fault Zone (Fig. 5). Deposition of CS3 in the EFB was terminated by the onset of the Isan Orogeny at ~1600 Ma, which was dominated by east-west compression and persisted until ~1500 Ma. The exact nature of Isan D1 deformation is uncertain, but seems to have involved overall north-south thrusting (Betts *et al.*, 2006), and resulted in a regional, steep, east-west foliation (Rubenach *et al.*, 2008).

Within the WFB, CS2 includes the 6 to 15 km thick Eastern Creek Volcanics (1790 to 1740 Ma) and equivalents, composed principally of amygdaloidal to massive metabasalt (with minor interbedded clastic sediments), considered to represent the remnants of an extensive igneous province overlapping the Wonga phase. To the east, a considerably condensed equivalent, the Magna Lynn Metabasalt, is found in the Kalkadoon-Leichhardt belt, lensing out into the EFB (Foster and Austin, 2008). The Eastern Creek Volcanics of the WFB and Wonga Granite would appear to represent an earlier mantle influenced phase preceding the 1600 to 1500 Ma mafic magmatism of the EFB of Rubenach *et al.* (2008).

The comprehensive national compilation and analysis of dated mafic and ultramafic magmatism by GeoScience Australia (Claoué-Long and Hoatson, 2009) has outlined a broad northnorthwest trending mafic igneous province

## Mount Isa Inlier ... cont.

that incorporates the Mount Isa Inlier and is composed of a series of eastward migrating pulses from ~1780 to ~1680, and locally ~1530 Ma (Fig. 5 inset). These overlap the major mafic Eastern Creek Volcanics in the WFB and the

possibly associated felsic magmatism of both the Wonga and Williams-Naraku Batholiths, and is taken to reflect a period of long lived underplating in section of the North Australian craton.

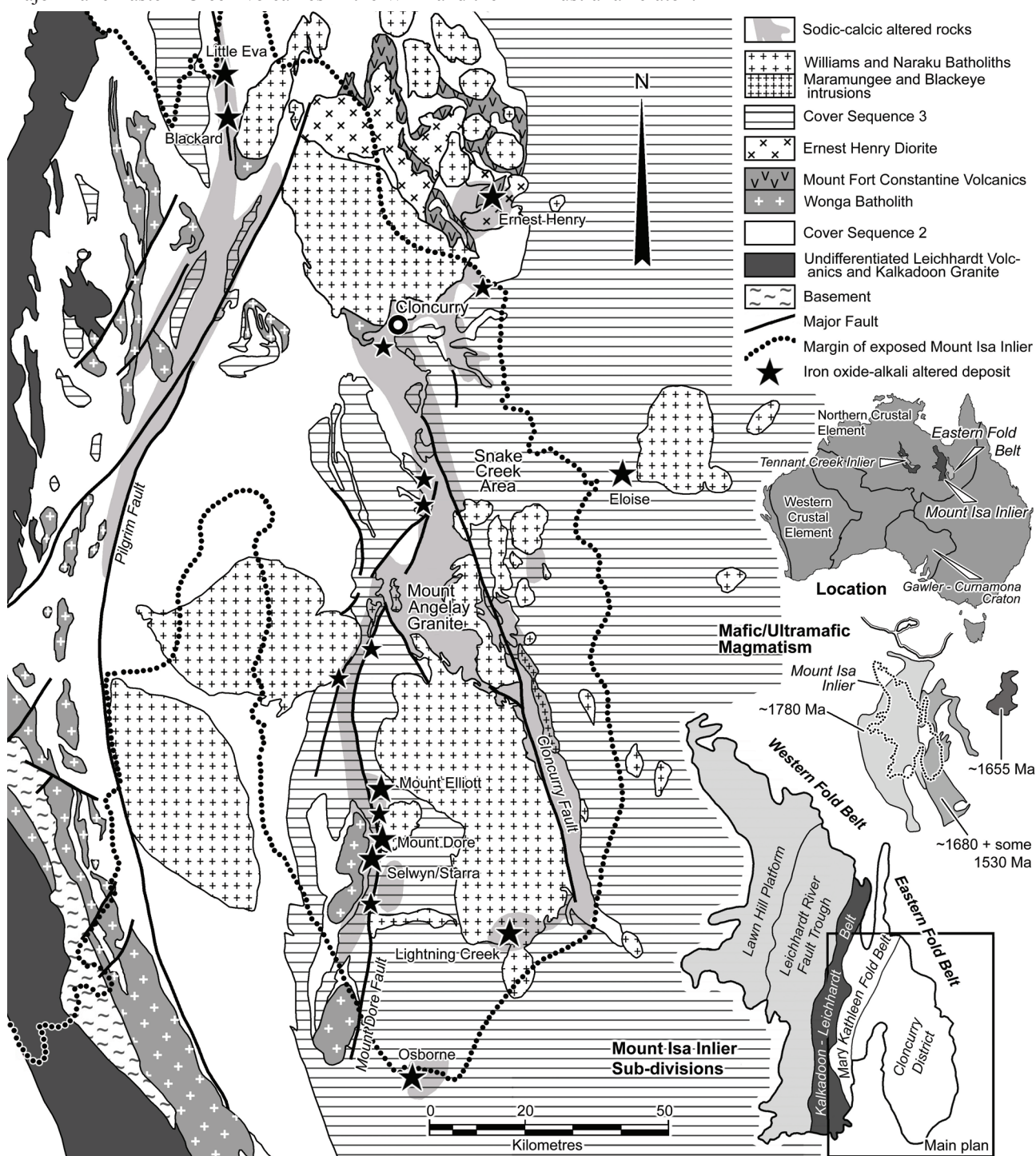


**Figure 5:** The tectonic framework and location of the main iron oxide-alkali altered mineralisation of the Palaeo- to Mesoproterozoic Mount Isa Inlier in northwest Queensland, Australia. The Subdivisions inset illustrates the western and eastern fold belts, separated by the 1870 to 1850 Ma Leichhardt Volcanics and Kalkadoon Granite of the central Kalkadoon-Leichhardt Belt. Both fold belts contain similarly aged 1790 to 1690 and 1680 to 1610 Ma cover sequences 2 and 3 sedimentary and volcanic rocks respectively, although the Western Fold Belt partially overlies a basement of either Archaean or Palaeoproterozoic rocks of Archaean provenance. The Eastern Fold Belt is composed of volcanic and sedimentary rocks deposited in extensional rift basins that young and thicken to the east, intruded by the voluminous Wonga (1750 to 1730 Ma) and Williams-Naraku (1550 to 1500 Ma) batholiths which are pre- and post-Cover Sequence 3 respectively. Note the general broad oval shaped distribution of the envelope encompassing exposures of these batholiths. The Mafic/Ultramafic Magmatism inset (after Claoué-Long and Hoatson, 2009) shows that the widespread and numerous small dykes, sills and stocks intruding these rocks also young to the east, although the ~1680 Ma population is overlapped by some 1530 Ma intrusions within granites to the immediate northeast of the Mount Angelay Granite. The extent of regional-scale, mainly sodic-calcic, alteration is illustrated on the main plan, largely controlled by trans-crustal fractures (particularly the Pilgrim, Mount Dore and Cloncurry faults) which influenced both facies distribution during extension, and were reversed as thrusts during basin inversion. The alteration also has a strong overlap with the carbonate (evaporitic) rocks of the Cover Sequence 2 Corella Formation and possible similar rocks of the Cover Sequence 3 Staveley Formation. Note the distribution of iron oxide-alkali altered and IOCG sensu stricto mineralisation. The geological interpretation is after Foster and Austin, 2008 and previous sources quoted therein, while the alteration is after Kendrick *et al.*, 2008; Mark *et al.*, 2005; Oliver, 1995.

Mount Isa Inlier ... cont.

## Regional Alteration

The Eastern Fold Belt (EFB) of the Mount Isa Inlier hosts regional-scale hydrothermal systems that include (1) barren regional sodic-calcic and lesser overprinting potassic alteration, and (2) granite-hosted hydrothermal alteration complexes with magmatic-hydrothermal transition features, e.g., Lightning Creek (Baker *et al.*, 2008; Oliver *et al.*, 2008; Oliver *et al.*, 2009; Perring *et al.*, 2000; Pollard, 2001).

Both, (1) laterally co-extensive fault related zones, and (2) linear networks of anastomosing, structurally controlled corridors of alteration that are developed over intervals of tens to hundreds of kilometres are evident within the EFB (Fig. 5; Kendrick *et al.*, 2008; Mark *et al.*, 2005; Oliver, 1995). Alteration within these zones is dominantly sodic-calcic and occurred periodically over a 250 m.y. interval. The earliest extensive alteration of this type is characterised by large-scale sodic-calcic-potassic metasomatism, NaCl-rich scapolite and skarn development associated with the ~1.7 Ga Wonga phase granites in the MKFB (Oliver, 1995). However, the bulk of the sodic-calcic assemblages were associated with fluids that were initially dominantly sedimentary formation waters with lesser magmatic components prior to and during peak metamorphism at 1595 to 1580 Ma (Kendrick *et al.*, 2008; Oliver *et al.*, 2008; Baker *et al.*, 2008). Fluid circulation was driven by the various pulses of magmatism and metamorphism caused by the inferred hot mafic underplate (and intraplate) underlying the region (Kendrick *et al.*, 2008). These fluids leached evaporite rich units (e.g., the Corella Formation) in the cover sequences to become hypersaline (Kendrick *et al.*, 2008), and are interpreted to have progressively scavenged metals from the volcanosedimentary pile to possibly be locally concentrated and sequestered into structurally focused fluid sites where they were available for further remobilisation (Oliver *et al.*, 2008). The regional sodic-calcic alteration is represented by assemblages of *albitic plagioclase + actinolite + titanite ± quartz ± magnetite ± diopside clinopyroxene* replacing metabasaltic, calc-silicate, metapelitic and felsic igneous rocks. Alteration is associated with complex, hypersaline H<sub>2</sub>O-NaCl-CaCl<sub>2</sub>-KCl-(?FeCl<sub>2</sub>) fluids with high Ca:Na ratios, overpressured in zones of retrograde brittle-ductile shear, brittle fracture and regional calc-silicate megabreccias. They occurred as multiple fluid buffered systems at 400 to 500°C and initial pressures of >200 MPa (de Jong and Williams, 1995). The major structures that have controlled the circulation of these fluids include the Cloncurry, Pilgrims and Mount Dore fault systems (Fig. 5), some of which have been shown to continue steeply to depths in excess of 30 km (Austin and Blenkinsop, 2008).

This alteration is divided by peak metamorphism at 1595 to 1580 Ma, with dominantly regional albite earlier, and subsequent more structurally controlled *albite-actinolite-magnetite-titanite ± clinopyroxene*, taking place synchronously with major granite (e.g., Williams-Naraku batholiths) emplacement (Baker *et al.*, 2008). Large parts of the latter regional sodic-calcic alteration is associated with the formation of breccia complexes that are particularly well exposed along the Cloncurry fault, predominantly in the roof and along the margins of the Williams and Naraku batholiths, developed during multiple episodes of granitoid intrusion (de Jong and Williams, 1995; Mark, 1998; Mark and de Jong, 1996). Breccia zones up to hundreds of metres across comprise large (metres across) subangular to angular and small rounded clasts of albitised host rock in

a matrix of sodic-calcic minerals. These textures suggest formation by upward escape of magmatic vapour phases, with alteration by later, high salinity magmatic fluids (Pollard, 2001). A direct connection between 1530 Ma intrusions, brecciation and alteration has been clarified by observations of sodic-calcic altered (albite, magnetite, hematite and actinolite with minor apatite) breccia pipes containing hydrothermal magnetite and local sulphides, emanating from contact aureoles to the Williams-Naraku batholith (e.g., in the Snake Creek area; Fig. 5), possibly spatially connected to significant mineralisation (Oliver *et al.*, 2006a; Cleverley and Oliver, 2005). This assemblage is similar to the mineralogy of veins and breccias found in the carapace of the Mount Angelay Granite (Fig. 5), also part of the Williams-Naraku batholith (Mark and Foster, 2000).

In the area around *Ernest Henry*, the regional sodic-calcic alteration is irregularly overprinted by a range of potassic-, iron- and manganese-bearing minerals, including *biotite, magnetite, almandine-spessartine garnet and K feldspar* which have an overall spatial association with the ore deposit, but are found up to several kilometres from the orebody (Williams *et al.*, 2005; Rusk *et al.*, 2010). These may represent regional alteration, or an early pre-ore assemblage.

The *Lightning Creek* prospect (Fig. 5) represents a major *granite-hosted hydrothermal complex with magmatic-hydrothermal transition features*. It is located within, and near the southern margin of, the Squirrel Hills granite (part of the ~1.53 Ga Williams and Naraku batholiths), and comprises a sill complex, developed over an area of 3000 × 430 m and persisting to a depth of 4750 m. The mineralised zone occupies a volume of ~6 km<sup>3</sup>, averaging ~10 vol.% magnetite, for over 2 Gt of contained iron (Perring *et al.*, 2000).

The dominant host rock is a coarse-grained quartz monzodiorite, comprising centimetre-sized phenocrysts of plagioclase and K feldspar set in a medium-grained groundmass of amphibole, biotite, K feldspar, magnetite, plagioclase, quartz and titanite, with accessory apatite and zircon. This quartz monzodiorite is intruded by quartz diorite enclaves, porphyritic monzogranite and fine-grained alkali-feldspar granite. Locally, these rocks were pervasively pyroxene-albite altered prior to the magnetite mineralisation. Much of the magnetite is variably distributed in veins that are spatially and temporally associated with a subsequent complex of minor quartzofeldspathic intrusives. These late intrusives range from a few millimetres to metres in thickness, are sub-horizontal and sill-like, and cannot generally be correlated between drill holes, although they may constitute up to 50% of the rock. They display considerable textural and mineralogical complexity and evolved from equigranular, quartzofeldspathic rocks (aplites) with magmatic chemistry, and include unusual iron-rich rocks (albite-magnetite-quartz) that exhibit a range of unusual spherulitic textures. The aplitic textured sills are composed of up to 75% albite <30% microcline, 25 to 30% quartz, and accessory apatite, calcite, chlorite, magnetite, titanite and zircon, with an unusual spherulitic texture. The spherulites are commonly dominated by albite with <15% K feldspar, 5 to 20% magnetite and 10 to 15% quartz. Fine-grained magnetite forms curved, balloon like surfaces, separating spherulitic albite-quartz ± magnetite from the original aplitic polygonal quartz-magnetite ± albite domains (Perring *et al.*, 2000; Pollard, 2001; Oliver *et al.*, 2008).

Experimental evidence (Iiyama, 1965) indicates that the Na/(Na+K) ratio of fluids in equilibrium with two alkali feldspars in CO<sub>3</sub><sup>2-</sup>-bearing fluids (0.96 at 600°C; 1 kbar) is significantly higher than the ratio is in chloride-bearing fluids (0.79). Unmixing of H<sub>2</sub>O-CO<sub>2</sub>-salt fluids within a crystallising melt, caused by decreases in temperature and/or pressure, will therefore result in Na exsolution and consequent albitisation of the wall rocks.

The large number of CO<sub>2</sub>-rich fluid inclusions in the district, both within the Williams and Naraku batholiths, and in the regional vein sets, are interpreted to be either from unmixing of complex NaCl-H<sub>2</sub>O-CaCl<sub>2</sub>-CO<sub>2</sub> brines upon their release from the crystallising mingled granite-gabbro batholith (Perring *et al.*, 2000; Pollard, 2001; Fu *et al.*, 2003), or derived directly from degassing of crystallising mafic intrusions (Oliver *et al.*, 2008). CO<sub>2</sub> unmixing is not commonly associated with potassic granites, except in cases where some involvement of mafic magmas or other mantle-derived melts is demonstrated (Mungall, 2002). Oliver *et al.* (2008) suggest simultaneous intrusion and magmatic mingling of CO<sub>2</sub>- and possibly Cu-bearing mafic magmas may have triggered the release of Cu and CO<sub>2</sub> during quenching of the mafic rocks (e.g., Wada *et al.*, 2004), which in turn forced exsolution of brines from the granitoids.

Fluid inclusions at Lightning Creek suggest crystallisation at >500°C and >1.5 kbar, while the spherulitic textures are taken to indicate crystallisation under hydrous conditions with episodic release of a fluid phase. This magmatic fluid phase was dominated by H<sub>2</sub>O, CO<sub>2</sub> and chlorine, and underwent phase separation into a CO<sub>2</sub>-rich vapour and a hypersaline brine (33 to 55 wt.% NaCl<sub>equiv.</sub>), enriched in iron (~10 wt.%) and copper (~1 wt.%; PIXE analysis), in addition to sodium, potassium and calcium. Although rich in copper, these magmatic fluids did not generate significant copper-(gold) mineralisation, possibly because of the high temperatures involved and/or a lack of reduced sulphur in the fluids or host rock. Where this fluid was retained within iron-rich portions of the sills, it caused calcic-iron±sodic alteration (pyroxene-albite±magnetite growth at the expense of quartz). Where it was expelled from the sills, it produced quartz-magnetite±clinopyroxene±albite veins, broadly coeval with the early magnetite veins (Perring *et al.*, 2000).

The Lightning Creek magnetite prospect demonstrates a process for the development of both large tonnage magmatic magnetite concentrations and a source of hydrothermal magnetite and copper mineralisation.

Baker *et al.* (2008) have identified three main fluid types from inclusions associated with iron oxide-alkali altered mineralising systems in the EFB. Two of these represent barren regional sodic-calcic alteration. These have high Br/Cl ratios, consistent with evaporite/bittern-derived fluids (~30 to 40 wt.% NaCl<sub>equiv.</sub> and ~5 to 36 wt.% NaCl<sub>equiv.</sub> respectively), moderate temperature (100 to 450°C) but low Cu contents of generally <300 ppm. The data allow for leaching of copper from crustal rocks by voluminous quantities of these non-magmatic fluids, as a source of copper. Oliver *et al.* (2008), propose this would involve scavenging of metals by circulating fluids that produced the regional barren alteration, which then sequestered their solutes into structurally focused fluid sites, or contributed to the pre-peak metamorphism ores (e.g., Osborne). Sequestered metal could then be reworked and concentrated by subsequent fluids generated or circulated by the Williams and Naraku batholiths and/or mafic intrusions (Oliver *et al.*,

2008). The third type of inclusion is largely confined to granite-hosted hydrothermal complexes (e.g., Lightning Creek), and IOCG deposits, as discussed below.

### **Deposit-scale Alteration and Mineralisation**

The last of the three main fluid types identified by Baker *et al.* (2008) in inclusions from iron oxide-alkali altered mineralising systems in the EFB, is largely confined to IOCG deposits and to granite-hosted hydrothermal complexes (e.g., *Lightning Creek*). It is characterised by abundant high temperature (~200 to 550°C), ultrasaline (30 to 60 wt.% total salts), complex multi-solid and high copper content inclusions (>300 to 10 000 ppm). Those of this latter type, originating from a granite-hosted environment alone, have Br/Cl ratios consistent with a magmatic origin, while those from IOCG deposits external to the intrusions, have wide ranges in salinity and homogenisation temperatures and evidence of multiple fluid sources, taken to support fluid mixing. Baker *et al.* (2008) interpret the data to support a model involving generation of a high-temperature, ultrasaline, copper-rich magmatic fluid exsolved from the Williams and Naraku batholiths which were channeled through large-scale structures to sites where it mixed with non-magmatic fluids with lower copper contents and evaporite-like halogen signatures. Baker *et al.* (2008) suggest larger IOCG deposits may best form from magmatic-derived fluids based on their higher Cu content (cf., the smaller Osborne deposit, proposed to be of basinal origin, as detailed below, compared to Ernest Henry, interpreted to be related to the release of magmatic-derived fluids; Oliver *et al.*, 2009).

Oliver *et al.* (2009) propose that there are two general styles of IOCG deposit in the Mount Isa Inlier, in adjacent but separate parts of the Inlier. These are the (1) Osborne (~1.68 to 1.6 Ga) and (2) Ernest Henry (~1.53 Ga) types, distinguished from each other on the basis of geochronology, structural association, metal-oxide and sulphide distribution, and radiogenic and stable isotope signals (Fisher and Kendrick, 2008; Kendrick *et al.*, 2007; Mark *et al.*, 2004; 2005a; Oliver *et al.*, 2008; 2009; Williams and Pollard, 2001). One of the key physical distinctions is that those of the Ernest Henry style are hosted in breccia pipes containing distinctly rounded and/or corroded clasts, whereas the Osborne type are more commonly associated with shear zones (Gauthier *et al.*, 2001; Mark *et al.*, 2006; Oliver *et al.*, 2008; Rubenach *et al.*, 2008). They regard the younger Ernest Henry type as having been formed as described by Baker *et al.* (2008) above.

The **Osborne** deposit in the southernmost part of the Mount Isa Block, is broadly conformable, and hosted in metamorphosed siliciclastic rocks and iron formation of the 1690 to 1650 Ma Soldiers Cap Group, surrounded by widespread sodic (albite) alteration. The host unit comprises feldspathic psammites ±thin layers of pelite, stromatolitic migmatites and local pre-metamorphic banded ironstone and schists. Sheet intrusions of amphibolite and post metamorphic pegmatites are also present. The ironstone is conformable and composed of well-banded (0.2 to 10 mm) magnetite, apatite and quartz. Carbon and oxygen isotope data suggest these ironstones were deposited at a similar time to the host sequence (Marshall *et al.*, 2006). Two ironstone lenses are developed over a 1.3 km strike length, the upper 10 to 40 m and the lower 8 to 15 m thick, separated by 6 to 40 m of psammite. Weak, disseminated copper-gold throughout the banded ironstones is associated with hematite-magnetite-pyrite.

*Mount Isa Inlier ... cont.*

Zones of massive, coarse-grained silicification/silica flooding with abundant wall rock relicts occur along strike as a continuation of the ironstones, and host the bulk of the copper-gold mineralisation. However, textural evidence indicates the main phase of copper-gold deposition post-dated the majority of the silica flooding and temporally associated pre-copper-gold pyrite±magnetite±siderite±talc and minor chlorine-bearing silicates (Adshead *et al.*, 1998). The ores (or ore precursors) are interpreted to have initially formed during or prior to the ~1.6 Ga regional metamorphic peak, by interaction of basinal or early metamorphic fluids with mafic rocks and ironstones. Rubenach *et al.* (2001) determined a 1595 Ma age for albitisation associated with peak metamorphic (S-type) pegmatites pre-dating copper-gold mineralisation, while Gauthier *et al.* (2001) determined a 1600 Ma Re-Os age for ore-related molybdenite. The involvement of saline basinal fluids in the genesis of Osborne mineralisation is suggested by syn-ore fluid inclusions with argon, halogen and noble gas data indicative of bitterns, halite dissolution and a 'metamorphic' component in which anatectic melts leave a signal (Fisher and Kendrick 2008). Subsequent to deposition of the ores, inversion and regional metamorphism associated with the main stages of the Isan Orogeny, may have also contributed anatectic fluids to the system, remobilising sulphides into axial planar features, and resetting isotopic systems, with the current morphology of the now shear-hosted orebody reflecting migration during peak metamorphism (1600 to 1595 Ma) of pre-D<sub>2</sub> stratigraphy-parallel ore into fold hinges during deformation (Oliver *et al.* 2008). The proposed fluids responsible for the initial mineralisation that predates peak metamorphism (~1.6 Ga) and Williams-Naraku batholith magmatism (1.55 to 1.50 Ga), may well involve the evaporite/bittern-derived fluids responsible for the barren regional pre-peak metamorphism sodic-calcic alteration as described by Baker *et al.* (2008) and Kendrick *et al.* (2008). Oliver *et al.* (2008) interpret these fluids to have progressively scavenged metals from the volcano-sedimentary pile to be sequestered them as either ore concentrations that are subject to further remobilisation (as they suggest occurred at Osborne), or as dispersed sulphides in structures that may be collected by subsequent fluids using the same conduits.

The ~1530 Ma **Ernest Henry** IOCG deposit is hosted by a breccia body, dominated by strongly K feldspar-altered clasts of the ~1740 Ma Mount Fort Constantine metavolcanics (dacite and andesite) with subordinate metabasalts and calc-silicate metasediments. It lies between two northeast trending shear zones and is basically a breccia pipe, plunging at approximately 45° to the southsoutheast, nested between the ductile shear zones (Rusk *et al.*, 2010).

Hydrothermal alteration and mineralisation at Ernest Henry is characterised by the regional pre-ore sodic-calcic event, overprinted by a pre-ore potassic-(manganese-barium) phase, represented by an intense biotite-magnetite assemblage, and less commonly K feldspar-garnet (manganese-rich) alteration. The host breccia clasts are usually pervasively altered to microcrystalline barian K feldspar. K feldspar alteration is most intense in the vicinity of copper-gold mineralisation, but forms a halo extending from several hundred meters up to 2 km beyond the ore body (Mark *et al.*, 2006a), although this outer halo may represent part of pre-ore regional alteration zone. Mineralisation is divided into two main stages, characterised by similar mineral assemblages: (1) associated with brecciation, and (2) a later vein-dominated episode. The

ore-bearing assemblage dominantly comprises magnetite, pyrite, chalcopyrite, carbonate and quartz, with lesser apatite, barite, titanite, actinolite, biotite and fluorite. In the levels of the deposit, the bulk of the ore is present as hypogene chalcopyrite infilling between K feldspar-altered breccia clasts, while at greater depths, it both infills between, and replaces clasts. Electrum and native gold are closely associated with pyrite and chalcopyrite (Foster *et al.*, 2007). Post-ore, volumetrically minor, carbonate±quartz veins containing minor coarse chalcopyrite, lack magnetite, and only carry a little gold. Deeper in the deposit, breccias include rounded clasts of previously mineralised breccias containing magnetite, pyrite and chalcopyrite, indicating multiple superimposed brecciation events (Rusk *et al.*, 2010; see Figs. 1 and 4 in the same paper, this volume).

Rusk *et al.* (2010) interpret the data from Ernest Henry to be consistent with the following genetic trend: (1) Rapid devolatilisation (of possibly both chloride-rich brines and CO<sub>2</sub>-rich fluids) within the source magma chamber; (2) Fluid over-pressuring in the roof of the magma chamber as a result of volatile exsolution and vapour expansion, assisted by a seal created by magma solidification, sodic-calcic alteration and/or contact metamorphism in the carapace of the igneous complex; (3) Possible leakage of over-pressured magmatic fluid along structures controlling the location of the later breccia pipe, producing a pre-ore potassic alteration halo; (4) The eventual failure of the seal and sudden release of fluid pressure, resulting in a high-energy fluid flow event driving brecciation and upward transported and milled clasts. The resultant breccia mass permitted the mixing and/or subsequent ingress of basinal brines circulating within fractured rocks several kilometres above the magma chamber. Fluid mixing, rapid depressurisation and resultant cooling led to ore precipitation within the matrix porosity between breccia clasts at the top of the orebody, where, as the fluid flow, temperature and pressure declined the breccia was sealed; (5) At depth, closer to the heat source, the temperature and pressure gradient degraded more slowly, allowing for fluid-rock reaction to be more protracted, such that prolonged chemical interaction between K feldspar-rich host rocks and ore fluids led to replacement style mineralisation within clasts, with the same mineral assemblage as observed in the shallower parts of the deposit. (6) At the deepest levels, repetition of the cycle may have resulted in the release of a new pulse of fluids which brecciated and tapped earlier-formed magnetite-chalcopyrite rich rocks, telescoping mineralised clasts upwards into the orebody along narrow channels, thereby upgrading ore. Several lines of evidence, including carbon, oxygen and sulphur isotopes, fluid inclusion halogen and argon isotope ratios are consistent with both a magmatic metal source and a basinal-brine fluid precipitating agent contributing to the hydrothermal system. These data include stable isotopes (Marshall *et al.*, 2006) which indicate a mixing trend between δ<sup>13</sup>C values of ~0‰ and δ<sup>18</sup>O of ~-21‰, to δ<sup>13</sup>C of around -7‰ and δ<sup>18</sup>O of around 11‰, which was interpreted to result from mixing between carbon and oxygen from marine meta-carbonates and a magmatic fluid at temperatures of ~450° C. Sulphur isotopes in chalcopyrite are mostly between δ<sup>34</sup>S of 0 and 4‰, but up to ~8‰ (Mark *et al.*, 2005b; Twyrould, 1997), which Rusk *et al.* (2010) consider to be consistent with a magmatic sulphur source. They also note that the spread to the most positive values for δS does not preclude a component of sulphur derived from marine metacarbonates. The signals recorded by argon isotopes and Cl/Br ratios in

*Mount Isa Inlier ... cont.*

fluid inclusions from Ernest Henry also indicate mixing between a mantle source ( $^{40}\text{Ar}/^{36}\text{Ar} \sim 29\,000$  and molar Cl/Br  $\sim 1000$ ) and a fluid derived from dissolution of evaporites ( $^{40}\text{Ar}/^{36}\text{Ar} < 1000$  and Cl/Br  $\sim 1000$ ; Kendrick *et al.*, 2007). This is in agreement with fluid inclusion halogen data from Baker *et al.* (2008) that also show fluid salinity derived from mixed magmatic and basinal brine components. For more detail and diagrams see Rusk *et al.* (2010) in this volume.

The **Mount Elliott** IOCG system is hosted within a succession of altered siliciclastic and carbonatic sediments, and volcanic rocks of the 1680 to 1610 Ma Cover Sequence 3 succession of the Mount Isa Inlier, Eastern Fold Belt, overlying a Palaeoproterozoic basement, and occurs within an enclave between 1550 to 1500 Ma A-type granitoids and gabbroids of the Williams batholith. It is located adjacent to the steeply east-dipping, transcrustal, reverse Mount Dore Fault, which also defines the boundary between the broadly equivalent eastern siliciclastic dominated and the western carbonate-bearing facies of Cover Sequence 3, and as such may represent a rejuvenated synsedimentary rift basin margin structure. Mineralisation is hosted by both calc-silicates of the Staveley Formation, and intensely skarn altered shales and meta-mafic rocks of the structurally overlying, but stratigraphically older Kuridala Formation of the Soldiers Cap Group. The bulk of the deposit is hosted within breccias, including infill replacing the matrix of a pre-ore, pipe-like, polymictic mass, cutting calcsilicates and amphibolites within the Staveley Formation, and a syn-ore (?) megabreccia with clasts of from 0.1 to 20 m across within phyllites and meta-mafic rocks of the Kuridala Formation. Mineralisation also replaces adjacent banded calcsilicates and occurs as late carbonate-sulphide veins. The main SWAN breccia within the Staveley Formation, comprises angular to rounded clasts, composed of strongly albite-altered calcsilicate and metadolerite set in a fine- to coarse-grained matrix which now contains hematite-stained albite, clinopyroxene, actinolite, magnetite, calcite, pyrite and chalcopyrite. The early, regional pre-breccia alteration (as represented by the clasts), is overprinted by multiple pulses of fracturing, brecciation and alteration, each composed of initial diopside-scapolite, followed by the deposition of actinolite and mineralisation, resulting in an assemblage of chalcopyrite, actinolite, scapolite  $\pm$  andradite  $\pm$  tourmaline  $\pm$  allanite  $\pm$  apatite  $\pm$  magnetite  $\pm$  pyrite  $\pm$  pyrrhotite and very abundant calcite and anhydrite, as well as minor biotite, chlorite and K feldspar. Skarn alteration, closely associated with the main copper-gold-bearing sulphides, has been dated at  $1510 \pm 3$  Ma, close to the age of the nearby batholithic granitoids, while stable isotope data are consistent with dominantly magmatic fluids during mineralisation, possibly influenced by a metamorphic fluid component. Potassic alteration is less well developed, compared to Ernest Henry, and much of the brecciation appears to predate ore. The skarn mineralogy is a reflection of the carbonate host of the Staveley Formation. For more details see Brown and Porter (2010), and Figs. 1, 2, 4, 5 and 6 in the same paper, this volume.

The **Starra-Selwyn** group of deposits represent a number of discrete high grade, structurally controlled shoots of gold-copper ore associated with magnetite-hematite-quartz "ironstones" (original mining reserve, 1988 of 5.3 Mt @ 1.98% Cu, 5.0 g/t Au; Kary and Harley, 1990), within a larger low grade resource (total resource of 253 Mt @ 0.34% Cu, 0.48 g/t Au, at a 0.2% Cu<sub>equiv</sub> cutoff; Sleight, 2002). Duncan *et al.* (2011; after Ivanhoe Mines

2008) quote past production + current resources totalling 37.4 Mt @ 1.2% Cu, 1.6 g/t Au.

Mineralisation occurs as 5 shoots, distributed over a  $\sim 5.5$  km strike length of an extensive ( $\sim 15$  km long) magnetite-hematite ironstone ridge that coincides with the Starra Shear high strain zone. This shear is located on the western margin of the major regional corridor of deformation, the Mount Dore fault zone. It is the western of two main, southward converging ironstone ridges evident at surface, and comprises a quartz-magnetite-hematite ironstone that hosts the known copper-gold mineralisation. The second, subparallel, eastern ridge, is a quartz-hematite ironstone that appears to only be mineralised close to where the two meet (Williams *et al.*, 2001).

A wide zone of chalcopyrite-pyrite mineralisation occurs within the Starra Shear, although the highest grades are confined to the ironstones package, usually within its easternmost layers. High gold grades are also typically restricted to the ironstones, particularly on the margins of individual ironstone bodies, but unlike copper, do not extend into the surrounding shear zone (Ivanhoe Australia website).

The gold-rich mineralised ironstone shoots at Starra plunge steeply to the north or south, and are hosted by metamorphosed siliciclastic-carbonate rocks of the Staveley Formation. The hanging wall comprises strongly altered, interbedded, calcareous sandstone and siltstone, and the weakly mineralized footwall is dominated by chloritised quartz-feldspar-biotite-magnetite schist. The sequence also contains numerous amphibolite bodies.

Structural criteria, and the paragenetic relationships between hematite and magnetite, indicate that the alteration and mineralisation at Starra overprint metamorphic scapolite and biotite. They also suggest very early hematite metasomatism was associated with the regional sodic-calcic alteration (quartz-albite-actinolite-scapolite-titanite) that post-dated peak metamorphism, but was syn-D<sub>4</sub>, in a brittle-ductile setting (Rotherham, 1997). This was overprinted by potassic-iron alteration (biotite-magnetite-hematite-quartz-pyrite) and then by the gold-copper mineralisation. The gold-copper mineralisation was emplaced in a brittle, although otherwise similar, deformation regime and consists of an early quartz-anhydrite-barite-calcite-hematite-gold assemblage (with extensive hematitisation of magnetite) that progressed to pyrite-bornite-chalcopyrite-chlorite-muscovite and then to magnetite mineralisation (Adshead-Bell, 1998; Rotherham *et al.*, 1998).

Fluid inclusion homogenisation temperatures and oxygen isotope geothermometry suggest that ironstone formation and mineralisation occurred at 550 to 400°C and 360 to 220°C respectively. Fluid  $\delta^{18}\text{O}$  compositions for ironstone formation (9.2 to 6.0‰) and gold-copper mineralisation (10.9 to 8.4‰) fall within the range of magmatic and metamorphic fluids, although a magmatic-metasomatic origin has been preferred on the basis of stable isotopic, fluid inclusion, and thermodynamic considerations (Rotherham *et al.*, 1998).

### **Structural Control and Brecciation**

In the southeastern *Mount Isa Inlier*, deposits such as Mount Elliot, Mount Dore and Starra/Selwyn are all associated with subsidiary parallel and branching faults distributed within 2 km on either side of the major Mount Dore Fault Zone, which has a lateral extent of  $>100$  km, and also controlled the distribution of regional alteration (Fig. 5). Some of the deposits within this zone, e.g., Mount Dore, are tabular and more closely controlled by shearing,

Mount Isa Inlier ... cont.

while the Mount Elliott mineralisation is hosted by a breccia pipe in a zone of cross-faulting on the margin of the Mount Dore Fault zone (Kendrick *et al.*, 2008; Mark *et al.*, 2005; Oliver, 1995; Brown and Porter, 2010; Rusk *et al.*, 2010).

Whereas deposits such as Mount Elliott, are closely associated with major transcrustal structures, further north, the Ernest Henry orebody is in a zone characterised by more evenly distributed structures. Nevertheless, the latter orebody is hosted by a zone of brecciation, sandwiched between two northeast trending shear zones, the hanging wall and footwall shear zones. Coward (2001) suggested these two shear zones form part of a linked duplex of at least four faults or shear zones. The strike of this combined structure varies between approximately north-northeast and east-northeast on a 10 km scale. The orebody is located at a pronounced flexure in the shear fabric of this structure. It is likely that these local zones of deformation reflect long-lived structures that have been reactivated and mineralised during the Isan orogeny (Blenkinsop *et al.*, 2008).

Two main types of regional breccia are recognised in the Mount Isa Inlier, as well as those associated with ore deposits. The first of the regional breccias, *type I*, which are 'tectonic-hydrothermal' in origin, are intimately associated with the regional sodic-calcic alteration patterns, but usually lack significant mineralisation. They are volumetrically the more significant, mostly containing poorly sorted angular clasts, which have been rotated, but only minimally transported, and have a high clast:matrix ratio. The matrix usually comprises calcite, actinolite, albite, clinopyroxene, epidote, hematite and magnetite. They have been interpreted to be the result of either (1) cycles of fluid overpressuring and/or fault movement, with subsequent underpressuring along faults, clast collapse and simultaneous matrix precipitation, or (2) fracturing during multiple fold overprinting and strain incompatibilities, all in the presence of, and facilitating the circulation of brines. *Type II* breccias are of fluidised hydrothermal origin, volumetrically minor, show evidence of high energy fluid and clast transport on the scale of hundreds of metres to kilometres, have rounded clasts, and are more likely to host ore deposits. They are typically polymictic, matrix supported, poorly sorted, cut bedding and form pipe- or dyke-like bodies. Many are dominated by a magnetite matrix, accompanied by lesser carbonate, actinolite, pyrite and sometimes chalcopyrite. Some type II breccias form caps to the 1550 to 1500 Ma Williams and Naraku batholiths and extend vertically and laterally into pipes and dykes, which Oliver *et al.* (2006) infer to have formed during high energy fluidisation, resembling diatreme emplacement.

The breccia that hosts the *Ernest Henry* ore deposit is very similar to regional type II breccias. It is developed such that its long axis is parallel to, and it is bounded above and below by shear zones, although in the hanging wall it decreases in intensity to a crackle breccia before the shear zone. The host breccia is milled, ranging from clast- to matrix-supported. The clasts are principally strongly K feldspar-altered metavolcanics (dacite and andesite of the ~1740 Ma enclosing country rock) with subordinate metabasalts and calc-silicate metasediments (Twyerould, 1997; Mark *et al.*, 2006a). The dominant ore-bearing assemblage comprises magnetite, pyrite, chalcopyrite, carbonate and quartz, with lesser apatite, barite, titanite, actinolite, biotite and fluorite. The bulk of the ore occurs as hypogene chalcopyrite that infills between breccia clasts at shallow levels, and both infills between, and replaces clasts at greater depths.

The mineralisation of the *Mount Elliott* deposit in the southeastern Mount Isa Inlier is predominantly (but not exclusively) hosted within two main breccia bodies. The larger of these, the SWAN breccia, varies from crackle to matrix-supported, hosts the majority of the mineralisation and is up to more than 400 m in diameter. It is composed of angular to rounded, strongly albite-altered calcsilicate and metadolerite clasts set in a fine- to coarse-grained matrix of hematite-stained albite, clinopyroxene, actinolite, magnetite, calcite, pyrite and chalcopyrite. The individual clasts vary from centimetres to metres in diameter, although the intensity of the albite alteration frequently precludes the identification of the protolith of the majority of fragments. The bulk of the mineralisation is within the matrix of the breccia. This breccia appears to predate the introduction of mineralisation, providing a large, porous and chemically suitable trap for the ingress of fluids and deposition of ore (Brown and Porter, 2010 and references cited therein). The more restricted Mount Elliot Breccia occurs within the phyllites and basaltic volcanic rocks that cap the calcsilicate unit in which the SWAN breccia is developed. It is a megabreccia, dominated by usually angular clasts that are 0.1 to 20 m across, and was formed within skarn-altered metapelites and volcanic rocks. Mineralisation occurs as open-space infilling by chalcopyrite-pyrite-pyrrhotite-magnetite-pyroxene (diopside-hedenbergite) ± calcite, anhydrite, apatite, gypsum and amethyst within inter-clast spaces of similar dimensions. It is characterised by very coarse-grained (as much as tens of centimetres across) sulphides, magnetite and pyroxene (Wang and Williams, 2001). In contrast to the SWAN breccia, it appears to have developed close to the time of mineralisation.

## Carajás Mineral Province

### *Crustal Setting*

The Carajás Mineral Province, which is located approximately 20 to 120 km west of the north-south trending preserved margin of the southern Amazonian craton in Pará, Brazil, hosts the world's largest known concentration of large-tonnage IOCG deposits, including, *Sossego, Salobo, Cristalino, Igarapé Bahia/Alemão, Gameleira, Alvo 118* and *Igarapé Cinzento/Alvo GT46* (Fig. 8; Xavier *et al.*, 2010; Requia and Fontboté, 2000; Ronzê *et al.*, 2000; Tazava and Oliveira, 2000; Souza and Vieira, 2000). These deposits are located within the east-southeast trending, 50 to 80 km wide, 150 km long Itacaiúnas Shear Belt (centred on the Carajás fault; Figs. 7 and 8), where it cuts obliquely across the eastern third of an east-west trending, 400 × 100 km belt of thick Neoproterozoic bimodal, but mainly mafic to intermediate volcanism. This belt of volcanism includes chemical and clastic sediments, gabbroic to granitic intrusions, and succeeding clastic sediments (Figs. 7 and 8), and overlies the Mesoarchean granitoid nucleus of the Amazonian craton.

The 4.4 million km<sup>2</sup> Amazonian craton is divided into two halves by the east-west trending Amazon Basin intracratonic rift that has been active from the late Neoproterozoic to the present, while its eastern margin is marked by the structural boundary with the deformed sediments of the Neoproterozoic Araguaia Belt, part of the Tocantins Orogen that developed during the collision between the Amazonian/West African and São Francisco/Congo palaeo-continent during the late Neoproterozoic (Fonseca *et al.*, 2004; Fig. 6). The Amazonian craton itself is composed of six northwest-trending terranes,

Carajás Mineral Province ... cont.

each with internally coherent structural and age patterns, and bounded by major structural features. The Itacaiúnas Shear Belt is developed towards the northeastern margin of, and within, the oldest of these terranes, the 400 to 500 km wide, 3.2 to 2.5 Ga Central Amazonian province which is composed of the larger Xingu-Iricoumé and smaller Roraima blocks to the southeast and northwest respectively (Fig. 6). The terrane boundary with the 2.25

to 2.05 Ga Maroni-Itacaiúnas province is immediately to the northeast of the Carajás Mineral Province IOCG deposits. This younger province is composed of a series of mobile belts containing metavolcanosedimentary and juvenile calc-alkaline granitic rocks, with large areas occupied by mantle derived Palaeoproterozoic greenstone belts/mafic lavas and tuffs. During the Neoproterozoic to Palaeoproterozoic, west Africa and the Amazonian craton

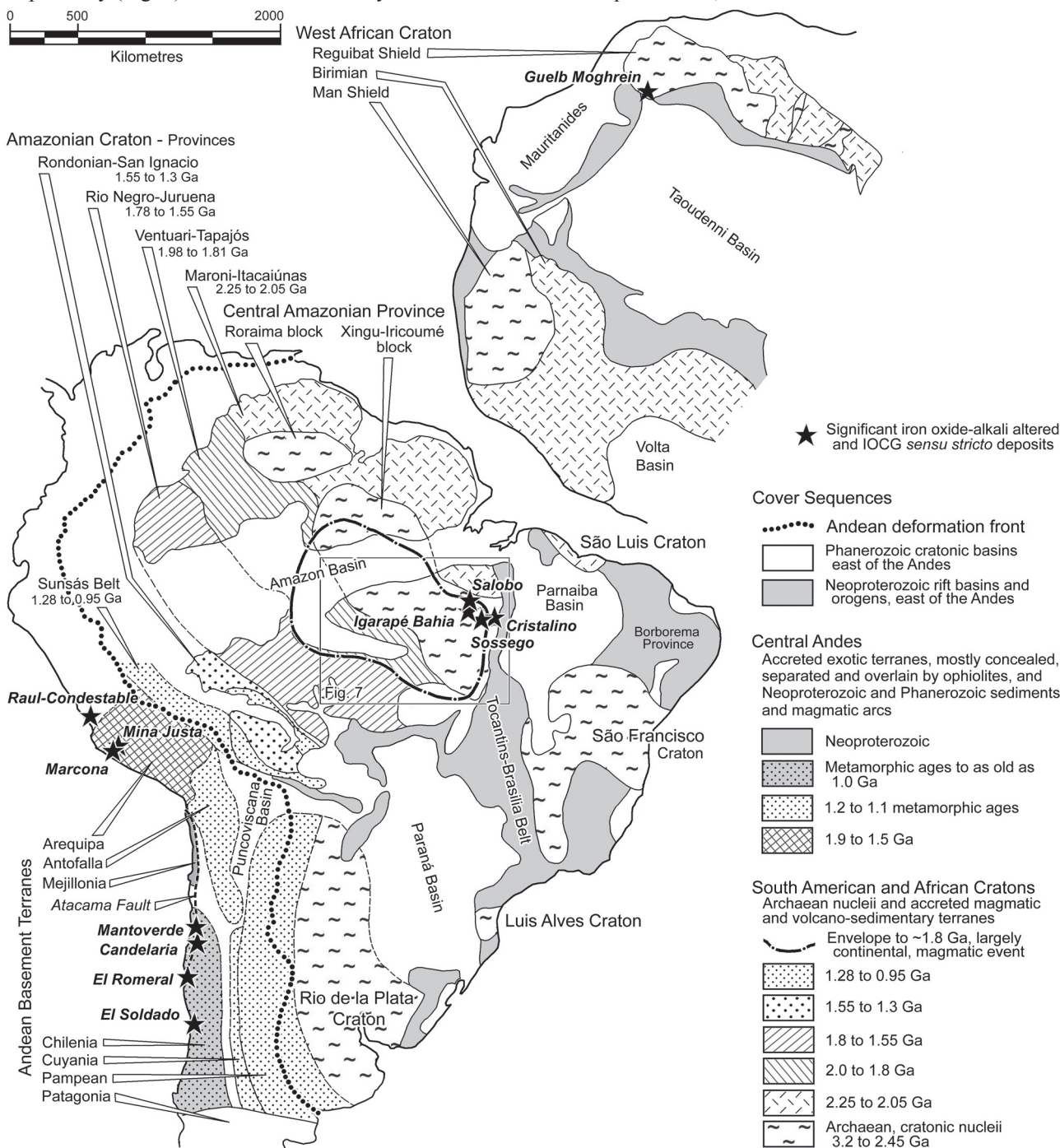


**Figure 6:** The tectonic framework and location of the IOCG *sensu stricto* and other iron oxide-alkali altered ore deposits of South America and West Africa. Those of the West African and Amazonian cratons are located towards the margin of Archaean nuclei of the Reguibat Shield (Guelb Moghrein) and the Xingu-Iricoumé block of the Central Amazonian Province of the Amazonian craton in Brazil (Carajás Mineral Province - Sossego, Salobo, Igarapé Bahia, Cristalino and a number of smaller deposits shown on Fig. 5). Note the outline of the ~1.8 Ga large igneous province, a vast sheet of largely felsic volcanic rocks and comagmatic granitoids that may influence the second generation, but smaller deposits of the Carajás Mineral Province (see also Figs. 4 and 5). The deposits of the Central Andean Belt in northern Chile and southern Perú, while hosted dominantly by Mesozoic (but also some Palaeozoic) rocks, overlie a thick basement composed largely of exotic terranes of Palaeo-, Meso and possibly Neoproterozoic metamorphics, specifically of the Arequipa (Perú) and Chilena (Chile) terranes. These older basement blocks are only very locally exposed, being separated and overlain by Neoproterozoic to Tertiary ophiolites, sedimentary sequences and magmatic arcs (shown on Fig. 6). However, they influence the controlling structures (e.g., the northern Atacama Fault) and the chemical and physical nature of the crust through which ore related fluids are introduced and circulated, as well as the thickness of underlying subcrustal lithospheric mantle. Details plotted are largely after Cordani and Teixeira (2007), Chew *et al.* (2010); Ramos (2008); (2004), Petters (1986).

*Carajás Mineral Province ... cont.*

were contiguous, and the Maroni-Itacaiúnas province and equivalent Eburnean/Birimian terranes of west Africa separated the Central Amazonian province and the Meso- to Neoproterozoic Man and Reguibat Shields of west Africa, the latter of which hosts the ~2.5 Ga Guelb Moghrein IOCG deposit in Mauritania (Fig. 6; Kolb *et al.*, 2010, in this volume; Strickland and Martyn, 2002).

During the Neoproterozoic and early Palaeoproterozoic, the southwestern edge of the Central Amazonian province marked the cratonic margin. The 1.98 to 1.81 Ga Ventuari-Tapajós province was accreted to this margin, and is composed of felsic volcanic and gneissic granitic rocks with juvenile isotopic signatures. This terrane is followed to the southwest by the progressively younger 1.78 to 1.55 Ga Rio Negro-Juruena, 1.55 to 1.3 Ga Rondonian-San Ignacio and 1.28 to 0.95 Ga Sunsás provinces (Fig. 6; Cordani and Teixeira, 2007).

The Itacaiúnas Shear Belt involved 2.85 to 2.76 Ga sinistral, transpressive, strike-slip ductile shearing, 2.7 to 2.6 Ga dextral transtension that produced the Carajás and Cinzento strike-slip fault systems, and a sinistral, transpressive regime that evolved at about 2.6 Ga.

The basement within this structural zone is composed of tonalitic to trondhjemitic gneiss and migmatite of the Mesoarchaeoan Xingu and Pium complexes of 3002±14 Ma protoliths, metamorphosed to granulite facies and extensive migmatites at 2861±12 Ma (e.g., Xavier *et al.*, 2010).

This older basement is overlain by sequences of metavolcanosedimentary and metamorphosed bimodal basic and felsic (but dominantly basaltic) volcanic rocks, iron formations and clastic sedimentary rocks of the 2.76 to 2.73 Ga Itacaiúnas Supergroup, including the 4 to 6 km thick Grão Pará group that is host to the giant, volcanic-hosted, 2.7 Ga Carajás banded iron formation iron deposits. The Itacaiúnas Supergroup is composed of a number of such volcanic sequences, some of which are equivalents whereas there are several tens of m.y. difference in age between others. The volcanic rocks of the Itacaiúnas Supergroup have been variously interpreted to reflect a continental extensional basin environment, or calc-alkaline magmas typical of subduction zones, back-arc basins and continental arcs (see Xavier *et al.*, 2010, this volume, for sources, details and discussion). However, trace element studies suggest crustal contamination of the volcanic rocks (Lobato *et al.*, 2005a), and that they were deposited on attenuated continental crust (Zucchetti, 2007; Zucchetti *et al.*, 2007). The volcanism of the Itacaiúnas Supergroup is part of the major global Neoproterozoic pulse of magmatism representing the most intense period of crustal growth in the geological record (Abbott and Isley, 2002).

This sequence is overlain in turn by poorly deformed platform siliciclastic and carbonatic sedimentary rocks and minor iron formations of the 2.7 to 2.6 Ga Águas Claras Formation cover sequence. All of these metamorphic, volcanic and sedimentary rocks are intruded by a series of granitoids, including 2.76 to 2.74 Ga syntectonic alkaline granites, 2.76 Ga mafic-ultramafic layered complexes, as well as 2.76 to 2.65 Ga gabbro sills and dykes, 2.70 Ga calc-alkaline monzogranite, 2.65 Ga porphyritic dacitic to rhyolitic rocks, 2.57 Ga A-type granites, 2.51 Ga peralkaline, meta-aluminous granitic rocks, and widespread late 'within-plate' A-type, alkaline to sub-alkaline granites associated with 1.88 to 1.87 Ga Palaeoproterozoic extensional events (e.g., Xavier *et al.*, 2010; Grainger *et al.*, 2008).

The Carajás Mineral Province is also located within the eastern sector of one of the largest felsic igneous

provinces in the world (Grainger *et al.*, 2008). This thick, oval-shaped, 1100 × 1400 km, incised but relatively flat-lying sheet of ~1.9 to ~1.8 (and 1.7?) Ga bimodal (felsic and intermediate) volcanic rocks and co-magmatic A-type granites (Figs. 6 and 7) overlaps both the Archaean Central Amazonian and Palaeoproterozoic Ventuari-Tapajós provinces. It covers over 1.2 million km<sup>2</sup> of the southern Amazonian craton and the southern margins of the northern part of the craton (Schobbenhaus *et al.*, 1995). The ~1.8 Ga A-type granites of the Carajás district are part of the eastern margin of this igneous province (Grainger *et al.*, 2008).

The Itacaiúnas Supergroup and the overlying sedimentary rocks of the Águas Claras/Rio Fresco Formations cover sequence, remained relatively stable during deposition (as evidenced by the, extensive, thick, finely banded, but lensoid BIFs), interspersed with recurrent structural subsidence and volcanic activity. This was because by the early Neoproterozoic the Central Amazonian province of the Amazonian craton was sufficiently rigid (stabilised) to retard the development of the unstable keel and dome granite-greenstone tectonics seen at the same period in cratonic nuclei such as the Yilgarn and Superior. The Archaean succession has subsequently been folded into a large "S-shaped" structure, dislocated near its centre by the Carajás Fault (shear zone), and buttressed by large igneous complexes such as the Mesoarchaeoan Pium Complex and Neoproterozoic granitoids (Rosière *et al.*, 2006).

Teixeira *et al.* (2009) interpret the Itacaiúnas Supergroup and related magmatic rocks of the Carajás Mineral Province to represent an intracontinental rift zone, with associated areally extensive, tholeiitic basaltic volcanism and anatexis that are the product of inferred mantle underplating. They suggest this mantle induced magmatism was responsible for the two major iron oxide rich mineralising episode within the Carajás Mineral Province: (1) the ~2.7 Ga volcanic hosted banded iron formations of the Carajás iron deposits, and (2) the multi-pulse 2.74 and 2.57 Ga IOCG deposits of the province. Both episodes are focused on deep transtensional faults. Teixeira *et al.* (2009) and Grainger *et al.* (2008) suggest, the subsequent, spatially overlapping, extensive ~1.8 Ga felsic igneous province resulted in a further phase of IOCG mineralisation and additional deposits in the same province, as outlined below. Teixeira *et al.* (2009) attribute the inferred underplating and magmatism from 2.75 to 2.5 Ga and at 1.8 Ga to mantle plume activity.

The bulk of the Carajás Mineral Province IOCG deposits are distributed in two structurally controlled belts, one to the northwest, associated with a structural corridor along the northern margin of the Itacaiúnas Shear Belt (Salobo, Igarapé Cinzento/Alvo GT46, and Gameleira), and the second on its southern margin to the southeast (Sossego, Cristalino and Alvo 118), while Igarapé Bahia/Alemão is located towards the western central part of the cluster of deposits, between the two main groups, possibly fault controlled in the core of a domal structure. The location of all, with the possible exception of Igarapé Bahia/Alemão, is substantially controlled by major, deep-seated faults/shears (Fig. 8).

Despite evidence for a common evolution of the Carajás IOCG deposits, detailed geochronologic data suggest that their formation may possibly be linked to three metallogenic events at ~2.74, 2.57 and ~1.8 Ga. Dating of ore-related minerals has revealed different ages, even in a single deposit (e.g., Igarapé Bahia, Gameleira and Salobo; Réquia *et al.*, 2003; Tallarico *et al.*, 2005; Pimentel *et al.*, 2003). A temporal relationship has been indicated between the

## Carajás Mineral Province ... cont.

widespread Archaean magmatism (~2.74 Ga) and these deposits, particularly at the Cristalino deposit (Huhn *et al.*, 1999), although robust geochronologic data also suggests an important metallogenetic event at 2.57 Ga (Réquia *et al.*, 2003; Tallarico *et al.*, 2005; Grainger *et al.*, 2008). However, except at Salobo, there is a lack of a clear spatial association between IOCG deposits and magmatism of this latter age in the province (Xavier *et al.*, 2010).

Xavier *et al.* (2010) conclude that, despite the importance of magmatism in providing heat and fluids for the development of extensive hydrothermal systems, the available geochronologic data may not be necessarily correlated to an individual magmatic event. They note that the ages may alternatively be the result of a long-term history of isotopic resetting due to the development and/or reactivation of Archaean ductile or ductile-brittle shear zones and/or Palaeoproterozoic anorogenic magmatism.

Grainger *et al.* (2008), suggest that the IOCG mineralisation of the Carajás Mineral Province can be subdivided into two groups, namely: (1) the larger deposits, which contain 0.2 to 1 Gt @ 0.95 to 1.4% Cu, 0.3 to 0.85 g/t Au, and include Salobo, Igarapé Bahia/Alemão, Cristalino and Sossego. These are dominantly hosted by the lower volcanic sequences and basement gneisses, and occur as pipe- or ring-like, generally breccia bodies that are strongly iron- and LREE-enriched, commonly with anomalous cobalt and uranium, and are quartz- and sulphur-poor, with iron oxides and iron-rich carbonates and/or silicates invariably present. As mentioned above, both 2.74 and 2.57 Ga ages of mineralisation are suggested for those members of this group that have been dated, comparable to the associated granitoids, the latter of which are A-type. (2) A group of smaller, commonly supergene-enriched

copper-gold deposits that generally comprise <50 Mt @ <2% Cu, <1 g/t Au in hypogene ore, with enrichment in granitophile elements such as tungsten, tin and bismuth, and which spatially overlap the Archaean IOCG deposits. These include Breves, Águas Claras, Gameleira and Estrela that are predominantly hosted by the upper sedimentary cover sequence, occurring as greisen-to ring-like or stockwork bodies. They generally lack abundant iron-oxides, are quartz-bearing and contain more sulphur-rich copper-iron sulphides. Precise Pb/Pb dating of hydrothermal phosphate of the Breves and Alvo 118 deposits indicate ages of 1872±7 Ma and 1868±7 Ma respectively, comparable with the adjacent young A-type granites and associated dykes which range from 1874±2 Ma to 1883±2 Ma. It is uncertain whether similar mineralisation occurs within the same 1.8 Ga magmatic complex outside of the Carajás Mineral Province, and if not, why?

### Regional Alteration

The host volcanic rocks to most large Carajás IOCG deposits also contain the major, stratabound, exhalative BIF (jaspilite) iron accumulations of the Carajás Mineral Province. The latter have undergone several stages of hydrothermal hypogene upgrading during the Neoproterozoic and possibly also the Palaeoproterozoic to produce the high grade iron ores of the province (~18 Gt @ >65% Fe; Figueiredo e Silva *et al.*, 2008). Lobato *et al.* (2005) speculate that the Carajás iron deposits could represent an exhalative end-member of the replacive iron oxide phase of the IOCG system in the province, having probably both involved saline fluids of meteoric as well as those of magmatic-hydrothermal origin. Alternatively, or in addition, both Neoproterozoic and late Palaeoproterozoic

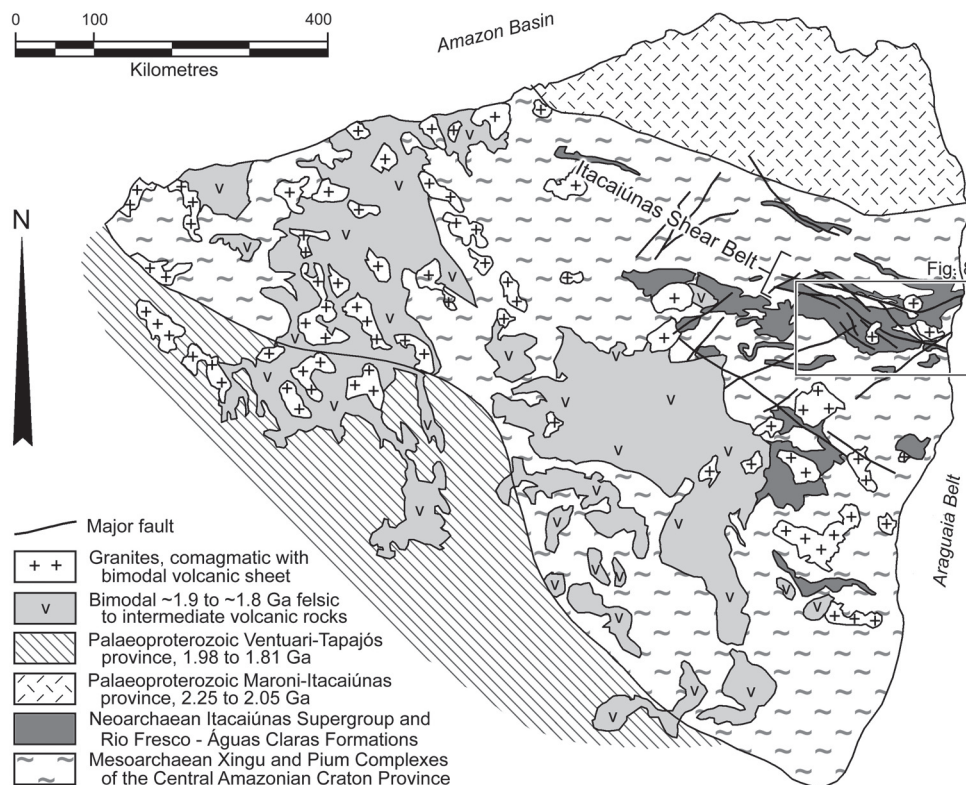


**Figure 7:** The tectonic and geological setting of the Carajás Mineral Province (largely the area of Fig. 5 as outlined) within the southern half of the Xingu-Iricoumé block of the Central Amazonian Cratonic Province. The outline of this figure is shown on Fig. 3. Note the extent of the mafic to intermediate volcanic host sequence of the Itacaiúnas Supergroup and the obliquely cross-cutting structures of the Itacaiúnas Shear Belt which influence the location of deposits, the major examples of which as currently known are clustered in the eastern third of the volcanic belt (for names and locations see Fig. 5). Note also the extent and distribution of the felsic to intermediate volcanic sheet and coeval A-type granites of the giant ~1.8 Ga large igneous province, and the overlap of the latter into the Carajás Mineral Province (after Schobbenhaus *et al.*, 1995 and Cordani and Teixeira, 2007).

## Carajás Mineral Province ... cont.

magmatic-hydrothermal iron oxide-rich fluids responsible for the magnetite of the IOCG deposits may be related to the hypogene upgrading of the BIF ores (Figueiredo e Silva *et al.*, 2008). Hagemann *et al.* (2005) consider the hypogene enrichment of Carajás BIFs (jaspilites) that produced the high grade iron ores, to be the result of iron-replacement by deep fault sourced, magmatic fluids associated with primitive, mantle-sourced, alkaline to hyperalkaline, mafic magmatic rocks, with an associated, very complex array of both compatible and incompatible elements.

The earliest alteration surrounding the Carajás IOCG deposits comprises regional sodic (albite-hematite) and actinolite-rich sodic-calcic assemblages, reflecting high salinity in the early regional hydrothermal fluids. Sodic-calcic alteration was closely controlled by regional ductile-brittle shearing, reflected by preceding mylonitisation and synchronous silicification (Xavier *et al.*, 2010), although the alteration is pervasive, with associated fracture controlled albite. Scapolite and tourmaline are conspicuous within the sodic assemblage in felsic volcanic rocks. Mylonitised metavolcanic rocks are characterised by alternating bands of albite, tourmaline and scapolite. Sodic-calcic assemblages overprint sodic alteration and are dominated by actinolite-albite with accompanying magnetite, calcite, epidote, quartz, titanite, allanite and thorianite, and may have associated massive magnetite bodies, as at Sequeirinho (Monteiro *et al.*, 2007).

Metal leaching from the host rocks during the sodic and sodic-calcic stages was probably enhanced by the high salinity of fluids, and driven by heat from the intrusive episodes recorded. The geochemical ore signatures of the IOCG mineralisation across the province is variable, and strongly dependent upon the chemistry of the leached

host rocks. Actinolite-rich sodic-calcic alteration is commonly associated with large massive magnetite bodies (distinct from the Carajás BIFs) enveloped by apatite-rich actinolite. Regional shear zones, associated with the known deposits, incorporate extensive biotite-scapolite zones representing early sodic alteration synchronous with shearing (Xavier *et al.*, 2010), over intervals of tens of kilometres and widths of a few hundred metres to a kilometre or more e.g., an area in excess of 20 km<sup>2</sup> of scapolite alteration surrounding the Sossego deposits which lies within a 60 km-long, up to several km wide shear zone, schematically shown on Fig. 8, generally following the southeastern margin between the Itacaiúnas Supergroup and basement, controlling the location of the Alvo 118, Sossego-Sequeirinho and Cristalino deposits (Xavier *et al.*, 2010). Sodic alteration is an early phase in all of the deposits, dominating at depth, overprinted by other, more localised ore-related assemblages at higher levels, as explained below.

## Deposit-scale Alteration and Mineralisation

Early regional sodic and sodic-calcic alteration was followed by a potassic phase, magnetite-(apatite) formation, chloritic, copper-gold mineralisation and hydrolytic alteration centred on the individual ore deposits. As these deposits are developed across the province, at varying crustal levels and local settings, there are corresponding variations in geochemical signature (e.g., tourmaline characterises those in metavolcano-sedimentary units as at Salobo and Igarapé Bahia/Alemão; fayalite, garnet and sillimanite in some hosted in ductile shear zones, including Salobo and Igarapé Cinzento/Alvo GT46; while silica and carbonate are important in brittle-ductile conditions such as Sossego and Alvo 118; Xavier *et al.*, 2010).

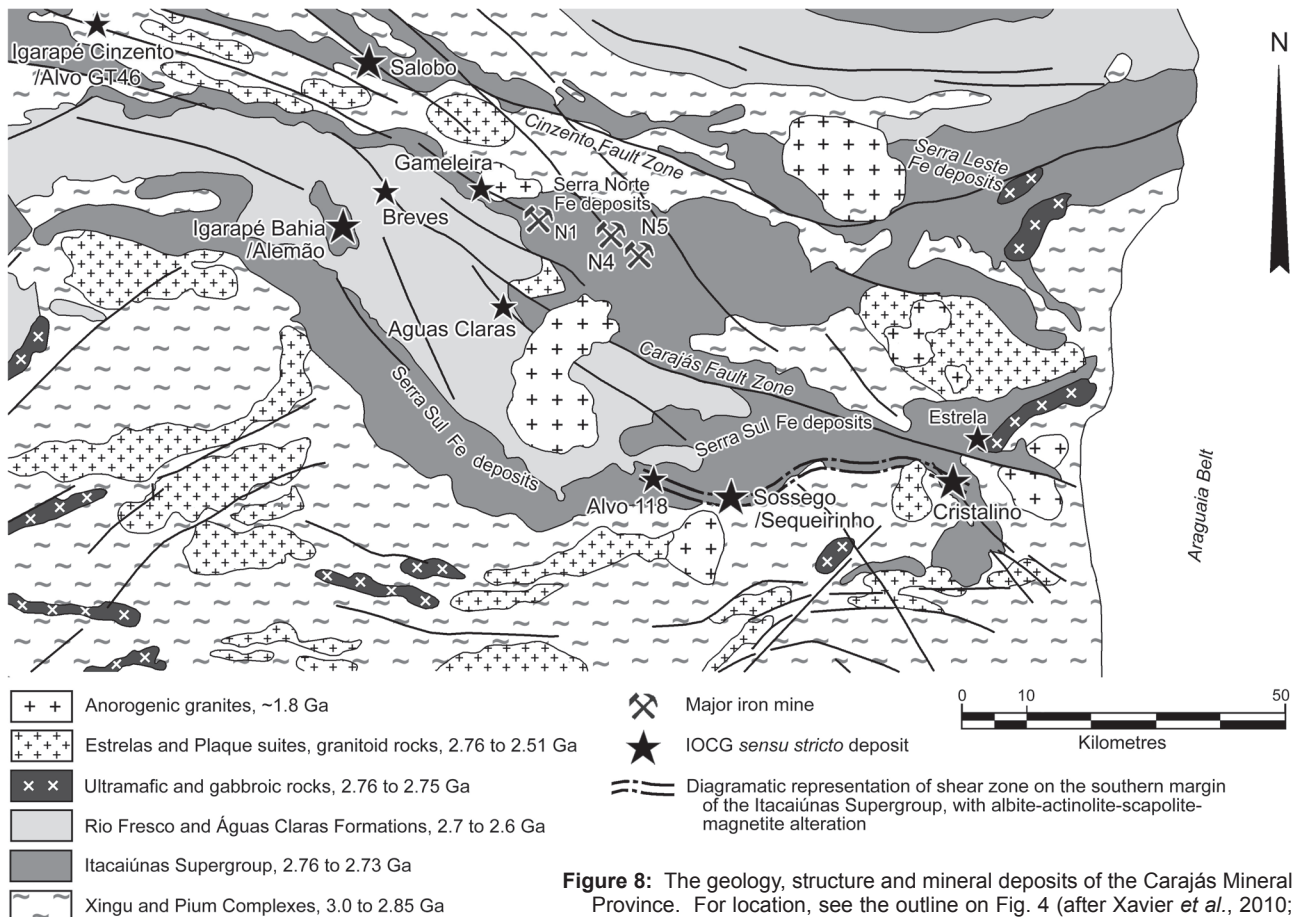


**Figure 8:** The geology, structure and mineral deposits of the Carajás Mineral Province. For location, see the outline on Fig. 4 (after Xavier *et al.*, 2010; Rosiere *et al.*, 2006).

Four types of fluid inclusions have been found in association with the IOCG deposits of the Carajás Mineral Province. These are: (1) hypersaline (35 to 70 wt.% NaCl<sub>equiv.</sub>), moderate to high temperature ( $T_{ht} = 250$  to  $570^{\circ}\text{C}$ ) brines, represented by halite-bearing or multi-solid aqueous inclusions; (2) lower temperature (usually  $<200^{\circ}\text{C}$ ) aqueous fluids with variable salinity ( $<5$  to  $30$  wt.% NaCl<sub>equiv.</sub>) represented by two phase inclusions; (3) low salinity ( $<6$  wt.% NaCl<sub>equiv.</sub>), moderate temperature ( $T_{decrep.} \geq 250^{\circ}\text{C}$ ) aqueous-carbonic ( $\text{CO}_2 \pm \text{CH}_4$ ) fluids; and (4) single phase carbonic ( $\text{CO}_2 \pm \text{CH}_4$ ) fluids (Xavier *et al.*, 2010). Type 1, hot metalliferous, hypersaline brines and lower temperature, low to intermediate salinity type 2 fluids are found at all deposits, while the aqueous-carbonic and carbonic fluids are only present in the west of the province at Salobo, Igarapé Bahia and Gameleira (Réquia and Fontboté, 2001; Ronchi *et al.*, 2001; Dreher, 2004). The lower temperature type 2 fluids predominate in the mineralisation stage and are regarded to represent an influx of surficially derived meteoric water. Ore precipitation was marked by a sharp temperature decrease to  $<300^{\circ}\text{C}$  in all IOCG deposits. Copper-gold mineralisation was invariably introduced in the late stages of all of the IOCG systems of the province, generally controlled by subsidiary brittle or brittle-ductile structures. Thus, Xavier *et al.* (2010) suggest copper deposition might be related to collapse of the early high temperature hydrothermal system, controlled by fluid flow in regional shear zones, and resulting from, or accompanying, the influx of meteoric fluids under hydrostatic, brittle conditions at the brittle-ductile to brittle transition. Stable isotope data do not unambiguously provide evidence for either a magmatic or evaporative/bittern source for type 1 fluids (Xavier *et al.*, 2010).

Individual deposits have been emplaced at differing vertical levels, with varying alteration patterns, although it is possible to construct a model based on progressive overlaps between deposits in the southeastern part of the district. At the deepest levels, regional- to district-scale sodic and sodic-calcic (albite-scapolite at  $\sim 500^{\circ}\text{C}$ ) alteration predominates, with associated magnetite mineralisation. At the next level up, actinolite appears in association with magnetite mineralisation (also at  $\sim 500^{\circ}\text{C}$ ) and sulphides, with the first potassic alteration represented by a relatively narrow biotite fringe to the ore, overprinting the still extensive sodic zone (e.g., Sequeirinho). Higher still, potassic alteration, comprising K feldspar and biotite is progressively more extensively developed at the expense of the earlier, higher temperature sodic assemblage, to become dominant (at  $\sim 460^{\circ}\text{C}$ ), where the first muscovite-sericite (hydrolytic) alteration appears (e.g., the Sossego orebody). In the upper levels (e.g., Alvo 118) chlorite-muscovite-hematite is dominant at temperatures of  $<250^{\circ}\text{C}$ , surrounding potassic remnants (Xavier *et al.*, 2010).

At Alemão, alteration and mineralisation is characterised by an assemblage, emplaced in the order, magnetite, chlorite (with lesser biotite), sulphides (in multiple pulses, dominantly chalcopyrite with subordinate bornite, lesser molybdenite, pyrite, pyrrhotite and minor galena, digenite and covellite), carbonate veining (mainly siderite, with lesser ankerite and ferruginous dolomite, and calcite) and late silica (with carbonate and local free native gold) (Ronzi *et al.*, 2000).

The protoliths and alteration of the deepest ( $\sim 12$  km) example at Salobo on the northwestern margin of the province, is uncertain. Interpretations vary from an iron formation that was metamorphosed to pyroxene-hornfels

facies (Lindenmayer, 1990; Villas and Santos, 2001), or basaltic-andesite and dacite of the Igarapé Salobo Group that have been subjected to extreme iron and potassic alteration at temperatures of  $>550^{\circ}\text{C}$  (Lindenmayer, 2003). Similar, structurally disrupted "iron formations" are distributed intermittently over tens of kilometres of strike length throughout the district (Siqueira and Costa, 1991). The ore zone is associated with a halo of variably magnetite-rich ( $<10$  to  $>50\%$ ) rocks with Mn-almandine, grunerite, Cl-rich hastingsite, fayalite, schorlitic tourmaline, Fe-biotite, allanite and quartz (Réquia *et al.*, 2003; Requia, and Fontboté, 2000). The ore occurs within strongly iron-potassic altered rocks in two main zones: (1) massive garnet-biotite-fayalite-grunerite accompanied by generally  $>50\%$  magnetite, minor graphite and fluorite, and (2) a foliated, granoblastic, almandine-biotite-grunerite-plagioclase-quartz assemblage with 10 to 50% magnetite. There is a direct relationship between copper and iron grades (Viera *et al.*, 1988; Souza and Vieira, 2000).

### Structural Control and Brecciation

Most of the known IOCG deposits of the Carajás Mineral Province are located along, or adjacent to, a regional shear zone that defines the contact between the metavolcano-sedimentary units of the host Itacaiúnas Supergroup and basement rocks of the Xingu Complex.

The major westnorthwest trending Cinzento shear zone, in the northwestern sector of the province, hosts the Salobo and Igarapé Cinzento/Alvo GT46 deposits. Salobo is entirely within the Cinzento shear zone, emplaced at  $\sim 12$  km depth, under brittle-ductile conditions, resulting in lenticular shaped ore shoots, with little brecciation (Souza and Vieira, 2000).

In the southeastern sector, an  $\sim 60$  km-long, up to several kilometres wide, overall east-west-striking shear zone, characterised by biotite-scapolite mylonites, controls the location of the Alvo 118, Sossego-Sequeirinho and Cristalino deposits, together with several other minor occurrences and a number of large, barren massive magnetite bodies (Fig. 8; Xavier *et al.*, 2010; Monteiro *et al.*, 2008).

In the Sossego-Sequeirinho district, the latter deposit comprises an "S" shaped, tabular orebody, whose tips are hosted by separate, parallel, sub-vertical eastsoutheast-trending shears in foliated granitoids and schists. These are linked by an offsetting northeast-southwest sinistral fault zone that hosts the bulk of the deposit within mineralised breccias. These two directions are the dominant structural trends in the district (Domingos, 2009). Intense hydrothermal alteration within a few hundred metres into the hanging wall of high angle faults belonging to these two structural trends, surrounds the other ore deposits at Sossego-Sequeirinho. Rocks in the immediate footwall of these same faults have been intensely mylonitised and subjected to biotite-tourmaline-scapolite alteration (Monteiro *et al.*, 2008).

Within the Carajás Mineral Province there are a number of variations in the occurrence and style of brecciation associated with IOCG mineralisation. No obvious ore related brecciation is recorded at the shear zone hosted, deeply emplaced Salobo deposit (Souza and Vieira, 2000).

The Igarapé Bahia deposit comprises three orebodies that are spatially disposed within a breccia unit that defines a semicircular shape at the surface, resembling a collapsed ring complex with a diameter of approximately 1.5 km. The breccia unit occurs as a 2 km long by 30 to 250 m thick string of fault dislocated bodies on the southern,

*Carajás Mineral Province ... cont.*

northeastern and northwestern sections of this structure, each dipping steeply outwards, nearly concordant with the metavolcanic-sedimentary wall rocks (Tallarico *et al.*, 2005). Each is situated at the interface between metamorphosed sedimentary/volcaniclastic and volcanic rocks, commonly brecciated near the contact with ore. High grade primary copper-gold mineralisation is largely restricted to the breccias, with millimetric to centimetric clasts of varied composition (BIF, meta-volcanic, meta-volcaniclastic and meta-sedimentary rocks) in a hydrothermal matrix containing copper-sulphides (chalcopyrite and bornite with minor molybdenite, digenite and pyrite), magnetite, carbonate (siderite to calcite), fluorite, gold, uraninite, apatite, REE minerals, tourmaline, stilpnomelane and ferropyrrosomalite (Tazava, 1999; Tazava and Oliveira, 2000). Much of the mined ore at Igarapé Bahia was strongly leached to form a lateritic gold deposit above the base of oxidation, passing down into refractory primary copper-gold sulphide mineralisation.

The **Alemão** deposit is a down-faulted, hypogene magnetite-copper-gold-rich body, that comprises a deeper, down-plunge continuation of the northwestern segment of the Igarapé Bahia mineralised structure, below the base of oxidation. Mineralisation at Alemão is represented by two classes of hydrothermal breccia: (1) magnetite-sulphide-breccia ore, composed of both massive bands of magnetite and chalcopyrite, and by polymictic breccias with clasts of volcanics, tuffs and banded iron formation, enclosed within a matrix of magnetite, chalcopyrite, siderite, chlorite, biotite and amphibole; and (2) chlorite-sulphide breccia ore, composed of angular to sub-angular clasts of chloritic, brecciated volcanic rocks with chalcopyrite, bornite, pyrite, chlorite, siderite, ankerite, tourmaline and molybdenite, both within the matrix and disseminated through the rock.

At **Cristalino**, copper-gold mineralisation is associated with mafic to felsic volcanic rocks overlain by (the Carajás) iron formation all of which have been locally brecciated. Mineralisation occurs as quartz-carbonate breccias, vein-stockworks, and to a lesser degree, as disseminations, and comprises chalcopyrite, pyrite, magnetite, marcasite, bravoite, cobaltite, millerite, vaesite and gold, with subordinate hematite, bornite, covellite, chalcocite, molybdenite and sphalerite (Huhn *et al.*, 1999).

At the **Sossego-Sequeirinho** orebodies, much of the mineralisation is associated with brecciation. At the deeper Sequeirinho deposit, an "S" shaped, tabular breccia is developed in a link fault between parallel two shears (which control the tips of the "S"). This breccia contains rounded fragments of massive magnetite and actinolite within a matrix of hydrothermal minerals. The development of the matrix commenced with coarse-grained actinolite, apatite and magnetite (a later generation to the sodic-calcic phase clasts), followed by epidote, chlorite, quartz, calcite and sulphides. Pyrite is the dominant early sulphide, overgrown by chalcopyrite, which also replaced magnetite. At the more shallowly emplaced Sossego orebody, sulphides are largely restricted to sub-vertical breccia pipes that contain open-vugs. These breccia bodies are sub-circular in plan, with sharp outer contacts, and a halo of radiating stockwork veins. The breccias are dominantly clast supported, with angular to sub-angular blocks (<0.5 to >10 cm) of locally derived host granophyric granite within a matrix of magnetite, actinolite, biotite, apatite, calcite, epidote with lesser pyrite and chalcopyrite (Domingos, 2009; Monteiro *et al.*, 2007; Xavier *et al.*, 2010).

## Central Andean Coastal Belt

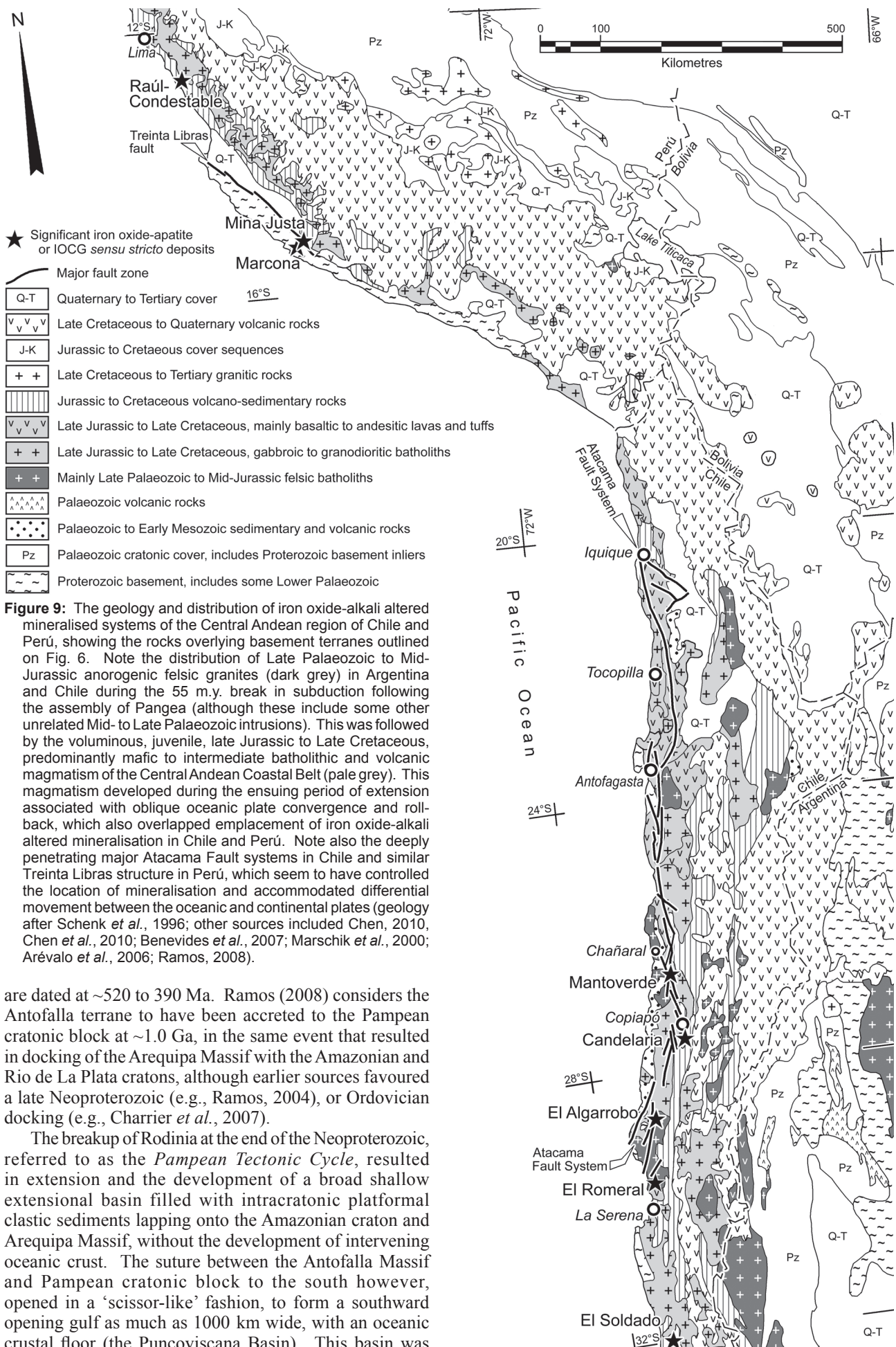
### Crustal Setting

The significant IOCG *sensu stricto* and other iron oxide-alkali altered deposits of the Central Andean Coastal Belt of Chile and Perú, including *Candelaria* (Marschik *et al.*, 2000; Marschik and Fontboté, 2001), *Mantoverde* (Rieger *et al.*, 2010; 2010a; Benevides *et al.*, 2007), *Raúl-Condestable* (de Haller *et al.*, 2006), *Marcona* and *Mina Justa* (Chen *et al.*, 2010; 2010a), fall within a Late Jurassic to Early Cretaceous volcano-plutonic belt (Sillitoe, 2003). This belt, which is characterised by voluminous tholeiitic to calc-alkaline volcanic piles and plutonic complexes of primitive mantle origin gabbro to granodiorite, is associated with an extensional to transtensional event when the underlying crust was attenuated and subjected to high heat flow. All of the intrusive rocks are oxidised and belong to the magnetite series (Charrier *et al.*, 2007; Sillitoe, 2003 and sources cited therein).

The IOCG *sensu stricto* ores have a close temporal and spatial association with the plutonic complexes of the volcanic belt and with major, broadly coeval, longitudinal fault systems. They share the belt with massive iron oxide-apatite, vein-type and manto copper-silver (with or without accompanying iron oxides), and small to moderate porphyry copper-gold deposits (Sillitoe, 2003; Chen, 2010).

The tectonic and geological history contributing to, culminating in, and then overprinting the mineralising episode, can be summarised as follows.

The Central Andean segment of western South America has been an active margin much of the time from the Mesoproterozoic, and is underlain by a series of accreted autochthonous terranes, and Proterozoic to Tertiary sedimentary and volcanosedimentary sequences. The main elements of the continent are the large Mesoarchean to late Mesoproterozoic Amazonian craton to the north, and the contiguous Rio de la Plata craton and Pampean cratonic terrane to the south (Fig. 6). The Pampean terrane is interpreted to have docked with both the Amazonian craton to the north, and the Rio de La Plata craton to the east during the Mesoproterozoic to form the original proto-South America (Ramos, 2008). The youngest rocks on the western Amazonian craton are deformed 1.28 to 0.95 Ga passive margin sedimentary rocks and syn- to late-tectonic 1.0 Ga granitic suites of the Sunsás province, outboard of the 1.55 to 1.3 Ga Rondonian-San Ignacio province (Fig. 6; Chew *et al.*, 2010). To the west of this, extending from 200 km south of Lima (Perú) to the Chilean border, is the first of the accreted terranes, the 800 × 100 km Arequipa Massif, the partially exposed section of the broader Arequipa Terrane (Fig. 6), composed of granulites with dioritic gneisses, basic meta-igneous rocks and migmatites dated at 1.9 Ga in the north, with juvenile magmatism further south of 1.5 to 1.4 Ga and rejuvenated metamorphic ages of around 1.0 Ga. This terrane was accreted to the Amazonian craton as part of the assembly of Rodinia at around 1.0 Ga, sandwiched by the advancing Laurentia (North America) and coincident with the Sunsás province orogenesis. The massif was subsequently intruded by substantial Ordovician (~470 Ma) granitoids of the Coastal Batholith in Perú (Ramos, 2008). A second block, the Antofalla Terrane, is contiguous with the Arequipa Massif on its southern margin, extending to around 100 km south of Antofagasta. This terrane is composed of gneisses, amphibolites and migmatites dated at ~1.2 to 1.0 Ga in the north, while further south high-grade metamorphic rocks and granitoids



are dated at ~520 to 390 Ma. Ramos (2008) considers the Antofalla terrane to have been accreted to the Pampean cratonic block at ~1.0 Ga, in the same event that resulted in docking of the Arequipa Massif with the Amazonian and Rio de La Plata cratons, although earlier sources favoured a late Neoproterozoic (e.g., Ramos, 2004), or Ordovician docking (e.g., Charrier *et al.*, 2007).

The breakup of Rodinia at the end of the Neoproterozoic, referred to as the *Pampean Tectonic Cycle*, resulted in extension and the development of a broad shallow extensional basin filled with intracratonic platformal clastic sediments lapping onto the Amazonian craton and Arequipa Massif, without the development of intervening oceanic crust. The suture between the Antofalla Massif and Pampean cratonic block to the south however, opened in a 'scissor-like' fashion, to form a southward opening gulf as much as 1000 km wide, with an oceanic crustal floor (the Puncoviscana Basin). This basin was

*Central Andean Coastal Belt ... cont.*

filled with several thousand metres of Neoproterozoic to Early Ordovician siliciclastic sediments, minor carbonate and mafic volcanic rocks cut by early Cambrian granitoids that form a narrow magmatic arc. To the south, this basin was open to the sea where an extensive carbonate shelf was developed grading westwards into fine siliciclastic sediments deposited on a basement of oceanic crust. Similar siliciclastic sequences were deposited to the west of the Antofalla Massif (Ramos, 2008).

The *Famatinian Tectonic Cycle*, a period from the late Cambrian to Early Devonian involved contraction, amalgamation and orogenesis, and included the development of a number of corresponding significant magmatic arcs of lower to middle Palaeozoic age. During the Ordovician, a compressive regime had been re-established and the Antofalla Massif was again accreted to the Pampean cratonic block by eastward subduction of the intervening oceanic crust before the beginning of the Silurian. During this period, and after the accretion, eastward subduction of the oceanic plate to the west had proceeded below both the Arequipa and Antofalla massifs, and below the Pampean cratonic block to the south of the latter. An additional exotic micro-continent, the Cuyania (Precordillera) terrane, believed to be derived from Laurentia after the Rodinia breakup, docked with the Pampean cratonic block in the Mid- to Late Ordovician, immediately to the south of the Antofalla Massif (Ramos, 2008). The Cuyania terrane comprises Grenville age (~1 Ga) basement and an exotic Cambrian to Ordovician cover succession (Cawood, 2005). A carbonate platform sequence was developed on this shallowly submerged microcontinent (Ramos, 2004). Following collision, marked by an ophiolitic suture zone, subduction stepped back and continued below the Cuyania terrane until at least the Mid- to Late-Devonian, when the exotic Chilenia terrane collided with the amalgamated Cuyania-Pampean cratonic block over the same interval of the continental margin. The Chilenia terrane is also masked by a Lower Palaeozoic passive margin foreland wedge, although minor erosional windows reveal schists and gneisses with metamorphic(?) ages as old as 1.0 Ga (Ramos and Basei, 1997). A further sliver of Laurentia, the Mejillonia terrane, largely masked by younger rocks, but outcropping sporadically along the coast from Antofagasta to Iquique, is interpreted to have accreted to the immediate west of the Antofalla Massif between 500 and 439 Ma, as indicated by subduction-obduction of ophiolites, and thrusting and folding of sedimentary rocks.

The succeeding *Gondwana Tectonic Cycle* commenced in the Mid-Devonian and continued to the Late Permian. At the close of the Famatinian Cycle, subduction retreated to near the current coastline, the subducting plate dipping east below the now amalgamated Arequipa, Antofalla, Mejillonia and Chilenia terranes, accompanied by the development of a growing accretionary prism and a complex sequence of both "I" and "S" type granitoids and associated volcanic rocks which are exposed in various parts of the Cordilleran Frontal and Coast Ranges. An arc is considered to have essentially been centred on the present day high cordillera, flanked progressively to the west by a forearc basin and accretionary complex (Charrier *et al.*, 2007). To the south of Santiago, the pattern of north-south elongated slivers of exotic terranes is broken by the parautochthonous Patagonian Terrane (Fig. 6), which collided with Gondwana from the south during the Early Permian, across an east-west suture, in the final stages of Pangean assembly (Charrier *et al.*, 2007; Ramos 2008).

The *Pre-Andean Tectonic Cycle* that followed, persisted from the latest Permian to earliest Jurassic and marks a 55 m.y. hiatus in orogenic magmatism between the amalgamation of Gondwana/Pangea and the commencement of its break-up. Over this period, following the final consolidation of the supercontinent, plate movement and subduction either ceased or was seriously curtailed. During this period, heat accumulated in the upper mantle below western Gondwana, melting of the lower crust, producing of enormous volumes of magma along the northern Chilean coast through to northern Argentina. This in turn resulted in crustal down-warping, extension of the upper, brittle crustal layer, and the development of extensional basins to produce the characteristic silicic magmatic activity and north-northwest oriented extensional basins of the continental margin. The orientation of these basins has been attributed to structures related to the sutures that bound the exotic terranes of the region (Charrier *et al.*, 2007 and sources cited therein). This magmatic activity includes substantial S- and A-type granitoids in north-western Argentina including the high Andes to the north, while similar aged intrusive rocks in the Coastal Range from north of Copiapó to south of La Serena in Chile may be of similar origin (Fig. 9; Charrier *et al.*, 2007 and sources cited therein).

The succeeding *Andean Tectonic Cycle* lasted from the late Early Jurassic to the present and corresponds to the break-up of Gondwana, with the eventual renewal of subduction activity, largely accommodating the split between South America and Africa, in the process generating Andean arc magmatism. Central and northern Chile (north of ~40°S), is characterised by the development of a magmatic belt parallel to, and on the western edge of the continental margin, bounded to the east by a backarc basin (Fig. 9). There was a gradual eastward migration of the axis of magmatic activity from the Late Cretaceous to Early Palaeogene, and development of foreland basins on the eastern side, to the current architecture from the Late Paleogene to the present (Charrier *et al.*, 2007).

During the first stage of the Andean Tectonic Cycle in northern Chile, magmatic activity commenced with a pile of as much as 5 to 10 km in thickness of subaerial to locally shallow submarine basaltic-andesitic, to andesitic to dacitic volcanic rocks, the Mid to Late Jurassic La Negra Formation and equivalents. This arc extended from near the Peruvian border in the north, to La Serena in the south. It is mostly conformable with the Pre-Andean anorogenic volcanic sequences and is host to IOCG-like vein mineralisation north of Antofagasta and the Mantoverde deposit further to the south. South of 26°S (Chanaral) to near 29°S (La Serena), succeeding Late Jurassic to Early Cretaceous arc volcanism is represented by up to 3 km of basaltic-andesitic, to andesitic to dacitic volcanic rocks of the Punta del Cobre Group that host the Candelaria-Punta del Cobre IOCG deposits (Marschik and Fontboté, 2001; Sillitoe, 2003). These volcanic and pyroclastic rocks extend eastward into the back-arc Tarapacá basin and interfinger in the east with carbonate rocks of the stable continental margin (Mpodozis and Ramos, 1990).

North of 27°S (Copiapó) the Tarapacá basin is dominated by marine carbonate and continental terrigenous clastic sedimentary rocks, with some interbedded volcanic rocks. South of La Serena, the Central Chile back-arc basin contains Jurassic marine carbonates, which includes a thick gypsum unit, overlain by Late Jurassic red beds and then by Early Cretaceous marine carbonate rocks. The arc to the west in this region is represented by an intra-arc

*Central Andean Coastal Belt ... cont.*

extensional basin containing up to 5 km of Early Cretaceous volcanic and volcanoclastic rocks of high-K calc-alkaline to shoshonitic basalt to andesite (Sillitoe, 2003; Ramos, 2000; Mpodozis and Ramos, 1990).

During the Late Jurassic, the changing tectonic pattern resulted in the back-arc basins in northern Chile being uplifted and progressing from marine to well developed evaporitic facies (Oyarzun *et al.*, 2003).

The Mid Jurassic to Early Cretaceous volcanic pile in Northern Chile is accompanied by voluminous, broadly contemporaneous, plutonic tholeiitic to calc-alkaline complexes of noritic and gabbroic, to quartz diorite and leucocratic tonalite and granodiorite in composition. These rocks are of primitive, mantle derived parentage in a series of batholiths, typically >50 km long. They are known to have been emplaced as a series of short pulses of between 3 and 15 m.y. where extensive dating has been undertaken between 25°30' and 27°30'S (Dallmeyer *et al.*, 1996; Lara and Godoy, 1998; Grocott and Taylor, 2002; Sillitoe, 2003). At least some of these batholithic masses (e.g., in the Candelaria mine area) are demonstrated to be gently dipping, tabular bodies, emplaced by roof uplift-floor depression mechanisms during regional extensional deformation (Arévalo *et al.*, 2006), although others from the Late Jurassic, may be steeply dipping slabs, localised by ductile shear zones (Grocott and Wilson, 1997).

In southern Perú, thick accumulations of mostly basaltic-andesitic volcanic arc rocks are found, similar to those in northern Chile, e.g., the Río Grande-Chala Formations, extending into the analogous back-arc basins which are filled with Early Jurassic basaltic volcanic (~1500 m) and several kilometres of Mid to Late Jurassic terrigenous sedimentary rocks in the Arequipa basin to the south, and high-K calc-alkalic and shoshonitic basalt and basaltic andesite with subordinate dacite and rhyolite in the contiguous Cañete basin to the north. These volcanic successions are underlain by clastic-carbonate rocks with very minor evaporites (Caldas, 1978; Romeuf *et al.*, 1993; Palacios *et al.*, 1992). The Middle to Upper Jurassic units in this succession, which host significant Early Cretaceous IOCG deposits, e.g., Mina Justa (Perú), were intruded by gabbroic plutons and dykes (Atherton and Webb, 1989; Pichowiak *et al.*, 1990), and then, from the Early Cretaceous, by the enormous dioritic to tonalitic Coastal Batholith (Pitcher and Cobbing, 1985; Grocott and Taylor 2002; de Haller *et al.*, 2006), which probably formed through wrench tectonics along crustal lineaments (Polliand *et al.*, 2005).

Sillitoe (2003) notes that the Jurassic and Early Cretaceous arc and intra-arc successions of the Coastal Cordillera are predominantly basaltic-andesite to andesite in composition, with subordinate dacite and rhyolite, which impart a bimodal signature. They range from tholeiitic to calc-alkaline in composition, but may be locally high-K calc-alkaline and shoshonitic. They apparently have a greater proportion of lava than pyroclastics, and lack volumetrically significant felsic volcanic rocks. There is also little evidence of major volcanic edifices typical of subduction related arcs, and the regime may well be more akin to a flood basalt province (Sillitoe, 2003). All of the intrusive rocks are oxidised and belong to the magnetite-series (Sillitoe, 2003). Sillitoe (2003) outlines isotope signatures and trace element characteristics of the Mid Jurassic to Early Cretaceous volcanic and intrusive rocks, consistent with maximal extension and crustal thinning, indicating that during the Early Cretaceous they were

derived from a subduction fluid modified mantle source without significant crustal contamination (e.g., Williams *et al.*, 2005).

In both Chile and Perú, these rocks are underlain by a basement of Palaeozoic sedimentary, volcanic and felsic intrusive rocks, which in turn overlie and separate Mesoproterozoic metamorphic rocks of the Arequipa, Antofalla and Mejillonia terranes (as described previously). The homoclinal dip of the La Negra volcanic succession, the total absence of tight folds and the observation that the volcanic rocks generally only exhibit low-grade, non-deformational hydrothermal-burial metamorphism (Aguirre, 1988; Atherton and Aguirre, 1992), has been taken to imply deposition under extensional conditions (Charrier *et al.*, 2007 and sources quoted therein). A regional extensional regime is also evidenced by geochemical data and the enormous thickness of volcanic rocks and back-arc sediments. This extension was accompanied by uplift of the asthenospheric wedge beneath the arc and back-arc basin, and is interpreted to reflect slab-steepening and roll-back of the subducting Phoenix plate slab over a period of ~90 m.y., from the late Early Jurassic to late Early Cretaceous, following the prolonged pause in subduction during the Pre-Andean cycle (Charrier *et al.*, 2007) and consequent cooling (and probable detachment) of the cold, dense, brittle slab.

It is suggested here that during the Pre-Andean tectonic cycle the prolonged break in subduction eventually resulted in the detachment of the cooled slab, triggering delamination and detachment of SCLM below the thickened leading edge of the adjacent continental crust (e.g., Fig. 2b). This led to upwelling of asthenospheric mantle and decompression melting to form an under-/intraplate magma chamber below the thinned lithosphere, anatectic melting of the lower crust, and production of anorogenic magmatism during the Pre-Andean cycle. At the beginning of the Andean cycle, the commencement of the advance of the now cooled, heavy Phoenix plate resulted in roll-back, and extension in the crust. By then the under-/intraplate had been fractionating for some time, and could release less dense fractions to exploit transcrustal fractures consequent upon the extension/transensional regime (e.g., the Atacama fault and related systems), to release large quantities of magma. The Phoenix plate, while rolling-back, was still sinking steeply and undergoing partial melting to fertilise the asthenospheric wedge and promote melting to recharge the under-/intraplate magma chamber and feed the magmatism within the crust.

This extensional phase was closed by a pulse of compressive deformation in the Late Cretaceous, which inverted the former back-arc basins and created a major regional unconformity (Charrier *et al.*, 2007).

Deformation in central and northern Chile during the late-Early Jurassic to late-Early Cretaceous was principally concentrated along the major, Atacama Fault Zone which developed during this stage as a deeply penetrating, continental-scale, strike-slip fault that can be traced for >1000 km, from Iquique in the north, to south of La Serena in the south, and runs through the plutonic rocks of this period, suggesting a reduction of crustal strength caused by the high heat flow. Both ductile and brittle deformation, and dextral (transensional) and sinistral (transpressional), as well as late vertical displacement is recognised. Two other structures, the ductile to brittle Tigrillo and Chivato fault systems are found to the west and east respectively of the Atacama fault. These three fault zones, which together

*Central Andean Coastal Belt ... cont.*

mark progressive younging to the east, had a marked control on the development of the associated Tarapacá and Central Chile basins in Chile, while comparable structures e.g., the deeply penetrating Treinta Libras fault system, are associated with the Arequipa-Cañete basin in southern Perú (Caldas, 1978; Atherton and Aguirre 1992; Sillitoe, 2003).

During the roll-back period, the advancing Phoenix plate behind the steepening slab approached the South American continent obliquely from the northnorthwest, from a generally northeast-southwest oriented spreading centre (Arévalo *et al.*, 2006). This produced direct strike-slip movement on the Treinta Libras fault system in Perú, parallel to the direction of approach, while the oblique advance towards the Chilean Coastal Belt would have caused transtensional-dextral and transpressional-sinistral displacement on the Atacama Fault respectively during extension and compression.

Both the axis of Mid Jurassic to Early Cretaceous magmatism and associated IOCG *sensu stricto* and iron oxide-apatite and other iron oxide-alkali altered deposits are diachronous, gradually migrating eastward with time (Sillitoe, 2003). This mineralisation, which occurs as either veins, hydrothermal breccias, replacement mantos, calcic "skarns" or a composite of more than one of these forms (which includes most of the larger examples), appears to have a close relationship with both plutonic complexes and broadly coeval fault systems. Mineralisation was introduced in two main periods, including from ~175 to 156 Ma (e.g., Marcona magnetite, Perú and the smaller vein system Cu deposits, north of Antofagasta in Chile, such as those near Tocopilla), and 120 to 112 Ma (e.g., Raúl-Condestable in Perú; Mantoverde and Candelaria near Copiapó in Chile). Other significant mineralisation includes the 140 Ma hematitic mantos at Mantos Blancos which lie to the south and east of the vein deposits north of Antofagasta; Chilean Iron Belt deposits, south of Copiapó and closer to the coast, which were emplaced between 130 and 116 Ma (e.g., El Romeral and El Algarrobo); and the El Soldado manto, further to south at 108 Ma. The Mina Justa copper deposit 3 to 4 km east of Marcona in Perú is dated at 109 to 95 Ma (all of these dates and sources are quoted in Chen, 2010 and Chen *et al.*, 2010).

A major change in plate interaction along the continental margin in the early-Late Cretaceous, was caused by the commencement of very rapid oceanic crust production at the mid-ocean ridges in both the Pacific and Atlantic oceans, and reduction of the slab-subducting angle below South America. This led to a period of intense contraction, emergence of the continental margin, inversion and consequent uplift and erosion of the Jurassic to Early Cretaceous backarc basins, the eastward migration of the axis of magmatism (several tens to a 100 km inland from the present coast), the formation of a continental foreland basin to the east and a wide forearc basin to the west. This activity produced more intense magmatic activity resulting in major plutons and abundant andesitic to rhyolitic-dacitic volcanic rocks, frequently associated with large calderas in a dominant extensional/transtensional regime, due to a very oblique convergence rate between the northward approaching Farallon (beneath the Pacific Ocean) and the South American plates (Charrier *et al.*, 2007 and sources quoted therein). By the early Miocene, the Nazca plate was being subducted below South America, with an increasing convergence rate from 49.5 to 42 Ma, until by 26 Ma the approach direction was almost orthogonal east-west directed.

The convergence rate increased to a maximum at 12 Ma. The main post-Incaic porphyry copper deposits of the Andean belt were formed during the Late Eocene to Oligocene north of La Serena and Late Miocene to Pliocene to the south.

This extended description illustrates the setting of the Mid Jurassic to Early Cretaceous rocks of the Central Andean Coastal Range above a complex collage of Palaeozoic to Mesozoic arcs and underlying exotic terranes of varying ages (from Palaeo- to Mesoproterozoic) and diverse compositions, separated by an array of sutures. All of these characteristics influence the composition and emplacement of any anorogenic magmatism, magma contamination, circulated fluids, structural framework or location of intrusions and volcanic conduits.

### ***District- to Deposit-scale Alteration and Mineralisation***

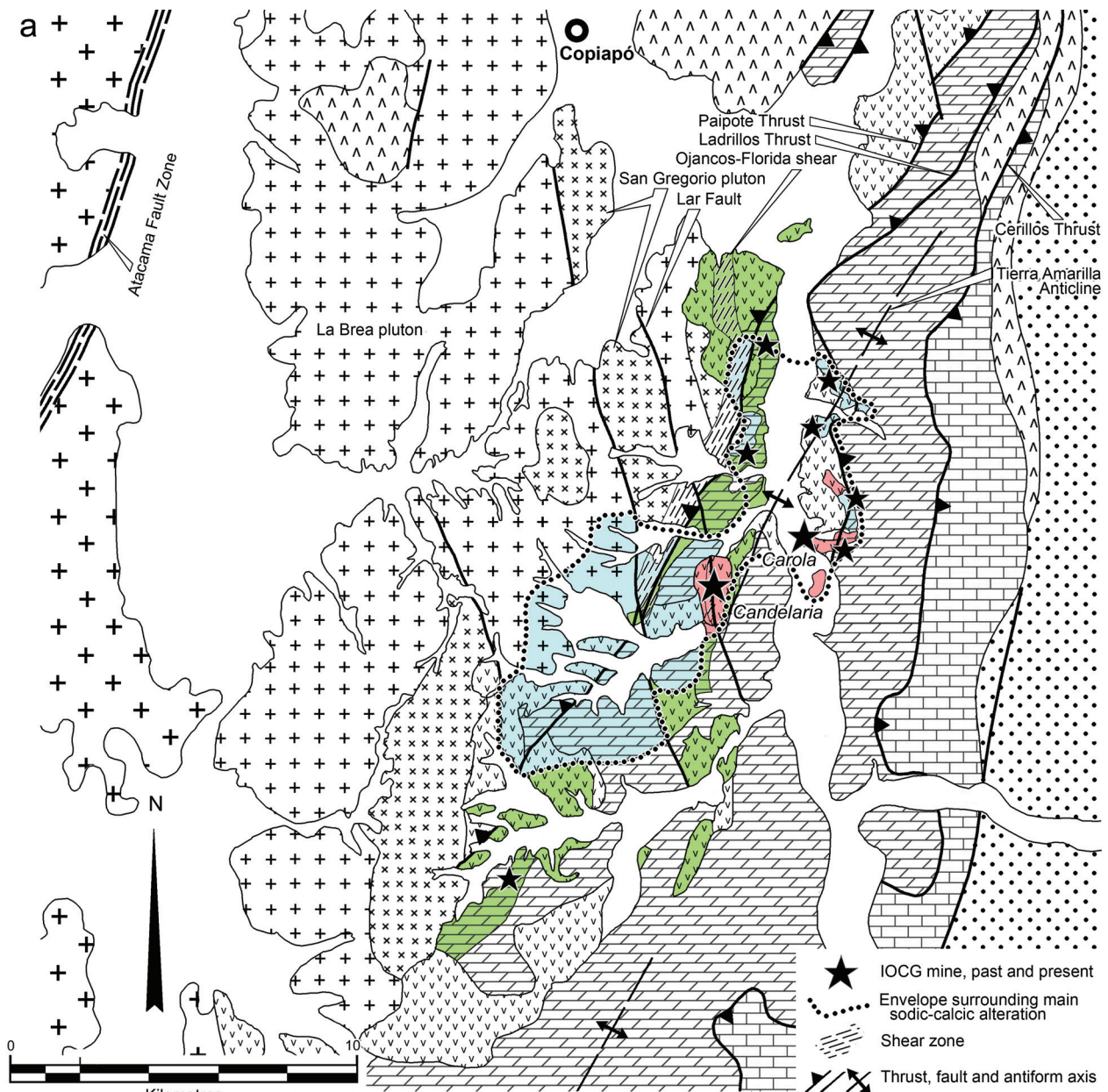
The iron oxide-alkali altered mineralised systems and deposits of the Central Andean Coastal Belt have been subdivided into a number of styles, including veins, hydrothermal breccias, tabular replacement bodies (mantos) and calcic-skarns, and composite deposits comprising two or more of the preceding. The veins tend to be hosted by intrusive rocks, particularly gabbrodiorite and diorite, whereas the larger composite bodies (e.g., *Candelaria*) are within volcanosedimentary sequences up to several kilometres from a pluton contact, intimately associated with major fault structures. All are accompanied by combinations of sodic, calcic, potassic and iron oxide alteration (Sillitoe, 2003).

During the period from 176 to 95 Ma, extensive, district-wide alteration events took place in southern Perú and northern Chile. It is recognised that the main IOCG *sensu stricto* mineralisation in northern Chile (e.g., *Candelaria*, Mantoverde) commonly postdates albite- and biotite-magnetite alteration, while magnetite-actinolite-albite-plagioclase mineralisation and alteration characterises the magnetite-apatite deposits of the Chilean Iron Belt (e.g., El Romeral), all of which are generally copper and gold (-silver)-barren (Chen, 2010).

Following the district scale alteration assemblages associated with the other main iron oxide-alkali altered mineralised systems of the Coastal Belt in northern Chile and southern Perú, each of the mineralised centres where copper±silver±gold was deposited, was accompanied by more restricted envelopes of alteration related to that mineralisation.

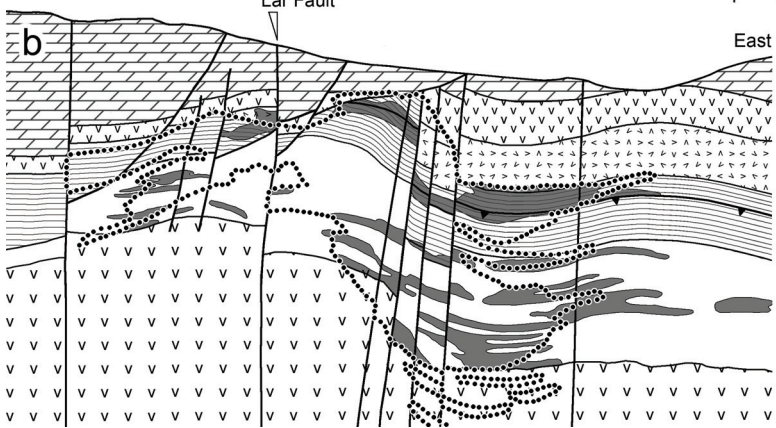
The *Candelaria* deposit lies within the almost continuously altered, but discontinuously mineralised, Punta del Cobre district, which occupies an area of ~20 × 5 km along the eastern margin of the 120 to 97 Ma Copiapó batholith (Williams *et al.*, 2005; Arévalo, 2006). This batholith, which lies immediately to the east of older Jurassic to Early Cretaceous (>125 Ma) granitoids, comprises the larger ~119 Ma La Brea pluton and ~110 Ma San Gregorio plutonic complex close to *Candelaria*, one of a group of smaller, similarly aged (111 to 106 Ma) intrusions on the eastern margin of the Copiapó batholith (Fig. 10; Arévalo *et al.*, 2006).

The district is characterised by a ~12 × 5 km envelope of sodic±calcic alteration, superimposed upon volcanic, sedimentary and intrusive rocks. This alteration is manifested as either (1) albite or sodic-plagioclase, and/or (2) scapolite, with or without calcic amphibole (mainly actinolite, ferro-actinolite, or actinolitic hornblende), pyroxene and/or epidote. Voluminous sodic scapolite-rich



- Quaternary sediments
  - Mid-Cretaceous Cerillos Formation, mainly volcanoclastic sandstone with basaltic-andesite intercalations
  - Early Cretaceous Totoralillo and Pabellón formations, marls, cherts, volcanoclastic rocks, thick limestone and sandstone
  - Early Cretaceous Abundancia and Nantoco formations, calc-mudstone, arkose, evaporites and calcareous breccias
  - Early to Mid Cretaceous Bandurrias Formation, red volcanic and volcanoclastic rocks
  - Late Jurassic to Early Cretaceous Punta del Cobre Formation, andesitic lavas, tuffs and volcanoclastic rocks
  - Mid Cretaceous monzodioritic to microgranitic and granodioritic to tonalitic intrusions - 111 to 106 Ma
  - Early Cretaceous dioritic La Brea batholith, ~120 Ma
  - Jurassic to Cretaceous granitoids, older than 125 Ma
- Alteration overprint
- Potassic or calcic-potassic alteration, biotite and/or K feldspar,  $\pm$ actinolite $\pm$ epidote $\pm$ chlorite $\pm$ calcite $\pm$ quartz, with magnetite
  - Sodic or sodic-calcic alteration, albite, sodic plagioclase or scapolite $\pm$ actinolite $\pm$ chlorite $\pm$ calcite $\pm$ epidote $\pm$ garnet $\pm$ amphibole
  - Thermal contact metamorphism and alteration, garnet $\pm$ pyroxene  $\pm$ scapolite; actinolite $\pm$ biotite; and epidote-chlorite $\pm$ calcite suites

- IOCG mine, past and present
- Envelope surrounding main sodic-calcic alteration
- Shear zone
- Thrust, fault and antiform axis



- Orebody outline, at 0.4% Cu cut-off
- Massive to semi-massive magnetite
- Candelaria Shear - highly foliated biotite schist and mylonites
- Abundancia Formation
  - Fine-grained calcareous sediments and mudstone
- Punta del Cobre Formation
  - Upper Andesites - biotite altered, massive and fine grained
  - Tuffs and volcanoclastic sediments
  - Lower Andesites - Coarse, stratified volcanoclastic breccias and massive andesites
  - Medium to fine-grained porphyritic andesite

*Central Andean Coastal Belt ... cont.*

assemblages, commonly (but not always) associated with calcic-amphibole and/or pyroxene  $\pm$ epidote  $\pm$ andradite, are usually stratabound, and within the Abundancia and upper Punta del Cobre formations (Figs. 10a and b), largely above the ore zone, possibly representing metamorphosed evaporitic beds in these Early Cretaceous units. These rocks also host small magnetite  $\pm$ chalcopyrite-pyrite mantos.

In contrast, where sodic alteration is predominantly albitisation, it is more commonly discordant and pervasive, occurring in igneous rocks, locally with associated minor pyrite  $\pm$ trace chalcopyrite and/or veinlets and disseminations of hematite (Marschik and Fontboté, 2001). Some of the early albite may be due to spilitisation of volcanics, rather than alteration (Ullrich and Clark, 1999).

The overall sodic-calcic zone is enveloped by rocks that were affected by propylitisation, and/or contact thermal metamorphic skarn/hornfels alteration related to the Copiapó batholith (Marschik *et al.*, 2003). The contact between the sodic and thermal metamorphism is gradational (Marschik and Fontboté, 2001).

The more extensive thermal metamorphic aureole of the batholith, extends over a length of >20 km and width of 2 to 5 km from the contact, producing hornfels and skarns with mineralogies that are dependent upon the host rock, and distance from the contact. Skarn minerals in the thermal aureole include proximal diopside-hedenbergite, pyroxene-scapolite  $\pm$ andraditic garnet, to distal biotite/quartz/pyroxene  $\pm$ epidote  $\pm$ K feldspar hornfels (Marschik *et al.*, 2000).

Early pervasive albitisation accompanied the introduction of widespread specularite, occurring in dilational fractures and open spaces. It preceded, and encloses cores of potassic alteration in the district, and occurs below and peripheral to the 116 to 114 Ma pervasive, brown biotite-quartz-magnetite stage (Mathur *et al.*, 2002), and associated almandine  $\pm$ cordierite alteration that accompanied early barren, more intense magnetite mineralisation. This early magnetite was mainly composed of mushketovite after hematite, indicating a shift to more reducing conditions and/or higher temperatures (Marschik and Fontboté, 2001), and more than one pulse and source of iron oxide alteration (Mathur *et al.*, 2002).

The deposit lies near the core of the district wide Tierra Amarilla antiform (Figs. 10a and b), part of the Paipote fold and thrust system, 20 km to the east of the main Atacama Fault Zone (AFZ). The ore zone is relatively flat lying, broadly concordant with the host sequence of coarse-grained volcanics and massive volcanic flows, breccias and tuffaceous rocks, and a broad, similarly flat-

dipping shear zone, with hanging wall evaporite-bearing limestone, shale and epiclastic rocks.

The deposit is capped by the base of the 2 km thick Chañarcillo Group (comprising the Abundancia, Nantoco, Totoralilio and Pabellón formations; Fig. 10a) that was laid down immediately prior to the mineralisation, and hence the depth of formation is assumed to correspond to the thickness of that unit.

The early pre-ore alteration described thus far, is overprinted by a younger (112 to 110 Ma; Mathur *et al.*, 2002), more areally restricted, ore-related intense potassic  $\pm$ calcic alteration (K feldspar-biotite-amphibole) phase, although Re-Os ages of 115 to 114 Ma for molybdenite (Mathur *et al.*, 2002) and two  $\sim$ 111 Ma dates for amphibole and biotite associated with chalcopyrite (Ullrich and Clark, 1999; Arévalo 1999), could represent the main sulphide mineralisation are hypersaline and CO<sub>2</sub>-bearing (Marschik and Fontboté, 2001).

The ore at Candelaria is associated with a complex, multistage event, and occurs: (1) as bodies that are roughly concordant with stratification and comprise replacements and pore filling (mantos); (2) in the matrix to hydrothermal breccias and pseudobreccias; (3) superimposed on massive magnetite replacement bodies; (4) as discontinuous veinlets and stringers in altered host rock; and (5) as massive veins (Marschik *et al.*, 2000; Marschik and Fontboté 2001).

The breccia ores represent intervals of high copper grade. They generally occur as irregular zones, and sometimes lens-shaped bodies, 1 to 3 m thick, which are concordant with stratification. They comprise a chalcopyrite-pyrite-magnetite matrix between brecciated, biotite altered, metavolcanic rock clasts. Clasts are very angular to locally rounded, from a few to tens of cm across. The margins of breccia bodies are diffuse and defined by a decrease in the amount of sulphide matrix. Individual clast borders are sharp and form jigsaw patterns, indicating limited transport and rotation after fragmentation, although some may represent replacive pseudo-breccia. The concordant lens-like replacement and pore-infill manto bodies resemble breccias where sulphides fill pore spaces between angular to rounded volcanic and sedimentary breccia clasts. Networks of veins as they are enlarged also form a pseudo-breccia texture (Arévalo *et al.*, 2006).

Copper ore is associated with magnetite and/or hematite and is dominantly composed of chalcopyrite and pyrite, with gold occurring as small inclusions in the chalcopyrite, within micro-fractures in pyrite and as a mercury-gold-silver alloy (Williams *et al.*, 2005).

**Figure 10: a.** The geology and superimposed alteration of the Candelaria-Punta del Cobre district of northern Chile. All of the known deposits lie within the Paipote fold and thrust system (which includes the steeply dipping Ojancos-Florida Shear Zone separating the Copiapó Batholith from the host Punta del Cobre Formation west of the Candelaria mine; as well as the Paipote, Ladrillos and Cerrillos thrusts and Tierra Amarilla anticline). This structural corridor is part of the regional Chivato fault system, which is  $\sim$ 20 km east of the main Atacama Fault Zone (top-left). The largest deposits, Candelaria and Carola are associated with potassic alteration within the broader sodic-calcic zone. Note the potassic core surrounding the Candelaria deposit is the exposure within the open pit mine, not an original pre-mine outcrop. The sodic-calcic alteration includes both stratabound alteration within the overlying Abundancia and Nantoco formations (possibly related to hydrothermal modification of evaporite-bearing beds within those units), and pervasive, discordant alteration within the volcanic and volcanoclastic rocks of the Punta del Cobre Formation (after Marschik *et al.*, 2000; Marschik and Fontboté, 2001; Arévalo *et al.*, 2006).

**b.** East-west cross section through the Candelaria mine (for reference, note the position of the Lar Fault on Figs. 7a and b). The diagram illustrates the distribution of the manto-like early magnetite and the outline of the overprinting +0.4% Cu orebody, both of which are largely confined to the coarse stratified volcanoclastic breccias and interlayered massive andesites of the Lower Andesites, and the flat-lying Candelaria Shear that caps this unit and the ore deposit. Note the concentration of steep faults near the core of the deposit. Distribution of alteration within the section comprises albite/sodic plagioclase-quartz-biotite-magnetite  $\pm$ K feldspar  $\pm$ minor Ca amphibole below the orebody; biotite-quartz-magnetite  $\pm$ K feldspar and abundant Ca amphibole (largely actinolite) within the ore zone; biotite-quartz-almandine  $\pm$ cordierite and common Ca amphibole within the upper Candelaria Shear; biotite-amphibole with K or Na feldspar in the tuffs and volcanoclastic sediments and Upper Andesites above the shear; and scapolite-quartz  $\pm$ pyroxene  $\pm$ Ca amphibole within the overlying Abundancia Formation (after Marschik *et al.*, 2000; Marschik and Fontboté, 2001; Arévalo *et al.*, 2006).

At the deeper levels in the mineralised system, chalcopyrite has a close spatial association with calcic amphibole (mainly actinolite) in an assemblage that also includes biotite, K feldspar  $\pm$  epidote  $\pm$  sodic plagioclase. Magnetite is ubiquitous, occurring as massive bodies, with or without superimposed sulphide mineralisation, although hematite is rare. Intermediate levels, are characterised by potassic alteration (biotite and/or K feldspar), with or without local developments of calcic amphibole  $\pm$  epidote, sodic plagioclase, and/or local anhydrite. In shallower and distal parts of the system, chlorite is developed at the expense of biotite and amphibole, and albite, chlorite and carbonate alteration increases in intensity. Peripheral to the mineralisation, hematite becomes the dominant iron oxide (Williams *et al.*, 2005). This alteration pattern is complicated by the influence of contact metamorphism related to components of the 120 to 97 Ma Copiapó batholith, as described above. The increasing sodic-calcic alteration in the upper levels of the Candelaria pit area, above the potassic and chloritic zones, may reflect the overlying evaporite-bearing Abundancia Formation (Marschik and Fontboté, 2001).

Marschik and Fontboté (2001), describe a paragenetic sequence over-printing the early, district scale stage of iron metasomatism and associated pervasive albite alteration, comprising: (1) a pre-ore high temperature (600 to 500°C), pre-ore iron oxide stage, comprising pervasive magnetite (mushketovite)-quartz-biotite; (2) the main sulphide ore stage at 500 to 300°C, represented by chalcopyrite and pyrite; and (3) the late stage at <250°C, with hematite-calcite and locally minor sulphides.

Sulphides from Candelaria and some other occurrences in the Punta del Cobre district yielded  $\delta^{34}\text{S}_{\text{CDT}}$  values largely between -3.2 and +3.1‰, with some as high as 7.2‰ for late stage mineralisation, or up to 6.8‰ in the marginal parts of the system (Rabbia *et al.*, 1996; Ullrich and Clark, 1999; Marschik and Fontboté 2001). Marschik and Fontboté (2001) interpret these isotopic data to be consistent with a dominantly magmatic source for sulphur, with a minor contribution during their stage 2, but definite influence in stage 3, from a peripheral evaporite-bearing sedimentary host sequence (e.g., Mathur *et al.*, 2002; Marschik and Fontboté 2001; Ullrich and Clark, 1999). Barton *et al.* (2005) reported that unpublished Sr isotope data for altered and host rocks in Candelaria-Punta del Cobre district, during both early sodic-calcic and late potassic stages of hydrothermal activity imply there are large contributions of non-igneous Sr, implying the ore systems involved influx of fluids from outside the local batholithic granitoids.

Arévalo *et al.* (2006) note that the sulphide ages quoted above, corresponds closely to that of the San Gregorio plutonic complex (Fig. 10a) of the Copiapó batholith, supporting a magmatic origin for the main sulphide mineralisation. They interpret the sulphide mineralisation to have been the product of magmatic fluids of a cooling hydrothermal system, emplaced during synplutonic deformation and dilation at the ductile-brittle transition, in the thermal aureole of the San Gregorio plutonic complex.

An isochron calculated by Re/Os ratios from hydrothermal magnetite and sulphides at Candelaria and the small satellite deposit Bronce, constrains initial  $^{187}\text{Os}/^{188}\text{Os}$  ratios of  $0.36 \pm 0.10$  and  $0.33 \pm 0.01$  respectively. These values are broadly similar to the calculated initial  $^{187}\text{Os}/^{188}\text{Os}$  ratio for magmatic magnetite in nearby batholithic rocks

that range from 0.20 to 0.41. These relatively radiogenic ratios also represent a mixture of mantle and crustal components in both the ores and batholithic rocks (Mathur *et al.*, 2002).

At **Mantoverde**, 150 km north of Candelaria, early district-wide sodic-calcic alteration is absent (Rieger *et al.*, 2010a), although widespread sporadic, weak selective albitisation of plagioclase is taken to represent sub-ocean floor spilitisation (Benevides *et al.*, 2007).

Benevides *et al.* (2007) interprets the following sequence of regional- to district-scale alteration: (1) Early, sporadic, widespread, but poorly exposed potassium-iron metasomatism which converted both granitoid and volcanic rocks to orthoclase (with subordinate biotite), accompanied by the deposition of magnetite (at 130 to 126 Ma; Chen, 2010), with associated fluorapatite, and minor pyrite, but no chalcopyrite. Homogenisation temperatures of 550 to 460°C are estimated for this phase (Benevides *et al.*, 2007). (2) Subsequent regional scapolitisation in the area between the Atacama fault system and the marginal basin, characterised by marialitic scapolite. Later in this second stage, much of the scapolite was replaced by chlorite as part of an episode of chlorite and sericite (hydrolytic) alteration and veining (at 350 to 300°C), with minor development of hematite, pyrite and trace chalcopyrite (Benevides *et al.*, 2007). This style of alteration grades from a slightly chloritised country rock, to chlorite-quartz veinlets, into chlorite-quartz-cemented hydrothermal breccias with mostly silicified, and occasionally K-altered, fragments, the Breccia Verde as detailed below (Rieger *et al.*, 2010).

The Mantoverde IOCG *sensu stricto* deposits, were subsequently emplaced along the main and, more commonly, subsidiary segments of the major Atacama fault system, together with chalcopyrite-bearing, but sub-economic metasomatic magnetite, and copper-barren magnetite-fluorapatite-pyrite bodies. All are hosted by Middle to Upper Jurassic andesites of the La Negra Formation, and by diorite and monzodiorite assigned to the Lower Cretaceous (126 to 120 Ma) Sierra Dieciocho plutonic complex (Benevides *et al.*, 2007). In the immediate Mantoverde district, mineralisation is developed within an intensely fractured structural block, delimited by the subvertical central and eastern branches of the north-south Atacama fault system, connected obliquely by the northnorthwest trending, brittle, Mantoverde fault (MVF). The MVF is a releasing strike-slip duplex, representing a transfer zone between the central and eastern branches of the Atacama fault system. Most of the Mantoverde deposits are closely associated with a 12 km interval of the MVF and sub-parallel minor faults (Benevides *et al.*, 2007; Rieger *et al.*, 2010; Rieger *et al.*, 2010a; Rieger *et al.*, 2009; see Figs. 2 and 4 in Rieger *et al.*, 2010, this volume).

A loosely constrained Early Cretaceous age of mineralisation is based on K-Ar dating of two samples of hydrothermal sericite from Mantoverde Norte, with minimum ages of  $117 \pm 3$  Ma from an andesite and  $121 \pm 3$  Ma from a granite dyke (Vila *et al.*, 1996). A two-point Re-Os isochron age derived from magnetite yielded 116 Ma, consistent with the alteration ages (Mathur *et al.*, 2002).

Five main ore-bearing geological groupings or mineralisation zones/styles are recognised at Mantoverde: (1) *Manto Atacama*, a specularite-cemented, hydrothermal breccia, averaging 80 m in thickness (locally up to 200 m), in the hanging wall (east) of the 40 to 50° east-dipping MVF. It is composed of sub-angular to sub-rounded clasts, a few centimetres across, of mainly andesitic or granitoid igneous

*Central Andean Coastal Belt ... cont.*

rocks in a mineralised, calcite-bearing, coarse-grained specularite matrix, altered to varying degrees by pervasive K feldspar, with more or less intense chlorite, sericite, silica and/or carbonate. (2) *Transition zone*, an adjacent specularite stockwork zone, immediately to the east and above the Manto Atacama, containing supergene copper oxide and hypogene sulphides, with essentially the same alteration as the Manto Atacama zone. (3) *Mantoverde Breccia*, a tectonic breccia in the footwall (west) of the main fault plane of the MVF, commonly 20 to 40 m thick. It comprises a rock flour matrix cataclastite, enclosing angular andesite and/or diorite clasts that are commonly a few millimetres to about 10 cm in diameter, with silica, chlorite and minor to moderate K feldspar alteration; (4) *Breccia Verde*, which is developed on both sides of the MVF, and has a gradational boundary with both the Transition zone and Mantoverde breccia. It is largely barren, and is composed of silicified and pervasively K feldspar altered volcanic and dioritic clasts within a matrix of chlorite-quartz, containing calcite and subordinate sericite, grading outwards into a chlorite-quartz stockwork. It is cut by sparse to moderately frequent sets of K feldspar  $\pm$ quartz, calcite  $\pm$ siderite, specularite,  $\pm$ quartz and sericite veinlets; (5) *Magnetite Zone*, developed between the Breccia Verde, an intrusion of the 120 to 127 Ma Sierra Dieciocho pluton to the west, and the Mantoverde Breccia to the east, and mainly at depth. It comprises magnetite-chlorite-sericite-K feldspar-cemented breccias, with clasts of igneous rock that are predominantly altered to magnetite (including mushketovite), K feldspar and quartz, cut by veinlets of K feldspar  $\pm$ quartz, calcite, sericite and late specularite-calcite. Pyrite and chalcopryrite occur as small patches, disseminations, or in discontinuous veinlets. This zone is representative of the other magnetite-sulphide bodies in the south of the district (Rieger *et al.*, 2010a).

The bulk of the mining to date has exploited supergene mineralisation which occurs within the zone of oxidation that consistently persists to a depth of 150 to 250 m below the surface. Mineralisation comprises chrysocolla, brochantite, atacamite, almagre, malachite and copper-bearing hematite, jarosite, and goethite, disseminated in the breccia matrix, as filling of veinlets, and as a patina on, or patches within rock fragments (Rieger *et al.*, 2010; Benevides *et al.*, 2007).

Below the base of supergene oxidation, in the Manto Atacama breccia, the specularite-rich matrix contains pyrite-chalcopryrite, with the chalcopryrite being locally replaced by digenite and bornite. The breccia is cut by veinlets of K feldspar  $\pm$ quartz, tourmaline, or sericite, with late stage calcite and specularite veinlets (Rieger *et al.*, 2010).

Neither native gold, nor electrum have been reported from the Mantoverde district, although there is a close correlation between gold and copper grades, and gold has been detected in both, chalcopryrite and pyrite (Rieger *et al.*, 2010).

In the northern half of the district, the mineralised tectonic breccias (e.g., Mantoverde Breccia), specularite-cemented, hydrothermal breccias (e.g., Manto Atacama), and outer halo of mineralogically identical veins (Transition zone) are characterised by primary specularite and largely developed in the hanging wall of the MVF. In contrast, in the southern half of the district, there are hypogene, crudely tabular, massive bodies of magnetite-pyrite and magnetite-chalcopryrite (e.g., the Magnetite zone), predominantly in the footwall of the Mantoverde fault, while massive and irregular bodies of magnetite-apatite  $\pm$ pyrite are developed along the eastern branch of the Atacama fault system (Benevides *et al.*, 2007).

The hypogene minerals of the Magnetite zone and the magnetite rich bodies in the south of the district comprise (1) magnetite stockworks and disseminations; (2) elongate magnetite-chlorite-sericite-K feldspar-cemented breccias, with igneous rock fragments that are mainly altered to an assemblage of magnetite, K feldspar and quartz; and (3) massive magnetite bodies. Both primary magnetite and mushketovite are present. These magnetite-rich rocks may be either barren, or contain chalcopryrite (and/or pyrite), mainly as small patches, disseminations and/or discontinuous veinlets (Rieger *et al.*, 2010).

Rieger *et al.* (2010), notes a vertical zonation of mineralisation-associated iron oxides, with a downward transition from upper hematite to magnetite at depth. Tilting and differential rotation across the MVF has resulted in the magnetite mineralisation being exposed to the south, while drilling confirms the continuity of similar magnetite dominant mineralisation at depth immediately below the Mantoverde Breccia ores in the footwall of the MVF in the north. A lateral transition between specularite breccias and magnetite is not evident to the north, although the two are juxtaposed across the MVF, again due to the differential rotation accommodated by that structure. However, in the south, the Manto Atacama is only poorly developed and gives way to magnetite-rich rocks in the hanging wall, footwall and at depth.

Benevides *et al.* (2007) conclude that on the basis of textural relationships in both breccias and veins, the crystallisation of specularite and chalcopryrite was coincident. However, Rieger *et al.* (2010) interpret them to have been emplaced at different times, with the main mineralising events being (1) an early high-temperature iron oxide stage, comprising the bulk of the specularite and magnetite in the district; (2) a sulphide stage responsible for the main copper-gold mineralisation; and (3) a late stage, represented mainly by calcite  $\pm$ specularite and specularite veining, and pervasive carbonatisation. They suggest the iron oxide stage comprises early hematite (hm-I), followed by early magnetite (mt-I) which wholly or partially replaced hm-I (to form mushketovite), accompanied by pervasive K feldspar alteration, minor tourmaline and weak scapolite. Subsequent, variably intense silicification, pervasive sericitisation and minor pyrite (py-I) was followed by a second phase of magnetite (mt-II) and chloritisation, with specularite locally developing rather than mt-II. Rieger *et al.* (2010) see the sulphide phase as occurring in isolation, after the development of iron oxides (including the specularite breccia matrix), K feldspar, sericite, silica and chlorite. The iron oxide stage of Rieger *et al.* (2010) corresponds to both the potassium-iron metasomatism, scapolitisation and sericite-chlorite phases of Benevides *et al.* (2007), described above (see Fig. 5 in Rieger *et al.*, 2010, this volume). Both agree on a terminal phase of alteration, which comprises largely barren calcite veining, variably accompanied by quartz.

Rieger *et al.* (2010) suggest the specularite associated with ore in the north of the district is their hm-I, on the periphery of the mineralised system, while the magnetite in the mineralisation at depth and to the south is both mt-I mushketovite after hm-I, and mt-II, which is deeper and hotter, proximal to the centre of mineralisation.

Rieger *et al.* (2010), noted a similar zonation in sulphur isotope signatures. Chalcopryrite in the Mantoverde district shows a wide range in sulphur isotope composition, with  $\delta^{34}\text{S}_{\text{VCDT}}$  of between -6.6 and +10.0‰ (Rieger *et al.*, 2010;

*Central Andean Coastal Belt ... cont.*

Benavides *et al.*, 2007). Systematic variation of these data reflect the spatial distribution of the sulphides in the orebodies and their position relative to the MVF. Sulphur isotopic compositions around 0‰  $\delta^{34}\text{S}_{\text{VCDT}}$ , which are compatible with a magmatic-derived sulphur component, are characteristic of chalcopyrite in orebodies with a close spatial relationship with the MVF in the southern and deeper, or proximal part of the Mantoverde district, representing the more internal parts of the hydrothermal system, while higher  $\delta^{34}\text{S}_{\text{VCDT}}$  values of around +6‰, are typical of the northern part of the district, or the shallower, levels, suggesting sulphur contribution from non-magmatic sources in the peripheral portions of the hydrothermal system (see Fig. 7 in Rieger *et al.*, 2010, this volume). Rieger *et al.* (2010a) report the  $\delta^{34}\text{S}$  values for pyrite (0.2 to 9.4‰) to similarly indicate a dominantly magmatic source, although also showing systematic variations across the district, interpreted to reflect both the relative distance from inferred fluid conduits and the level of deposition within the hydrothermal system, and possible non-magmatic components on the peripheries of the system.

Homogenisation temperatures of between 550 and 460°C have been reported from hypersaline fluid inclusions (32 to 56 wt.% NaCl<sub>equiv.</sub>) in quartz coexisting with magnetite (Vila *et al.*, 1996; Benavides *et al.*, 2007 and unpublished sources quoted therein), while the main hypogene specularite breccia sulphide mineralisation is calculated to have formed at between 250 and 180°C (Benavides *et al.*, 2007). Homogenisation temperatures of a number of determinations for late calcite-chalcopyrite and calcite veins from two and three phase fluid inclusions with salinities of from 32 to 40 wt.% NaCl<sub>equiv.</sub> and 1 to 10 wt.% NaCl<sub>equiv.</sub> returned values of 360 to 160°C and 260 and 112°C respectively (Vila *et al.*, 1996 and unpublished sources quoted therein).

The majority of initial  $^{87}\text{Sr}/^{86}\text{Sr}$  values of altered volcanic rocks and hydrothermal calcite from the district (0.7031 and 0.7060) are similar to those of the igneous rocks of the region. Lead isotope ratios of chalcopyrite are consistent with lead (and by inference copper) derived from Early Cretaceous magmatism. The sulphur, strontium and lead isotope data of chalcopyrite, calcite gangue and altered host rocks respectively, are compatible with the cooling of metal and sulphur-bearing magmatic hydrothermal fluids (with deposition at <350°C) that mix with meteoric waters or seawater at relatively shallow crustal levels. They suggest, input of additional exotic sulphur is likely, though not essential, for the deposition of copper mineralisation, occurring mainly in the shallow, and distal parts of the ore system.

Magnetites from the Mantoverde deposit have Os and Re concentrations of 11 to 17 ppt and 4 to 6 ppb, respectively. An initial  $^{187}\text{Os}/^{188}\text{Os}$  ratio calculated from these is ~0.20, compared to ~0.36 to 0.33 at Candelaria, and from 0.20 to 0.41 for magmatic magnetite from Early Cretaceous batholithic intrusions in the district. These relatively radiogenic ratios are taken to represent a mixture of mantle and crustal components in the ores and batholithic rocks (Mathur *et al.*, 2002).

Benavides *et al.* (2007) interpret isotopic and temperature data they quote from regional and shallow hematitic mineralisation to indicate their potassium-iron metasomatism stage was caused by magmatic fluids, possibly products of the second boiling of granitoid magmas, such as the nearby 126 to 120 Ma Sierra Dieciocho complex. However, they suggest the data indicates a

change, probably during the scapolitisation and sericite-chlorite phases, possibly due to evaporite derived brines mobilised by marginal basin inversion reflected in the regional sodic alteration event, but even more likely during the deposition of chalcopyrite ore.

The *El Romeral* and *El Algarrobo* iron oxide-apatite deposits are two of the largest of the string of similar accumulations that constitute the Chilean Iron Belt.

The Chilean Iron Belt is up to 30 km wide and extends over a north-south interval of approximately 700 km, from 25 to 31°S. It embraces a large number of magnetite-apatite accumulations, ~40 of which are of economic significance and a more limited number (~5) that are mined for iron on a large scale (Bookstrom, 1977). K-Ar ages of alteration minerals and post-ore dykes from a number of these deposits are between 128 and 102 Ma (Zentilli, 1974; Pichon, 1981)

The El Romeral deposit lies within a composite, north-south elongated, 8 × 4 km sliver of late Palaeozoic metasedimentary, Lower Jurassic volcanoclastic and Early Cretaceous intrusive rocks. The sliver is bounded to the west and east by pre-ore quartz monzonite and post-ore granodiorite batholiths respectively. The late Palaeozoic metasedimentary rocks comprise schists, phyllites and quartzite, and are locally overlain by erosional remnants of volcanoclastic andesitic rocks, possibly equivalent to the Lower Jurassic La Negra Formation. Elsewhere in the district, the latter are overlain in turn by Lower Cretaceous marine andesitic rocks (Bookstrom, 1977).

Intrusive rocks in the sliver include the north-south elongated ~500 m wide, Early Cretaceous La Liga andesite porphyry, which hosts the main orebody, and the Romeral diorite, occurring as two larger masses to the east and west. A wedge of Palaeozoic metasedimentary rocks separate the La Liga andesite and eastern Romeral diorite to the north (Bookstrom, 1977).

The diorite is very similar to the andesite intrusive, except that it is more phaneritic, has less calcic plagioclase and contains less augite and ilmenite. A network of post- and intra-mineral dioritic dykes cut the orebody. The Romeral diorite predates the ore, although along its contacts, it has strongly metasomatised both the La Liga andesite and Palaeozoic metasedimentary rocks (Bookstrom, 1977).

The sliver is cut by a series of north-south trending faults that are part of the Atacama Fault System complex, which underwent sinistral displacement during ore deposition (Bookstrom, 1977).

The lenticular 800 × 250 m main orebody persists to a depth of 400 m below surface and comprises an up to 200 m wide core of >50% Fe, as almost massive magnetite, enveloped by progressively lower grade shells. The high grade ore is intergrown with very fine actinolite and discontinuous veinlets of gangue minerals. Microscopically, the ore is composed of spongy intergrowths of skeletal magnetite grains and actinolite prisms, with minor clinozoisite, titanite, apatite, albitic-plagioclase, marialitic-scapolite, chlorite and quartz. Magnetite veinlets are common. A second orebody is hosted by Palaeozoic biotite schists ~500 m to the north (Bookstrom, 1977).

Ore zone boundaries are gradational, and the enclosing country rocks contain an alteration assemblage of magnetite, actinolite, albitic plagioclase, dioside, clinozoisite, titanite, chlorapatite, marialitic scapolite, tourmaline, chlorite, pyrite, calcite, micas and clays. This alteration accompanied the ore formation and is dominated by magnetite and actinolite that formed at temperatures in the range 550 to 475° C,

*Central Andean Coastal Belt ... cont.*

followed by late chloritisation. A pronounced actinolite alteration halo that is at least 4.5 km long and up to 500 m wide surrounds the deposits. The diorite has been strongly altered to albitic-plagioclase (Ab<sub>80-90</sub>) to resemble an aplite to the west, overlapping and external to the actinolite envelope over a width of several hundred metres from the orebody and strike length of ~3 km. A similar, less intense albitic plagioclase alteration halo is also evident to the east of the main orebody, but over a narrower width. In addition, much the Romeral diorite contains 26±5% pervasive, interstitial actinolite throughout, beyond the main alteration zones, accompanied by fine dustings of magnetite and fine actinolite stockworks (Bookstrom, 1977).

At El Algarrobo, similar mineralisation is hosted by a comparable diorite (110 Ma) and Early Cretaceous andesites which have undergone strong associated actinolite/tremolite-apatite alteration in association with magnetite mineralisation (Ménard, 1995). On the basis of petrological and geochemical studies, Ménard (1995) concluded that the magnetite-actinolite/tremolite-apatite mineralisation is related to clino- and orthopyroxene diorite intrusions which crystallised at ~4 km depth under increasing  $fO_2$ , when a supercritical fluid phase exsolved during cooling and consolidation at 900 to 800°C, to release H<sup>+</sup> and Cl<sup>-</sup>, and Na (resulting in sodic alteration), followed by sequential leaching of Fe (at <700°C), Ca and Mg (between 600 and 500°C) from minerals of the primary diorite assemblage i.e., titanomagnetite-ilmenite, plagioclase (An<sub>70-40</sub>), augite and hypersthene. The same author suggests the Fe, Mg and Ca were transported by fluids in cationic form by Cl<sup>-</sup>, to cooler rocks for precipitation.

However, Mathur *et al.* (2002) collected magnetite from three magnetite-apatite deposits of the Chilean iron belt, including El Romeral. They found that these samples have Re and Os concentrations of 0.8 to 3 ppb, and 11 to 76 ppt respectively. Calculated initial <sup>187</sup>Os/<sup>188</sup>Os ratios of from 1.2 to 8.4 are distinctly different from those of Candelaria and Mantoverde (determined by the same authors and quoted above) and from magmatic rocks of the arc. They therefore conclude that the Os in these magnetite-apatite ores could be derived from sedimentary rocks, suggesting a dominant input from basin-derived, non-magmatic brines.

In **southern Perú**, two cycles of regional alteration are evident over the period from 176 to 95 Ma, i.e., the Late Jurassic to Early Cretaceous, extending over an area of >75 km<sup>2</sup>, encompassing both the *Marcona* and *Mina Justa* deposits. This part of southern Perú covers section of the Cañete basin, an extensional rift trough filled by tuffs, amygdaloidal and porphyritic andesite flows and medium to fine-grained andesitic volcanoclastic rocks, with minor sandstone, siltstone and limestone of the Late Jurassic Río Grande Formation. This succession overlies a basement of Palaeoproterozoic to Mesozoic plutonic, metasedimentary and volcanic rocks. The alteration and mineralisation related to the Marcona magnetite ores was emplaced during the extensional phase of the basin, hosted mainly by Palaeozoic metasediments and lesser Mesozoic volcanic rocks. In contrast, the Mina Justa copper mineralisation is hosted by Jurassic volcanic rocks and was deposited during the inversion of the basin (Chen *et al.*, 2010).

The following is summarised from a detailed study reported in Chen *et al.* (2010) and (2010a).

The *first cycle* culminated in the formation of the **Marcona** magnetite deposits, evolving as follows: (1) a precursor phase, characterised by the Mg-Fe amphibole cummingtonite (~176 Ma); (2) K-Mg-Fe metasomatism which produced a

phlogopite-magnetite assemblage (171 Ma); followed by, (3) widespread albitic ±marialitic scapolite (i.e., Na-Cl metasomatism), bracketed between 171 and 162 Ma. This latter assemblage is not as intense as the similar phase at Candelaria, but in contrast to the latter, is associated with neither magnetite nor sulphides; (4) the main magnetite stage at Marcona, from 162 to 159 Ma, resulted in the deposition of *en echelon* swarms of massive (>90%) magnetite orebodies (the largest containing 400 Mt of ore), comprising a sulphide-free assemblage of magnetite-biotite-actinolite/tremolite ±phlogopite ±fluorapatite. In contrast to the preceding stages, which were characterised by high temperature metasomatism, Chen *et al.*, (2010a) report that these magnetite bodies exhibit no convincing mega- or microscopic evidence of large scale iron-metasomatism. Rather, they interpret the textures and character of the magnetite orebodies to represent fault- and bedding-controlled intrusions of bimodal magnetite and dacite, occurring as “amoeboid”, commingled immiscible melts, exsolved during the mixing of juvenile andesitic and rhyolitic (or rhyodacitic) parental magmas, enhanced by dissolution of quartz from the intruded host metasediments. However, although there is no evidence of iron-metasomatism within the actual orebodies, the process of exsolution and crystallisation of the oxide melts at 700 to 800°C released large volumes of brines responsible for the intense potassic and/or sodic metasomatic halos to the orebodies; (5) Oxygen and sulphur stable-isotope geothermometry indicate that quenching of these magmatic fluids from >800 to <450°C resulted in the precipitation between ~159 and 156 Ma of a late, but metasomatic magnetite-sulphide mineralisation, overprinting the magnetite bodies at Marcona. The resultant assemblage comprised substantial pyrrhotite and pyrite, and minor chalcopyrite, only contributing very weak copper grades. This phase was accompanied by actinolite/tremolite, the termination of K feldspar alteration, and by phlogopite supplanting biotite. This low-magnetite, sulphide-dominated stage formed in a relatively reduced and cooler (≤360°C) regime; (6) This was followed from ~156 to 154 Ma by a more distinct phase of polymetallic sulphide mineralisation, comprising a magnetite-free assemblage of mainly pyrite, chalcopyrite and pyrrhotite, responsible for an average grade of 0.12% Cu, with local zones of >0.45% Cu, corresponding to a decrease in pyrrhotite and increase in pyrite-chalcopyrite (Chen *et al.*, 2010). This mineralisation was deposited from lower temperature, <360°C brines coeval with small dacite porphyry plugs marking the terminal phase of the volcanic cycle (Chen *et al.*, 2010a). The *Marcona* orebodies were deposited in Early Palaeozoic clastic sediments, and to a lesser extent in the base of the overlying Early Jurassic volcanic rocks, and were restricted to an extensional rift trough, coeval with the deposition of the thick Late Jurassic volcanic pile (Chen *et al.*, 2010).

The *second cycle* of alteration, followed from, and geographically overlapped the first, and influenced the hosts to the **Mina Justa** copper deposit, which is located 3 to 4 km northeast of Marcona. It initially comprised temporally separated and possibly unrelated alteration pulses spanning the gap before the build-up from ~110 Ma, of the phase that culminated in the Mina Justa mineralisation, as follows: (1) a barren albitic-actinolite assemblage, coeval with the late sulphide stages at Marcona (159 to 154 Ma); (2) potassic metasomatism (~142 Ma), occurring as an assemblage of K feldspar ±magnetite; (3) green

*Central Andean Coastal Belt ... cont.*

actinolite  $\pm$ magnetite  $\pm$ diopside (110 Ma), which was widespread within the Mina Justa orebody area; (4) early hematite-calcite, (between 110 and 104 Ma), subsequently entirely pseudomorphed in the next phase by magnetite (mushketovite); (5) major magnetite-pyrite-K feldspar, emplaced at high temperature ( $\sim$ 600°C) from 104 to 101 Ma, to produce massive, lensoid and brecciated bodies of medium- to coarse-grained magnetite-pyrite which host the highest grade copper sulphide mineralisation at Mina Justa; followed by (6) copper-sulphide mineralisation from 99 to 95 Ma, dominantly occurring as replacement of massive magnetite-pyrite bodies or veins, but also as lesser cross-cutting sulphide veins. The principal sulphides in decreasing order of abundance are chalcopyrite, bornite, chalcocite and digenite, often accompanied by specular hematite and calcite; (7) late specular hematite in the upper parts of the orebodies, where a copper-barren hematite zone is locally developed (Chen *et al.*, 2010).

The Mina Justa deposit comprises two main, complex, shallowly southeast plunging, 10 to 200 m thick, fault-controlled, lensoid orebodies, the Main and Upper (see Fig. 2B, in Chen, 2010, this volume). The Main body outcrops as a  $\sim$ 400 m long, northeast striking zone of discontinuous copper oxides and K feldspar-actinolite alteration, dipping at 10 to 30° to the southeast. The Upper orebody has a similar surface expression and size, approximately 400 m southeast of the Main zone. Each is composed of a massive magnetite-sulphide core, enclosed by hydrothermal breccias with strongly altered clasts in a magnetite+sulphide matrix. These breccias are in turn surrounded by extensive stockwork veining. Each is zoned upwards and outward from pyrite-chalcopyrite to bornite-chalcocite ( $\pm$ digenite). Hypogene hematite (partly specularite) occurs in the upper parts of the copper mineralisation in each lens. Similarly striking, but northwest dipping magnetite lenses carry minor copper and are cut by the ore lenses. The hypogene copper sulphide mineralisation of the Main and Upper orebodies represent emplacement along reactivated listric-normal detachment faults during the Mid-Cretaceous inversion of the contiguous, plate boundary-parallel, Cañete basin, temporally coincident with the earliest (from  $\sim$ 109 Ma), largely granodioritic-dioritic, stocks of the Coastal batholith. A swarm of 20 to 50 m thick andesitic (ocöite) dykes, which constitute up to 35% of the rock volume in the deposit area, post date mineralisation (Chen *et al.*, 2010).

Chen *et al.* (2010) and Chen (2010) conclude that the Mina Justa deposits is representative of the significant IOCG *sensu stricto* deposits of the central Andes on the basis of the following features: (1) emplacement in significantly older, largely volcanic strata, rather than in broadly syn-mineralisation granitoids; (2) localisation of sulphide mineralisation by older, sulphide-deficient and tenuously related, magnetite bodies, dominantly in hydrothermal breccia and stockwork; and (3) channeling of brines by regionally extensive fault systems accommodating the contractional inversion of arc-parallel, evaporite bearing volcano-sedimentary basins.

The same authors conclude that at Mina Justa, brines released during inversion of the arc-parallel, evaporite bearing Cañete basin, were responsible for low temperature (<250°C) sulphide mineralisation, which overprinted high temperature (600 to 540°C) magnetite-pyrite concentrations. The high temperature potassic metasomatism and magnetite-pyrite formed during emplacement of the major Coastal batholith and yields  $\delta^{34}\text{S}$  values of 1 to 4‰

(Chen, 2010) from the pyrite, consistent with a magmatic source, whereas the subsequent introduction of basinal brines and the consequent mineralising event taking place approximately 5 to 10 m.y. later. The influence of the basinal brines in depositing ore is in accordance with  $\delta^{34}\text{S}$  values from ore sulphides of >20‰ (Chen, 2010)

The **Raúl-Condestable** deposits are located 90 km south of Lima, in central Perú. Unlike most IOCG *sensu stricto* deposits, it appears to be spatially, as well as temporally, closely associated with an intrusions and as such is unusual. Like the other iron oxide-alkali altered mineralised systems described above from the Central Andean Coastal Belt, it is hosted by a series of volcanic, plutonic, and sedimentary units of Upper Jurassic to Lower Cretaceous age, which are part of a large volcanic island- to continental-volcanic belt that was active from Late Jurassic to Early Tertiary time. The host volcano-sedimentary sequence is  $\sim$ 6 km thick, dips at  $\sim$ 40° WSW, and is divided into four units (see Fig. 2A in Chen, 2010, this volume). Two of the lower of these, units I and III, which are basalt and basaltic-andesite in composition, represent the bulk of the volcanic sequence. The sandwiched unit II is around 1.5 km thick and dominantly detrital sediments. The 2 to 3 km of intermediate dacitic and andesitic volcanic rocks of unit IV are dated between  $116.7\pm 0.4$  and  $114.8\pm 0.4$  Ma. This magmatism was accompanied by a 500 to 600 m thick, 116.5 Ma quartz-diorite sill (within unit III), and two narrow, nested, tonalite stocks with minor apophyses, within the core of a dacitic volcano. The tonalite stocks dip at around 50° ENE, normal to stratification, extend for over  $\sim$ 1.6 km vertically, are 300 m wide, and were emplaced at  $\sim$ 115 Ma (de Haller *et al.*, 2006; Williams *et al.*, 2005).

The main tonalite stock is surrounded by a halo of pervasive potassic (biotite) alteration, mostly within mafic rocks. The biotite alteration is cut by a quartz stockwork and locally by actinolite veinlets (<5 mm thick) associated with the transition to the overprinting pervasive actinolite alteration shell that laterally surrounds the quartz stockwork and biotite alteration core. The actinolite alteration is accompanied by albite and chlorite ( $\pm$ scapolite and magnetite) and largely affects rocks of unit III and the quartz-diorite porphyry sill. The latter shell can be intense in tuffs, mafic lava, and impure limestone, with the rocks being locally completely replaced by amphibole (actinolite). This shell, and the biotite core, grades upwards into Fe-chlorite and sericite that caps the tonalite stock in unit IV. A peripheral halo of hematite-chlorite ( $\pm$ epidote-calcite-albite) surrounds both the Fe-chlorite and actinolite shells in units III and IV (de Haller *et al.*, 2006; Williams *et al.*, 2005).

Mineralisation surrounds, and is largely external to the tonalite stock, predominantly within unit III, although extending from units II to IV. It is developed in the biotite-quartz and actinolite-albite-chlorite shells, and the Fe-chlorite-sericite cap, particularly in carbonate, tuffaceous and pyroclastic rocks, and volcanic breccias. Conformable, tabular (manto) replacements, disseminations and veinlets occur within permeable volcaniclastic and carbonate-rich rocks, surrounding structurally controlled feeder veins which are perpendicular to bedding and cut units II to IV, the quartz-diorite stock and locally the main tonalite. Massive fine-grained, to large scapolite crystals accompany the feeder veins. Scapolite is cut by veinlets filled with titanite (in part altered to ilmenite), K-feldspar, muscovite, pyrite, sphalerite and galena, and chalcopyrite (in paragenetic order). This hydrothermal titanite has been dated (U-Pb) by de Haller *et al.* (2006) at  $115.2\pm 0.3$  Ma.

*Central Andean Coastal Belt ... cont.*

and is assumed to approximate the age of mineralisation. Apatite precipitated after hematite, together with, or just before, magnetite and pyrrhotite.

Specular hematite alteration followed the introduction of actinolite, occurring as open-space filling and massive replacement bodies, to be replaced and pseudomorphed by magnetite. The main ore stage is characterised by two end-member assemblages (i.e., coexisting mineral suites that did not precipitate at the same time and were therefore not in equilibrium), (1) an early, extensive, oxidised, hematite-magnetite-pyrite-chalcocopyrite within and adjacent to the feeder veins/structures, and (2) a reduced suite that progressed from molybdenite, to pyrrhotite, pyrite and finally chalcocopyrite, gold and minor sphalerite and galena within the mantos, disseminations and veins. Early specularite is transformed to musketovite. These assemblages are cut by late stage calcite-sulphide veins (de Haller *et al.*, 2006).

De Haller and Fontboté (2009) conclude, on the basis of ore paragenesis and zoning, sulphur isotopes, thermodynamic constraints, alteration mineralogy and geochemistry, that the Raúl-Condestable deposits were formed by cooling and wall-rock buffering of metal-bearing magmatic brines, which on mass balance estimates, after sulphur isotope data, they infer contributed ~70% of the sulphur. This is supported by  $\delta^{34}\text{S}$  values of sulphides from 1.0 to 6.3‰ (median ~3.5‰, close to the  $0 \pm 5\%$  of magmatic fluids) in the deep feeder veins. In the (mainly) upper parts of the system, these brines mixed with varying proportions of seawater-derived fluids, which contributed a subordinate part of the sulphur. Sulphides from the pyrrhotite-pyrite-chalcocopyrite suite from shallower levels have wide variations of  $\delta^{34}\text{S}$  values of 2.7 to 26.3‰ (median ~7.5‰), suggesting a mixing of fluids. Values of  $14 \pm 1\%$  are estimated for sea water of that period. The late-stage calcite-sulphide veins show strongly negative  $\delta^{34}\text{S}$  values of -32.7 to -22.9‰, indicating a possible biogenic influence. They also conclude that, in the absence of rocks which could have oxidised the hot (>300°C) fluids to the field of hematite stability, the oxidised assemblage (hematite-magnetite-pyrite-chalcocopyrite) was precipitated from magmatic brines, following the  $\text{SO}_2\text{-H}_2\text{S}$  gas buffer at elevated temperature (>350°C) and high fluid/rock ratio. Mass balance calculations from sulphur isotope data infers sulphides of the oxidised assemblage have a larger component of magmatic sulphur than those of the reduced mineral association. The deposition sequence from hematite to chalcocopyrite is taken to reflect the cooling of the magmatic fluid, and redox and pH buffering by the basaltic-andesitic volcano-sedimentary host rocks. As such, the occurrence of musketovite followed by iron-bearing sulphides is interpreted to be direct field evidence for precipitation from oxidised magmatic brines (De Haller and Fontboté, 2009).

## Khetri and Alwar Copper Belts

### Crustal Setting

The Khetri and Alwar copper belts are located approximately 190 km southwest of New Delhi, in the states of Rajasthan and Haryana, in northwestern India. They lie within the 100 to 200 km wide Aravalli mobile belt (Singh *et al.*, 2010) on the northwestern margin of the Archaean Aravalli-Bundelkhand proto-continent (Meert *et al.*, 2010; or Aravalli craton of Naqvi and Rogers, 1987). The Aravalli-Bundelkhand proto-continent is bounded to the

north by the current Himalayan Fold Belt and to the south by the continental scale, east-northeast-trending, Proterozoic Narmada-Son lineament and the parallel Satpura mobile belt immediately to its south. These structures also mark the northern limit of the Dharwar (East and West), Bhandara (Bastar) and Singhbhum cratons, which are each separated by north-northwest-trending sutures, and form the bulk of Peninsular India (Fig. 11).

The northeast-trending Great Boundary fault divides the Aravalli-Bundelkhand proto-continent into the main Bundelkhand craton to the east and the Aravalli block (Meert *et al.*, 2010; or Mewar craton of Rao and Reddy, 2002), which broadly coincides with the Aravalli Mobile Belt, to the west. The Aravalli and Satpura mobile belts would appear to be continuous from the southern to western margins of the Aravalli-Bundelkhand proto-continent.

Much of the Bundelkhand craton is occupied by the Bundelkhand Igneous Complex, which includes the late Bundelkhand Granite (2492±10 Ma). These intrude older Archaean granite-greenstone enclaves and gneisses formed between 3.2 and 2.5 Ga. The exposed basement to the Aravalli block comprises the 3.3 to 2.45 Ga Banded Gneissic Complex (or Mewar Gneisses), composed of migmatites, tonalite-trondhjemite-granodiorite gneisses, meta-sedimentary rocks and sporadic greenstone belts/amphibolites, intruded by the 2530±3.6 Ma Berach Granite (Meert *et al.*, 2010; Singh *et al.*, 2010 and sources quoted therein). The stabilised metamorphic basement of the Aravalli block was unconformably overlain by the 2.15 to 1.8 Ga Aravalli Supergroup. This unit comprises shallow water, stromatolite-bearing facies in the east, and deep water carbonate-pelite facies to the west. These facies-domains are separated by the gabbro-norite (ophiolite?)-bearing Rakhabdev shear zone, interpreted to define a subduction zone, along which the Aravalli basin closed at 1.8 Ga (the absence of any preserved magmatic arc would challenge this interpretation). The sequence is also cut by 1.85 Ga granites (Singh *et al.*, 2010).

Within the Aravalli mobile belt, the Aravalli Supergroup succession is overlain by the >5 km thick Delhi Supergroup, which comprises the basal Raialo Group (carbonate, conglomerate and sandstone, with mafic and felsic volcanic rocks), overlain by the Alwar Group (conglomerate and sandstone), which is followed in turn by the Ajabgarh Group (stromatolitic carbonate, siltstone and shale). Minor felsic and mafic volcanic rocks occur throughout the Ajabgarh and Alwar Groups. The age of this succession is poorly constrained, between 1.7 and 0.8 Ga (Meert *et al.*, 2010; Singh *et al.*, 2010).

The Aravalli mobile belt is composed of a series of terranes. These terranes are separated by major shear zones, and represent the surface expression of different stratigraphic levels and degrees (depths) of metamorphism, e.g., in some terranes, the Aravalli Supergroup is only metamorphosed to low- to medium grades, while in others it has been modified to granulite facies and subjected to migmatization (Singh *et al.*, 2010). The main pulse of metamorphism took place between 1725 and 1621 Ma, at the onset of the Delhi Orogenic Cycle. Two distinct phases of magmatism are also recognised, the first between 1810 and 1660 Ma in the south, and largely between 1810 and 1780 Ma in the north, have an A-type geochemistry, attributed to an extensional setting (Meert *et al.*, 2010).

The second, younger ~0.85 to ~0.73 Ga (with some examples ~1.0 Ga) 'Erinpura Granite' pulse is best represented to the south, although it is also developed in

*Khetri and Alwar District ... cont.*

the Khetri area, to the north. This extensive young granite phase temporally overlaps the bimodal 0.77 to 0.75 Ga Malani Igneous Suite (MIS), which forms the largest felsic magmatic province in India, covering an area in excess of 55 000 km<sup>2</sup> (Li *et al.*, 2008; Singh *et al.*, 2010; Vallinayagam and Kumar, 2010). It is characterised by voluminous

magmatism that began with minor basaltic, followed by predominant felsic volcanic rocks and then by granitic emplacement, with a final, predominantly felsic magmatic cycle, and minor mafic dyke swarms. The MIS includes both peralkaline and peraluminous phases and is interpreted to represent ‘anorogenic magmatism’, related either to

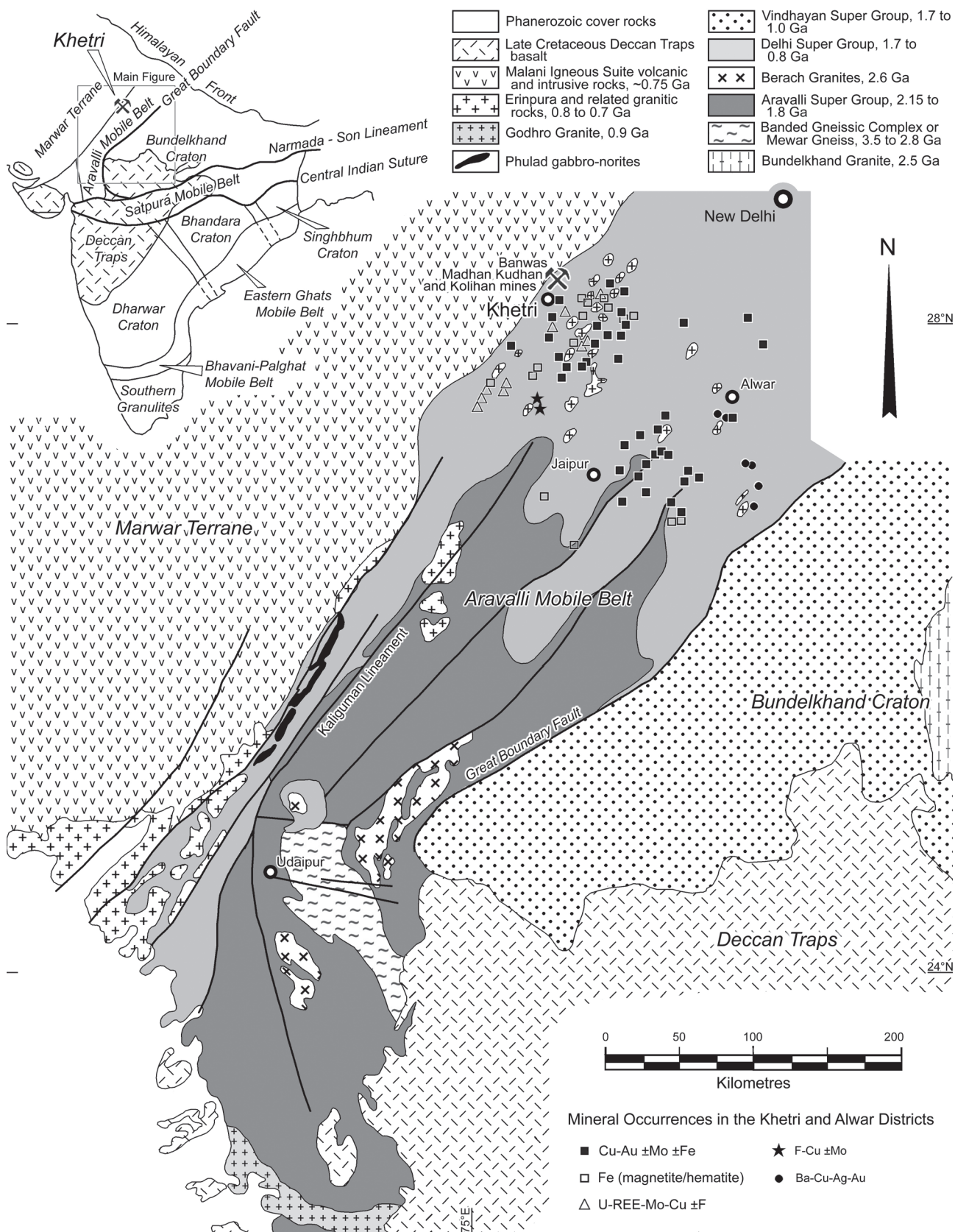


**Figure 11:** The tectonic framework, geological setting and distribution of main iron oxide-alkali altered mineralisation in the Aravalli-Bundelkhand Craton, Northwestern India. Note that only the mineral occurrences of the Khetri-Alwar district are shown (after Knight *et al.*, 2002; Meert *et al.*, 2010; Singh *et al.*, 2010).

*Khetri and Alwar District ... cont.*

crustal melting during extension or to an active 'hot spot' (Eby and Kochhar, 1990; Bhushan, 2000; Sharma, 2004).

The MIS constitutes the bulk of the exposed basement (below superficial cover) in the Marwar terrane, which forms the western margin to the Aravalli mobile belt, although the complex also overlaps well into the core of the mobile belt, mainly in the form of intrusive roots. No Archaean basement is exposed, or indicated by isotopic signatures within the Marwar terrane, suggesting it marks the western edge of the Archaean craton. The MIS is unconformably overlain by the red beds and evaporites of the Neoproterozoic to Cambrian Marwar basin (Meert *et al.*, 2010).

To the east of the Aravalli mobile belt (i.e., east of the Great Boundary fault), the bulk of the Bundelkhand craton is covered by the extensive, flat lying, 600 to 4500 m thick, Mesoproterozoic (1.7 to 1.0 Ga) Vindhyan Supergroup. This unit is made up of a sequence that includes conglomerates, sandstones, shales and a variety of limestones, including stromatolites (Meert *et al.*, 2010; Naqvi and Rogers, 1987).

Mineralisation within the Khetri district is controlled by shear zones, related to the major northeast-southwest trending Kaliguman lineament. It is hosted by the Mesoproterozoic Delhi Supergroup, described above. In the Khetri-Alewar district, the sequence comprises shallow-water, locally evaporitic, sedimentary, and lesser mafic and felsic volcanic rocks. This sequence is likely to have been deposited within a series of intra-cratonic rift basins, developed over an Archaean basement (Knight *et al.*, 2002, and sources cited therein). A regionally-continuous, stratigraphically conformable, breccia horizon, the Hornstone Breccia (Heron, 1917), is developed near the contact between the Alwar and Ajabgarh groups. It comprises angular fragments of quartz and quartzite in a massive iron oxide-rich chert matrix, interpreted to represent a breccia formed by evaporite dissolution (cf., Corella Formation, Mt Isa; Blake *et al.*, 1990).

The Delhi Supergroup rocks of both the Khetri and Alwar districts have been metamorphosed to low- to mid-amphibolite facies, deformed into northeast-southwest striking, doubly-plunging folds, and intruded by numerous 1.7 to 1.5 Ga syntectonic, and 0.85 to 0.75 Ga post-tectonic granitoids. The latter are broadly coeval with the Erinpura Granite and MIS events and comprise biotite- and hornblende-bearing tonalite to syenite, containing accessory magnetite, titanite, allanite, apatite and fluorite, and are geochemically characterised by  $Al_2O_3/(CaO+Na_2O+K_2O)$  ratios of <1.1, low Al and Ca, high Th and HFSE, and enrichment in LREE, indicating A-type affinities (Knight *et al.*, 2002).

### **District-scale Alteration and Mineralisation**

The Khetri line of deposits extends over a strike-length of >10 km and contains ~140 Mt @ 1.1 to 1.7% Cu, 0.5 g/t Au. It is hosted by garnet-chlorite schists, andalusite- and graphite-bearing biotite schists, and feldspathic quartzites, within sub-vertical northeast-striking shear zones. Mineralisation forms sub-vertical lens-like zones of stockwork, massive and vein-hosted chalcopyrite-pyrite-pyrrhotite with magnetite and hematite (Knight *et al.*, 2002).

This belt of copper deposits occurs on the western margin of a regional 50 × 100 km zone of calc-silicate and albite-haematite alteration that overprints and cross-cuts metamorphic fabrics, and contains widespread  $Cu \pm Au \pm Ag \pm Co \pm Fe \pm REE \pm U$  mineralisation. The calc-silicate assemblages occur as coarse-grained clinopyroxene-hornblende-epidote-apatite-scapolite-

titanite-magnetite. The albite-hematite alteration comprises albite-amphibole (actinolite)-hematite-magnetite-calcite, with variable K feldspar, biotite, epidote, scapolite, titanite, apatite and fluorite, and locally abundant pyrite and chalcopyrite. The albite-hematite alteration is spatially related to vein systems and breccias, which commonly contain copper and gold mineralisation, massive magnetite-hematite vein-deposits, fluorite and rare uraninite occurrences. Alteration is zoned, with calc-silicates found dominantly on the margins of the regional alteration system, while albite-hematite forms a central core, locally overprinting calc-silicate assemblages. Mineralisation-style within the system is also zoned, from (1) chalcopyrite-pyrite-pyrrhotite in graphitic schists at Akwali; and (2) chalcopyrite-pyrite-pyrrhotite-magnetite-hematite at Khetri, both in the northwest; (3) magnetite-hematite-chalcopyrite-pyrite in albite-haematite alteration, in the core, and (4) hematite-chalcopyrite-barite to the east. A SHRIMP U-Pb titanite age from the albite-hematite-amphibole-calcite-titanite assemblage constrains the timing of regional alteration to  $847 \pm 8$  Ma, which overlaps the fission-track ages of garnet from ore assemblages at the Madhan-Kudhan Cu mine at Khetri ( $897 \pm 125$  Ma). As such, this mineralisation temporally overlaps the post tectonic A-type granitoids of the district (Knight *et al.*, 2002).

## **Lao Cai District**

### **Crustal to Local Setting**

The Lao Cai district, which includes the producing Sin Quyen copper-gold mine, is located in northern Vietnam and neighbouring southern China, broadly following the northwest-trending Red River (Song Hong) fault zone.

The Red River fault zone is a major structural complex accommodating lateral strain associated with the Himalayan collision between the Indo-Australian and Eurasian plates. It lies within, and close to the northeastern margin of the similarly northwest-trending, ~200 km wide, Song Da mobile belt, which was developed over the southwestern edge of the South China plate/Yangtze craton, immediately adjacent to the suture with the Indochina plate to the south (Fig. 12a; Metcalfe, 1995).

The southern margin of the Song Da mobile belt is defined by the major northwest-trending Song Ma fault, and by the Cambrian to Devonian greenschist facies oceanic sediments (metagreywackes, greenschists, amphibolites, and marbles) and calc-alkaline to mafic volcanics (including ophiolites) of the "anticlinorial" Song Ma terrane immediately to its north. This terrane also includes low to high-grade unfossiliferous schists intruded by Devonian and Triassic granitoids and is characterised by large scale folding, thrusting and nappe formation, interpreted to indicate continent-continent collision in the early to middle Carboniferous (Metcalfe, 1995).

The Song Da rift zone occupies much of the interval between the Song Ma terrane and the Red River fault zone. It developed during the Permo-Triassic and was filled by marine volcanic and sedimentary rocks, deposited in an extensional basin on continental crust. The volcanic rocks include spilites, tholeiitic to calc-alkaline porphyritic basalts and komatiites. Basin inversion followed in the Jurassic, as evidenced by a period of folding and thrusting, and deposition of red-beds. During the Cretaceous to Miocene, calc-alkaline to alkaline felsic volcanism, with associated alkaline granitoids (144 to 89 Ma) and lesser gabbroids, commenced within the core of the earlier rift

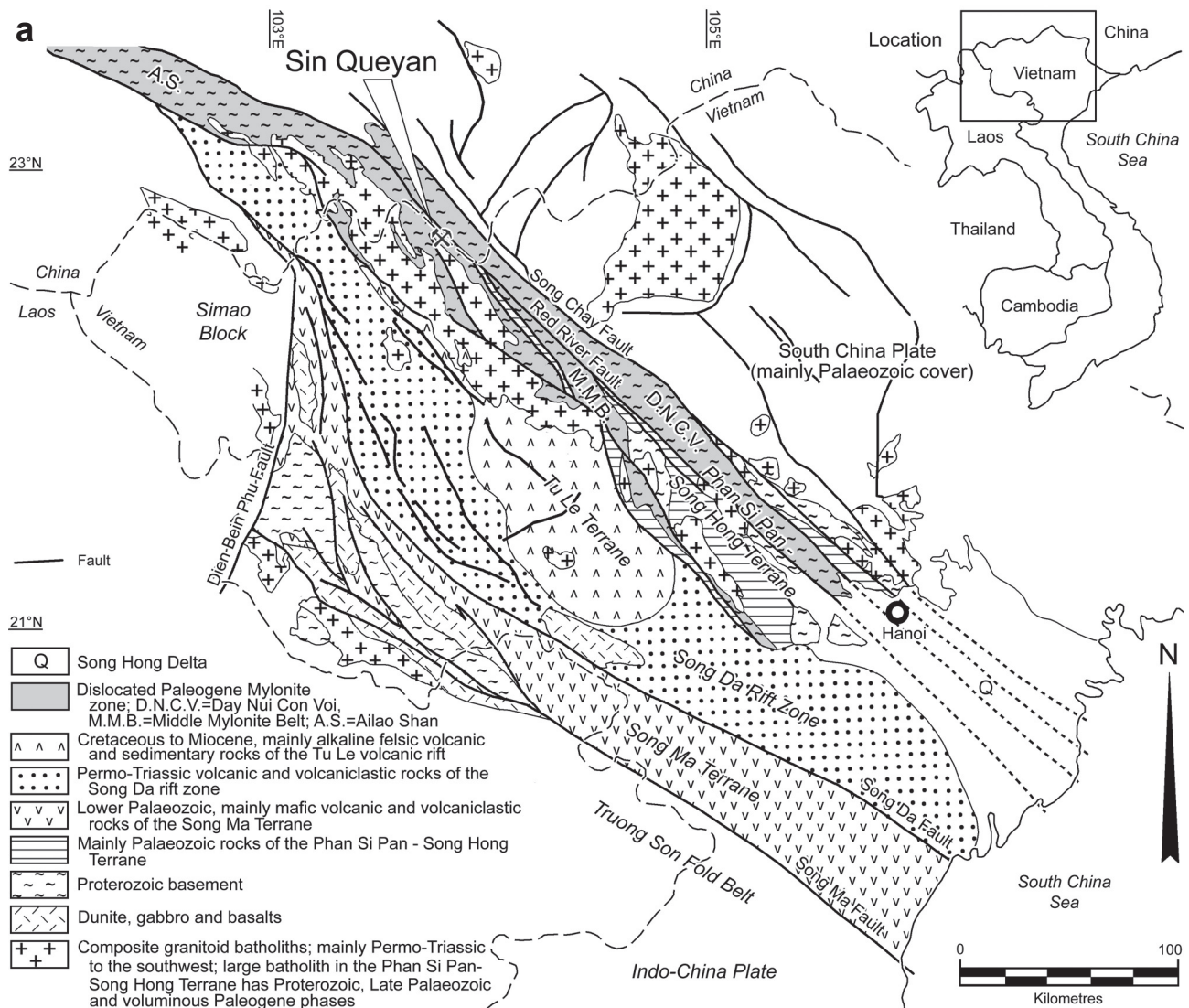
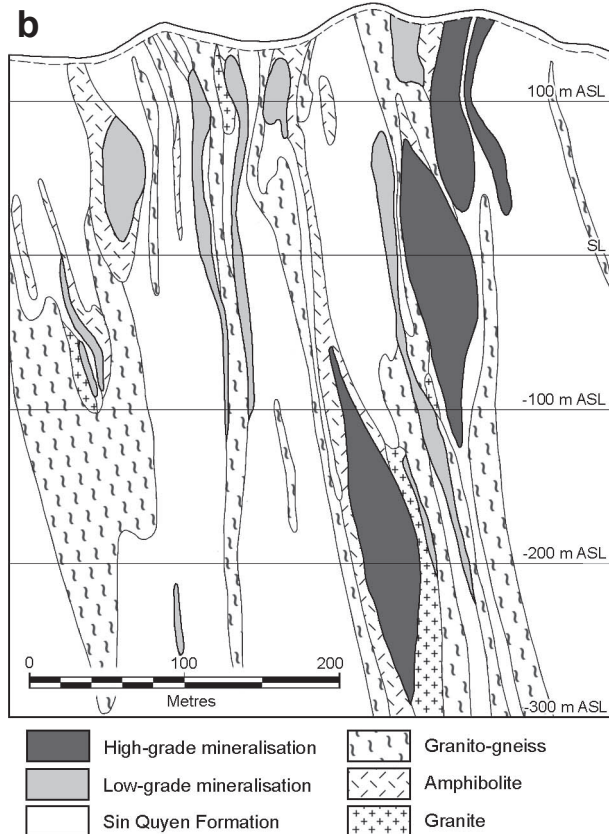


**Figure 12:** a - The tectonic framework and geological setting of the Song Da Mobile Belt in northern Vietnam, and the location of the Sin Queyan deposit of the Lao Cai District (after McLean, 2002; Khuong, 2010; Burchfiel *et al.*, 2008). b - Generalised cross section through the Sin Queyan deposit (after McLean, 2002).



basin, to define the Tu Le terrane (Khuong, 2010; McLean, 2001, and sources cited therein).

The northern edge of the Song Da mobile belt is occupied by the Phan Si Pan-Song Hong terrane, a broad band of Proterozoic metamorphic basement rocks, largely gneisses and schists, representing mafic volcanic and volcano-sedimentary rocks that have undergone multiple deformation and are locally migmatized. The principal regional metamorphism and deformation has been constrained between 2.36 and 1.96 Ga, although Permo-Triassic ages of 245 to 220 Ma (Carter *et al.*, 2001) are also recorded, all of which are overprinted by a diachronously partitioned Cenozoic mylonitisation with ages variably dated between 60 and 12 Ma (Burchfiel *et al.*, 2008).

Intrusive pulses within the Phan Si Pan-Song Hong terrane include late Palaeo- to Mesoproterozoic mafic and felsic rocks (as described below from the Sin Queyan deposit area); late Neoproterozoic (750 to 760 Ma) Po Sen complex diorite-granodiorite-granites; Devonian to Carboniferous Song Chay complex; Cretaceous (75 Ma) alkaline granitoids (granosyenite and granite) of the Muong Hum complex; and extensive Palaeogene (~35 Ma) I- and A-type granitoids (Khuong, 2010; and numerous sources cited therein).

Lao Cai District ... cont.

Sin Quyen and the other related iron oxide-alkali altered deposits of the Lao Cai district are hosted by the basement metamorphics of the Phan Si Pan-Song Hong terrane.

The Red River fault zone is predominantly restricted to the Phan Si Pan-Song Hong terrane. It represents a series of late brittle, dextral faults, which dislocated what may have originally been a single continental-scale mylonitic shear zone with sinistral, transpressive shear kinematic indicators. This mylonite zone is interpreted to have dipped northeast, underlain by a thrust that flattened into the middle crust, and overlain by a normal fault. The late brittle fault dislocation produced an *en echelon*, overlapping complex of at least three broad (up to 30 km wide) zones of intensely mylonitised rocks, represented in Vietnam by the Day Nui Con Voi, Middle Belt and Ailao Shan zones (Burchfiel *et al.*, 2008).

The Day Nui Con Voi is bounded to the northeast and southwest respectively by the brittle Song Chay and Red River faults. The Middle Belt is developed to the southwest of the Red River fault zone, while the southeastern extremity of the Ailao Shan zone occurs to the south of that again, tapering to the southeast and bounded by brittle faults (Fig. 12a; Burchfiel *et al.*, 2008).

Burchfiel *et al.* (2008) conclude that the metamorphosed and mylonitised lithologies on the northeastern margin of the Song Da mobile belt are largely metamorphosed Proterozoic rocks, but may also include mylonitised Palaeozoic and Mesozoic protoliths. Triassic and younger rocks locally separate the mylonite zones across brittle faults. During the early Cenozoic, all were metamorphosed to mid-amphibolite facies within the middle crust, and subsequently extruded within the mylonite zones, largely between 40 and 28 Ma (Burchfiel *et al.*, 2008 and sources cited therein).

The Sin Quyen deposit, which is located 300 km northwest of Hanoi, is hosted within strongly deformed, steeply dipping, amphibolite facies, migmatized gneiss and schist of the 800 m thick, Proterozoic Sin Quyen Formation. This formation, is divided into a lower, predominantly graphitic (~15 to 20%) quartz-feldspar-biotite-muscovite interleaved schist and gneiss unit, and an upper plagioclase-quartz-biotite gneiss. The lower Sin Quyen Formation, which is intruded by extensive "granito-gneiss", granite, pegmatite and amphibolite, is host to the bulk of the Sin Quyen alteration and mineralisation.

The Sin Quyen Formation conformably overlies metasediments of the Proterozoic Lung Po Formation, and at the surface, is overlain, across a faulted contact, by dolostones and shales of the Cambrian Cam Duong Formation. At depth, the upper Sin Quyen Formation is in faulted contact with limestones and marbles of the Neoproterozoic to Lower Cambrian Sa Pa suite (McLean, 2001).

The oldest intrusives within the deposit area are small, irregular, lensoidal, banded 5 to 50 × 10 to 100 m Proterozoic gabbros and amphibolites and albitised gabbro-dolerites (1777 Ma, Rb-Sr; 1036, Ar-Ar; Khuong 2010). These rocks are intimately associated with mineralisation, particularly where altered, and may contain up to 70% of the ore, and include all of the high grade zones (McLean, 2001).

Strongly deformed, gneissic and migmatized Proterozoic felsic intrusive rocks occur as 2 to 200 × 10 to 300 m lenses and dykes, overprinted by mylonitic fabrics. These "granito-gneisses" enclose enclaves of both amphibolite and biotite gneiss country rock (McLean, 2001).

Small, generally lensoid, younger granitoids, many being plagiogranites, are found intruding along faults, commonly occurring in close association with mineralisation. They are seen to cut the Neoproterozoic to Cambrian Sa Pa Suite. Ta Viet Dung *et al.* (1975) recorded these intrusives to be mineralised, and preceding sulphide development, and further, that magnetite accumulations only contained sulphide where they were present. McLean (2001) however, logged the same intrusives as post-mineralisation as they separate mineralised intervals and are themselves barren. Other young intrusives include plagioclase-quartz pegmatites and minor gabbro-dolerites.

### Alteration and Mineralisation

The Sin Quyen area is characterised by early widespread sodic alteration (albitisation), overprinted by more localised sodic-calcic and potassic-iron assemblages. The latter has completely altered amphibolites and biotite gneisses at Sin Quyen to form a hastingsite-biotite-quartz rock with accessory apatite, calcite, chlorite and epidote, that hosts virtually all of the magnetite and orthite mineralisation and the bulk of the sulphides (McLean, 2001).

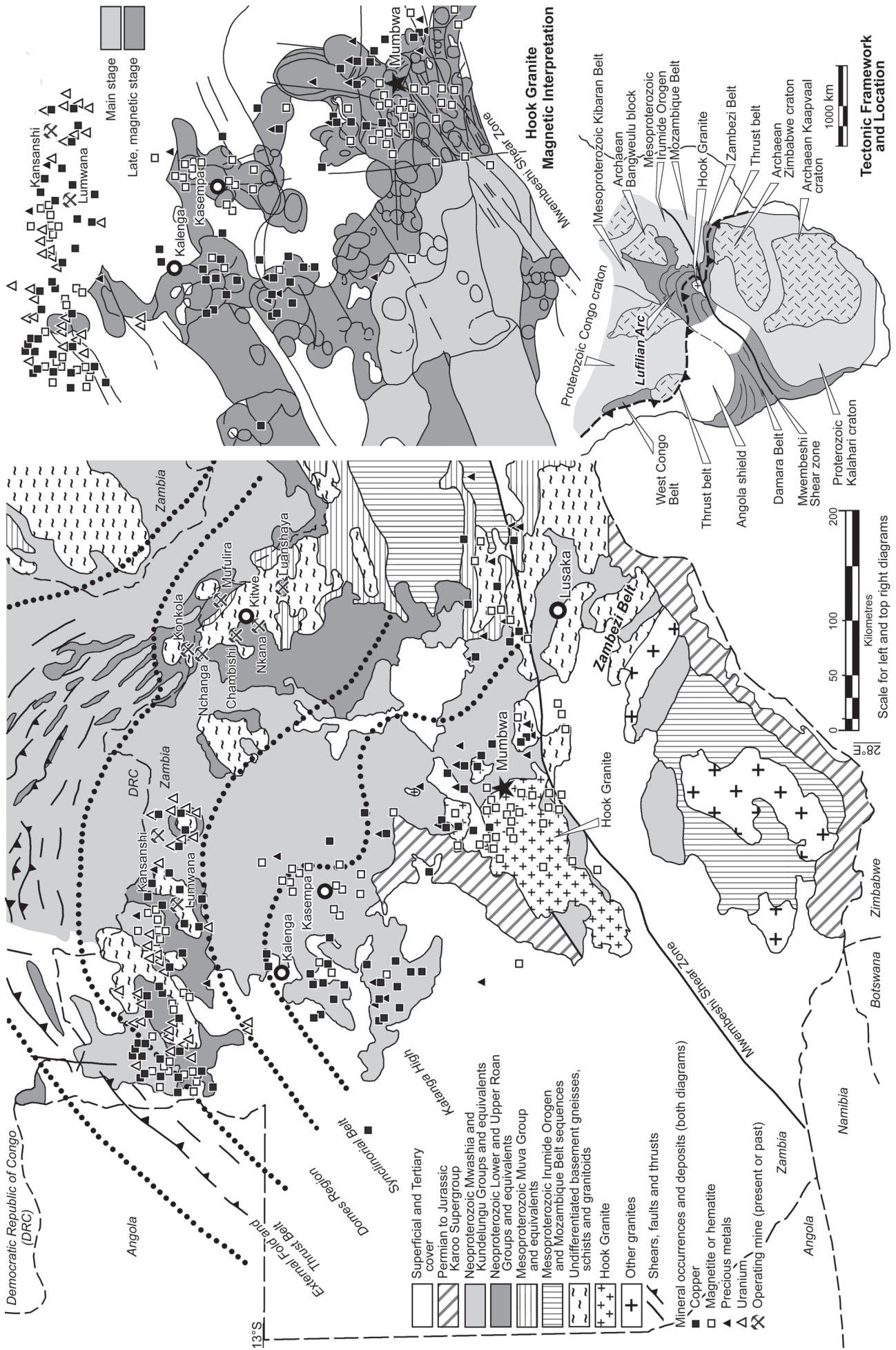
Alteration and mineralisation is interpreted to have taken place in two stages, an early metasomatic phase, characterised by early albite, followed by biotite and hastingsite, and lesser hedenbergite, epidote and garnet, with late stage magnetite and orthite, with lesser uraninite. This was followed by a hydrothermal phase accompanied by chalcopyrite, pyrrhotite and lesser pyrite (Ta Viet Dung *et al.*, 1975).

Magnetite occurs as disseminations and veins and is strongly developed as bands along foliations and as massive accumulations, generally in metasomatite, but also in adjacent biotite gneiss. It is generally closely associated with biotite and hastingsite, but is also found as mono-mineralic bands. Orthite is commonly associated with magnetite within the metasomatite, occurring as disseminations, but also in magnetite- and sulphide-poor hedenbergite-garnet skarn assemblages (McLean, 2001).

Sulphides are dominantly present as disseminations and foliation parallel bands and fracture fillings, also occurring as breccia cement within fractured magnetite bands. Two main generations of sulphide are recognised. The older is an early, minor, commonly deformed, phase of chalcopyrite-pyrrhotite-pyrite associated with quartz, forming veins cutting the magnetite and metasomatites. The second, dominant variety, which has not been deformed, comprises chalcopyrite and pyrrhotite with lesser pyrite. A number of sub-stages of the latter are also recognised, representing deposition at progressively declining temperatures (McLean, 2001). Gold is recognised both within the sulphides (both chalcopyrite and pyrrhotite-pyrite) and in the native form (~15%) (McLean, 2001).

Numerous occurrences of magnetite, from high to low grade, and variable associated copper mineralisation are found over an interval of several hundred kilometres along the Red River fault zone in Vietnam and China (McLean, 2001).

Ta Viet Dung *et al.* (1975) favoured a Proterozoic age for the metasomatic alteration and associated magnetite, orthite and uraninite (due to the close association of this assemblage with Proterozoic lithologies), and a Permo-Triassic emplacement, of sulphides on the basis of their lack of deformation, and interpreted association with Permo-Triassic plagiogranites. McLean (2001) suggested all of the mineralised phases are of Proterozoic origin, based on his observation that the younger plagiogranites



Lao Cai District ... cont.

post-dated mineralisation. However, the coincidence with the Red River fault zone would seem fortuitous, unless it represents a reactivated Proterozoic structure. Similarly the lack of influence by the Cenozoic mylonitisation would seem anomalous. Further work is required to resolve these relationships.

### **Structural Control and Brecciation**

Mineralisation at Sin Quyen is concentrated adjacent to major faults that parallel and are interpreted to be splays of the Red River fault zone. The deposit is reported to be hosted by extensive fault zones adjacent to the Sin Quyen reverse fault, which was described as a 50 m wide zone of “crushed, sheared and folded rock” (Ta Viet Dung *et al.*, 1975). Ore occurs as steeply northeast-dipping, anastomosing lenses (Fig. 12b), within a northwest-trending, 100 to 200 × 2500 m zone, that persists to depths of generally <500 m. Although northeast dipping, these lenses are stacked in a steeply southwest dipping envelope. In plan the mineralised zone has a gentle “S” shape, with the best grades concentrated in the central limb, consistent with sinistral dilation (McLean, 2001).

The main ore zone represents the largest of four discontinuous “broken zones” within banded, upper Sin Quyen formation quartz-feldspar gneiss, interpreted to be splays of the Sin Quyen fault. These zones are characterised by strong fracturing and dislocation of the gneissic fabric and the development clay-matrix tectonic breccias. Sulphide mineralisation appears to post-date deformation (McLean, 2001).

## **Lufilian Arc**

### **Crustal Setting**

The ~800 km long Lufilian Arc is developed within the Katangan fold belt in western Zambia, separating and lapping onto the Kalahari and Congo cratons of southern Africa. It is one of a number of similar Pan-African fold belts (West Congo, Damaran, Katangan and Zambezi) that fringe and/or separate these two cratons, and which may be interconnected below intervening Phanerozoic cover.

The Kalahari and Congo cratons are composites of earlier Archaean nuclei (e.g., the Kaapvaal and Zimbabwe cratons within the former) and Palaeo- and Mesoproterozoic elements amalgamated during the assembly of Rodinia.

The oldest basement rocks exposed as inliers within, and marginal to the Lufilian Arc, comprise a Palaeoproterozoic (~2.05 to 1.85 Ga) calc-alkaline magmatic arc sequence of metasediments, metavolcanics and intrusive granitoids of the Lufubu Metamorphic Complex (Rainaud *et al.*, 2005; Selley *et al.*, 2005). These rocks are part of a larger north-south to northwest-trending Ubendian magmatic arc, mainly underlying the Lufilian Arc in the east (Petters, 1986). Within the Zambian Copper Belt, these are unconformably overlain by a ~1.3 to 1.1 Ga supracrustal sequence of quartzite and metapelite, the Muva Group (Selley *et al.*, 2005).

The Archaean to early Palaeoproterozoic basement rocks of the Kalahari and Congo craton are separated from the Neoproterozoic sequence of the Lufilian Arc by the Mesoproterozoic Kibaran and Irumide successions respectively. These rocks represent the extensive, generally northeast-trending, Kibaran mobile belt. They comprise thick (>10 km) sequences of variously metamorphosed conglomerates, sandstones, shales with lesser dolerite flows, and overlying graphitic shales, stromatolitic limestones and dolostones. Deposition commenced at ~1.4 Ga, in response to extension caused by the impending breakup or Nuna/Columbia. Two main styles of granitoid intrusion are recognised, syn- and post-orogenic phases at ~1.25 to 1.3 and 1.2 to 0.95 Ga respectively. The syn-orogenic gneissic to un-metamorphosed granitoids accompanied compression and basin inversion, while those of post-orogenic origin are alkaline (Petters, 1986 and sources quoted therein).

In each of the Pan-African mobile belts of southern Africa, a ~200 m.y. period of tectonic quiescence followed the assembly of Rodinia, before extension and Neoproterozoic sedimentation heralded the commencement of its breakup. In the Lufilian Arc, the resultant Katanga Supergroup included an initial sequence of coarse grained, fluvial conglomerates and sandstones, dominantly siliciclastics, devoid of volcanic activity, within interconnected, but relatively restricted, fault controlled intracontinental rift basins. These depositional centres were subsequently enlarged and filled with organic-rich, marginal marine siltstone-shale sediments and then early evaporites. This package of rocks is represented by the Lower Roan Subgroup. The succeeding post-rift, thermal sag phase, produced the laterally more extensive platformal sequence of the Upper Roan Subgroup, comprising mixed carbonate and clastic rocks with abundant evaporitic textures and chaotic breccia (interpreted to represent the dissolution of evaporites). A second period of extension ensued, reflected by the local intrusion of ~765 to 736 Ma gabbroic sills in Zambia and equivalent pyroclastic and extrusive rocks in the northern part of the Arc (and possibly some A-type granitoids). This magmatism was accompanied by the deposition of a thick sequence of mixed carbonate and clastic sedimentary rocks, emplaced within a shallow to deeper marine setting, and included significant carbonaceous shales. This sequence, which overlies the Upper Roan Subgroup across either an unconformity, or a tectonic breccia, is divided into the Mwashia Subgroup and overlying Nguba Group, separated by the 10 to 1300 m thick Grand Conglomérat, a regional sequence of debris flows and glacial diamictites. Toward its northern limits, this succession is capped by the Kundelungu Group, comprising a basal glacial diamictite (Petit Conglomérat), and mixed carbonate and clastic rocks. The total thickness of the Katangan sequence varies from ~4 to ~9 km (Petters, 1986 and sources quoted therein; Selley *et al.*, 2005).

The equivalent sequence in the Zambezi belt includes a thick syn-rift, 879±19 Ma bimodal volcanic suite, which

**Figure 13** (facing page): The tectonic framework, geological setting and distribution of copper, iron oxide, gold and uranium mineralisation in the Lufilian Arc in Zambia, southern Africa. The location of the Mumbwa/Kitumba project deposit is shown with a star on the eastern margin of the Hook Granite. The geological map (left) is summarised from a range of published sources, including the Geological Survey Department of Zambia and Selley *et al.*, 2005. The top-right image is after Nisbet *et al.*, 2000 and shows their magnetic interpretation of the extent and distribution of the two main phases of the exposed and sub-surface Hook Granite in the Katanga High region of the Lufilian Arc, versus the distribution of copper, iron oxides, gold and uranium. This image is at the same scale, and has common reference points to the geological map on the left. It illustrates the wide extent of magnetite alteration/disseminations in the district. Note that the distribution of mineral occurrences is only shown for the area within and to the north of the Mwembeshi Shear Zone and west of the main mine sequence exposures of Zambian Copper Belt, which is indicated by the location of the major mines. The lower right diagram illustrates the tectonic setting of the Lufilian Arc (after Selley *et al.*, 2005, Porada and Berhorst (2000) and Kampunzu, and Cailteux, 1999).

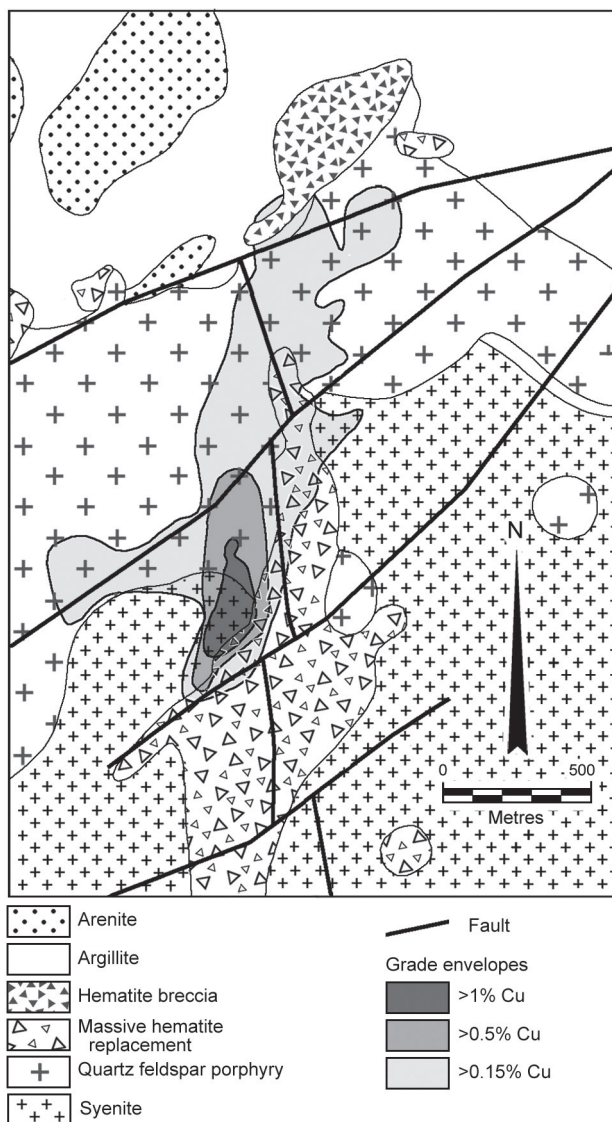


**Figure 14:** Geological plan of the Kitumba deposit, Mumbwa project, Zambia, showing the outline of the mineralised body projected to the surface (after Blackthorn Resources ASX releases, 2009, 2010).

is earlier than the commencement of sedimentation in the Lufilian Arc, which is limited by the basement ~880 Ma Nchanga Red Granite.

Small, but widespread developments of ~765 to 735 Ma mafic to intermediate magmatism, brackets the basal units of the Nguba Group, suggesting the main deposition may have ceased before 700 Ma (Selley *et al.*, 2005, and sources cited therein).

The main (post-Katangan) Lufilian orogenesis appears to span a period of >100 m.y., with the oldest metamorphic ages of ~590 Ma, the main stage orogenesis from 560 to 530 Ma and widespread dates of 510 to 465 Ma possibly recording post-orogenic cooling (Selley *et al.*, 2005, and sources cited therein). The late-tectonic composite Hook Granite, which cuts the Nguba Group, comprises an older, magnetically flat set of medium-grained biotite-hornblende granitoid intrusions, dated at  $559 \pm 18$  and  $566 \pm 5$  Ma in two samples. These are cut by numerous, younger microcline-biotite-hornblende megacrystic phases, reflected by donut-shaped magnetic anomalies with diameters of from <10 to 50 km, interpreted to represent anorogenic ring complex intrusions. Samples of these intrusions have been dated at  $533 \pm 3$  Ma (Hanson *et al.*, 1993; Nisbet *et al.*, 2000; Lobo-Guerrero, 2010).

The Lufilian Arc comprises four distinct, north-convex, arcuate tectonic subdivisions, the: (1) External fold and thrust belt to the northeast (hosting the Central African Copper Belt), characterised by thin-skinned thrust/nappe-dominated deformation, absence of exposed basement, low-grade metamorphism and repetition of the Katangan stratigraphy; (2) Domes region (which includes the Zambian Copper Belt in its outer margins), representing a thicker skinned deformation with upright folds, exposed basement domes (interpreted to represent culminations above thrust ramps), and upper-greenschist to upper-amphibolite facies metamorphism; (3) Synclinal belt, where sediments are subjected to large scale folding during at least two deformation events, and low grade metamorphism, which it has been suggested, reflects a change from a marginal shelf in the north, to a deeper basin (Cosi *et al.*, 1992; Porada and Berhorst, 2000); and (4) Katanga High to the southwest, in which only the upper parts of the Katangan Supergroup and almost all of the outcropping granitic intrusions of the Lufilian Arc are exposed (Petters, 1986; Selley *et al.*, 2005).

The northern margin of the Lufilian Arc is represented by the relatively undeformed top of the Kundelungu Group, whereas the southern limit is defined by the major, east-west trending, sinistral Mwembeshi shear zone which separates it from the Zambezi Belt. Kinematics suggest northwest to northeast directed thrusting during the Late Neoproterozoic to Lower Cambrian basin inversion orogenesis, with displacement vectors radiating perpendicular to the arcuate trend of the fold belt (Selley *et al.*, 2005). Porada and Berhorst (2000) and Kapunzu and Cailteux (1999) suggest the arcuate shape is the result of oblique compression during this event, between the northern margin of the Kalahari craton and the southwestern edge of the Congo craton (Fig. 13).

### Alteration and Mineralisation

A number of iron oxide-alkali altered mineralised systems occur around and within the Hook Granite in the Katanga High zone of the Lufilian Arc, apparently related to its magnetically anomalous younger (~533 Ma) stage (Hitzman, 2001; Nisbet, 2000). These include Kitumba (Mumbwa), the most significant IOCG *sensu stricto* deposit currently known in Zambia, located ~200 km west of Lusaka (Nisbet, 2000; Blackthorn Resources).

The Hook Granite batholith has proven to be complex, with numerous phases, both foliated and unfoliated, and extensive biotite-silica-K feldspar-tourmaline-epidote-magnetite-hematite-pyrite alteration. A detailed study of aeromagnetic data revealed the geophysical character described above that differentiates the younger stage of the Hook Granite apparently associated with iron oxide-alkali altered mineralisation. Extrapolation of this study has enabled the identification of areas with a similar expression, suggesting the presence of the same granitoids below wide areas of Phanerozoic cover in western Zambia, and at a relatively shallow depth within the Katanga Supergroup (Nisbet *et al.*, 2000).

The main exposed Hook Granite batholith in the Mumbwa area contains numerous iron and copper mineral occurrences while iron, gold and copper-silver mineralisation is found within the surrounding Katanga Supergroup sediments (Geological Survey of Zambia Mineral Maps; Nisbet, 2000). These occurrences are characterised by structurally-controlled, vertically oriented,

*Lufilian Arc ... cont.*

hematite-rich, pipe-like breccia zones, from a few hundred metres, up to several kilometres in length (Hitzman, 2001; Nisbet, 2000).

Studies within the external fold and thrust belt and domes divisions of the Lufilian Arc have identified a succession of regional alteration styles, largely reflecting the abundance of evaporites within the lower parts of the Katangan sequence. The earliest is a low temperature Ca-Mg-SO<sub>4</sub> anhydrite-, dolomite- and phlogopite-dominant stage, involving brine reflux below the Upper Roan Subgroup evaporites. This was followed by a potassic-dominant phase, also relatively low temperature, characterised by widespread, frequently intense development of K feldspar and locally sericite, best developed in rocks of the Lower Roan Subgroup, and associated with, but more extensive than, sediment hosted ore of the Zambian Copper Belt. The third phase is sodic, characterised by albite, commonly at the expense of K feldspar, best developed in the Upper Roan Subgroup, and locally within the Mwashia Subgroup and Nguba Group. This alteration is of regional extent, significantly more widespread than the Copper Belt mineralisation (Selley *et al.*, 2005).

In the Katanga High core of the Lufilian Arc, intrusive and sedimentary rocks within iron oxide-alkali altered mineralised systems have undergone initial albitisation (e.g., Kitumba; Lobo-Guerrero, 2010; 2005). The relationship of this sodic phase with that in the external fold and thrust belt and domes divisions, is unclear, other than possibly both being caused by the circulation of hypersaline brines generated from the abundant evaporites within the sequence. This early albitisation is overprinted by potassic alteration, characterised by the formation of K feldspar. Magnetite is subsequently introduced into these altered rocks, to be in turn replaced by hematite during a late hydrolytic (sericite-chlorite) alteration event (Hitzman, 2001; Lobo-Guerrero, 2010). These breccias have a matrix of metallic hematite and/or magnetite, with evidence of explosive hydrothermal activity. Densely packed, polymictic, 'round-clast' breccias, cemented by iron oxides, are a common feature (Lobo-Guerrero, 2010). Lobo-Guerrero (2010) suggests textures indicate the clast rounding is the result of silica leaching and corrosion by extremely alkaline and/or acid (F-rich) hydrothermal solutions which have etched angular rock fragments, rather than by milling.

Iron oxide altered breccia may be overprinted by a final sulphidation event, resulting in the precipitation of pyrite and then chalcopyrite, frequently accompanied by fluorite, galena and sphalerite. Mineralisation is hosted by the Hook Granite, and argillaceous and carbonate rocks of the Katanga Supergroup, sometimes with associated syenite. Gold mineralisation is usually found in silicified breccias hosted within a variety of rock types (Nisbet, 2000; Hitzman, 2001).

Lobo-Guerrero (2010; 2005), notes that sodic alteration is widespread and very important in the iron oxide-alkali altered mineralised systems of the Lufilian Arc, with scapolitisation and albitisation being observed surrounding these systems, at times extending outwards in various rock-types for up to more than a hundred kilometres.

A number of massive, breccia-hosted and vein-like magnetite-apatite deposits have been identified in central and northern Zambia, accompanied by sodic and sodic-calcic alteration. These magnetite bodies are associated with gabbro, "diorite" and syenite stocks or sills (~765 to 736 Ma?) which have undergone extreme sodic alteration,

resulting in the formation of albite-actinolite-scapolite assemblages and may represent an early phase of iron oxide-alkali altered mineralisation (Hitzman, 2001). One of the better examples of the latter is a north-south elongated, 150 × 50 km zone passing through Kasempa (~300 km northwest of Mumbwa) which contains ~230 Mt @ 66% Fe in 10 deposits, hosted by brecciated Upper Katanga Supergroup rocks associated with a suite of syenites. This mineralisation occurs as hematite or magnetite with sulphides as veins and replacements (Nisbet *et al.*, 2000).

Hitzman (2001) notes that a number of copper-(U-Au) deposits associated with intense sodic alteration (e.g. Kansanshi) are also observed in the inner portion of the Lufilian arc. The mineralisation at Kansanshi comprises three sets of high-angle, sheeted quartz-carbonate-sulphide veins (512 to 502 Ma) with envelopes of disseminated sulphides, cutting a sequence of Mwashia Subgroup (?) carbonaceous phyllites, quartz-biotite schists, biotite-garnet schists, impure marbles and quartz-muscovite phyllites (Torrealdy *et al.*, 2000). Although these deposits lack significant iron oxides, the intense sodic alteration is somewhat similar to that observed in many of the magnetite-apatite systems of the region (Hitzman, 2001).

The Kitumba IOCG *sensu stricto* mineralised system at Mumbwa is centred on a copper-gold anomalous hematite-sericite-quartz-apatite-barite-siderite alteration zone, with overlapping geophysical anomalies (magnetic, electrical, gravity and radiometric). It is located at the southern extremity of a north-south oriented, 25 km long corridor of continuous, but fluctuating geophysical anomalism associated with the eastern margin of the Hook Granite. Kitumba is the main and only significant resource delineated to date. The remainder of the trend has only returned narrow higher- (~0.9% Cu) or broad low-grade (~0.2% Cu) copper mineralisation in drill intersections (Blackthorn Resources releases; Lobo-Guerrero, 2010).

The mineralisation at Kitumba is associated with a large-scale and highly variable magmatic-hydrothermal iron oxide breccia complex, that exhibits signs of multiple brecciation. The dominant feature is a north-south oriented massive hematite replacement breccia zone that is ~1750 m long, by 100 to 500 m in width. The breccia is centred on a north-south fault zone that has been dislocated into at least four segments with offsets of ~100 m each, by northeast trending faults, with the breccia outline also influenced by the cross faults. The breccia is developed within syenite and quartz feldspar porphyry of the Hook Granite, to within 200 m of the northeast-trending contact with argillite and arenite of the Nguba Group. Numerous other hematite breccias are also found along the intrusive contact (Blackthorn Resources releases).

Copper mineralisation at Kitumba, comprises a simple hypogene pyrite-chalcopyrite assemblage, that has been extensively modified by deep weathering and oxidation, resulting in a redistributed supergene oxide assemblage of native copper and secondary copper minerals in the form of malachite, copper phosphate minerals, covellite, digenite, chalcocite and bornite. The secondary copper minerals are distributed within fractures and as linings in cavities. Higher grade zones are related to supergene-enriched sulphides and oxides, particularly concentrations of native copper, malachite and chalcocite (Blackthorn Resources releases).

The main Kitumba deposit contains an *in situ* JORC compliant inferred mineral resource of 87 Mt @ 0.94% Cu, (using a 0.5% Cu cut-off), enclosing a high grade core of

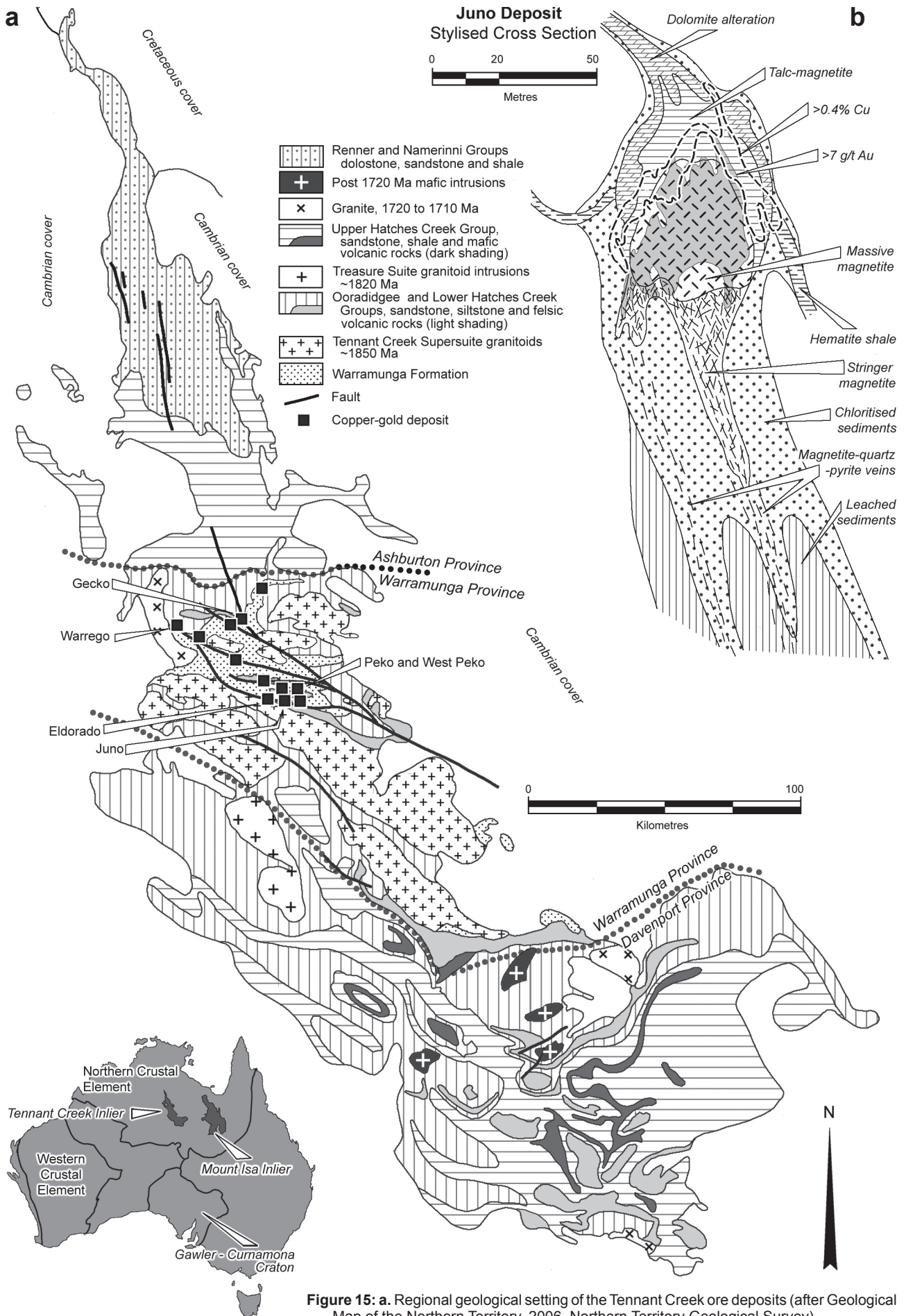


**Figure 15:** a. Regional geological setting of the Tennant Creek ore deposits (after Geological Map of the Northern Territory, 2006, Northern Territory Geological Survey).  
 b. Stylised cross section through the Juno orebody showing the geology, alteration and distribution of mineralisation (after Wedekind *et al.*, 1989).

Lufilian Arc ... cont.

22 Mt @ 1.73% Cu, 0.05 g/t Au, 1.20 g/t Ag, 0.036 kg/t U (using a 1.0% Cu cut-off). The 0.5% Cu cutoff encloses a coherent body that extends from a depth of ~120 to 600 m below the surface, that is around 600 m long by 200 m wide. These are in turn enclosed within a much larger resource of 345 Mt @ 0.47% Cu, using a 0.2% Cu cut-off (Blackthorn Resources releases).

East-west to eastnortheast-trending faults appear to be an important control on the distribution of alteration, mineralisation and intrusion within the inner (southwestern) sections of the Lufilian Arc, although due to the degree of cover and lack of detailed mapping many of the inferred structures have not been confirmed (Lobo-Guerrero, 2010).

## Tennant Creek Inlier

### Crustal Setting

The Tennant Creek Inlier is located ~900 km southsoutheast of Darwin in the Northern Territory of Australia. It hosts a cluster of small, but high grade gold-copper-bismuth deposits, associated with magnetite and/or hematite ironstones, that are distributed over an area of ~70 × 50 km. Examples of the largest and highest grade deposits include Peko (3.2 Mt @ 4% Cu, 3.5 g/t Au, 0.2% Bi, 14 g/t Ag) and Juno (0.45 Mt @ 0.4% Cu, 57 g/t Au, 0.6% Bi, 7 g/t Ag). The total production to 2000 was in excess of 156 tonnes of gold and 345 000 tonnes of copper since mining commenced in the 1930s.

The Palaeoproterozoic Tennant Creek Inlier is elongated in a northnorthwest to northwest direction, covering an area of ~44 000 km<sup>2</sup>, ~500 km west of the Mount Isa Inlier (Le Messurier *et al.*, 1990). It is composed of three elements, the central of which, the Warramunga Province, hosts all of the mineralisation. The mineralised province is bounded to the north and south by overlying sequences of the coeval Ashburton and Davenport provinces respectively, while the inlier as a whole is surrounded by flat lying, mainly carbonate facies Cambrian rocks of the Wiso and Georgina basins to the west and east respectively, and by Mesozoic and younger cover (Shaw *et al.*, 1996).

The exposed Warramunga Province is the central portion of a largely concealed block of Palaeoproterozoic rocks that extends over an area of ~350 × 60 km, elongated in a eastsoutheast direction (Shaw *et al.*, 1996), almost perpendicular to the trend of the inlier, but parallel to, and approximately 200 km north of the southern boundary of the North Australia craton. Assembly of this craton commenced prior to 1.9 Ga, to be consolidated and cratonised by ~1.83 Ga, although repeated terrane accretion and orogenic activity continued along its southern margin to ~1.40 Ga (Plumb 1979, Myers *et al.*, 1996).

Deposition within the Warramunga Province commenced with a thick turbidite succession, the Warramunga Formation, which is unconformably overlain by sedimentary and felsic volcanic rocks of the Ooradidgee Group. Pre-Warramunga Formation basement is not exposed, although drill holes 30 km to the south west of the exposed Warramunga Province have intersected almandine-amphibolite facies gneisses with a Rb-Sr age of 1920±60 Ma, and Sm-Nd and Rb-Sr modal ages of crystallisation of at least 2.4 Ga.

The Warramunga Formation, which is ~3000 m thick, was deposited in a rift basin at ~1.86 to 1.85 Ga, and hosts the bulk of the known mineralisation of the Tennant Creek Inlier (Donnellan *et al.*, 1994; Compston 1995). It is composed of turbiditic greywacke, siltstone and shale,

which are in part tuffaceous, and notably iron-rich. The sequence contains abundant disseminated detrital and metamorphic magnetite, and numerous thin hematitic carbonate-bearing siltstones and shales, including an argillaceous banded ironstone that is known locally as the 'hematite shale'. An interbedded dacite lava is dated at 1862±5 Ma (Smith, 2001).

The angular unconformity at the top of the Warramunga Formation corresponds to the Tennant Event, when the sequence was metamorphosed to greenschist facies and the ~1850 Ma (Page 1995) Tennant Creek Super-suite was emplaced, comprising syn- to post-tectonic I-type granitoids, quartz-feldspar porphyry and minor mafic intrusions. This magmatism and tectonic activity represents the early stages of the Barramundi Orogeny, that is recognised across northern Australia (Donnellan 2005; Donnellan *et al.*, 1994; Compston 1995; Skirrow, 2000; Stolz and Morrison, 1994; Etheridge *et al.*, 1987)

The up to 5000 m thick Ooradidgee Group immediately overlies the Tennant Event unconformity and comprises a suite of felsic volcanic rocks, predominantly dacitic to rhyolitic ignimbrites, (but with broadly coeval basalts, representing bimodal volcanism) with associated felsic sills and a possible monzodiorite, emplaced between 1845±4 and 1827±9 Ma (Compston, 1995). The sequence was emplaced within a continental rift setting (Hussey *et al.*, 1994), associated with continuing, localised extension belonging to the late stages of the Barramundi orogenic cycle. The sequence also includes sandstones, siltstones, shales, cherts and tuff. Deposition ceased soon after the emplacement of the ~1820 Ma Treasure Suite granites, granophyre, and monzodiorite-diorite (and comagmatic volcanic rocks) and the variably developed 1810 Ma Murchison Event unconformity which separates the Ooradidgee and the Tomkinson Creek and Hatches Creek groups. In places this contact appears to be transitional, with volcanism and any break in deposition diachronously migrating southward. This event also marks the transition from rift to sag phase sedimentation in the Davenport geosyncline (Smith, 2001, and sources cited therein).

The temporally equivalent Tomkinson Creek and Hatches Creek groups are composed of thick, well stratified sequences, respectively comprising ~6 km of silicified marine sandstone in the Ashburton Province to the north, and in the Davenport Province to the south, up 10 000 m of sandstone, siltstone and shale, with felsic volcanic rocks and basaltic lava towards the base. Both of these groups were terminated by the ~1720 Ma Davenport Event which was accompanied by a suite of post-mineralisation 1720 to 1710 Ma S-type granites (Page, 1995; Smith, 2001, and sources cited therein).

### Alteration and Mineralisation

Mineralisation within the Tennant Creek field is associated with ironstone bodies, characterised by ellipsoidal, lens, cigar-like and irregular geometries, that range in size from a few tonnes to several tens of millions of tonnes. In excess of 650 ironstone bodies are recorded in the Inlier, although only 25% contained any ore grade Cu, Au or Bi, many of which were only very minor in size, and only 100 of these have been mined in any way. Barren ironstones are dominantly composed of magnetite and/or hematite with variable amounts of quartz, chlorite, dolomite and talc, whereas those that are mineralised, also contain sulphides, sulphosalts, and minor muscovite. The ironstones display a range of textural variations, including

*Tennant Creek Inlier ... cont.*

iron oxides that occur as: (1) massive fine to medium grained intergrowths; (2) diffusely-banded to mottled with quartz and chlorite; (3) fine-grained, colloform-banded varieties with quartz; and (4) skeletal and growth-zoned magnetite. Both replacement and infill textures are evident (Wall and Valenta, 1990; Davidson and Large, 1998). Large (1975) observed microtextures suggesting the earliest assemblages involved hematite or hydrated iron-oxides, which were overprinted by magnetite.

Both the barren and mineralised ironstones are zoned, grading downward from massive accumulations, into root zones of replacement and networks of magnetite-quartz±hematite stringer veins, together forming pipe-like geometries that may persist in some cases for up to several hundred metres vertically, all of which are enveloped by chloritic alteration extending for centimetres to metres out from the iron oxides. Talc and dolomite alteration are also observed, and both host sediments and ironstones are frequently variably brecciated on a deposit- to local-scale (Skirrow, 2000; Skirrow & Walshe, 2002).

Ironstones generally vary from transgressive to bedding localised in a variety of structural settings including antiformal fold closures, faults, shears and contacts of felsic porphyry intrusions (Ivanac, 1954), particularly in conjunction with contacts between rheologically contrasting lithologies. A strong structural control is also indicated by several east-west lines or trends of ironstones. Some ironstones are also spatially related to locally calcite-bearing 'hematite shale' units which may have acted as chemical triggers to ironstone precipitation where they were encountered by conduits carrying magnetite-stable fluids (Large, 1975; Wedekind *et al.*, 1989).

Well developed  $S_1$  foliation in the chlorite alteration suggests early- to syn-  $D_1$  timing for the development of the ironstones. The colloform textures of early hematite and/or hydrated iron oxide deposition (Large, 1975) are consistent with a relatively low temperature of initial formation, supported by fluid inclusion homogenisation temperatures of 120 to 180°C (not pressure-corrected; Khin Zaw *et al.*, 1994; Huston *et al.*, 1993; Skirrow, 1993). However, calculated chlorite formation temperatures, and oxygen isotope geothermometry on quartz-magnetite pairs, in both barren and mineralised ironstones, indicate a temperature of formation of ~300 to 400°C, for magnetite-chlorite replacing the early hematite assemblage (Skirrow, 1993), consistent with formation during lower greenschist facies regional metamorphism (Wall and Valenta, 1990). The ironstone bodies are also calculated to have formed from hot (350 to 400°C) NaCl+CaCl<sub>2</sub> brines at pressures of ~2.5 to 5 kb (Wedekind and Love, 1990; Skirrow and Walshe, 2002).

Khin Zaw *et al.* (1994), Huston *et al.* (1993), Skirrow (1993) and Skirrow and Walshe (1994) agree that the fluids responsible for ironstone-formation were calcic brines with 10 to 20 wt.% NaCl<sub>equiv.</sub>

Although deposits across the district share many key characteristics, they have widely varying Au:Cu and magnetite:hematite ratios, iron-sulphide mineralogies, and sulphur isotope composition (Wedekind *et al.*, 1989; Wall and Valenta, 1990; Huston *et al.*, 1993; Skirrow, 1993; Davidson and Large, 1998). These variations may be regarded as representing a spectrum of ironstone-related styles between two compositional end-members: (1) reduced (magnetite-pyrrhotite), copper-rich deposits with narrow ranges of  $\delta^{34}\text{S}_{\text{sulphide}}$  values (0 to 4‰) and magnetite-muscovite-Mg chlorite alteration assemblages (e.g., West Peko), and (2) oxidised (hematite-

magnetite±pyrite), gold-rich deposits with wide ranges of  $\delta^{34}\text{S}_{\text{sulphide}}$  values (-15 to 7‰) and hematite-chlorite-muscovite±pyrite alteration (e.g., Eldorado; Skirrow & Walshe, 2002). Many of the larger, high grade gold deposits lie between these extremes, characterised by minerals of intermediate oxidation-reduction state (Skirrow, 2000).

At the West Peko deposit, gold-copper-bismuth is interpreted to have formed at 300 to 340°C from pyrrhotite±magnetite-stable, weakly acidic, sulphur- and N<sub>2</sub>±CH<sub>4</sub>-rich, low salinity (3 to 10 wt.% NaCl<sub>equiv.</sub>) hybrid metamorphic and/or formation fluids (Skirrow, 1999; Skirrow and Walshe, 2002). The same authors suggest these fluids flowed along shear and fault zones which trapped reduced rock packages below oxidised Warramunga Formation, with gold and bismuth deposited in response to desulphidation±oxidation of the reduced fluid as it reacted with magnetite±hematite ironstone. They also suggest desulphidation could have been driven by precipitation of chalcopyrite, pyrite, pyrrhotite and bismuth-sulphides or sulphosalts in response to increased pH of the fluids (Skirrow, 1999; Skirrow and Walshe, 2002).

Mineralisation at Eldorado is interpreted to have formed from an intermediate  $fO_2$ , low- to moderate-salinity fluid, which mixed with hematite-stable Ca-Na-Cl brine in the presence of magnetite-rich ironstone (Skirrow and Walshe, 2002). Fluid mixing likely caused an increase in copper solubility leading to undersaturation of copper minerals and the deposition of copper-deficient gold-bismuth mineralisation.

According to Skirrow (2001), with the exception of several data from West Peko, all oxygen-hydrogen isotopic compositions of fluids lie outside and above the generally accepted field for magmatic waters ( $\delta^{18}\text{O}_{\text{fluid}} = 0$  to 6‰;  $\delta\text{D}_{\text{fluid}} = -40$  to -10‰; Wedekind, 1990; Huston, 1991; Skirrow, 1993). Input of evolved surficial waters (e.g., formation waters or their higher temperature equivalents) appears necessary to generate the oxygen-hydrogen isotopic compositions, but contributions of magmatic or metamorphic waters cannot be precluded. All of the textures and mineral relationships point to the copper and iron sulphides, bismuth minerals (including bismuthinite and a range of seleniferous Bi±Pb sulphosalts; Large, 1975), and gold overprinting the magnetite-rich ironstones.

Published <sup>40</sup>Ar/<sup>39</sup>Ar ages for gold-copper-bismuth-mineralisation in the Tennant Creek region range from 1825 to 1829 Ma, apparently younger than the timing of deformation bracketed by <sup>207</sup>Pb/<sup>206</sup>Pb zircon ages of igneous rocks at ~1850 Ma. Recalculation using revised estimates of the <sup>40</sup>K decay constant and age of the <sup>40</sup>Ar/<sup>39</sup>Ar standard shifts the <sup>40</sup>Ar/<sup>39</sup>Ar ages to 1851 to 1847 Ma, in excellent agreement with <sup>207</sup>Pb/<sup>206</sup>Pb zircon ages from Tennant Supersuite igneous rocks and with local geological constraints (Fraser *et al.*, 2008) and the Barramundi orogenic cycle volcanic rocks of the Ooradidgee Group. This implies the Tennant Event metamorphism and continuing magmatism is coeval with mineralisation.

District-wide iron oxide alteration is evident, although no regional sodic alteration has been recognised in the Warramunga Province, possibly reflecting the apparent lack of evaporites in the sequence. Strongly developed deposit scale magnetite-hematite with chlorite-muscovite and biotite alteration is characteristic of the ores. Ore fluid temperatures of ~340 to 400°C for the earlier ironstone formation during early  $D_1$  and ~300 to 350°C for the late  $D_1$  emplacement of sulphide mineralisation are generally lower than in many IOCG *sensu stricto* deposits.

## Great Bear Magmatic Zone

### Crustal Setting

The Great Bear Magmatic Zone (GBMZ) is located on the western margin of the exposed Canadian Shield in the Northwest Territories of Canada. It is an extensive, 1.88 to 1.84 Ga, largely felsic, volcano-plutonic complex, developed along a continental suture zone. It overlies a Palaeoproterozoic, ~2.1 to 1.88 Ga magmatic arc, the Hottah terrane, which had been accreted to the western margin of the Archaean Slave craton during the short-lived ~1.90 to 1.88 Ga Calderian orogeny (Corriveau *et al.*, 2010 and sources quoted therein). The GBMZ is exposed over an area of 450 × 100 km, although, magnetic data suggest it may have a total length of 1200 km below cover. Felsic and intermediate magmatism predominates, occurring as batholiths, subvolcanic intrusions and volcanic rocks, with coeval mafic magmatism as minor volcanic rocks, dykes and sills (see Fig. 4, in Corriveau *et al.*, 2010 in volume 4 of this series). The complex is cut by a series of northeast trending, deeply penetrating, dextral faults that Mumin *et al.*, 2009 interpret to reflect southeast-directed extension. These faults host the mafic dykes mentioned above. Regional scale iron oxide-alkali altered mineralised systems are documented throughout the exposed GBMZ. The magmatism, which is interpreted to have been both a thermal catalyst and fluid source to hydrothermal activity, ceased at 1.84 Ga. The GBMZ is interpreted to represent a voluminous accumulation of continental magmas emplaced after arc-continent collision and orogenic collapse, on top of an eroded arc and suture (Hildebrand *et al.*, 2010). Isotopic signatures of GBMZ volcanic and plutonic rocks do not indicate the presence of underlying Archaean crust, although magnetotelluric data reflects the upper surface of a west dipping, wedge-shaped Archaean lithospheric root extending from the Slave craton exposed to the east. At depth, the edge of this root reaches a position that is below the eastern margin of the exposed Hottah terrane. In addition, to the west, a resistive cratonic root imaged to a depth of ~200 km occurs below the Hottah terrane, with a less resistive region underlying the GBMZ, separating the two roots. Each of these discontinuities is sharply defined. The magnetotelluric data shows the Wopmay Fault Zone, which marks the eastern limit of the GBMZ, only extending to mid-crustal levels where it intersects the Archaean lithospheric wedge. The currently known IOCG systems in the GBMZ occur above some of these discontinuities.

The bulk of the IOCG-style mineralisation in the GBMZ is associated with alteration systems that are developed systematically outwards from sub-volcanic intrusions i.e., unlike most IOCG mineralisation, they do exhibit a close spatial relationship with intrusions.

### District-scale Alteration and Mineralisation

Corriveau *et al.*, (2009 and 2010) have studied excellent cross-sectional exposures of alteration and mineralisation systems from the Port Radium-Echo Bay, NICO-Sue Dianne, DeVries and Fab Lake districts within the Great Bear Magmatic Zone (GBMZ) that illustrate the regional-scale build-up of hydrothermal systems coeval with, but also spatially related to the magmatism of the region. See Corriveau *et al.* (2010), in volume 4 of this series, for locations mentioned below, geological diagrams and detailed descriptions. This section will briefly summarise two deposits in the south, NICO and Sue-Dianne, and

compare their characteristics with conclusions from the Port Ray-Echo Bay district, further north.

The southern of these two districts contains "IOCG", uranium and iron occurrences, with associated magnetite-rich, K feldspar and magnetite-to-hematite vein, breccia and replacive alteration. This mineralisation and alteration is hosted by remnants of the pre-1.88 Ga supracrustal marine metasedimentary rocks (siltstones, subarkosic-wacke and arenite) of the Treasure Lake Group, and by an unconformably overlying 1.86 Ga rhyolite to rhyodacitic volcanic complex (Faber Group). The Faber group is composed of thick-bedded rhyolite to rhyodacite tuffs, flows and lesser volcanoclastic rocks. It includes basal heterolithic breccias (containing clasts from the underlying sediments), massive to flow-banded, potassium feldspar-altered rhyolite (felsite), with or without magnetite laminae, overlain in turn by thick-bedded, ash-flow tuffs with lesser porphyritic flows, lapilli tuff and volcanoclastics. Granitoids of the Marian River Batholith underlie and intrude the Treasure Lake Group, and are source plutons for, and partially intrude the volcanic rocks of the Faber Group. Sub-volcanic porphyry stocks and bimodal porphyritic dyke swarms link the Marion River batholith with zones of economic mineralisation at Sue-Dianne and NICO respectively. At both of these deposits, the IOCG alteration was temporally coeval with extrusion of these GBMZ volcanic rocks.

The Sue-Dianne copper-gold-silver deposit is hosted by a structurally controlled hydrothermal breccia complex, constrained entirely within the pre-existing 400 m wide, northeast-trending, Dianne Lake fault zone, where it intersects the north trending MAR fault (Goad *et al.*, 2000). Textural evidence indicates these structures were active both during and after mineralisation. The breccia complex was developed within well-preserved rhyodacite ignimbrite sheets of the Faber Group (Gandhi, 1989). Hydrothermal brecciation emanates from the apex of an albitised porphyry stock low in the complex, extending upwards for approximately 300 m to where it is assumed to have breached the palaeosurface. These breccias are now capped by an interpreted fall-back breccia and palaeogolith. Breccia clasts are strongly altered to K feldspar ± epidote, chlorite, hematite and sulphide, and are composed of rounded to sub-angular fragments of welded and crystal tuff, and occasionally of altered porphyry stock. The core of the complex comprises both clast- and matrix-supported breccia, and grades progressively outwards into structurally controlled fracture breccia. The hydrothermal matrix is composed of magnetite, hematite, K feldspar, chlorite, epidote, garnet, fluorite, chalcocopyrite and pyrite. Distal hydrothermal effects take the form of giant quartz veins, stockwork and breccia complexes, and pervasive silicification, accompanied by minor K feldspar, epidote, sericite and/or hematite. At depth, the core of the deposit is barren magnetite-pyrite, grading upwards to magnetite-hematite-chlorite-epidote-fluorite-andradite-chalcocopyrite matrix breccias. The peripheral and structurally higher levels of the system are dominated by hematite with bornite mineralisation (Goad *et al.*, 2000; Mumin *et al.*, 2010; Corriveau *et al.*, 2010).

Economic mineralisation at NICO, which is 25 km south of Sue-Dianne, occurs over a vertical stratigraphic interval of ~300 m, from the base of the Faber Group volcanic rocks where minor mineralisation is hosted, downward into the Treasure Lake Group, predominantly within strongly altered siltstone and arkose. Mineralisation occurs as a series of subparallel stratabound lenses, individually up to ~50 m in

*Great Bear Magmatic Zone ... cont.*

thickness and ~1 km in length. These are accompanied by intense hydrothermal iron oxide (dominantly magnetite)-hornblende-biotite-K feldspar  $\pm$ tourmaline  $\pm$ carbonate, carbonate-magnetite or K feldspar replacement alteration, and by veins, stockworks and breccias. At depths of >300 m, metasediments are hornfelsed, possibly through contact metamorphism by the immediately underlying Marion River Batholith. There is a general outward progression of alteration, from core to periphery, of albite, magnetite=pyrrhotite or pyrite, magnetite-hornblende-biotite-tourmaline, hematite-hornblende-biotite, biotite, K feldspar and distal sericite. The most peripheral and/or youngest hydrothermal effects include giant quartz complexes and quartz-epidote veining and alteration. Brecciation and intense K feldspar and other alteration styles are common at the interface of porphyritic dykes and altered sediments and within some of the mineralisation zones (Corriveau *et al.*, 2010). Gold, cobalt, bismuth and copper mineralisation is thought to have been introduced in two phases: (1) an early iron oxide event dominated by magnetite with minor chalcopyrite, native bismuth and possibly some gold; and (2) the main economic mineralisation during a later overprinting phase, mainly of cobaltian arsenopyrite, cobaltite, bismuthinite, native gold, gold-bismuth-tellurium alloys and pyrite=chalcopyrite (Corriveau *et al.*, 2010).

Corriveau *et al.* (2010), interpret the Port Radium-Echo Bay district, 250 km to the north, to represent a large 1.87 to 1.86 Ga stratovolcano/cauldron collapse structure, dominantly composed of porphyritic to amygdaloidal andesitic tuff, flows, breccia and debris flows, with a comagmatic core comprising a complex of dioritic sub-volcanic stocks and plutons. Alteration is centred on, and most intense within, the core sub-volcanic diorite intrusions, with a progressive outward mineral zonation into the andesitic wallrocks. This zonation includes sodic=calcic (albite=amphibole), calcic-iron=sodic (magnetite-actinolite-apatite=albite), high-temperature and lower-temperature potassic-iron (K feldspar/biotite-magnetite and sericite-hematite respectively,  $\pm$ local skarn alteration), phyllic (quartz-sericite-pyrite), propylitic (chlorite-epidote-carbonate $\pm$ sericite-albite) and distal to late epithermal quartz-carbonate-hematite veins. Alteration and mineralisation is present as early replacive impregnations, overprinted by veins, stockworks or breccias, all occurring at varying intensities. A variety of mineralisation occurs within various zones of this system including, vanadium bearing iron oxide-apatite; breccia, replacive and skarn-hosted base metals (Zn, Pb, Ag, Cu, Co, Ni); and distal, epithermal-like quartz-carbonate-hematite-sulphide-arsenide veins containing variable U, Cu, Ag, Co, Bi, Ni, Pb and Zn. For detail, see Corriveau *et al.* (2010, in volume 4 of this series).

Corriveau *et al.*, (2009 and 2010), after comparing the Sue-Dianne and NICO systems with those of the Port Radium-Echo Bay district to the north, conclude that within the known alteration and mineralising systems of the GBMZ, coalescing hydrothermal cells temporally and spatially evolved from: (1) Sodic (albite) alteration, which is usually through replacement, and most intense within or proximal to major heat sources or next to splays of the trans-crustal Wopmay fault. This zone generally occurs distal to, and at depth, with respect to known mineralisation and sulphide occurrences; to (2) Calcic-iron (magnetite-amphibole-apatite  $\pm$ biotite  $\pm$ epidote) alteration, which is also deep in the system, superimposed upon, or peripheral to, sodic and/or an

early, extensive, mild to an intense potassic phase; most commonly occurring as breccia matrix, or as disseminations, veins, stockworks or replacement; to (3) High-temperature magnetite-group mineralisation, which ranges from barren (where monomineralic or accompanied by amphibole  $\pm$ apatite  $\pm$ epidote), to fertile, with associated K feldspar or biotite, chalcopyrite and pyrite  $\pm$ gold and silver (e.g., *Sue-Dianne*), and the development of breccias; sometimes accompanied by late overprinting cobalt- and bismuth-bearing arsenides and gold-bismuth-tellurides (e.g., *NICO*); to (4) Skarn alteration and associated mineralisation; to (5) Low-temperature hematite-group mineralisation, which is highly variable, present as either specularite or earthy varieties; occurring as massive to finely dispersed replacements, veins, stockworks or breccia fill; commonly associated with one or more of magnetite, K feldspar, chlorite, tourmaline, epidote, quartz, carbonate, sericite or pyrite. In a number of cases, the best mineralisation occurs at the transition between magnetite and hematite fields (e.g., *Sue Dianne*; Mumin *et al.*, 2007; 2010; Corriveau *et al.*, 2010a).

Corriveau *et al.*, (2009 and 2010) further suggest that crustal-scale, and regional-volcanic-associated structures and rheological variation provided hydrological pathways, and access to chemically receptive rocks that resulted in a wide variation of alteration and mineralisation styles. They interpret the intense silicification zones (e.g., adjacent to hematite-carbonate breccias), and giant quartz stockworks and vein systems observed along transcurent faults, to represent high level epithermal mineralisation released from the IOCG systems.

## Southeast Missouri Iron Province

This province includes eight known major magnetite and hematite deposits (including Pea Ridge, Bourbon, Kratz Spring, Camels Hump and Lower Pilot Knob), totalling in excess of 1 Gt of ore, and numerous (>30) minor occurrences. They are hosted by the volcanic rocks of the Eastern Granite-Rhyolite Province (EGRP) where it is exposed in the Saint Francois Mountains of Missouri, USA. The 1.48 to 1.45 Ga EGRP is contiguous with the 1.40 to 1.34 Ga Southern Granite-Rhyolite Province (SGRP) that is locally exposed in the Arbuckle Mountains of Oklahoma. Both are ~12 km thick, relatively undeformed, and together cover a 250 to 600 km wide curvilinear belt outboard of the Archaean Superior craton of Canada and north-central USA. They are respectively separated from the craton, by the intervening, fringing, 1.88 to 1.83 Ga Penokean, and 1.70 to 1.63 Ga Central Plains orogens. The combined EGRP and SGRP, extend for over 2500 km from southern Ontario in Canada, to New Mexico (USA). Over this interval, they form part of the stable basement to the Phanerozoic sedimentary basins that cover the interior of the continent. The EGRP is overprinted to the east by the 1.3 to 1.0 Ga Grenville Front, and to the west and northwest by the 1.1 Ga Mid-continental Rift. Sm-Nd depleted mantle model ages ( $T_{DM}$ ) of <1.55 Ga (Fig. 16) in the south and east of the two provinces, imply both granite and rhyolite were essentially juvenile, incorporating little crust of appreciably greater age, while to the north and west, ages are considerably greater, suggesting they incorporated significant amounts of Palaeoproterozoic crust. Where exposed in the Saint Francois Mountains, the EGRP is dominantly composed of anorogenic granites, intruding coeval rhyolite, rhyolitic and minor intermediate alkalic

Great Bear Magmatic Zone ... cont.

rocks, but elsewhere is also intruded by significant gabbroid masses, and may overlie a more mafic layer (Seeger, 2000; Pratt *et al.*, 1992; Atekwana, 1996; Van Schmus *et al.*, 1993; 1996; Rohs and Van Schmus, 2007).

More than 1500 m of these rhyolites, dominantly ash flow tuffs, with rare trachytes, are preserved in the Saint Francois Mountains. The rhyolites typically contain perthitic alkali feldspar phenocrysts and iron-rich mafic minerals, including fayalite, ferrosilite and ferrohastingsite, and are characterised by very high SiO<sub>2</sub>, K<sub>2</sub>O:Na<sub>2</sub>O, Fe:Mg and fluorine (locally up to 20% F), and low CaO, MgO and Al<sub>2</sub>O<sub>3</sub>. The trachyte suite includes magnetite trachyte, trachyte, trachyandesite and trachybasalt (Kisvarsanyi and Kisvarsanyi, 1989).

Granitoids found within the district are of three types, (1) sub-volcanic massifs, which are comagmatic with the rhyolites, and contain perthitic alkali feldspars, biotite and ubiquitous magnetite, occurring as fine-grained granophyre, grading down into coarse rapakivi granites; (2) ring intrusions, that define the ring structures, and are composed of intermediate to high silica porphyritic trachyandesites, trachytes, syenites and amphibole-biotite granites, and (3) central plutons that form the core of the ring complexes, and are typically high-silica, two-mica granites with accessory fluorite, topaz, apatite, spinel, orthite, titanite and cassiterite. They also characteristically contain high uranium and thorium contents (Kisvarsanyi and Kisvarsanyi, 1989).

Iron oxide deposits are generally associated with, but not necessarily hosted by, the magnetite trachytes, which may carry up to 10 vol.% magnetite over significant areas. These deposits are generally spatially associated with ring structures, and are considered to be related to the phase in the evolution of the complex that produced the ring plutons,

which are comagmatic with the trachytes (Kisvarsanyi and Kisvarsanyi, 1989).

Mineralisation is controlled by structures which provided fluid migration paths and sites of ore localisation. Breccias formed by explosive volcanic eruptions and caldera collapse were especially favourable sites. The ore occurs as dykes, veins, open-space fillings, breccia matrix and replacement deposits of magnetite and hematite, with ores containing 35 to 56% Fe. In most deposits, the contact between ore and wall rocks is sharp, although locally, narrow fringes of partial or total replacement of wall rock by fine-grained magnetite is evident. In the massive (often ~100%) magnetite sections of some deposits, unaltered or slightly altered, suspended rhyolite blocks are suspended within the massive magnetite near the contact, locally forming jigsaw breccias, leading to the suggestion the magnetite may represent an ore-magma injection (Kisvarsanyi and Kisvarsanyi, 1989).

Low tonnage accumulations of mainly hematite, may also occur at high levels in the volcanic pile as conformable, bedded or bedding replacement, tuffaceous deposits, representing vapour-phase condensates or fumarolic precipitates in caldera lakes. At Pilot Knob, a 3 to 10 m thick band of conformable, finely banded (2 to 20 mm), steel grey specular hematite, with structure interpreted as mudcracks, ripple marks and rain drip or hail imprints is interbedded with a clay seam and volcanic conglomerate, and overlain by rhyolite. The gangue is principally angular quartz and feldspar (Seeger, 1989; Kisvarsanyi and Kisvarsanyi, 1989).

The most complex deposits occur near intrusive contacts between ring intrusion syenites and late-stage central plutons, at the deepest levels of the terrane, where, in addition

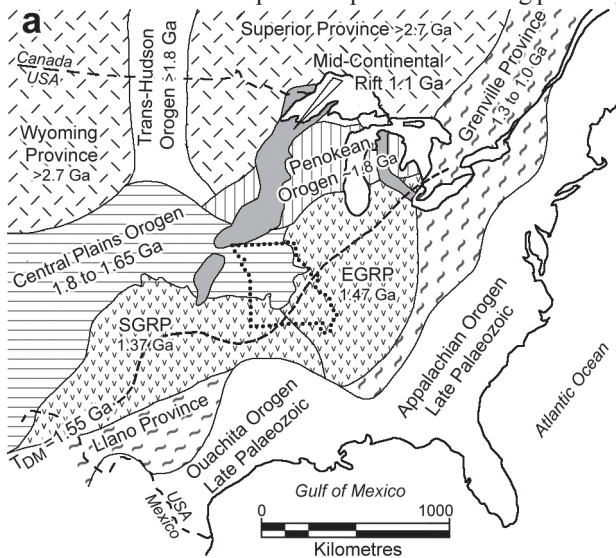
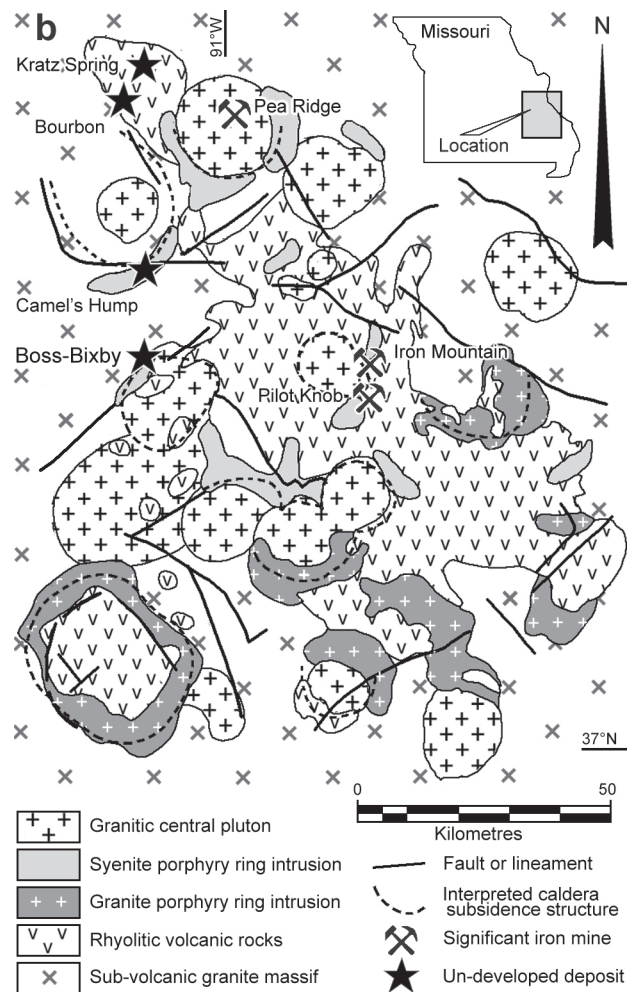


**Figure 16:** Tectonic and geological setting of the Southeast Missouri Iron Province, USA. The dotted outline of Missouri shown on the regional diagram (a) allows comparison with the location shown on (b).

**a** The extent and setting of the Eastern and Southern Granite Rhyolite Provinces (EGRP and SGRP respectively) relative to the main tectonic elements of southeastern North America (after Van Schmus *et al.*, 1993; 1996).

**b** The geology, structure and mineral deposits of the Saint Francois Mountains of Southeastern Missouri. Boss-Bixby is the only occurrence with significant associated copper and gold. The other deposits shown are magnetite-hematite-apatite resources. The main features to note are the granite ring complexes and cauldron subsidence structures of the EGRP and the alkaline syenite porphyry ring intrusions (after Kisvarsanyi and Kisvarsanyi, 1989; Seeger, 2000)



*Southeast Missouri Iron Province ... cont.*

to magnetite and hematite, copper sulphides, uranium and thorium minerals, REE and gold are found (e.g., Boss-Bixby). Late stage breccia-pipes and hydrothermal quartz veins have been responsible for the enrichment in uranium, thorium, REE and gold in some of these latter deposits. (Kisvarsanyi and Kisvarsanyi, 1989).

The **Boss-Bixby** prospect, which contains ~70 Mt of copper mineralisation at an unspecified grade, was discovered in 1956 by drilling a blind magnetic anomaly below Palaeozoic cover. It lies on a major regional, northeast-trending lineament, where it intersects the northwestern margin of a 20 km diameter ring complex structure. The deposit is hosted within a syenite pluton, the Boss Plutonic Complex, part of a ring of intrusions surrounding an inferred central granite pluton. The syenite ring intrusion and its associated mineralisation, which is elongated along the regional lineament over an interval of ~1200 m, intrudes brecciated rhyolitic volcanic rocks and is cut by post-mineralisation diorite, granite and aplite dykes. The host syenite is believed to be the latest of a series of steep, dyke-like, northeast-southwest elongated intrusions on the margin of the ring complex (Seeger, 2000; Kisvarsanyi, 1989; Kisvarsanyi and Kisvarsanyi, 1989).

The deposit is a composite of several pods of higher grade copper mineralisation, separated by low-grade zones, within the iron oxide mass. The mineralisation is disseminated throughout the syenite intrusion, although the main developments are concentrated in breccias and irregular fracturing on the hanging wall of the syenite body and in the adjacent, brecciated, structurally overlying, rhyolitic volcanic rocks. The principal "ore minerals" comprise magnetite, chalcopyrite and bornite, with lesser hematite, ilmenite and rutile as well as pyrite, carrollite, molybdenite, cobaltite, sphalerite, galena, chalcocite, covellite, cubanite and enargite. Boss-Bixby is notable for the presence of ilmenite and titaniferous magnetite in some phases, and the absence of apatite. In contrast, most other magnetite deposits in the district comprise low TiO<sub>2</sub> magnetite and include apatite, which has associated REE. Two varieties of magnetite, blue and brown, are observed, the former of which is found at depth, progressively rimmed by the brown (more oxidised) variety, until a boundary, above which the latter dominates in the upper part of the deposit. The magnetite locally contains some chalcopyrite, bornite and pyrite inclusions, which are interpreted as sulphide crystals trapped or exsolved at the time of crystallisation, although later chalcopyrite replacement of magnetite is common. The distribution of hematite and magnetite is also zoned, with magnetite dominating in the lower parts of the deposit, hematite in the upper, with a mixed transition zone straddling the blue to brown magnetite boundary. A zonation is also evident between upper oxide and lower sulphide dominant assemblages, with the interface being at higher levels on the margins of the deposit, but plunging to depth in the core of the system (Kisvarsanyi, 1989; Kisvarsanyi and Kisvarsanyi, 1989).

Hagni and Brandom (1989) divide the mineralising system at Boss-Bixby into 5 stages, corresponding to a gradual decrease in temperature: (1) an initial magmatic iron oxide stage (800 to 700°C), where titaniferous magnetite, and lesser specular hematite (commonly containing ilmenite exsolution lamellae) occurs as very fine grains and disseminations throughout the syenite, most likely magmatic in origin. This stage was followed by an episode of brecciation and (2) high-temperature (700 to 600°C), metasomatic-hydrothermal iron oxide (low TiO<sub>2</sub>?), occurring

as coarse-grained magnetite that coats and separates breccia fragments; (3) endoskarn alteration, throughout the syenite, producing an assemblage of andraditic garnet, scheelite, quartz, epidote and molybdenite, followed by martitisation of magnetite; (4) sulphide and precious metals stage, which post-dates all of the magnetite, although it is difficult to determine whether martitisation preceded or accompanied the introduction of sulphides, which occur as pods within the overall iron oxide mass. This sulphide stage commenced with the deposition of early pyrite and carrollite, where carrollite rims zoned, cobaltiferous pyrite, followed by the precious metals, predominantly in the form of electrum and hessite, with lesser galena, before the main late episode of copper-iron sulphides, principally involving pyrite, chalcopyrite and bornite, with small amounts of enargite and chalcocite. Chalcopyrite occurs as a replacement of host rock and earlier oxide minerals, and locally forms veins. Bornite is found adjacent to, and partially replacing chalcopyrite grains. Both chalcopyrite and bornite rim magnetite, hematite and pyrite; (5) late oxide and sulphide stage, which includes chalcopyrite, and specular hematite that may occur as small vugs within the chalcopyrite and replaces bornite. Fluorite is a late addition.

Hagni and Brandom (1989) show that strong metasomatic K feldspar (orthoclase) alteration was after syenite intrusion and accompanied the brecciation and iron oxide mineralisation, followed by alteration that is principally garnet, calcite, fluorite, gypsum, chlorite and quartz associated with the skarn and sulphide stages (Kisvarsanyi, 1989).

Depth of burial (350 m of Palaeozoic sedimentary rocks) and low grades have resulted in the resource remaining unexploited (Seeger, 2000).

## Wernecke Breccia

### Crustal Setting

The Wernecke Breccia, in the Wernecke and Ogilvie Mountains of north-central Yukon Territory, Canada, comprise at least 65 sub-economic iron oxide-copper-gold ±uranium ±cobalt (IOCG) prospects associated with a large scale Proterozoic breccia system (Hunt *et al.*, 2010; Corriveau *et al.*, 2010). The individual breccia bodies are spatially associated with local and regional faulting, and are developed within the Palaeoproterozoic (>1.6 Ga) Wernecke Supergroup (WSG). They are distributed over an area of ~100 km in diameter and 100 × 50 km in the Wernecke and Ogilvie Mountains respectively, separated by an interval of ~150 km. Both areas lie within the Foreland Fold and Thrust Belt of western Canada, which is bounded to the west by the northwest-trending, continental-scale Tintina Fault zone that marks the boundary with the accreted, strongly deformed Mesozoic to Cenozoic Cordillera. To the east, the Foreland Fold and Thrust Belt both overthrusts and is overlain by poorly deformed Phanerozoic cover sequence sediments of the broad (>500 km wide) Interior Platform, separating it from the Precambrian Shield. From 2.3 to 1.8 Ga that Shield had comprised a collage of Archaean cratons fringed and separated by active margins and continental arcs, including the Great Bear Magmatic Zone (Hoffman, 1989). See Fig. 1 in Hunt *et al.* (2010) in volume 4 of this series.

The shield area of northwestern North America, is believed to have been rifted from somewhere to the east of the Tasman Line in eastern Australia, following the break-up of the Rodinia super-continent in the Late Neoproterozoic (Fig. 4). The ~1.6 Ga Wernecke Breccia, with little associated

*Wernecke Breccia ... cont.*

contemporaneous magmatism, may have originally been located in what is now central New South Wales, ~1500 km to the southeast of the Mount Isa Inlier (major IOCG related magmatism of ~1.55 to 1.5 Ga), and 1000 km east of the Gawler Craton/Curnamona Province with major 1.6 to 1.57 Ga magmatism coeval with IOCG mineralisation (Conor *et al.*, 2010; Glen, 2005).

The base of the WSG sequence is not exposed, but is interpreted to sit on  $\geq 1.84$  Ga crystalline basement representing the westward continuation of the Canadian shield. It is an ~13 km-thick, deformed and weakly metamorphosed sequence comprising fine-grained marine sedimentary and carbonate rocks, that were deposited as two clastic to carbonate grand cycles, in an extensional basin. Halite-facies meta-evaporites occur in the upper part of the 4 km thick lower cycle (e.g., Norris, 1997; Thorkelson, 2000).

The WSG is locally overlain by the amygdaloidal, intermediate to mafic Slab Volcanics in the Wernecke Mountains. No volcanic rocks have been found in the Ogilvie Mountains, although rare amygdaloidal mafic dykes are known. Locally, dykes and intrusions of diorite, syenite, gabbro and lesser basalt cut the sequence. In the Wernecke Mountains, limited developments of the dioritic to syenitic Bonnet Plume River series of intrusions are dated at 1720 to 1710 Ma (Thorkelson *et al.*, 2001), although, in contrast to the major iron oxide-alkali altered mineral provinces of the world, no batholithic-scale anorogenic or juvenile magmatism is evident at the current level of erosion (Gillen *et al.*, 2009).

The breccia complexes, which are interpreted to have formed at ~1.6 Ga, vary greatly in size from a few centimetres to several hundred metres to several kilometres across. Within individual breccia masses, the degree of brecciation gradually decreases outwards, from strongly disrupted sedimentary rocks to fractured country rock. Their morphology is also variable. They are generally elliptical in plan view, elongate, or irregular in shape, and in vertical section, can be discordant or parallel to layering with no or numerous offshoots. They exhibit evidence of multiple phases of brecciation, probably growing over an interval of time during which crack-and-seal hydrothermal activity was prevalent (Hunt *et al.*, 2010; Corriveau *et al.*, 2010).

The breccia bodies vary from clast to matrix supported, with generally sub-angular to sub-rounded altered clasts in a fine-grained matrix of rock fragments. Clasts range from <1 cm to several hundred metres across, and are predominantly of Wernecke Supergroup sediments, although some igneous fragments (including Slab volcanics) are also locally evident. Some clasts contain veins of hematite that do not penetrate into the matrix, indicating multiple episodes of hydrothermal activity and brecciation. Outward transitions from Wernecke breccia through broken host rock and veined (carbonate=quartz) to undisturbed host rock are common, and occur over intervals of 5 to 500 m (see Figs. 2, 3 and 5 in Hunt *et al.*, 2010, in volume 4 of this series). "IOCG-style" mineralisation, comprising trace to significant amounts of copper, cobalt, gold and uranium, occurs as multiple episodes of veining and disseminations within and peripheral to the breccia bodies (Hunt *et al.*, 2010; Corriveau *et al.*, 2010).

***District-scale Alteration and Mineralisation***

Metasomatic alteration is observed within, and is largely restricted to the extensive Wernecke Breccia, extending outward into the into host rocks for only a few, to several

tens of metres (e.g., Thorkelson, 2000). The alteration type appears to be largely controlled by the host rock, and consists of dominantly sodium- or potassium-rich minerals, overprinted by carbonate. Grey, sodic-altered rocks, containing abundant albite and lesser scapolite, are largely restricted to that part of the sequence that includes halite-facies meta-evaporites (Hunt *et al.*, 2005). Pink to red potassic alteration, caused by abundant orthoclase  $\pm$ sericite, is dominant in breccia hosted by fine-grained clastic rocks. Carbonate, in the form of calcite and dolomite-ankerite, overprints sodic and potassic alteration respectively, forming veins up to 2 m thick that crosscut Wernecke Breccia. Siderite, in addition to dolomite and ankerite (and barite), is locally abundant (Hunt *et al.*, 2010, in volume 4 of this series; see Figs. 4 and 6 in that paper).

Gillen *et al.* (2010), details evidence from fluid inclusion, alteration chemistry and halogen data. These data suggest the dominant hydrothermal fluids associated with formation of the Wernecke Breccia originated as seawater-derived bittern brine (with low Cl/Br basal fluid signatures), that variably dissolved evaporitic halite (high Cl/Br halite dissolution values in samples from some prospects), suggesting halite dissolution within the WSG was variable (Gillen *et al.*, 2010).

Noble gas data also indicate the significant involvement of sea water derived sedimentary formation water (low  $^{40}\text{Ar}/^{36}\text{Ar}$  ratios of <2000), although a limited number of values from one prospect (high  $^{40}\text{Ar}/^{36}\text{Ar}$  ratios of ~11 000 to 40 000) are consistent with mixing with either a mantle-derived magmatic, or deeply sourced metamorphic fluid (Kendrick *et al.*, 2008a). Because of the limited population of the latter, a basement metamorphic component is favoured by Kendrick *et al.* (2008a).

Hunt *et al.* (2010) reported breccia forming and mineralising fluids were at moderate temperature (~80 to 350°C), moderate to high salinity (~5 to 40 wt.%  $\text{NaCl}_{\text{equiv.}}$ ),  $\text{NaCl-CaCl}_2\text{-H}_2\text{O}$  brines whose composition is taken to reflect significant interaction with the host rocks (Hitzman *et al.*, 1992; Gillen *et al.*, 2004; Hunt, 2005; Kendrick *et al.*, 2008a; Hunt *et al.*, 2007).

Most of these fluid characteristics can be explained by the evolution of this brine as it ascended through sedimentary strata of the Wernecke Supergroup. The varying fluid compositions at different levels in the stratigraphy are consistent with this conclusion, and the occurrence of both bittern and halite dissolution brines can be attributed to two separate paths of fluid flow. A basement-derived metamorphic contribution has locally mixed with the bittern or halite dissolution fluids, but only accounts for a minor component of the overall fluid in one of the fluid flow paths. Sampling of fluids from different points along the paths highlight an evolving fluid chemistry that was strongly controlled by temperature, salinity and redox conditions (Gillen *et al.*, 2010).

Hunt *et al.* (2010, in volume 4 of this series) suggest the breccias are the result of periodic over-pressuring of dominantly evolved formational/metamorphic fluids, leading to repeated brecciation of host strata and coincident mineral precipitation, most likely as a response to fluid pH changes, temperature and/or pressure during expansion. Permeable pathways, e.g., faults or shear zones, focussed the fluids leading to multiple brecciation events in the same location as pressure repeatedly built up and was released. Consult Hunt *et al.* (2010) for the observations and reasoning upon which this hypothesis is based and for a more detailed descriptions, images and discussion of these deposits.

## Fennoscandian Shield

### Crustal Setting

The northern Fennoscandian Shield in the Kola Peninsular of Russia, and in Finland, and northern Sweden and Norway, largely comprises Archaean and Palaeoproterozoic rocks, with the bulk of known economic mineral deposits restricted to the latter (Billström *et al.*, 2010).

The Meso- and Neoarchaeic Kola and Karelian cratons in the east, are composed of 3.5 to 2.9 Ga gneissic tonalite-trondhjemite-granodiorite (TTG), followed by 2.9 to 2.6 Ga greenstones, calc-alkaline volcanic rocks and further TTG magmatism, before consolidation after the last major stage of granitoid intrusion at 2.65 Ga.

The early Palaeoproterozoic interval, between 2.5 and 1.9 Ga, was characterised by extension/intracratonic rifting and sedimentary basin evolution, and recurrent mantle plume activity, resulting in numerous komatiitic eruptions, layered intrusions (komatiitic, picritic and tholeiitic to calc-alkaline) over the partly concealed Norrbotten craton in the west and the contiguous Karelian and Kola blocks to the east (Fig. 17). No indication of accretionary phases or formation of major new felsic crust is indicated during this period. The large layered intrusions (hosting significant chromium, nickel, titanium, vanadium

and/or PGE mineralisation) represented a major magmatic input between 2.45 and 2.39 Ga, sometimes with associated high grade granulite facies metamorphism of the intruded rocks, while major basaltic and komatiitic stages (with intercalated arenites) which occurred between 2.2 and 2.0 Ga were associated with extensional pulses (Mutanen, 1997; Lehtonen *et al.*, 1998; Rastas *et al.*, 2001; Fig. 17).

A change took place between 1.96 and 1.75 Ga, during the commencement of assembly of the Nuna/Columbia supercontinent, when felsic and calc-alkaline andesites and related volcaniclastic sedimentary rocks were deposited in subaerial to shallow water settings, mainly over the Norrbotten craton. These rocks were underlain by significant granite, syenoid, dioritoid and gabbroid intrusions. This series involved strong reworking of older crust within the Karelian and Norrbotten cratons. It commenced with 1.90 to 1.86 Ga grey, deformed, metaluminous, tonalite and granodiorite, with associated gabbros, diorites and rare true granites. The Archaean basement, supracrustal rocks and up to 10 km thick pile of Palaeoproterozoic sedimentary and volcanic rocks to the southwest of, and lapping onto the Archaean cratons, were multiply deformed and metamorphosed during the intrusion of these voluminous granitoids and associated gabbros.

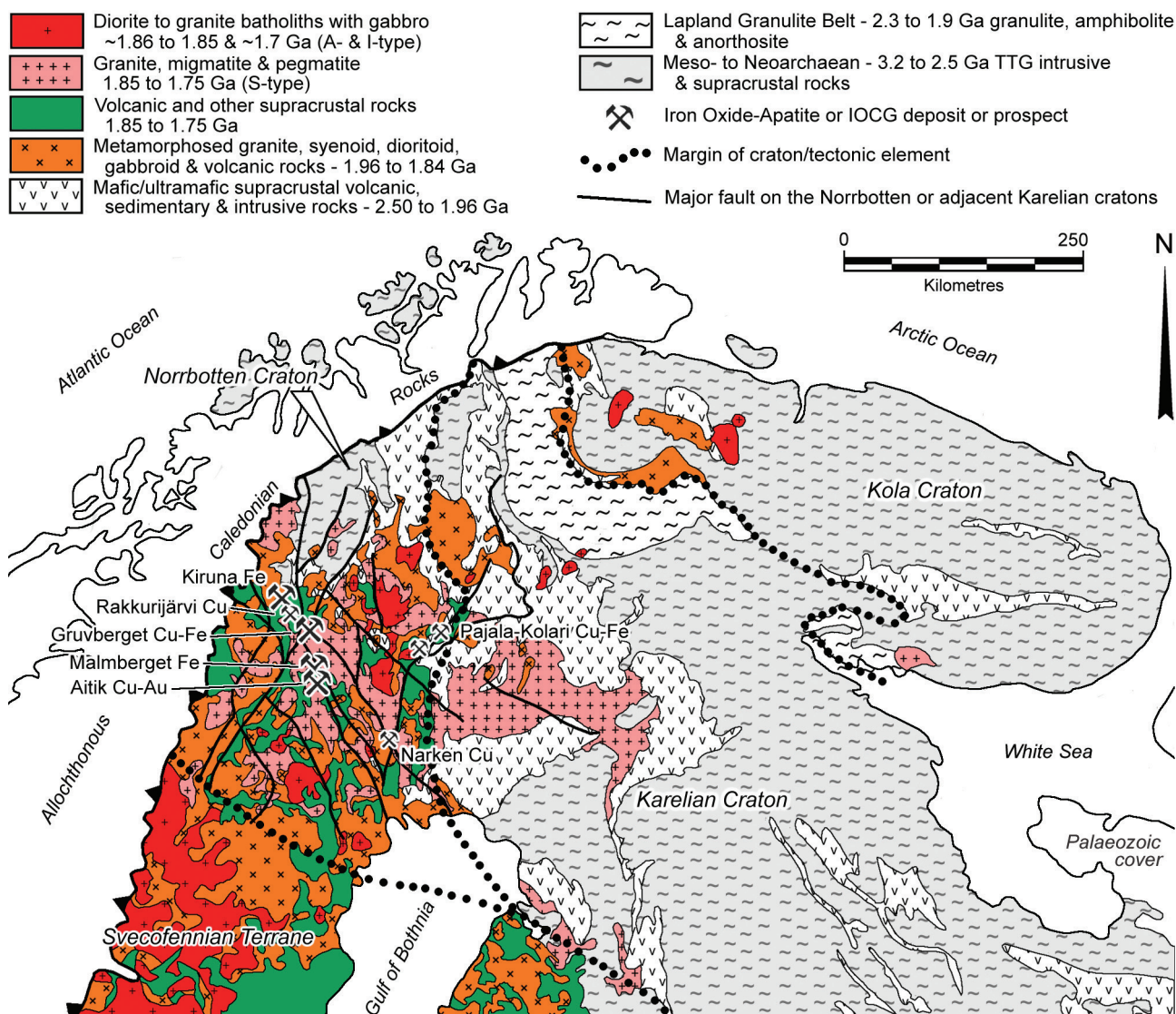


**Figure 17:** Geological summary of the Fennoscandian Shield, northern Norway, Sweden, Finland and Russia, showing the location of the significant magnetite-apatite deposits and IOCG sensu stricto mineralisation. After Billström *et al.*, 2010 and sources quoted therein, and Lahtinen *et al.*, 2011.

*Fennoscandian Shield ... cont.*

These intrusions were followed by a 1.88 to 1.86 Ga undeformed calc-alkaline quartz monzonite-adamellite-granite suite, and then between 1.85 and 1.75 Ga, by major batholithic developments of S-type granite, migmatite and pegmatite in the core of the amalgamated Norrbotten-Karelian craton. Finally, two pulses of extensive north-south oriented anatectic A- and I-type quartz monzodiorite-quartz monzonite-adamellite-granite batholiths at ~1.8 and ~1.7 Ga, were generated during another major stage of deformation and metamorphism, extending into, and mainly within, the Svecofennian terrane to the south (Billström *et al.*, 2010 and sources quoted therein). These two sets of granitoids have calc-alkaline to alkali-calcic compositions (Wanhainen and Martinsson, 2010).

These intrusive phases were followed by, or overlapped with the interpreted accretion of several volcanic arc complexes, associated with an inferred subduction zone along the SW margin of the Norrbotten and Karelian cratons. Lahtinen *et al.* (2005) suggest this phase of subduction involved five partly overlapping pulses and the amalgamation of several microcontinents and island arcs onto the southwestern margins of the combined Archaean Karelian and Norrbotten cratons.

The major magnetite-apatite deposits at Kiirunavaara and Malmberget, as well as the epigenetic copper-gold deposits of the region, are hosted by the geographically restricted 1.89 Ga Kiirunavaara Group (formerly Kiruna Porphyries) and equivalents that overlie Archaean basement of the Norrbotten craton in the Kiruna-Gällivare district (Weiher *et al.*, 2005). The host Kiirunavaara Group volcanic rocks are interpreted to be comagmatic with the 1.88 to 1.86 Ga quartz monzonite-adamellite-granite suite described above. These deposits are located ~250 km to the northeast of the northwest-southeast trending Proterozoic to Archaean basement boundary and inferred subduction zone. Prior to the initiation of subduction, the same district lay within a northeast-trending extensional rift trough (Wanhainen and Martinsson, 2010).

The volcanic rocks of the Kiirunavaara Group, have trachyandesitic to rhyodacitic compositions, and are taken to represent an early and chemically distinct phase compared to the dominant calc-alkaline andesites and related volcanoclastic sedimentary units of the subduction complex to the southwest. However, recent dating (Storey *et al.*, 2007) suggest they may have started to develop much earlier at ~2.05 Ga, during the extensional phase.

For more detail and illustrations, see Billström *et al.* (2010), and Wanhainen and Martinsson (2010) in volume 4 of this series.

### ***District-scale Alteration and Mineralisation***

Large-scale fluid migration of variable salinity, from ~2 Ga, during the multiple stages of pre- and synorogenic magmatism, metamorphism and deformation resulted in regional scapolite, K feldspar-phlogopite, albite and albite-carbonate alteration (Billström *et al.*, 2010). Regional scapolite has been variously attributed to felsic intrusions (Ödman, 1957) and to mobilised evaporites from supracrustal successions (Tuisku, 1985; Frietsch *et al.*, 1997; Vanhanen, 2001). Fluid inclusions from areas of regional albite-scapolite alteration in Fennoscandia, indicate Ca-Na-Cl brines with salinities of 30 to 40 wt.% NaCl<sub>equiv.</sub> and temperatures of 500 to 200°C (Billström *et al.*, 2010).

Around 40 iron oxide-apatite deposits are known within northern Norrbotten, with ~1600 Mt of ore having been mined from 10 of these during the last 100 years. These deposits are

mainly restricted to the volcanic rocks of the Kiirunavaara Group, with very few occurrences known outside the immediate Kiruna-Gällivare area (Billström *et al.*, 2010).

Within the **Kiruna** district, which hosts the major *Kiirunavaara* and *Malmberget* iron oxide-apatite deposits, there is a progression upwards from albite-rich sodic alteration at depth, to intermediate potassic (K feldspar-sericite) to sericite-quartz at shallower levels. In the footwall of the main, conformable, tabular magnetite-apatite body at Kiirunavaara, the dominant assemblage is magnetite-albite-actinolite-chlorite, with the density of veins carrying these minerals increasing towards the base of the ore. The orebody is primarily composed of magnetite, with intergrown apatite, actinolite and minor quartz. It comprises a 5 km long by 100 m thick body that persists for at least 1500 m down dip. The ore is bimodal, with high (>1% P) and low (<0.05% P) apatite ore. The apatite-rich ore is locally banded and predominates in the hanging wall and peripheral parts of the deposit, and in varying amounts in the footwall, whereas the apatite-poor variety is found close to the footwall, as slightly irregular and branching bodies of massive and fine-grained magnetite ore (Billström *et al.*, 2010). Magnetite-actinolite veining/brecciation is found in both the hanging wall and footwall, including large blocks of volcanic wall rocks that may be partially or wholly replaced by actinolite. Blocks of wall-rock within the ore may be replaced by albite or have albitite rims. The deposit follows the contact between the underlying pile of trachyandesitic lava and hanging wall pyroclastic rhyodacite. The hanging wall is locally affected by biotite-chlorite alteration, commonly accompanied by weak enrichment of copper, cobalt and molybdenum. Post-ore alteration is evident in dykes that transect the deposit, and are altered to K feldspar, sericite and disseminated hematite, while hematite ± quartz, barite and/or fluorite veins cut the ore. The upper and lower contacts of the small, conformable magnetite-hematite (Per Geijer ores) lenses at the top of the rhyodacite are occupied by breccias of volcanic clasts in a hematite, magnetite and/or apatite matrix, with highly K feldspar-sericite-silica altered wall rocks (Billström *et al.*, 2010; Hitzman *et al.*, 1992).

Billström *et al.* (2010), conclude that most features of the Kiirunavaara ores are compatible with both a magmatic magnetite intrusive origin, and over-printing by hydrothermal processes. In the deposit area, there is evidence of pre-ore metasomatic magnetite-albite-actinolite-chlorite alteration and mineralisation, followed by massive, columnar jointed magnetite-apatite ore with the characteristics of a magnetite magma, overprinted by further metasomatic magnetite mineralisation and associated alkalic alteration.

The Palaeoproterozoic **Aitik** hybrid porphyry copper-gold/IOCG deposit is located ~200 km northeast of the northwest-southeast-trending Archaean-Proterozoic palaeoboundary in the Fennoscandian shield. The deposit, which is located ~16 km southeast of Malmberget, is considered to have formed at ~1.9 Ga, in a volcanic arc environment over the cratonic margin, related to distal subduction of oceanic crust from the southwest, beneath the Archaean craton. The country rocks comprise metamorphosed intermediate volcanic and clastic sedimentary rocks that were intruded by plutonic rocks of granitic, dioritic and gabbroic composition. Aitik is associated with the major, long-lived, northnorthwest-trending Nautanen deformation corridor of multiple shear zones (Wanhainen and Martinsson, 2010).

*Fennoscandian Shield ... cont.*

The rocks at Aitik have experienced at least two metamorphic events (Bergman *et al.*, 2001), and four main phases of alteration (Wanhainen and Martinsson, 2010). An early, pre-metamorphic potassic porphyry alteration took the form of replacement of amphibole by biotite, and microcline growth in the groundmass. The second phase comprises minerals characteristic of amphibolite facies peak metamorphic conditions (e.g., amphibole and garnet), followed by a third assemblage indicative of retrograde conditions (e.g., biotite, sericite, chlorite, epidote and calcite) that are widespread and common within the groundmass of most of the rocks. Chlorite and sericite are abundant in the footwall and hanging wall rocks, while biotite and sericite alteration dominate in the ore zone. The fourth and final phase is characterised by K feldspar, magnetite, scapolite, amphibole, tourmaline, garnet, muscovite, apatite, allanite and quartz, occurring locally within all rock types, together with chalcocopyrite and pyrite.

A metamorphosed quartz monzodioritic intrusion, related to the early porphyry copper-gold mineralisation, is situated in the footwall of the deposit. The ore zone comprises biotite and quartz-muscovite-sericite schists towards the footwall and hanging wall respectively, with disseminated and quartz-stockwork hosted chalcocopyrite and pyrite.

A high salinity fluids (30 to 38<sub>equiv.</sub> wt.% NaCl + CaCl<sub>2</sub>) were released during emplacement of the intrusion at ~1.89 Ga, resulting in the observed mineralisation, veining and alteration of the intrusive and surrounding volcanoclastic rocks. Remnants of the primary porphyry copper mineralisation are best preserved in the footwall intrusion, in intrusive units within the volcanoclastic rocks of the ore zone, and in quartz stockworks at the margins of the quartz monzodiorite.

An overprinting mineralisation and alteration event characteristic of an iron oxide-alkali altered mineralised system occurred ~100 m.y. later, accompanying compression, monzonitic-granitic magmatism, ductile deformation, and block movements across northern Norrbotten. Magnetite and sulphide enrichments, are found within the deposit, locally occurring as disseminations and within late veins of mainly amphibole, K feldspar, tourmaline, garnet, quartz and epidote, together with late scapolite alteration (Wanhainen and Martinsson, 2010; Billström *et al.*, 2010).

These mineral assemblages are associated with regionally extensive sodic-calcic alteration which is distributed throughout the entire northern Norrbotten ore province, although extensive Phanerozoic and superficial cover do not allow the continuity of this alteration to be established. However, similar, characteristic, scapolite-, amphibole- and K feldspar-rich mineral assemblages are extensively developed throughout the province, overprinted by intense K feldspar alteration in areas of copper-mineralisation and along deformation zones (Edfelt, 2005).

This implies that the widely circulated fluids responsible for iron-oxide copper-gold and related mineralisation, and extensive sodic-calcic alteration in the region during this tectonic event, also affected the Aitik deposit, and probably involved addition of copper and gold. This late mineralising fluid was highly saline (30 to >60<sub>equiv.</sub> wt.% NaCl + CaCl<sub>2</sub>) and contained solids of ferropyrrosmalite and hematite. The preceding was summarised from Wanhainen and Martinsson (2010, in volume 4 of this series).

## Angara-Ilim District

The Angara-Ilim cluster of iron oxide deposits (Soloviev, 2010b) is located approximately 500 km northwest of Irkutsk, in south-central Siberia. Over 50 iron deposits are known within the district, with the total mineable magnetite iron ore reserves of the 11 largest being ~18 Gt @ 20 to 50% Fe. Three of these (Korshunovskoe, Rudnogorskoe and Tatianinskoe), which are currently being mined, account for a collective remaining iron ore reserves of some 450 Mt (Soloviev, 2010b, and sources quoted therein). Alkaline-ultramafic and carbonatite intrusions are also found within the same district.

The Angara Ilim district is situated within the southwestern part of the Siberian craton, some 400 km inboard of the margin, near the intersection of a triple junction of lineaments. The approximately 4 million km<sup>2</sup> Siberian craton/platform comprises limited exposed Archaean inliers in the Anabar and Aldan shields and Yenisey Ridge (see Fig. 1, in Soloviev, 2010b, in volume 4 of this series). The remainder is covered by poorly deformed Proterozoic and Phanerozoic shelf sediments. In the Angara-Ilim district, the >3 km thick cover sequence largely comprises Cambrian dolostones, and includes an up to 600 m thick Lower Cambrian halite-bearing evaporite unit. Nearly half of the craton is overlain by the Permo-Triassic "Siberian traps", mantle-derived continental, mostly low-Ti, tholeiitic flood-basalts, their possible feeders and comagmatic intrusions. These volcanic rocks are dominantly flood-basalt lavas in the northern and northwestern parts of the Siberian craton, and mostly tuffs in the south, including the Angara-Ilim region. They are not homogenous in composition, with several distinct igneous suites being united under this one grouping (Soloviev, 2010b).

The Angara-Ilim region is in the southern, marginal part of the 'Tungus Syncline', a large, gently dipping, cratonic-scale synform in the Palaeozoic-Mesozoic cratonic cover, overlying Precambrian basement. The region is characterised by gentle, rounded to oval-shaped domes and depressions, up to 60 to 130 km across, folding Palaeozoic to Lower Triassic sedimentary rocks, and likely the Precambrian basement. These structures are believed to largely control clusters of iron oxide deposits and are characterised by a larger number of mafic intrusives and dykes, uplifted Precambrian basement and dense fault networks (Strakhov, 1978; Odintsov *et al.*, 1980). Nikulin *et al.* (1991) correlate these deposit clusters with inferred magmatic chambers in the upper asthenospheric mantle or SCLM. The Siberian traps are interpreted to be the result of a major mantle plume event and represent the largest known preserved large igneous province (LIP) on the Earth.

The Angara-Ilim deposits occur as large, sub-vertical, upwardly flaring diatreme-like breccia pipes, some accompanied by maar-like depressions at the surface. Breccia pipes and magnetite mineralisation extends to depth, generally >2 km, persisting to as much as 4.5 km below the surface in one deposit, most likely extending into Precambrian basement. They penetrate through the gently dipping sedimentary sequences of the cratonic cover and are characterised by a gradual increase of mafic igneous material with depth, comprising rocks associated with the Siberian traps. Tholeiitic, calc-alkaline, dolerite sills are intersected by the pipes, which are in turn cut by younger basaltic dykes and stocks, that are possibly alkalic and exhibit a shoshonitic affinity (Strakhov, 1978; Odintsov *et al.*, 1980).

Angara-Ilim District ... cont.

Breccia pipes are up to 3000 × 500 m across at surface, as at *Korshunovskoe*, where the pipe cuts a sequence of Upper Cambrian and Ordovician sediments comprising argillites, limestones, evaporites, siltstones, sandstones and clays. The pipe incorporates fragments and larger blocks of sedimentary and igneous (gabbro-dolerites, dolerites and basalts) rocks cemented by essentially chloritic material as well as by fine-grained, largely skarn-altered, carbonate. Hydrothermal fluids that caused the mineralisation and brecciation also produced a halo of skarn in carbonate units, while the fine carbonate of the matrix is also altered to a skarn assemblage. The core of the pipe is characterised by intense multiple brecciation, with breccia clasts represented mostly by variably altered dolerites. The breccia is cemented by a finely dispersed matrix, completely replaced by pyroxene and pyroxene-garnet skarns, post-skarn calcite-serpentine-chlorite and iron oxides, predominantly magnetite. Magnetite is disseminated in the matrix, occurring as fracture fill and large vein-like tabular masses, as well as sub-horizontal tabular bodies in the wall rocks and as concretionary accumulations on clasts (Soloviev, 2010a, and sources quoted therein).

Outside of the central zone, intense fracturing is evident, with local brecciation in altered sedimentary rocks. The fractures are filled with magnetite, accompanied by chlorite and calcite. Finally, the outermost zone is characterised by weak, predominantly sub-horizontal fractures within sedimentary rocks, locally replaced by skarn in carbonate lithologies. Steeply-dipping dykes of gabbro-dolerite, dolerite, dolerite-porphyr and basalt-porphyr are present, both within and outside the breccia pipes; sub-horizontal dolerite sills are found at depth. The deposit incorporates magnetite bodies of various structural types, including steeply-dipping, columnar, vein-like masses in zones of intense brecciation and replacement by skarns. Sub-horizontal bodies are present at a depth of some 700 to 1500 m from the surface. The mineralisation is mostly magnetite, with minor magnomagnetite, hematite and martite (Soloviev, 2010a).

The Angara-Ilim deposits are characterised by abundant magnesian and calcic skarns, with varying pyroxene/garnet ratios, intense retrograde and hydrosilicate (mostly chlorite-serpentine) alteration. All of these assemblages include magnetite, although it is especially abundant in association with chlorite and serpentine forming brecciated, disseminated and massive ores. Late massive magnetite ( $\pm$ apatite, calcite) veins crosscut the early assemblages and often contain concentric, spherulitic, ball-like magnetite aggregations nucleated on clasts as well as magnetite-halite accumulations (Soloviev, 2010a).

In general, only minor sulphides, mostly pyrite, pyrrhotite and chalcopyrite are present in these deposits, occasional accompanied by trace bornite, pentlandite, sphalerite and galena. More intense sulphide mineralisation tends to occur at higher deposit levels. Up to 10 to 15 vol.% pyrite may occur in narrow fracture-controlled quartz-carbonate-sulphide zones overprinting magnetite mineralisation. Occasionally, minor chalcopyrite is found in micro-fractures and as interstitial disseminations within magnetite, garnet and pyroxene, although local, higher chalcopyrite contents (up to 1% Cu) have been reported within magnetite ore at Oktyabrskoe. Elevated gold values are locally associated with quartz-carbonate-pyrite zones, mostly on the upper levels at Neryunda, Korshunovskoe and Rudnogorskoe (Odintsov *et al.*, 1980; Strakhov, 1978; Vakhrushev *et al.*, 1973; Vakhrushev and Vorontsov, 1976).

## Bushveld and Palabora Complexes

The *Vergenoeg* iron oxide-fluorite and *Palabora* iron oxide-copper-apatite-REE carbonatite deposits are both associated with 2.05 Ga mantle related magmatism in the northern Kaapvaal craton of South Africa, hosted respectively by the Rooiberg-Bushveld mafic-felsic complex, and the satellite Palabora pyroxenite complex 150 km to the east which surrounds the late stage mineralised carbonatite core. The Vergenoeg deposit, occurs as a downward tapering breccia-pipe within anorogenic Rooiberg Group felsic volcanic rocks related to the underlying mantle-derived source of the Bushveld Complex.

The *Rooiberg-Bushveld Complex* was emplaced into and over the Mesoarchaeon to Palaeoproterozoic Kaapvaal craton, close to its northern margin, at 2.05 Ga. The Kaapvaal craton comprises a Palaeo- to Mesoarchaeon granite-greenstone basement, overlain by a thick stratified pile of late Mesoarchaeon to early Palaeoproterozoic mafic volcanic and intracratonic sedimentary rocks (Fig. 18). These include the ~8 km thick clastic successions of the Mesoarchaeon Dominion Group and Witwatersrand Supergroup, the ~5 km of mafic volcanic rocks that constitute the Neoarchaeon Ventersdorp Supergroup and the 15 km late Neoarchaeon to early Palaeoproterozoic (2.64 to 2.05 Ga), Transvaal Supergroup, composed of intracratonic clastic, chemical (BIFs) and carbonatic sedimentary and lesser volcanic rocks. This pile remained relatively undeformed, because by the late Mesoarchaeon, the craton was sufficiently rigid (stabilised) to retard the development of the unstable granite-greenstone tectonics seen at the same period on many other cratonic nuclei (Eglington and Armstrong, 2004).

The Transvaal Supergroup is unconformably overlain by the *Rooiberg Group* (sometimes included as the uppermost volcanic unit of the Transvaal Supergroup; e.g., Button, 1986). This group is almost entirely composed of volcanic rocks that total up to 3.5 km in thickness and are preserved over >50 000 km<sup>2</sup>, although they are estimated to have originally covered an oval-shaped 450 × 350 km (>110 000 km<sup>2</sup>) area (Kinnaird, 2005). The Rooiberg Group occurs directly over the centre of, and forms the intruded roof to the Bushveld Complex. It has been subdivided into four parts, as follows: (1) Dullstroom Formation, comprising at least three compositional groups, low- and high-Ti mafic to intermediate units, and high-Mg felsic units; (2) Damwal Formation, marking the last high-Mg felsites and the first sedimentary intercalations and pyroclastics, accompanied by high-Fe, Ti, P volcanics, overlain by dacites and rhyolites; (3) and (4) Kwaggasnek and Schrikkloof Formations, dominated by dacitic pyroclastics, rare rhyolite flows and intercalated sedimentary horizons. Precise U-Pb zircon dating of Kwaggasnek Formation felsites gives an age of 2059.9±1 Ma, consistently younger than the main layered mafic stage of the Bushveld Complex (zircons from the Merensky Reef and from late stage pegmatoids give ages of 2055.3±1.2 Ma and 2056.3±0.7 Ma respectively; Armstrong *et al.*, 2010). The Rooiberg Group is conformably overlain by the Loskop formation clastic sediments with minor volcanic intercalations. Clastic sediments in this latter unit include eroded clasts of the main mafic stage of the Bushveld Complex (Schweitzer *et al.*, 1995; Kinnaird, 2005).

Widespread, but not voluminous, 2061.8±5.5 Ma granophyre masses of the Rashedoop Granophyre Suite are found below the Rooiberg Group, but above the layered

*Bushveld and Palabora Complexes ... cont.*

mafic phases of the Bushveld complex which it predates (Kinnaird, 2005).

The main mafic to ultramafic phase of the Bushveld Complex, the 7 to 8 km thick *Rustenburg Layered Suite* (RLS), was emplaced as a series of sub-concordant sills along the unconformable contact between the top of the Transvaal Supergroup and the base of the Rooiberg Group, with the floor being the upper sections of the Pretoria Group. The RLS dips to the north, and covers an area of ~65 000 km<sup>2</sup>, elongated east-west parallel to the margin of the craton. It was formed in five chambers that were most likely connected with each other and with a sixth at depth. The RLS was fed by repeated injections of magma from depth, changing composition with time, and has a complex-wide "stratigraphic layering", including the: (1) Marginal zone (mostly norites); (2) Lower zone, (harzburgite between two pyroxenites); (3) Critical zone, (a lower suite of orthopyroxene cumulates and an upper package of chromitite, harzburgite, pyroxenite, through norite to anorthosite); (4) Main zone, (the Merensky Reef then gabbronorite, and infrequent anorthosite and pyroxene); (5) Upper zone, (strongly banded gabbros). In the eastern limb of the complex, the Upper Zone of the RLS is characterised by banded gabbros with up to 25 layers of cumulate, massive and net-textured, titaniferous and vanadiferous magnetite, the thickest being 7 m, while the most consistent averages 2 m. Each layer has a sharp base

and gradational upper margin (Kinnaird, 2005; Cawthorn and Molyneux, 1986). Sections of the Upper zone are also cut by magnetite breccia pipes of similar composition to the layers, reflecting upward expulsion of magnetite from the cumulate layers (Cawthorn and Molyneux, 1986).

The final phase of the Bushveld Complex is the 1.5 to 3.5 km thick, sheeted *Lebowa Granite Suite* (LGS) that has an areal extent of 30 000 km<sup>2</sup>, and with ages of 2054±2 Ma (Armstrong *et al.*, 2010) postdates the RLS. The granite underlies the older, less dense Rooiberg Group and Rashedoop Granophyre Suite, but overlies the denser RLS, through which feeder dykes are mapped. Wilson *et al.* (2000) suggest foliations and lineations are horizontal, reflecting vertical host-rock compression and horizontal magma flow during emplacement, with space being created for the granites by roof uplift and floor depression. They are predominantly alkali feldspar granites with iron-rich ferromagnesian minerals and have been categorised as A-type (Kleemann and Twist, 1989).

All of the data available suggests the whole complex, including the Rooiberg Group volcanic rocks, associated granophyres, A-type granites of the LGS, and the layered ultramafic complex of the RLS, was emplaced over a period of only 3 to 5 m.y. (Kinnaird, 2005; Armstrong *et al.*, 2010). Kinnaird, 2005 discusses a range of opinion on the formation of the Bushveld Complex, but favours the Kaapvaal craton having undergone northeast-

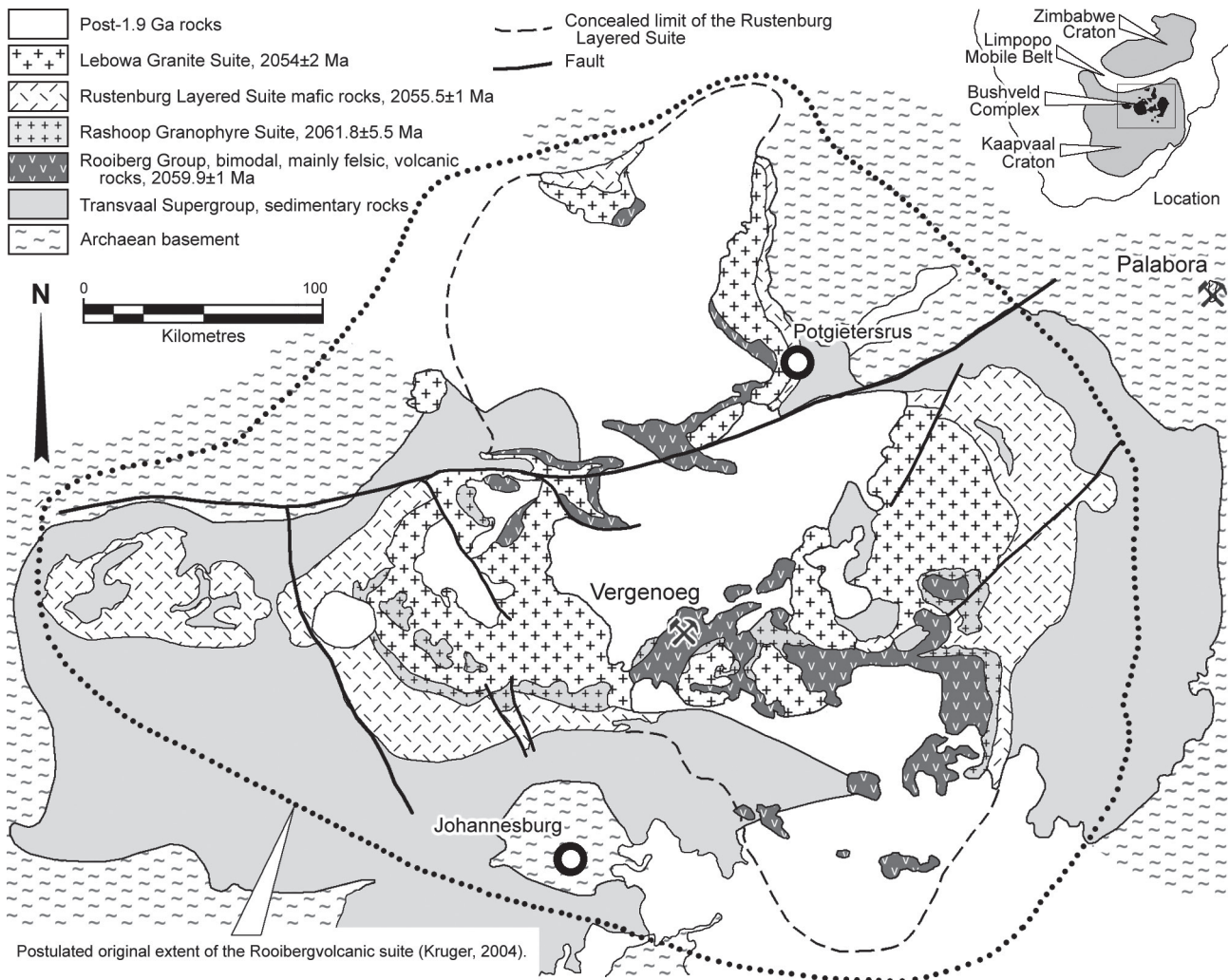


**Figure 18:** Geological summary of the Bushveld-Rooiberg Complex, South Africa, showing the location of the Vergenoeg magnetite-fluorite deposit and the Palabora mine and mafic igneous/carbonatite complex. Note also the estimated original areal extent of the Rooiberg volcanic suite.

*Bushveld and Palabora Complexes ... cont.*

southwest extension and strike-slip reactivation, as suggested by the lack of pre-Bushveld deformation of the Transvaal Supergroup and its preservation over large parts of the craton, as well as the generation of A-type granites, usually associated with crustal extension. In addition, the preservation of the volcanic and shallow-level intrusive rocks of the Bushveld Complex indicates that the significant magmatic thickening related to the Bushveld event must have been compensated by coeval crustal thinning (Gibson and Stevens, 1998). However, as Late Proterozoic to Cretaceous diamondiferous kimberlites in the adjacent Kaapvaal contain a ~3.1 Ga diamond population (Richardson *et al.*, 1984; Shirey *et al.*, 2003), a lithospheric root in excess of 140 km must have existed beneath the craton in the Archaean and survived the Bushveld event (Gibson and Stevens, 1998). Gibson and Stevens (1998) suggest from a study of the deep section of the crust exposed by the 2.02 Ga (post-Bushveld) Vredefort Impact Structure, that the metamorphic profile revealed is consistent with heating by craton-wide intraplate of mantle-derived magmas when a mantle plume head reached the base of the Kaapvaal lithosphere at ~2.06 Ga and underwent partial decompression melting. Once formed the melts rose to levels within the SCLM, or at the base of the crust (Moho) where partial fractional crystallisation occurred within an intraplate magma chamber. The heat released from these magmas resulted in an elevated crustal geotherm to values approaching 40 to 50°C/km, and regional metamorphism of the adjacent crust. They conclude that anatexis in the deeper, high-grade sections of this metamorphosed terrane produced the magmas that rose to form the felsic volcanic rocks of the Rooiberg Group, and high-level granophyre intrusions. However, as the whole of the RLS is enriched in Si, K and Rb relative to many mafic magmas and <sup>87</sup>Sr/<sup>86</sup>Sr and Re-Os isotope are too radiogenic for a purely mantle-derivation of the magmas, there was contamination of the magmas by a crustal source. On the basis of Pb isotope data (Kruger, 2000), there may be a significant component of upper crustal source, especially for the Main Zone with little evidence that the lower crust contributed to the Bushveld magmas, while the very uniform chemistry of individual magma pulses across the complex implies that whatever the contaminant was, the magma spent sufficient time at deep crustal levels to achieve thorough mixing with the crustal components.

After the anatectic Rooiberg Group volcanic and Rashoop Granophyre intrusive rocks were emplaced, pulses of progressively fractionated and contaminated mafic to ultramafic magmas (with reduced, buoyant densities to rise above the Moho) from the deep chamber were ejected and rose to be ponded beneath the less dense felsites. At a later stage, further anatectic felsic magma from the wall rocks of the deeper chamber produced the LGS granites, rising though the denser RLS, to be emplaced at their level of buoyancy immediately below the Rooiberg felsites.

The *Vergenoeg* breccia-pipe iron oxide-fluorite deposit (~175 Mt at 28% CaF<sub>2</sub>, ~42% Fe) is developed within massive red rhyolites of the upper Rooiberg Group Kwaggasnek and Schrikkloof Formations. The upper part of the ~900 m diameter breccia-pipe is filled with volcanic debris and volcanoclastics, the uppermost units of which are only found beyond the limits of the pipe, whereas the lower members grade into the discordant breccia-pipe. This succession, informally known as the Vergenoeg Suite (Fourie, 2000), is possibly an equivalent

of the Loskop Formation (Crocker, 1985), and is regarded by Fourie (2000) and Borrock *et al.* (1998) to have been emplaced at ~1.95 Ga, coeval with the Bobbejaankop Granite of the Lebowa Granite Suite. A number of similar, but smaller, iron oxide-fluorite deposits within a 100 km radius, as well as the Slipfontein hematite-fluorite-magnetite body with accompanying copper and gold, are closely associated with the Bobbejaankop Granite (Fourie, 2000; Kerrich *et al.*, 2005; Pirajno, 2009). However, Goff *et al.* (2004) suggest that on the basis of the silica-undersaturated nature (SiO<sub>2</sub> < 30%) of the pipe and its extreme enrichment in Ca, F, Fe, Nb, P and REE compared to granites, all of these occurrences might instead be related to alkaline magmas similar to Palabora which are also found cutting the Rooiberg-Bushveld Complex over a wide area.

The Vergenoeg Suite comprises: (1) an uppermost, 10 m thick sedimentary unit, mainly a stratiform banded iron formation (thin interbedded hematite and chert beds, with minor cross bedding, ripple marks, mud cracks and dewatering slump structures) with associated shale and conglomerates, that persists for kilometres beyond the pipe; (2) a number of stratified hematite and hematite-fluorite units which are scattered around the volcanic pipe, representing spill over remnants of lava and pyroclastics, e.g., small fragmental lens-shaped, concordant massive, grey and specularitic hematite bodies, interstratified with felsite, including red to greyish, massive hematite containing euhedral fluorite phenocrysts; (3) breccia agglomerate, which occupies the hills surrounding the pipe, composed of angular to rounded felsic volcanic clasts in a matrix of fine ferruginous and hematite tuff; (4) ignimbrite, comprising a siliceous, welded, coarse to fine tuff which overlies felsites of the Schrikkloof Formation. The ignimbrite is found in the pit and grades down into the discordant breccia pipe; (5) the discordant breccia pipe, interpreted to have been formed by a violent gas-vapour felsic volcanic eruption. The pipe has been completely replaced and has a vertical zonation, from hematite-fluorite (and gossan cap) at surface, followed by a deeper zone of un-oxidised magnetite-fluorite, then a magnetite-fayalite transition zone and finally a fayalite zone at the deepest levels. Fluorite, siderite and pyrite veins, dykes and lenses are present throughout all zones (Fourie, 2000).

Borrock *et al.* (1998) recognised two main stages of mineralisation that produced the pattern described above. The first represents the primary assemblage that made up the original intense hydrothermal alteration of the felsic volcanic pipe, and is now only preserved at depth. This assemblage comprises fayalite, fluorite and ilmenite with lesser magnetite, apatite, pyrrhotite and REE minerals. It was altered during a secondary hypogene stage that occupies the upper parts of the pipe, comprising an early ferroactinolite, grunerite and titanian magnetite assemblage, and a late secondary stage of hematite, siderite, low-Ti magnetite, ferropyrrosmalite, stilpnomelane, biotite, titanite, quartz, and apatite (Borrock *et al.*, 1998).

Borrock *et al.* (1998) showed that inclusion petrography, heating-freezing and gas analyses indicate the primary assemblage formed from a high-salinity (>67 wt.% NaCl<sub>equiv.</sub>), high-temperature (>500°C), fluid that coexisted with a CO<sub>2</sub>-rich vapor phase. Stable isotope analyses of deep primary fayalite and titanian magnetite yield calculated water compositions for these temperatures that are typical of magmatic water ( $\delta^{18}\text{O}_{\text{H}_2\text{O}} = 7$  to 8‰ at 500°C). Fluid inclusions related to the secondary

*Bushveld and Palabora Complexes ... cont.*

alteration assemblages homogenise at 150 to 500°C and have salinities of 1 to 35 wt.% NaCl<sub>equiv.</sub>. Stable isotope analyses of hematite and inclusion waters in fluorite suggest that these fluids consist of a mixture of magmatic and meteoric water. The meteoric water is envisaged as supplying the large amount of oxygen required to alter fayalite to magnetite and hematite in the upper part of the deposit (Borrock *et al.*, 1998).

Fourie (2000) concludes that mineralisation was emplaced in the waning phase of volcanic activity centred on the Vergenoeg pipe, which represents the core of a now eroded volcanic cone, and was responsible for the surrounding Vergenoeg Suite volcanic rocks. Late stage magmatic-hydrothermal fluids completely replaced the brecciated felsic volcanic neck after the last eruption to produce the primary assemblage described above, which was essentially 90% fayalite (olivine) with accessory fluorite, ilmenite and magnetite, reflecting the very high Fe- and F-content of the fluids compared to the  $fO_2$ . The final phase was the introduction of fluorite dykes and veins, and siderite bodies. Fluorite was not affected by the secondary stages of mineralisation which converted the fayalite to magnetite and hematite, resulting from the influx of oxidised meteoric waters in the upper sections of the deposit. Fluorite is best developed in the upper magnetite and hematite zones, decreasing with depth, with concomitant increases in iron oxides and fayalite and a base of ore at ~360 m. The pipe continues to beyond 650 m depth.

The **Palabora** copper deposit in South Africa is hosted by the Loolekop carbonatite pipe within the Phalaborwa mafic-carbonatite plug, a satellite of the main Rooiberg-Bushveld Complex, 150 km to the east. It comprises a ~2 × 1 km carbonatite pipe in the core of an ~8 × 3 km alkaline complex of dominantly dunite, pyroxenite and apatite-rich pegmatoidal pyroxenite. As such it may represent a more deeply-sourced, lower volume, low-degree partial melt from below the margin of the main chamber that fed the Rooiberg-Bushveld complex (e.g., Farmer, 2005). Other alkaline/carbonatite complexes are also found well within the confines of the Rooiberg-Bushveld Complex (Harmer, 2000).

The composite multi-stage Palabora Complex represents ultramafic- to peralkaline-magmatic and metasomatic activity in three coalescent centres over an area of ~16 km<sup>2</sup>. It is an elongated, 8 km long pipe-like body that plunges at ~80°E and intrudes Archaean granites, gneisses, quartzites, granulites, amphibolites, and talc- and serpentine-schists, close to the eastern margin of the Kaapvaal Craton. It consists of concentrically zoned, multiple intrusions, which decrease in age from the margin to the cores. The oldest, outer parts, are predominantly variably metasomatised clinopyroxenites, composed of diopside, phlogopite and apatite (comprising a feldspathic outer rind surrounding the bulk that is micaceous). This was followed by an alkaline phase, reflected by the intrusion of plug like bodies of syenite peripheral to the pyroxenite, and by extensive, texturally destructive metasomatism (finitisation) of the Archaean country rocks, by K-Na-Ca-Mg-Fe- and CO<sub>2</sub>-rich magmatic water, dominated chloride brines (with abundant volatiles, particularly fluorine) at a depth of ~12 km, pressure of ~450 MPa and temperature of ~1000°C. During this latter phase, passive emplacement of a more limited, pegmatoidal pyroxenites took place, possibly with metasomatic input, at three centres within the main pipe, North and South Palabora and Loolekop in the centre.

The intrusive cycle culminated with the emplacement of the carbonatite complex. At Loolekop, this entailed, (1) foskerite (olivine/serpentine-magnetite-apatite-calcite rock) and then (2) a banded carbonatite, which were emplaced within the pegmatoidal pyroxenites, followed by (3) a transgressive carbonatite that was intruded as the last magmatic phase along fracture- and shear-zones, and contains the main copper resource. The foskerite at Loolekop, within which the two carbonatite phases are closely nested, covered a surface area of ~1300 × 750 m (Harmer, 2000; Vielreicher *et al.*, 2000; Groves and Vielreicher, 2001).

The main economic metals/minerals are largely restricted to the foskerite and carbonatites. Apatite is a primary igneous phase in the pegmatoidal pyroxenite, foskerite and carbonatites, although at Loolekop, the highest phosphate grades are in the foskerite, where it can constitute up to 56% of the rock, occurring as disseminated grains or as vertical bands. Iron oxides (magnetite) and copper-sulphides are concentrated in the last phases of each of the two magmatic cycles, i.e., (1) the foskerite-banded carbonatite and (2) the transgressive carbonatite, with in both instances, magnetite preceding the copper sulphides. However, the main magnetite with lesser copper is found in the earlier cycle, while minor magnetite and the bulk of the copper is in the transgressive carbonatite cycle. Magnetite, which is assumed to have an orthomagmatic origin in the first (foskerite-banded carbonatite) phase, averages 27% of the ore and is distributed antithetically to copper. There is a variation in the titanium content of magnetite, from ~4 to <0.1 wt.% TiO<sub>2</sub> in foskerite and transgressive carbonatite respectively, possibly reflecting a change from orthomagmatic to hydrothermal. Economic copper grades are dominantly associated with the transgressive carbonatite, although it also occurs within both the banded carbonatite and foskerite. In the transgressive carbonatite, it is found as disseminated grains and sulphide veinlets up to 1 cm thick of chalcopyrite, with lesser bornite and cubanite. Chalcopyrite-(bornite-cubanite), bornite and bornite-(chalcocite) are the dominant copper sulphides in the transgressive and banded carbonatites, and foskerite respectively. The copper sulphides associated with the foskerite and banded carbonatite are interpreted to be orthomagmatic (Verwoerd, 1986), whereas that accompanying the transgressive carbonatite is a secondary hydrothermal generation (Harmer, 2000; Vielreicher *et al.*, 2000; Groves and Vielreicher, 2001).

Vielreicher *et al.* (2000) interpret the Palabora Complex and its mineralisation to be the product of the interaction of multiple pyroxenitic and carbonatitic magmas and their volatiles, which were ultimately derived from decompression melting of metasomatised mantle during extension at the transition from thick Archaean to thinner post-Archaean lithosphere. However, both Harmer (2000) and Vielreicher *et al.* (2000) note that the Sr and Nd isotopic signatures of the Palabora carbonatites are highly anomalous compared to the pyroxenite, indicating its exposure to a cratonic rather than a mantle reservoir alone, thereby precluding the possibility that the carbonatites evolved in a closed system from the same magma responsible for the pyroxenites (Eriksson, 1989). The association of the (finitised) altered halo surrounding the complex indicates exchange between the magmatic/mineralising system and the crust. It has been experimentally indicated that to be maintained as a melt, calcite and dolomite (the principal components of carbonatite) require accompanying fluxing components of

*Bushveld and Palabora Complexes ... cont.*

fluorine (Gittins and Tuttle, 1964; Jago and Gittins, 1991) and alkalis (Cooper *et al.*, 1975; Harmer and Gittins, 1997). Consequently, upon the crystallisation of carbonatites, large volumes of these components would be released as alkali- and CO<sub>2</sub>-rich magmatic brines to alter, and interact with the enclosing country rock. This interaction is reflected in the overprinting of the Palabora Complex and Archaean country rocks by a destructive metasomatic halo, evident as satellite syenite intrusions, large alkaline alteration zones, and aeromagnetic anomalies that extend for tens of kilometres from Palabora itself (Groves *et al.*, 2010; Harmer, 2000; Vielreicher *et al.*, 2000).

## Ossa Morena Zone

The Ossa Morena Zone (OMZ), which is located in southwestern Iberia, is one of the southernmost terranes of the European Variscan Belt, and probably the most complex. It includes a late Neoproterozoic (Cadomian - 620 to 550 Ma) volcanic arc formed during the accretion of an exotic terrane to the Iberian Autochthon (Dallmeyer and Quesada, 1992; Eguíluz *et al.*, 2000). The same arc was reactivated, during Variscan times (372 to 332 Ma), when it hosted a second magmatic belt, formed during the oblique collision of the amalgamated Iberian terrane (which included the OMZ on the leading edge) with the South Portuguese Zone (Silva *et al.*, 1990; Quesada, 1992). Both the OMZ and Iberian terrane are of continental affinity and yield U-Pb zircon ages between 2.0 and 1.7 Ga and Nd isotope model ages between 2.0 and 1.4 Ga (Nägler, 1990; Nägler *et al.*, 1995; Fernández- Suarez *et al.*, 2000; De la Rosa *et al.*, 2002). These data suggest the underlying lower crust is at least of Palaeoproterozoic age, and possibly older, consistent with the presence of a microcontinent (see Figs. 1, 2 and 3 from Carriedo and Tornos, 2010, in volume 4 of this series).

The OMZ is composed of three sequences, two of Proterozoic age, the other Palaeozoic. The former comprise Neoproterozoic dark schist, metagreywacke, quartzite and amphibolite, unconformably overlain by a Late Neoproterozoic to Lower Cambrian, synorogenic calc-alkaline volcanosedimentary sequence of dacitic to rhyolitic composition, with phyllite, greywacke and heterolithic breccia. Abundant magnetite is found within Lower Cambrian rocks, occurring as discontinuous stratabound magnetite-rich horizons 5 to 6 km long, usually either interbedded with volcanic rocks, or located at the contact with underlying limestone, interpreted variously as exhalative or skarn related respectively (Vázquez and Fernández Pompa, 1976; Coullaut, 1979). A broadly coeval, Late Neoproterozoic to Early Cambrian complex of geochemically similar plutonic rocks intrudes these sequences, including up to kilometre sized Cambrian (530 to 500 Ma) magmatic albitite intrusions, emplaced at depths of ~7 to 15 km (Carriedo and Tornos, 2010).

The Palaeozoic sequence commenced with a succession of bimodal volcanics, and thick, Late Cambrian to Ordovician, fine grained clastic rocks, intruded by a complex suite of mid- to late-Cambrian granites that are the roots of the bimodal volcanism. Variscan deformation (370 to 330 Ma) is characterised by sinistral strike-slip faulting which produced a transpressional-transensional regime that controlled magmatism and hydrothermal activity. The Variscan orogeny was accompanied by oblique subduction of the Rheic Ocean beneath the southern OMZ, accompanied by obducted fragments of oceanic crust, a modest magmatic arc, sedimentation during both

compressive and extensional phases, and the eventual oblique collision with the Portuguese Zone in the Early Permian. The Variscan magmatic arc includes small, sometimes magnetite-rich, albitites, occurring as 340 Ma elongate stocks, that crosscut large Variscan plutons (Carriedo and Tornos, 2010 and sources quoted therein).

The most significant geological event during this period was the intrusion of large plutons of sub-volcanic, I-type, high-K, 352 to 332 Ma calc-alkaline rocks. Magma emplacement was at 1.5 to 3 km and comprised diorite, tonalite and granodiorite with minor gabbro and norite. The origin of these plutons is uncertain, as they are not related to major volcanic activity typical of magmatic arcs.

The deep IBERSEIS seismic profiles have revealed an extensive reflective body, compatible with a large, discontinuous, sub-horizontal, mantle derived, mafic to ultramafic intrusion (the IBERSEIS Reflective Body, or IRB) with dimensions of 150 to 170 × ~70 km, and 1 to 5 km thick, emplaced in a mid-crustal decollement at a depth of 15 to 20 km. This structural setting likely represents the brittle-ductile transition where the Variscan thrusts are rooted. The interpretation of the IRB as a complex of large layered intrusions is supported by a regional magnetic anomaly and the systematic juvenile <sup>207</sup>Pb/<sup>206</sup>Pb signatures of Variscan mineralisation (Tornos and Chiaradia, 2004). A structural reconstruction and projection shows that the IRB should outcrop in the Aracena Metamorphic Massif where highly crust contaminated mafic-ultramafic rocks dated at 336±2 Ma are hosted by high-temperature/low-pressure metamorphic rocks and are considered to be the surface expression of this intrusive mass (Carriedo and Tornos, 2010).

Tornos *et al.* (2006) suggest the IRB may be the product of melting of the upper asthenospheric mantle, induced by slab roll-back, or by lithosphere delamination, with break-off and sinking of the subducted oceanic crust in the asthenosphere or detachment of a collisionally thickened lithospheric keel, which is possibly a common feature of syn- to late-collisional settings adjacent to a zone of subduction. The IBERSEIS seismic profiles show the underlying Moho discontinuity, at a depth of ~30 km, is flat, with no remnants of a subduction zone or preserved orogenic roots.

Carriedo and Tornos (2010) consider that the intrusion of the voluminous, high-T juvenile rocks of the IRB (high level intraplate) into low metamorphic grade middle crust produced major crustal melting, intracrustal ponding, fractionation and the consequent formation of water-rich, highly contaminated melts, synchronous with high-T/low-P metamorphism and widespread anatexis. Both processes are regarded as having been critical to the formation of the magmatic nickel(-copper) and IOCG mineralisation found in the OMZ. The anatexis resulting from the intrusion of the IRB was most likely responsible for the Early Carboniferous (352 to 332 Ma) sub-volcanic, I-type, high-K, calc-alkaline plutons described above (Tornos and Casquet, 2005).

## District-scale Alteration and Mineralisation

Two different styles of mineralisation within the Ossa Morena Zone of southern Iberia have been described as representing iron oxide-alkali altered and IOCG *sensu stricto* deposits. These are described as: (1) replacive magnetite deposits related to albitite-rich leucogranites (65 to 78 wt.% SiO<sub>2</sub>) of both Cambrian and Variscan (Lower

*Ossa Morena Zone ... cont.*

Carboniferous) age; and (2) shallower, complex, Variscan hydrothermal magnetite-(copper-gold) replacements related to trans-crustal shear zones. The district also contains older stratabound massive magnetite accumulations of Cambrian age, interpreted to be of exhalative origin, which are cut by the Cambrian albitites (Carriedo and Tornos, 2010).

Two major groups of albitite have been recognised. The dominant group occurs as discrete, Cambrian (530 to 500 Ma), mid-crustal (~7 to 15 km depth), up to 1 km diameter intrusions containing 65 to 78 wt.% SiO<sub>2</sub>. These albitites (albite-rich leucogranites) have a groundmass of albite with scarce phenocrysts of quartz and albite, and common accessories of apatite, fluorite, titanite and zircon. The lack of alteration selvages to albitite dykes, the presence of stockscheider and mirmekitic textures, and preliminary melt inclusion data, suggest that the albitite is a primary magmatic rock and not the product of the metasomatic alteration of leucogranite by sodic fluids. There are, however, ghosts of likely amphibole phenocrysts which have been almost totally replaced by albite (Carriedo *et al.*, 2009; Carriedo and Tornos, 2010).

Carriedo and Tornos (2010) point out the origin and petrogenetic significance of these albitites is controversial. Those of Cambrian age have been interpreted as the sub-volcanic equivalent of the rift-related volcanism of Early Cambrian age (Sánchez-García *et al.*, 2008). Their REE patterns are interpreted to be consistent with a derivation from the crystallisation of residual melts produced during the fractional crystallisation of juvenile basalt.

Mineralisation associated with Cambrian albitites occurs as lenseoid albite-actinolite-magnetite replacements of both the albitite itself, and limestone and calc-silicate hornfels wall rocks along the contact. Zones of hydrothermal brecciation in the uppermost skin of the albitite has been observed, possibly related to exsolution of iron-rich hypersaline aqueous magmatic fluids. Fluid inclusion, and stable and radiogenic isotope data indicate the alteration is related to the circulation of iron-rich aqueous brines equilibrated with the albitite. In some occurrences, possible magmatic breccias comprise rounded albitite clasts supported by massive magnetite (Carriedo *et al.*, 2009; Carriedo and Tornos, 2010).

Variscan albite-leucogranites occur as widespread anatectic products in high-grade metamorphic zones, and as dyke swarms crosscutting Variscan plutons dated at 340±4 Ma (Montero *et al.*, 2000). Unusual 340 to 338 Ma albite-magnetite dykes of magmatic origin (Carriedo, unpublished PhD thesis) are rooted in anatectic zones that encompass magnetite-rich siliciclastic metasediments and amphibolite. These dykes show pegmatite-like features with common stockscheider structures. Preliminary radiogenic isotope data from the Variscan albitites seems to reflect mixing between magmas of dioritic derivation and a dominant crustal component, likely resulting from the partial melting of siliciclastic rocks (Bachiller, 1996). The nature of the protolith appears to control the composition of the albitite, ranging from pure albite to albite and magnetite or even massive apatite-rich rocks. Accessory phases within these dykes include quartz, K feldspar, actinolite, biotite and titanite.

These Variscan dykes evolve vertically to magmatic/hydrothermal breccias and are interpreted to be associated with the development of large distal stratabound magnetite-actinolite-albite bodies. The stratabound bodies are formed

by syn-extensional metasomatic replacement of sequences, including calc-silicate hornfels, schist and carbonate-rich rocks of early Cambrian age by fluids interpreted to have been exsolved from albitites. They are lenticular, with mylonitic fabrics, with an ore assemblage of magnetite, actinolite, albite, variable scapolite and sulphides (mostly pyrite). Garnet rich skarns are locally present (Carriedo *et al.*, 2009; Carriedo and Tornos, 2010).

In summary, these magnetite rich albitites represent both a variety of magnetite-apatite mineralisation spatially and temporally related to intrusions, and a mechanism to produce magmatic-hydrothermal fluids that may contribute to the formation of IOCG mineralisation distal to the intrusive. Carriedo and Tornos (2010) suggest these deposits and observed processes indicate the formation of albitites through mingling of fractionated juvenile magmas and anatectic partial melts of iron-rich metasediments during high-temperature/low-pressure metamorphism. In addition, assimilation of equivalent rocks during the intrusion of albitite may also contribute to their composition. These albitites can produce magnetite concentrations ranging from immiscible iron melts, to albite-magnetite rocks, or iron-saturated magmatic fluids exsolved from albitite that can form replacive accumulations.

## Turgai District

The Turgai district of northwestern Kazakhstan is developed within the Carboniferous Valerianovskoe volcanic belt on the western margin of the Kazakh Collage.

The first of two sequences containing volcanic rocks in this belt, the Valerianovo Supergroup, comprises a pile of andesitic lavas and pyroclastics, which both overlie and grade up into successions of rift-related clastic sedimentary and carbonate rocks. The overlying Kachar Supergroup, commences with polymictic conglomerates, tuffs and sediments, interbedded with basaltic and andesitic flows and their subaerial pyroclastic equivalents. Parts of this sequence are intruded by a series of gabbros and diorites of the Sarbai-Sokolovsky complex, considered to be comagmatic with the Kachar Supergroup volcanic suite. A second intrusive complex also cuts the earlier gabbros and diorites within the belt. This volcanic rift sequence is developed over an east dipping subducted slab involved in the closure of the Trans-Uralian Zone to the immediate west. As such, the terrane might be interpreted to represent a post-collisional extensional/rift setting, closely following continent-continent collisional closure, accompanied by deep mantle sourced magmatism, as indicated by the presence of large gabbro masses.

As well as the three major magnetite-apatite deposits (*Kachar, Sarbai and Sokolovsk*), which have total resources of more than 2.7 Gt @ 43% Fe, there are a number of porphyry/skarn copper deposits within the same belt. Gabbro-diorite-granodiorite intrusives of the Sarbai-Sokolovsky complex (progressively emplaced from the Mid Carboniferous to Permian) occur in the vicinity of the Sarbai and Sokolovsk deposits, although the largest of the trio, Kachar, is distinctive for the absence of any proximal intrusive mass, the closest being 2 to 2.5 km distant at depth. Large scale, marginally younger orthomagmatic titanite-magnetite bearing gabbros are found at depth in the same district.

*Turgai District ... cont.*

The hosts to these ores include carbonates and consequently the resultant alteration assemblage includes a "skarn" assemblage, similar to that associated with other magnetite-apatite and accepted IOCG *sensu stricto* deposits (e.g., Candelaria, Prominent Hill, Hillside, etc.).

The early stages of hydrothermal activity in the Turgai district is represented by widespread calcic alteration, reflected by an assemblage of wollastonite, calcic-amphiboles (actinolite/tremolite) and calcic-pyroxenes (diopside/augite), with apatite and quartz, and evidence of early regional scapolite around some deposits.

The second phase, which accompanies the introduction of the massive magnetite deposits, is inferred to have taken place at temperatures of >500°C and is characterised by a sodic-calcic-(potassic) assemblage accompanying the dominantly massive to banded magnetite. It comprises intergrown coarse epidote, augite/diopside, andradite (calcic garnet), actinolite/tremolite, calcite and pyrite (up to 10%), with minor titanite and apatite. The assemblage is influenced by the composition of the host rocks, e.g., at Sokolovsk, the felsic intrusive and silicate volcanic rocks are altered to albite, actinolite, diopside/augite, biotite and K feldspar, while those lithologies composed of aluminosilicates in the hanging wall are converted to pyroxene (diopside/augite) and scapolite (a chlorine rich variety) and the carbonates to pyroxene and pyroxene-garnet skarns. At Kachar, in particular, magnetite ore is closely associated with more extensive zones of scapolite and albite alteration, which have been overprinted and replaced by diopside-garnet and garnet skarns. The major magnetite phase was locally overprinted by a sulphide-sodic-potassic stage with up to 10% each of chalcopyrite and pyrite, characterised by albite-scapolite, K feldspar and chlorite. This sulphide mineralisation is mainly evident in the centres of the deposits, where sulphide-rich calcite veins are developed, comprising coarse sparry calcite, sulphides, magnetite and minor quartz. Subsequent chloritisation, with associated hematite and magnetite is followed by the more widespread late development of coarse barren veins of calcite, albite, scapolite and K feldspar that extend for kilometres beyond some of the deposits. This is part of an extensive marialitic scapolite zone, with accompanying sodic-pyroxene, that post-dates all of the intrusive activity of the district (Hawkins *et al.*, 2010 and sources quoted therein; Sokolov and Grigor'ev, 1977).

Traditionally these deposits have been regarded as "skarns". However, neither Kachar or Sarbai are in direct contact with Sarbai-Sokolovsky complex intrusives, and consequently the contained iron must have been introduced in hydrothermal fluids, whether intimately associated with the intrusives, or from another deeper source, and the skarn assemblage is a reflection of the interaction between hot, volatile-rich fluids and the calcic country rocks.

## Acknowledgements

Thanks are due to all of the authors who have contributed to these two volumes, for the benefit of their experience and research, and the discussion that has accompanied the review and editing of their papers and influenced this overview and review. Particular thanks to Tim Baker and Nick Hayward who gave of their time to review the original version of this compilation and suggest major changes which has significantly improved the final product.

## References

- Adshead-Bell, N.S., 1998 - Evolution of the Starra and Selwyn high-strain zones, Eastern fold belt, Mount Isa inlier: implications for Au-Cu mineralization; *Economic Geology*, v. 93, pp. 1450-1462.
- Abbott, D.H. and Isley, A.E., 2002 - The intensity, occurrence and duration of superplume events and eras over geological time; *Journal of Geodynamics*, v. 34, pp. 265-307.
- Adshead, N.D., Voulgaris, P. and Muscio, V.N., 1998 - Osborne copper-gold deposit; in Berkman, D.A. and Mackenzie, D.H., (eds.), *Geology of Australian and Papua New Guinean Mineral Deposits, The AusIMM, Melbourne*, Monograph 22, pp. 793-799
- Aguirre, L., 1988 - Chemical mobility during low-grade metamorphism of a Jurassic lava flow: Río Grande Formation, Perú; *Journal of South American Earth Sciences*, v. 1, pp. 343-361.
- Allen, S., McPhie, J., Simpson, C., Kamenetsky, V., Chambefort, I., Agangi, A., Bath, A., Garner, A. and Morrow, N., 2009 - A Mesoproterozoic silicic LIP in South Australia: the Gawler Range Volcanics and Hiltaba Suite; <http://www.largeigneousprovinces.org/09feb.html>
- Altona Mining Limited, 2010 - ASX/Media Announcement, 14 December, 2010.
- Anderson, D.L., 2009 - Energetics of the Earth and the missing heat source mystery; [www.mantleplumes.org/Energetics.html](http://www.mantleplumes.org/Energetics.html)
- Arévalo, C., 1999, The coastal Cordillera-Precordillera boundary in the Copiapó area, northern Chile and the structural setting of the Candelaria Cu-Au ore deposit: Unpublished Ph.D. dissertation, *Kingston University, Kingston-upon-Thames, U.K.*, 244p.
- Arévalo, C., Grocott, L., Martin, W., Pringle, M. and Taylor, G., 2006 - Structural setting of the Candelaria Fe oxide Cu-Au deposit, Chilean Andes (27°30'S); *Economic Geology*, v. 101, pp. 819-841.
- Arculus, R.J., 1994 - Aspects of magma genesis in arcs: *Lithos*, v. 33, pp. 189-208.
- Armstrong, R.A., Kamo, S. and Harmer, R.E., 2010 - Rapid emplacement of the one of the world's greatest continental magmatic provinces - precise age constraints on the Bushveld Complex; *ANU Research School of Earth Sciences, Canberra*, <http://rses.anu.edu.au/highlights/view.php?article=194>
- Artemieva, I.M. and Mooney, W.D., 2001 - Thermal thickness and evolution of Precambrian lithosphere: A global study; *Journal of Geophysical Research*, v. 106, pp. 16 387-16 414.
- Atekwana, E.A., 1996, Precambrian basement beneath the central Midcontinent United States as interpreted from potential field imagery, in van der Pluijm, B.A. and Catascosinos, P.A., (eds.), *Basement and Basins of Eastern North America, Geological Society of America, Boulder, Colorado*, Special Paper 308, pp. 33-44.
- Atherton, M.P. and Aguirre, L., 1992 - Thermal and geotectonic setting of Cretaceous volcanic rocks near Ica, Perú, in relation to Andean crustal thinning; *Journal of South American Earth Sciences*, v. 5, pp. 47-69.
- Atherton, M.P. and Webb, S., 1989 - Volcanic facies, structure, and geochemistry of the marginal basin rocks of central Peru; *Journal of South American Earth Sciences*, v. 2, pp. 241-261.
- Austin, J.R., Blenkinsop, T.G., 2008 - The Cloncurry Lineament: Geophysical and geological evidence for a deep crustal structure in the Eastern Succession of the Mount Isa Inlier; *Precambrian Research*, v. 163, pp. 50-68.
- Bachiller, N., 1996 - Las alteraciones hidrotermales de los leucogranitos del complejo intrusivo de Burguillos del Cerro (Badajoz). Edad, Geoquímica y modelo de procedencia y evolución de los fluidos; Master's Thesis, *Universidad Complutense de Madrid*, 151p. (in Spanish)

- Baker, T., 2002 - Emplacement depth and carbon dioxide-rich fluid inclusions in intrusion-related gold deposits; *Economic Geology*, v. 97, pp. 1109–1115.
- Baker, T., 2003 - Lindgren's legacy: magmas, fluids and ore deposits; in Baker, T., Cleverley, J.S. and Fu, B., (eds.), *Magmas, Fluids and Porphyry-Epithermal Deposits Symposium, James Cook University, Townsville*, v. 97, pp. 1109–1115.
- Baker, T., Mustard, R., Fu, B., Williams, P.J., Dong, G., Fisher, L., Mark, G. and Ryan, C., 2008 - Mixed messages in iron oxide–copper–gold systems of the Cloncurry district, Australia: insights from PIXE analysis of halogens and copper in fluid inclusions; *Mineralium Deposita*, v. 43, pp. 599–608.
- Barton, M.D. and Johnson, D.A., 1996 - Evaporitic source model for igneous related Fe oxide-(REE-Cu-Au-Au) mineralization; *Geology*, v. 24, p. 259–262.
- Barton, M.D. and Johnson, D.A., 2000 - Alternative brine sources for Fe oxide (-Cu-Au) systems: implications for hydrothermal alteration and metals; in Porter T.M., (ed.), *Hydrothermal Iron Oxide Copper-Gold and Related Deposits: A Global Perspective*, *PGC Publishing, Adelaide*, v. 1, pp. 43–60.
- Barton, M.D. and Johnson, D.A., 2004 - Footprints of Fe oxide (-Cu-Au) systems; *University of Western Australia, Special publication 3*, pp. 12–116.
- Barton, M.D., Jensen, E.P. and Ducea, M., 2005 - Fluid sources for IOCG (Candelaria, Punta del Cobre) and porphyry Cu-style mineralization, Copiapo batholith, Chile: Geologic and Sr isotopic constraints; [http://gsa.confex.com/gsa/2005AM/finalprogram/abstract\\_96645.htm](http://gsa.confex.com/gsa/2005AM/finalprogram/abstract_96645.htm)
- Bastrakov, E.N., Skirrow, R.G. and Davidson, G.J., 2007 - Fluid Evolution of Iron Oxide Cu-Au Prospects in the Olympic Dam District, Gawler Craton, South Australia; *Economic Geology*, v. 102, pp. 1413–1440.
- Begg, G.C., Hronsky, J.A.M., Arndt, N.T., Griffin, W.L., O'Reilly, S.Y. and Hayward, N., 2010 - Lithospheric, cratonic, and geodynamic setting of Ni-Cu-PGE sulfide deposits; *Economic Geology*, v. 105, pp. 1057–1070.
- Bekker, A., Slack, J.F., Planavsky, N., Krapez, B., Hofmann, A., Konhauser, K.O. and Rouxel, O.J., 2010 - Iron formation: the sedimentary product of a complex interplay among mantle, tectonic, oceanic, and biospheric processes; *Economic Geology*, v. 105, pp. 467–508.
- Bell, R.T., 1982 - Comments on the geology and uraniferous occurrences of the Wernecke Mountains, Yukon and District of Mackenzie; *Canadian Geological Survey Paper*, 82-1B, pp. 279–284.
- Belousova, E., Griffin, W. and O'Reilly, S., 2009 - The Gawler Craton, South Australia: Unexpected discoveries and mysteries; *GEMOC ARC National Key Centre, Annual Report, Macquarie University, Sydney*, <http://www.gemoc.mq.edu.au/Annualreport/annrep2009/Reshigh09.html>
- Belperio, A., Flint, R. and Freeman, H., 2007 - Prominent Hill: A hematite-dominated, iron oxide copper-gold system; *Economic Geology*, v. 102, pp. 1499–1510.
- Benavides, J., Kyser, T.K., Clark, A.H., Oates, C., Zamora, R., Tarnovschi, R. and Castillo, B., 2007 - The Mantoverde iron oxide-copper-gold district, III Región, Chile: the role of regionally-derived, non-magmatic fluid contributions to chalcopyrite mineralization; *Economic Geology*, v. 102, pp. 415–440.
- Bergman, S., Kübler, L. and Martinsson, O., 2001 - Description of regional geological and geophysical maps of Northern Norrbotten county; Geological Survey of Sweden, Ba 56, pp. 5–100.
- Betts, P.G., Giles, D., Mark, G., Lister, G.S., Goleby, B.R. and Ailleres, L., 2006 - Synthesis of the Proterozoic evolution of the Mt Isa Inlier; *Australian Journal of Earth Sciences*, v. 53, pp. 187–211.
- BHP Billiton, 2010 - Annual Report; [www.bhpbilliton.com](http://www.bhpbilliton.com).
- Bhushan, S.K., 2000 - Malani Rhyolites – a review; *Gondwana Research*, v. 3, pp. 65–77.
- Billström, K., Eilu, P., Martinsson, O., Niiranen, T., Broman, C., Weihed, P., Wanhainen, C. and Ojala, J., 2010 - IOCG and related mineral deposits of the northern Fennoscandian Shield; in Porter, T.M., (ed.), *Hydrothermal Iron Oxide Copper-Gold and Related Deposits: A Global Perspective - Advances in the Understanding of IOCG Deposits*; *PGC Publishing, Adelaide*, v. 4, pp. 381–414.
- Blake, D.H., 1987 - Geology of the Mount Isa Inlier and environs, Queensland and Northern Territory; Bureau of Mineral Resources, Bulletin 225, 83p.
- Blenkinsop, T.G., Huddleston-Holmes, C.R., Foster, D.R.W., Edmiston, M.A., Leping, P., Mark, G., Austin, J.R., Murphy, F.C., Ford, A. and Rubenach, M.J., 2008 - The crustal scale architecture of the Eastern Succession, Mount Isa: The influence of inversion; *Precambrian Research*, v. 163, pp. 31–49.
- Bookstrom, A.A., 1977 - The magnetite deposits of El Romeral, Chile; *Economic Geology*, v. 72, pp. 1101–1130.
- Boric, R., Holmgren, C., Wilson, N.S.F. and Zentilli, M., 2002 - The geology of the El Soldado manto type Cu (Ag) deposit, central Chile; in Porter, T.M., (ed.), *Hydrothermal Iron Oxide Copper-Gold and Related Deposits: A Global Perspective*, *PGC Publishing, Adelaide*, v. 2, pp. 163–184.
- Borrok, D.M., Kesler, S.E., Boer, R.H. and Essene, E.J., 1998 - The Vergenoeg magnetite-fluorite deposit, South Africa: support for a hydrothermal model for massive iron oxide deposits; *Economic Geology*, v. 93, pp. 564–586.
- Bott, M.H.P., 1982 - The interior of the Earth: its structure, constitution and evolution; *Arnold, London*, 403p.
- Brenan, J.M., Shaw, H.F., Phinney, D.L. and Ryerson, F.J., 1994 - Rutile aqueous fluid partitioning of Nb, Ta, Hf, Zr, U and Th: Implications for high field strength element depletions in island arc basalts; *Earth and Planetary Science Letters*, v. 128, pp. 327–339.
- Brown, M. and Porter, T.M., 2010 - The Mount Elliott IOCG system, Eastern Fold Belt, Mount Isa Inlier, Northwest Queensland; in Porter, T.M., (ed.), *Hydrothermal Iron Oxide Copper-Gold and Related Deposits: A Global Perspective - Advances in the Understanding of IOCG Deposits*; *PGC Publishing, Adelaide*, v. 3, pp. 219–232 (*this volume*).
- Bryan, S., 2007 - Silicic Large Igneous Provinces; *Episodes*, v. 30, pp. 20–31.
- Burchfiel, B.C., Chen, L., Wang, E. and Swanson E., 2008 - Preliminary investigation into the complexities of the Ailao Shan and Day Nui Con Voi shear zones of SE Yunnan and Vietnam; in Burchfiel, B.C. and Wang, E., (Eds.), *Investigations into the Tectonics of the Tibetan Plateau*, *The Geological Society of America*, Special paper 444, pp. 45–58.
- Button, A., 1986 - The Transvaal sub-basin of the Transvaal Sequence; in Anhaeusser, C.R. and Maske, S., (eds.), *Mineral Deposits of Southern Africa*, *Geological Society of South Africa, Johannesburg*, v. 1, pp. 811–817.
- Caldas, J., 1978 - Geología de los cuadrangulos de San Juan, Acari y Yauca; *Instituto Geológico Minero y Metalúrgico del Perú, Lima, Perú*, Boletín 30. (*in Spanish*)
- Campbell, I.H., 2005 - Large Igneous Provinces and the Mantle Plume Hypothesis; *Elements*, v. 1, pp. 265–269
- Carriedo, J., Tornos, F. and Tomé, C., 2009 - Coexistence of different styles of the IOCG-like deposits in SW Iberia; in Williams, P.J. *et al.*, (eds.), *Smart Science for Exploration and Mining, Proceedings of the 10<sup>th</sup> Biennial SGA Conference, 17–20 August, 2009, Townsville, Australia*, Extended abstracts, v. 2, pp. 611–613.

- Carriedo, J. and Tornos, F., 2010 - The iron oxide copper-gold belt of the Ossa Morena Zone, southwest Iberia: implications for IOCG genetic models; in Porter, T.M., (ed.), *Hydrothermal Iron Oxide Copper-Gold and Related Deposits: A Global Perspective - Advances in the Understanding of IOCG Deposits*; PGC Publishing, Adelaide, v. 4, 441-460.
- Carter, A., Roques, D., Bristow, C. and Kinny, P., 2001 - Understanding Mesozoic accretion in Southeast Asia: significance of Triassic thermotectonism (Indosinian orogeny) in Vietnam; *Geology*, v. 29, pp 211-214.
- Cawood, P.A., 2005 - Terra Australis Orogen: Rodinia breakup and development of the Pacific and Iapetus margins of Gondwana during the Neoproterozoic and Paleozoic; *Earth-Science Reviews*, v. 69, pp. 249-279.
- Cawthorn, R.G. and Molyneux, T.G., 1986 - Vanadiferous magnetite deposits of the Bushveld Complex; in Anhaeusser, C.R. and Maske, S., (eds.), *Mineral Deposits of Southern Africa*, Geological Society of South Africa, Johannesburg, v. 2, pp. 1251-1266.
- Chambefort, I., Kamenetsky, V., McPhie, J., Bth, A., Agangi, A., Allen, S.R., Ehrig, K and Green, N., 2009 - The Olympic Dam Cu-Au-U deposit, South Australia: Was fluorine a key in forming this giant?; in Williams, P.J. et al., (eds.), *Smart Science for Exploration and Mining, Proceedings of the 10<sup>th</sup> Biennial SGA Conference, 17-20 August, 2009, Townsville, Australia*, Extended abstracts, v. 2, pp. 207-209.
- Chambefort, I., McPhie, J., Kamenetsky, V., Ehrig, K. and Green, N., 2009 - Diverse Mafic Facies in the Olympic Dam Cu-Au-U Deposit, South Australia; in Williams, P.J. et al., (eds.), *Smart Science for Exploration and Mining, Proceedings of the 10<sup>th</sup> Biennial SGA Conference, 17-20 August, 2009, Townsville, Australia*, Extended abstracts, v. 2, pp. 614-616.
- Charrier, R., Pinta, L. and Rodríguez, M.P., 2007 - Tectonostratigraphic evolution of the Andean Orogen in Chile; in Morena, T. and Gibbobs, W., (eds.), *The Geology of Chile*, The Geological Society, Bath, UK, pp. 21-114.
- Chen, H.Y., 2010 - Mesozoic IOCG mineralisation in the central Andes: an updated review; in Porter, T.M., (ed.), *Hydrothermal Iron Oxide Copper-Gold and Related Deposits: A Global Perspective - Advances in the Understanding of IOCG Deposits*; PGC Publishing, Adelaide, v. 3, pp. 259-272. (this volume).
- Chen, H.Y., Clark, A.H., Kyser, T.K., Ullrich, T.D., Baxter, R., Chen, Y.M. and Moody, T.C., 2010 - Evolution of the Giant Marcona-Mina Justa Iron Oxide-Copper-Gold District, South-Central Perú; *Economic Geology*, v. 105, pp. 155-185.
- Chen, H.Y., Clark, A.H., Kyser, T.K., 2010a - The Giant Marcona magnetite deposit, Ica, South-Central Perú: a product of hydrous, iron oxide-rich melts ?; *Economic Geology*, v. 105, pp. 1441-1456.
- Chew, D.M., Cardona, A. and Miškovic, A., 2010 - Tectonic evolution of western Amazonia from the assembly of Rodinia to its break-up; *International Geology Review*, 12p.
- Chiaradia, M., Banks, D. Cliff, R., Marschik, R. and de Haller, A., 2006, Origin of fluids in iron oxide-copper-gold deposits: Constraints from  $\delta^{37}\text{Cl}$ ,  $^{87}\text{Sr}/^{86}\text{Sr}$ , and Cl/Br; *Mineralium Deposita*, v. 41, p. 565-573.
- Claoué-Long, J.C. and Hoatson, D.M., 2009. Guide to using the Map of Australian Proterozoic Large Igneous Provinces; *Geoscience Australia*, Record 2009/44, 37p.
- Cleverley, J.S. and Oliver, N.H.S., 2005 - Crustal scale volatile transfer: melts and breccias in the Mount Isa Eastern Fold Belt; in Hancock, H. (ed.), *Structure, Tectonics and Ore Mineralisation Processes*, Economic Geology Research Unit, James Cook University, Townsville, p. 26.
- Cline, J.S., 1995 - Genesis of porphyry copper deposits: the behavior of water, chloride, and copper in crystallizing melts; in Pierce, F.W. and Bolm, J.G., (eds.), *Porphyry Copper Deposits of the American Cordillera*, *Arizona Geological Society Digest*, v. 20, pp. 69-82.
- Cline, J.S. and Bodnar, R.J., 1991 - Can economic porphyry copper mineralization be generated by a typical calc-alkaline melt?; *Journal of Geophysical Research*, v. 96, pp. 8113-8126.
- Compston, D.M., 1995 - Time constraints on the evolution of the Tennant Creek block, northern Australia; *Precambrian Research*, v. 71, pp. 107-129.
- Condie, K.C., 2001 - Mantle plumes and their record in Earth history; *Cambridge University Press, Cambridge*, 305p.
- Condie, K.C., 2002 - The supercontinent cycle: Are there two patterns of cyclicality?; *Journal of African Earth Sciences*, v. 35, pp. 179-183.
- Condie, K.C., 2004 - Supercontinents and superplume events: Distinguishing signals in the geologic record; *Physics of the Earth and Planetary Interiors*, v. 146, pp. 319-332.
- Condie, K.C., 2005 - Earth as an evolving planetary system; *Elsevier, Amsterdam*, 447p.
- Condie, K.C., O'Neill, C. and Aster, R., 2009 - Evidence and implications for a widespread magmatic shutdown for 250 m.y. on Earth; *Earth and Planetary Science Letters*, v. 282, pp. 294-298.
- Conor, C., Raymond, O.L., Baker, T. and Lowe, G., 2010 - Aspects of structural control on alteration and mineralisation in the Moonta-Wallaroo Cu-Au Mining Field, Olympic Domain, South Australia; in Porter, T.M., (ed.), *Hydrothermal Iron Oxide Copper-Gold and Related Deposits: A Global Perspective - Advances in the Understanding of IOCG Deposits*; PGC Publishing, Adelaide, v. 3, pp. 147-170. (this volume).
- Cooper, A.F., Gittins, J. and Tuttle, O.F., 1975 - The system  $\text{Na}_2\text{CO}_3$ - $\text{K}_2\text{CO}_3$ -CaCO at 1 kilobar and its significance in carbonatite petrogenesis; *American Journal of Science*, v. 275, pp. 534-560.
- Cordani, U.G. and Teixeira, W., 2007, Proterozoic accretionary belts in the Amazonian Craton; in Hatcher, R.D.J., Carlson, M.P., McBride, J.H. and Martínez, C.J.R., (eds.), *4-D Framework of Continental Crust*, Geological Society of America, Boulder, Colorado, Memoir, v. 200, pp. 297-320.
- Corriveau, L., 2007 - Iron oxide copper-gold deposits: a Canadian perspective; in Goodfellow, W., (ed.), *Mineral Deposits of Canada: a Synthesis of Major Deposit-Types, District Metallogeny, the Evolution of Geological Provinces and Exploration Methods*, Geological Association of Canada, Mineral Deposits Division, Special Publication no. 5, pp. 307-328
- Corriveau, L., Williams, P.J. and Mumin, H., 2010a - Alteration vectors to IOCG mineralization: from uncharted terranes to deposits; in Corriveau, L. and Mumin, A.H., (eds.), *Exploring for Iron Oxide Copper-Gold Deposits: Canada and Global Analogues*, Geological Association of Canada, Short Course Notes 20, pp. 89-110.
- Corriveau, L., Mumin, H. and Setterfield, T., 2010 - IOCG environments in Canada: characteristics and geological vectors to ore; in Porter, T.M., (ed.), *Hydrothermal Iron Oxide Copper-Gold and Related Deposits: A Global Perspective - Advances in the Understanding of IOCG Deposits*; PGC Publishing, Adelaide, v. 4, pp. 311-344.
- Cosi, M., De Bonis, A., Gosso, G., Hunziker, J., Martinotti, G., Moratto, S., Robert, J.P. and Ruhlman, F., 1992 - Late Proterozoic thrust tectonics, high-pressure metamorphism and uranium mineralisation in the Domes area, Lufilian Arc, northwestern Zambia; *Precambrian Research*, v. 58, pp. 215-240.

- Coullaut, J.L., 1979 - Geología y metalogenia del criadero de San Guillermo Colmenar, Jerez de los Caballeros, Badajoz; *Curso Rosso de Luna, IGME*, pp. 1-20. (in Spanish)
- Coward, M., 2001 - Structural controls on ore formation and distribution at the Ernest Henry Cu-Au deposit, NW Queensland; BSc (Honours) Thesis, *James Cook University, Townsville*.
- Creaser, R.A., 1989 - The geology and petrology of Middle Proterozoic felsic magmatism of the Stuart Shelf, South Australia; Unpublished Ph.D. thesis, *La Trobe University, Melbourne, Australia*.
- Creaser, R.A., 1995 - Neodymium isotopic constraints for the origin of Mesoproterozoic silicic magmatism, Gawler Craton, South Australia; *Canadian Journal of Earth Sciences*, v. 32, pp. 469-471.
- Creaser, R.A., 1996, Petrogenesis of a Mesoproterozoic quartz latite-granitoid suite from the Roxby Downs area, South Australia; *Precambrian Research*, v. 79, pp. 371-394.
- Creaser, R.A., White, A.J.R., 1991 - Yardea Dacite - large-volume, high-temperature silicic volcanism from the Middle Proterozoic of South Australia; *Geology*, v. 19, pp. 48-51.
- Crocker, I.T., 1985 - Volcanogenic fluorite-hematite deposits and associated pyroclastic rock suite at Vergenoeg, Bushveld Complex; *Economic Geology*, v. 80, pp. 1181-1200.
- Daliran, F., 2002 - Kiruna-type iron oxide-apatite ores and "apatites" of the Bafq district, Iran, with an emphasis on the REE geochemistry of their apatites; in Porter, T.M. (ed.), *Hydrothermal Iron Oxide Copper-Gold and Related Deposits: A Global Perspective*, *PGC Publishing, Adelaide*, v. 2, pp 303-320
- Dallmeyer, R.D. and Quesada, C., 1992 - Cadomian vs. Variscan evolution of the Ossa-Morena Zone (SW Iberia): field and  $^{40}\text{Ar}/^{39}\text{Ar}$  mineral age constrains; *Tectonophysics*, v. 216, pp. 339-364.
- Dallmeyer, R.D., Brown, M., Grocott, J., Taylor, G.K. and Treloar, P.J., 1996 - Mesozoic magmatic and tectonic events within the Andean plate boundary zone, 26-2730°S, north Chile; constraints from  $^{40}\text{Ar}/^{39}\text{Ar}$  mineral ages; *Journal of Geology*, v. 104, pp. 19-40.
- Davidson, G.J., 1989 - Starra and Trough Tank: iron formation-hosted gold and copper deposits of north-west Queensland, Australia; Unpublished Ph.D. thesis, *University of Tasmania, Hobart, Australia*, 376 p.
- Davidson, J.P., 1996 - Deciphering mantle and crustal signatures in subduction zone magmatism; *Geophysical Monograph* 96, pp. 251-262.
- Davidson, G.J. and Large, R.R., 1998 - Proterozoic copper-gold deposits; *AGSO Journal of Australian Geology and Geophysics*, v. 17, pp. 105-113.
- Davidson, G.J., Paterson, H.L., Meffre, S. and Berry, R.G., 2007 - Characteristics and Origin of the Oak Dam East Breccia-Hosted, Iron Oxide Cu-U-(Au) Deposit: Olympic Dam Region, Gawler Craton, South Australia; *Economic Geology*, v. 102, pp. 1471-1498.
- Davies, G.F., 1992, On the emergence of plate tectonics; *Geology*, v. 20, pp. 963-966.
- de Haller, A., Corfú, F., Fontboté, L., Schaltegger, U, Barra, F., Chiaradia, M., Frank, M. and Alvarado, J.Z., 2006 - Geology, geochronology, and Hf and Pb isotope data of the Raúl-Condestable iron oxide-copper-gold deposit, central coast of Perú; *Economic Geology*, v. 101, pp. 281-310.
- de Haller, A. and Fontboté, L., 2009 - The Raúl-Condestable iron oxide copper-gold deposit, central coast of Perú: ore and related hydrothermal alteration, sulfur isotopes, and thermodynamic constraints; *Economic Geology*, v. 104, pp. 365-384.
- de Jong, G. and Williams, P.J., 1995 - Giant metasomatic systems formed during exhumation of mid-crustal Proterozoic rocks in the vicinity of the Cloncurry fault, northwest Queensland; *Australian Journal of Earth Sciences*, v. 42, pp. 281-290.
- de la Rosa, J.D., Jenner, G.A. and Castro, A., 2002 - A study of inherited zircons in granitoid rocks from the South Portuguese and Ossa-Morena zones, Iberian massif: Support for the exotic origin of the south Portuguese zone; *Tectonophysics*, v. 352, pp. 245-256.
- de Hoog, J.C.M., Mason, P.R.D. and van Bergen, M.J., 2001 - Sulfur and chalcophile elements in subduction zones: Constraints from a laser ablation ICP-MS study of melt inclusions from Galunggung Volcano, Indonesia; *Geochimica et Cosmochimica Acta*, v. 65, pp. 3147-3164.
- Direen, N.G. and Lyons, P., 2007 - Regional Crustal Setting of Iron Oxide Cu-Au Mineral Systems of the Olympic Dam Region, South Australia: Insights from Potential Field Modelling; *Economic Geology*, v. 102, pp. 1397-1414.
- Domingos, F., 2009 - The structural setting of the Canaã dos Carajás region and Sossego-Sequeirinho deposits, Carajás - Brazil; Unpublished Doctoral thesis, *Durham University, Durham, U.K.*, 483p.
- Donnellan, N., Hussey, K.J. and Morrison, R.S., 2001 - Short Range, Northern Territory; *Northern Territory Geological Survey*, 1:100 000 geological map series and explanatory notes, 5659.
- Donnellan, N., Morrison, R.S. and Hussey, K.J., 1994 - A brief summary of stratigraphy and structure of the Tennant Creek Block, central Australia; Proceedings, Annual Conference, Darwin, 5-9 August 1994, *Australian Institute of Mining and Metallurgy, Melbourne*, pp. 161-164.
- Dreher, A.M., 2004 - O depósito primário de Cu-Au de Igarapé Bahia, Carajás: Rochas fragmentárias, fluidos mineralizantes e modelo metalogênico; Ph.D. thesis, *Universidade Estadual de Campinas*, 221p. (in Portuguese)
- Drexel, J.F., Preiss, W.V. and Parker, A.J., 1993 - The geology of South Australia. The Precambrian, v. 1: *South Australia Geological Survey Bulletin*, v. 54, 242p
- Duncan, R., Hitzman, M., Nelson, E., Stein, H., Zimmerman, A. and Kirwin, D., 2009 - Re-Os molybdenite ages for the southern Cloncurry IOCG district, Queensland, Australia: Protracted Mineralisation Over 210 myr; in Williams, P.J. et al., (eds.), *Smart Science for Exploration and Mining, Proceedings of the 10<sup>th</sup> Biennial SGA Conference, 17-20 August, 2009, Townsville, Australia*, Extended abstracts, v. 2 pp. 626-628.
- Duncan, R., Stein, H., Evans, K., Hitzman, M., Nelson, E. and Kirwin, D., 2011 - A new geochronological framework for mineralization and alteration in the Selwyn-Mount Dore corridor, Eastern Fold Belt, Mount Isa Inlier, Australia: genetic implications for iron oxide copper-gold deposits; *Economic Geology*, v. 106, pp. 169-192.
- Eby, G.N. and Kochhar, N., 1990 - Geochemistry and petrogenesis of the Malani igneous suite, north Peninsular India; *Journal of the Geological Society of India*, v. 36, pp. 109-130.
- Edfelt, Å., Armstrong, R.N., Smith, M. and Martinsson, O., 2005 - Alteration paragenesis and mineral chemistry of the Tjårrojåkka apatite-iron and Cu (-Au) occurrences, Kiruna area, northern Sweden; *Mineralium Deposita*, v. 40, pp. 409-434.
- Eglington, B.M. and Armstrong, R.A., 2004 - The Kaapvaal Craton and adjacent orogens, southern Africa: a geochronological database and overview of the geological development of the craton; *South African Journal of Geology*, v. 107, pp. 13-32.

- Eguiluz, L., Gil Ibarra, J.I., Ábalos, B. and Apraiz, A., 2000 - Superposed Hercynian and Cadomian orogenic cycles in the Ossa Morena zone and related areas of the Iberian massif; *GSA Bulletin*, v. 112, pp. 1398-1413.
- Ehrig, K., 2010 - Olympic Dam: 35 years since discovery, 2.3 million metres of diamond core, and new (?) ideas; Proceedings, Giant Ore Deposits Down-Under, 13th Quadrennial IAGOD Symposium 2010, Adelaide, South Australia, 6 to 9<sup>th</sup> April, 2009, *International Association on the Genesis of Ore Deposits*, Abstracts CD volume, pp. 9-10.
- Einaudi, M.T. and Oreskes, N., 1990 - Progress towards an occurrence model for Proterozoic iron-oxide (Cu, U, REE, Au) deposits - a comparison between the ore provinces of South Australia and SE Missouri; in Pratt, W.P. and Sims, P.K. (eds.), *The Mid-continent; Permissive Terrain for an Olympic Dam Deposit? U.S. Geological Survey, Bulletin 1932*, pp. 58-69.
- Eriksson, S.C., 1989 - Phalaborwa: a saga of magmatism, metasomatism and miscibility; in Bell, K., (ed.), *Carbonatites, Genesis and Evolution, Unwin Hyman, London*, pp. 221-254.
- Eriksson, P.G., Altermann, W., Catuneanu, O., van der Merwe, R. and Bumby, A.J., 2001 - Major influences on the evolution the 2.67 – 2.1 Ga Transvaal basin, Kaapvaal craton; *Sedimentary Geology*, v. 141-142, pp. 205-231.
- Ernst, R.E. and Buchan, K.L., 2002 - Maximum size and distribution in time and space of mantle plumes: Evidence from large igneous provinces; *Journal of Geodynamics*, v. 34, pp. 309-342.
- Ernst, W.G., 2009 - Archean plate tectonics, rise of Proterozoic supercontinentality and onset of regional, episodic stagnant-lid behavior; Special Issue: Supercontinent Dynamics, *Gondwana Research*, v. 15, pp. 243-253.
- Etheridge, M.A., Rutland, R.W.R. and Wyborn, L.A.I., 1987 - Orogenesis and tectonic process in the early to middle Proterozoic of northern Australia; in Kroner, A., (ed.), *Proterozoic Lithospheric Evolution, Geodynamic Series, American Geophysical Union*, v. 17, pp. 115-130.
- Fanning, C.M., Reid, A. and Teale, G., 2007 - A geochronological framework for the Gawler craton, South Australia; *South Australia Geological Survey, Bulletin 55*, 258p.
- Farmer, G.L., 2005 - Continental basaltic rocks; in Rudnick, R.L., (ed.), *The Crust, Elsevier, Netherlands*, v. 3, pp. 85-122.
- Farnetani, C.G. and Samuel, H., 2005 - Beyond the thermal plume paradigm; *Geophysical Research Letters*, v. 32, L03711.
- Fernández-Suarez, J., Gutiérrez-Alonso, G., Jenner, G.A. and Tubrett, M.N., 2000 - New ideas on the Proterozoic-Early Palaeozoic evolution of northwest Iberia: Insights from U-Pb detrital zircon ages; *Precambrian Research*, v. 102, pp. 185-206.
- Figueiredo e Silva, R.C., Lobato, L.M., Rosiere, C.A., Hagemann, S., Zucchetti, M., Baars, F.J., Morais, R., and Andrade, I., 2008 - A hydrothermal origin for the jaspilite-hosted, giant Serra Norte iron ore deposits in the Carajas Mineral Province, Para State, Brazil; in Rosiere, C.A., Spier, C.A., Rios, F.J. and Suckau, V.E., (eds.), *Banded Iron Formation-Related High-Grade Iron Ore, Reviews in Economic Geology*, v. 15, pp. 255-290.
- Fisher, L.A. and Kendrick, M.A., 2008 - Metamorphic fluid origins in the Osborne Fe oxide Cu-Au deposit, Australia: evidence from noble gases and halogens; *Mineralium Deposita*, v. 43, pp. 483-497.
- Flament, N., Coltice, N. and Rey, P.F., 2008 - A case for late-Archaean continental emergence from thermal evolution models and hypsometry; *Earth and Planetary Science Letters*, v. 275, pp. 326-336.
- Foley, S.F., Barth, M.G. and Jenner, G.A., 2000 - Rutile/melt partition coefficients for trace elements and an assessment of the influence of rutile on the trace element characteristics of subduction zone magmas; *Geochimica et Cosmochimica Acta*, v. 64, pp. 933-938.
- Fonseca, M., de Oliveira, C. and Evangelista, H., 2004 - The Araguaia Belt, Brazil: part of a Neoproterozoic continental-scale strike-slip fault system; in: Weinberg, R., Trouw, R., Fuck, R. and Hackspacher, P., (eds.), *The 750-550 Ma Brasiliano Event of South America, Journal of the Virtual Explorer*, v. 17, Paper 6.
- Foster, A.R., Williams, P.J. and Ryan, C.G., 2007 - Distribution of gold in hypogene ore at the Ernest Henry iron oxide copper-gold deposit, Cloncurry District, NW Queensland; *Exploration and Mining Geology*, v. 16, pp. 125-143.
- Foster, D.R.W. and Austin, J.R., 2008 - The 1800-1610 Ma stratigraphic and magmatic history of the Eastern Succession, Mount Isa Inlier, and correlations with adjacent Paleoproterozoic terranes; *Precambrian Research*, v. 163, pp. 7-30.
- Fourie, P.J., 2000 - The Vergenoeg fayalite iron oxide fluorite deposit, South Africa: some new aspects; in Porter, T.M., (ed.), *Hydrothermal Iron Oxide Copper-Gold and Related Deposits: A Global Perspective, PGC Publishing, Adelaide*, v. 1, pp. 309-320.
- Fraser, G.L., Hussey, K. and Compston, D.M., 2008 - Timing of Palaeoproterozoic Au-Cu-Bi and W-mineralization in the Tennant Creek region, northern Australia: Improved constraints via intercalibration of <sup>40</sup>Ar/<sup>39</sup>Ar and U-Pb ages; *Precambrian Research*, v. 164, pp. 50-65.
- Fraser, S.I., Fraser, A.J., Lentini, M.R. and Gawthorpe, R.L., 2007 - Return to rifts - the next wave: fresh insights into the petroleum geology of global rift basins; *Petroleum Geoscience*, v. 13, pp. 99-104.
- Freeman, H. and Tomkinson, M., 2010 - Geological setting of iron oxide related mineralisation in the southern Mount Woods Domain, South Australia; in Porter, T.M., (ed.), *Hydrothermal Iron Oxide Copper-Gold and Related Deposits: A Global Perspective, v. 3 - Advances in the Understanding of IOCG Deposits; PGC Publishing Adelaide*, v. 3, pp. 171-190. (this volume).
- Frietsch, R., 1978 - On the magmatic origin of the iron ores of the Kiruna type; *Economic Geology*, v. 73, pp. 478-485.
- Frietsch, R., Tuisku, P., Martinsson, O. and Perdahl, J.-A., 1997 - Cu-(Au) and Fe ore deposits associated with Na-Cl metasomatism in early Proterozoic rocks of northern Fennoscandia: A new metallogenic province; *Ore Geology Reviews*, v. 12, pp. 1-34.
- Gauthier, L., Hall, G., Stein, H. and Schaltegger, U., 2001 - The Osborne deposit, Cloncurry district: a 1595 Ma Cu- Au skarn deposit; in: Williams P.J., (ed.), *A Hydrothermal Odyssey, Economic Geology Research Unit, James Cook University, Townsville, Extended Abstracts*, Contribution no.59, pp. 58-59.
- Gandhi, S.S., 1989 - Rhyodacite ignimbrites and breccias of the Sue-Dianne and Mar Cu-Fe-U deposits, southern Great Bear Magmatic Zone, Northwest Territories; *Geological Survey of Canada, Paper 89-1C*, pp. 263-273.
- Geoscience Australia - Australian Stratigraphic Names Database; *Geoscience Australia, Canberra*. <http://www.ga.gov.au/products-services/data-applications/reference-databases/stratigraphic-units.html>
- Ghandi, S.S. and Bell, R.T., 1990 - Metallogenic concepts to aid exploration for the giant Olympic Dam-type deposits and their derivatives; *8<sup>th</sup> IAGOD Symposium, Ottawa, Canada, August, 1990, Program and Abstracts*, p. A7.

- Gibson, R. L. and Stevens, G., 1998 - Regional metamorphism due to anorogenic intracratonic magmatism. What drives metamorphism and metamorphic reactions?; *Geological Society, London, Special Publication*, v. 138, pp. 121-135.
- Giles, C.W., 1988 - Petrogenesis of the Proterozoic Gawler Range Volcanics, South Australia; *Precambrian Research*, v. 40/41, pp. 407-427.
- Gillen, D., Baker, T. and Hunt, J.A., 2004 - Fluid inclusion studies in Fe-oxide Cu-Au deposits, Wernecke Mountains; in McPhie, J. and McGoldrick, P., (eds.), 17th Australian Geological Convention, Hobart, Dynamic Earth: Past, Present and Future, *Geological Society of Australia, Abstracts 73*, p. 82.
- Gillen, D., Baker, T., Ryan, C. and Kendrick, M., 2009 - Evolution of basin-derived IOCG-related hydrothermal fluids in the Wernecke Mountains, Canada; in Williams, P.J. et al., (eds.), Smart Science for Exploration and Mining, *Proceedings of the 10<sup>th</sup> Biennial SGA Conference, 17-20 August, 2009, Townsville, Australia*, Extended abstracts, v. 2, pp. 629-631.
- Gittins, J. and Tuttle, O.F. 1964 - The system  $\text{CaF}_2\text{-Ca(OH)}_2\text{-CaCO}_3$ ; *American Journal of Science*, v. 262, pp. 66-75.
- Glen, R.A., 2005 - The Tasmanides of eastern Australia; in Vaughan, A.P.M., Leat, P.T. and Pankhurst, R.J., (eds.), Terrane Processes at the Margins of Gondwana, *Geological Society of London, Special Publication 246*, pp 23-96.
- Goad, R.E., Mumin, A.H., Duke, N.A., Neale, K.L. and Mulligan, D.L., 2000 - Geology of the Proterozoic iron oxide-hosted NICO cobalt-gold-bismuth and Sue-Dianne copper-silver deposits, southern Great Bear Magmatic Zone, Northwest Territories, Canada; in Porter, T.M., (ed.), Hydrothermal Iron Oxide Copper- Gold and Related Deposits: a Global Perspective, *PGC Publishing, Adelaide*, v. 1, pp. 249-267.
- Goff, B.H., Weinberg, R., Groves, D.I., Vielreicher, N.M. and Fourie, P.J., 2004 - The giant Vergenoeg fluorite deposit in a magnetite-fluorite-fayalite REE pipe: a hydrothermally-altered carbonatite-related pegmatoid?; *Mineralogy and Petrology*, v. 80, pp. 173-199
- Goldfarb, R.I., Bradley, D. and Leach, D.L., 2010 - Secular variations in economic geology; *Economic Geology*, v. 105, pp. 459-465.
- Gow, P.A., Wall, V.J., Oliver, N.H.S. and Valenta, R.K., 1994 - Proterozoic iron oxide (Cu-U-Au-REE) deposits: Further evidence of hydrothermal origins; *Geology*, v. 22, pp. 633-636.
- Gow, P., 1996 - Geological evolution of the Stuart Shelf and Proterozoic iron oxide-associated mineralization: insights from regional geophysical data; Unpublished PhD thesis, *Monash University, Melbourne, Australia*.
- Grainger, C.J., Groves, D.I. and Costa, C.H.C., 2002 - The epigenetic sediment hosted Serra Pelada Au-PGE deposit and its potential genetic association with Fe-oxide Cu-Au mineralisation, Amazon craton, Brazil; in Porter, T.M. (ed.), Hydrothermal Iron Oxide Copper-Gold and Related Deposits: A Global Perspective, *PGC Publishing, Adelaide*, v. 2, pp. 227-245.
- Grainger, C.J., Groves, D.I., Tallarico, F.H.B. and Fletcher, I.R., 2008 - Metallogenesis of the Carajás Mineral Province, Southern Amazon Craton, Brazil: Varying styles of Archean through Paleoproterozoic to Neoproterozoic base- and precious-metal mineralisation; *Ore Geology Reviews*, v. 33, pp. 451-489.
- Grocott, J. and Wilson, J., 1997 - Ascent and emplacement of granitic plutonic complexes in subduction-related extensional environments; in Holmes, M.B., (ed.), Deformation Enhanced Fluid Transport in the Earth's Crust and Mantle. *Chapman and Hall, London*, pp. 173-195.
- Grocott, J. and Taylor, G., 2002 - Magmatic arc fault systems, deformation partitioning and emplacement of granitic complexes in the Coastal Cordillera, north Chilean Andes (25°30' to 27°00' S); *Journal of the Geological Society of London*, v. 159, pp. 425-442.
- Groves, D.I. and Vielreicher, N.M., 2001 - The Phalaborwa (Palabora) carbonatite-hosted magnetite-copper sulfide deposit, South Africa: an end-member of the iron-oxide copper-gold-rare earth element deposit group?; *Mineralium Deposita*, v. 36, pp. 189-194.
- Groves, D.I., Vielreicher, R.M., Goldfarb, R.J. and Condie, K.C., 2005 - Controls on the heterogeneous distribution of mineral deposits through time; in McDonald, I. Boyce, A.J., Butler, I.B., Herrington, R.J. and Polya, D.A., (eds.), Mineral Deposits And Earth Evolution: *Geological Society, London, Special Publication*, v. 248, pp. 71-101.
- Groves, D.I., Bierlein, F.P., Meinert, L.D. and Hitzman, M.W., 2010 - Iron oxide copper-gold (IOCG) deposits through Earth history: implications for origin, lithospheric setting, and distinction from other epigenetic iron oxide deposits; *Economic Geology*, v. 105, pp. 641-654.
- Hagemann, S.H., Rosiere, C.A., Lobato, L., Baars, F. and Zucchetti, M., 2005 - Controversy in genetic models for Proterozoic high-grade, banded iron formation (BIF)-related iron deposits - unifying or discrete model(s)?; in Iron Ore 2005 Conference, Perth, WA, September 19-20, 2005, *The AusIMM, Melbourne, Publication Series 8*, pp. 67-71
- Hagni, R.D. and Brandom, R.T., 1989 - The mineralogy of the Boss-Bixby, Missouri copper-iron-cobalt deposit and a comparison to the Olympic Dam deposit at Roxby Downs, South Australia; in Brown, V.M., Kisvarsanyi, E.B. and Hagni, R.D. (eds.), "Olympic Dam-Type" Deposits and Geology of Middle Proterozoic Rocks in the St. Francois Mountains Terrane, Missouri, *Society of Economic Geologists, Guidebook no. 4*, pp. 82-92.
- Hamilton, W.B., 2007 - Earth's first two billion year - the era of internally mobile crust; in Hatcher, R.D.J., Carlson, M.P., McBride, J.H. and Martínez, C.J.R., (eds.), 4-D Framework of Continental Crust, *Geological Society of America, Boulder, Colorado, Memoir*, v. 200, pp. 233-296.
- Hand, M., Reid, A. and Jagodzinski, L., 2007 - Tectonic framework and evolution of the Gawler Craton, southern Australia; *Economic Geology*, v. 102, pp. 1377-1395.
- Hanson, R.E., Wardlaw, M.S., Wilson, T.J. and Mwale, G., 1993- U-Pb zircon ages from the Hook Granite massif and Mwembeshi dislocation: constraints on Pan-African deformation, plutonism, and transcurrent shearing in Central Zambia; *Precambrian Research*, v. 63, pp. 189-209.
- Harmer, R.E. and Gittins, J., 1997 - The origin of dolomitic carbonatites: Field and experimental constraints; *Journal of African Earth Sciences*, v. 25, pp. 5-28.
- Harmer, R.E. 2000 - Mineralisation of the Phalaborwa complex and the carbonatite connection in iron oxide-Cu-Au-U-REE deposits; in Porter, T.M., (ed.), Hydrothermal Iron Oxide Copper-Gold and Related Deposits: A Global Perspective, *PGC Publishing, Adelaide*, v. 1, pp. 331-340.
- Harné, D.M.W. and Von Gruenewaldt, G., 1995 - Ore-forming processes in the upper part of the Bushveld complex, South Africa; *Journal of African Earth Sciences*, v. 20, pp. 77-89.
- Hart, C.J.R., Mair, J.L., Goldfarb, R.J. and Groves, D.I., 2004 - Source and redox controls on metallogenic variations in ore systems, Tombstone-Tungsten Belt, Yukon, Canada: Transactions, Royal Society Edinburgh: Earth Sciences, v. 95, pp. 339-356.

- Hauck, S.A. and Kendall, E.W., 1984 - Comparison of middle Proterozoic iron oxide-rich ore deposits, mid-continent U.S.A., South Australia, Sweden and Peoples's Republic of China; Abstract, *13<sup>th</sup> Annual Institute on Lake Superior Geology, Wasau, Wisconsin*, pp. 17-18.
- Hauck, S.A., Hinze, W.J., Kendall, E.W. and Adam, S.S., 1989 - A conceptual model of the Olympic Dam Cu-U-Au-REE-Fe deposit: a comparison of central North America and South Australian terranes; *Geological Society of America, Abstracts with Program*, v. 21, pp. A32-33.
- Hauck, S.A., 1990 - Petrogenesis and tectonic setting of middle Proterozoic iron oxide-rich ore deposits: an ore deposit model for Olympic Dam-type mineralization; in Pratt, W.P. and Sims, P.K. (eds.), *The Mid-continent; Permissive Terrain for an Olympic Dam Deposit ? U.S. Geological Survey, Bulletin 1932*, pp. 4-39.
- Hawkins, T., Herrington, R., Smith, M., Maslenikov, V. and Boyce, A., 2010 - The iron skarns of the Turgai Belt, northwestern Kazakhstan; in Porter, T.M., (ed.), *Hydrothermal Iron Oxide Copper-Gold and Related Deposits: A Global Perspective - Advances in the Understanding of IOCG Deposits; PGC Publishing, Adelaide*, v. 4, 461-474.
- Haynes, D.W., Cross, K.C., Bills, R.T. and Reed, M.H., 1995 - Olympic Dam ore genesis: A fluid mixing model; *Economic Geology*, v. 90, pp. 281-307.
- Haynes, D.W., 2000 - Iron oxide copper (-gold) deposits: their position in the ore deposit spectrum and modes of origin, in Porter T.M., (ed.), *Hydrothermal Iron Oxide Copper-Gold and Related Deposits: A Global Perspective, PGC Publishing, Adelaide*, v. 1, pp. 71-90.
- Hayward, N., 2008 - The geodynamic setting and magmatic controls on genesis of world-class IOCG ore deposits; *Geological Society of Australia, Abstracts*, v. 89, p. 130.
- Hayward, N. and Skirrow, R.G., 2010 - Geodynamic setting and controls on iron oxide Cu-Au ( $\pm$ U) ore in the Gawler craton, South Australia; in Porter, T.M., (ed.), *Hydrothermal Iron Oxide Copper-Gold and Related Deposits: A Global Perspective - Advances in the Understanding of IOCG Deposits; PGC Publishing, Adelaide*, v. 3, 119-146. (*this volume*).
- He, B., Xu, Y.-G., Chung, S.-L., Xiao, L. and Wang, Y., 2003 - Sedimentary evidence for a rapid kilometer-scale crustal doming prior to the eruption of the Emeishan flood basalts; *Earth and Planetary Science Letters*, v. 213, pp. 391-405.
- Heron, A.M., 1917 - Geology of Northeastern Rajputana and adjacent district; *Memoir Geological Survey of India*, v. 45, pp. 1-29.
- Hildreth, W. and Moorbath, S., 1988 - Crustal contributions to arc magmatism in the Andes of central Chile: *Contributions to Mineralogy and Petrology*, v. 98, pp. 455-489.
- Hoffmann, A.W. and Hart, S.R., 2007 - Another Nail in Which Coffin?; *Science*, v. 215, pp. 39-40.
- Hoffman P F, 1989 - Precambrian geology and tectonic history of North America; in Bally W A, Palmer A R (Eds), *The Geology of North America, Vol A, The Geology of North America - An Overview, DNAG Series, Geological Society of America, Boulder, Colorado*, pp. 447-512.
- Hildebrand, R.S., Hoffman, P.F. and Bowring, S.A., 2010 - The Calderian orogeny in Wopmay orogen (1.9 Ga), northwestern Canadian Shield; *Geological Society of America Bulletin*, v. 122, pp. 794-814.
- Hitzman, M.W., Oreskes, N. and Einaudi, M.T., 1992 - Geological characteristics and tectonic setting of Proterozoic iron oxide (Cu-U-Au-LREE) deposits; *Precambrian Research*, v. 58, pp. 241-287.
- Hitzman, M.W., 2000 - Iron oxide-Cu-Au deposits: what, where when and why; in Porter T.M., (ed.), *Hydrothermal Iron Oxide Copper-Gold and Related Deposits: A Global Perspective, PGC Publishing, Adelaide*, v. 1, pp. 1-17.
- Hitzman, M.W., 2001 - Fe oxide-Cu-Au systems in the Lufilian Orogen of southern Africa; SEG Special Session I: Iron-Oxide(-Copper-Gold) Systems-Deposit Studies to Global Context, GSA Annual Meeting, November 5-8, 2001, Boston, Massachusetts, Abstract: 1p.
- Hitzman, M.W. and Valenta, R.K., 2005 - Uranium in iron oxide-copper-gold (IOCG) systems; *Economic Geology*, v. 100, pp. 1657-1661.
- Huhn, S.R.B., Souza, C.I.J., Albuquerque, M.C., Leal, E.D. and Brustolin, V., 1999 - Descoberta do depósito Cu(Au) Cristalino: Geologia e mineralização associada região da Serra do Rabo - Carajás - PA; in VI Simpósio de Geologia da Amazônia, Proceedings, *Sociedade Brasileira de Geologia, Belém*, pp. 140-143. (*in Portuguese*)
- Hunt, J.A., Baker, T. and Thorkelson, D.J., 2005 - Regional-scale Proterozoic IOCG-mineralized breccia systems: examples from the Wernecke Mountains, Yukon, Canada; *Mineralium Deposita*, v. 40, pp. 492-514.
- Hunt, J.A., Baker, T. and Thorkelson, D.J., 2007 - A review of iron oxide copper-gold deposits, with focus on the Wernecke Breccias, Yukon, Canada, as an example of a non-magmatic end member and implications for IOCG genesis and classification; *Exploration and Mining Geology, CIM*, v. 16, pp. 209-232.
- Hunt, J.A., Baker, T. and Thorkelson, D.J., 2010 - Wernecke Breccia: Proterozoic IOCG mineralised breccia system, Yukon, Canada; in Porter, T.M., (ed.), *Hydrothermal Iron Oxide Copper-Gold and Related Deposits: A Global Perspective - Advances in the Understanding of IOCG Deposits; PGC Publishing, Adelaide*, v. 4, pp. 345-356.
- Huston, D.L., 1991 - Follow-up studies of C-O-H isotopes in the Tennant Creek district, Northern Territory; AMIRA Workshop Manual No. 5, Proterozoic gold-copper project, *University of Tasmania, CODES, Hobart*, pp. 31-42.
- Huston, D.L., Bolger, C. and Cozens, G., 1993 - A comparison of mineral deposits at the Gecko and White Devil deposits: Implications for ore genesis in the Tennant Creek district, Northern Territory, Australia; *Economic Geology*, v. 88, pp. 1198-1225.
- Huynh, T., Betts, P.G. and Ailleres, L., 2001 - Three dimensional modelling of lithospheric-scale structures of South Australia; in Jessell, M. J., (ed.), *General Contributions: 2001, Journal of the Virtual Explorer*, v. 3. <http://virtualexplorer.com.au/journal/2001/03>.
- Iiyama, J.T., 1965 - Influence des anions sur les équilibres d'échange d'ions Na-K dans les feldspaths alcalins à 600°C sous une pression de 1000 bars; *Bulletin Société Française de Minéralogie et Cristallographie*, v. 88, pp. 618-622.
- Isley, A.E., 1995 - Hydrothermal plumes and the delivery of iron to BIF; *Journal of Geology*, v. 103, pp. 169-185.
- Isley, A.E. and Abbott, D.H., 1999 - Plume-related mafic volcanism and the deposition of banded iron formation; *Journal of Geophysical Research*, v. 104, pp. 15461-15477.
- Ivanac, J.F., 1954 - The geology and mineral deposits of the Tennant Creek Goldfield, N.T., Australia; *Bureau of Mineral Resources, Bulletin 22*, 164p.
- Jagodzinski, E.A., 2005 - Compilation of SHRIMP U-Pb geochronological data, Olympic Domain, Gawler Craton, South Australia, 2001-2003; *Geoscience Australia Record*, v. 2005/20.
- Jago, B.C. and Gittins, J., 1991 - The role of fluorine in carbonatite magma evolution; *Nature*, v. 349, pp. 56-58.
- Johnson, J.P. and Cross, K.C., 1995 - U-Pb geochronological constraints on the genesis of the Olympic Dam Cu-U-Au-Ag deposit, South Australia; *Economic Geology*, v. 90, pp. 1046-1063.

- Johnson, J.P. and McCulloch, M.T., 1995 - Sources of mineralizing fluids for the Olympic Dam deposit, (South Australia): Sm-Nd isotopic constraints; *Chemical Geology*, v. 121, pp. 177-199.
- Kamunzu, A.B. and Cailteux, J., 1999 - Tectonic Evolution of the Lufilian Arc (Central Africa Copper Belt) During Neoproterozoic Pan African Orogenesis; *Gondwana Research*, v. 2, pp. 401-421.
- Kary, G.L. and Harley, R.A., 1990 - Selwyn copper- gold deposits; in Hughes, F.E. (ed.), *Geology of the Mineral Deposits of Australia and Papua New Guinea*, *The Australasian Institute of Mining and Metallurgy, Melbourne*, Monograph 14, v. 1, pp. 955-960.
- Kendrick, M.A., Mark, G. and Phillips, D., 2007 - Mid-crustal fluid mixing in a Proterozoic Fe oxide-Cu-Au deposit, Ernest Henry, Australia: evidence from Ar, Kr, Xe, Cl, Br, and I; *Earth and Planetary Science Letters*, v. 256, pp. 328-343.
- Kendrick, M.A., Baker, T., Fu, B., Phillips, D. and Williams, P.J., 2008 - Noble gas and halogen constraints on regionally extensive mid-crustal Na-Ca metasomatism, the Proterozoic Eastern Mount Isa Block, Australia; *Precambrian Research*, v. 163, pp. 131-150.
- Kendrick, M.A., Honda, M., Gillen, D., Baker, T. and Phillips, D., 2008a - New constraints on regional brecciation in the Wernecke Mountains, Canada, from He, Ne, Ar, Kr, Xe, Cl, Br and I; *Chemical Geology*, v. 255, pp. 33-46.
- Kerrick, R., Goldfarb, R.J. and Richards, J.P., 2005 - Metallogenic provinces in an evolving dynamic framework; in Hedenquist, J.W., Thompson, J.F.H., Goldfarb, R.J. and Richards, J.P. (eds.), *Economic Geology*, 100<sup>th</sup> Anniversary Volume, *Society of Economic Geologists*, pp. 1097-1136.
- Khin Zaw, Huston, D.L., Large, R.R., Mernagh, T. and Ryan, C.G., 1994 - Geothermometry and compositional variation of fluid inclusions from the Tennant Creek gold-copper deposits: implications for ore deposition and exploration; *Mineralium Deposita*, v. 29, pp. 288-300.
- Khuong The Hung, 2010 - Overview of magmatism in northwestern Vietnam; *Annales Societatis Geologorum Poloniae*, v. 80, pp. 185-226.
- Kinnaird, J.A., 2005 - The Bushveld Large Igneous Province; <http://www.largeigneousprovinces.org/Downloads/BushveldLIP.pdf>
- Kisvarsanyi, G., 1989 - The Boss iron-copper deposit, Missouri; in Brown, V.M., Kisvarsanyi, E.B. and Hagni, R.D. (eds.), "Olympic Dam-Type" Deposits and Geology of Middle Proterozoic Rocks in the St. Francois Mountains Terrane, Missouri, *Society of Economic Geologists*, Guidebook no. 4, pp. 69-81.
- Kisvarsanyi, G. and Kisvarsanyi, E.B., 1989 - Precambrian geology and ore deposits of the Southeast Missouri Iron Metallogenic Province; in Brown, V.M., Kisvarsanyi, E.B. and Hagni, R.D. (eds.), "Olympic Dam-Type" Deposits and Geology of Middle Proterozoic Rocks in the St. Francois Mountains Terrane, Missouri, *Society of Economic Geologists*, Guidebook, no. 4, pp. 1-40.
- Kleeman, G. J. and Twist D., 1989 - The compositionally-zoned sheet-like granite pluton of the Bushveld Complex: Evidence bearing on the nature of A-type magmatism; *Journal of Petrology*, v. 30, pp. 1383-1414.
- Knutson, J., Donnelly, T.H., Eadington, P.J. and Tonkin, D.G., 1992 - Hydrothermal alteration of Middle Proterozoic basalts, Stuart Shelf, South Australia - a possible source for Cu mineralisation; *Economic Geology*, v. 87, pp. 1054-1077.
- Kolb, J., Meyer, F.M., Vennemann, T., Sindern, S., Prantl, S., Böttcher, M.E. and Sakellaris, G.A., 2010 - Characterisation of the hydrothermal fluids of the Guelb Moghrein iron oxide-Cu-Au-Co deposit, Mauritania: ore mineral chemistry, fluid inclusions and isotope geochemistry; in Porter, T.M., (ed.), *Hydrothermal Iron Oxide Copper-Gold and Related Deposits: A Global Perspective - Advances in the Understanding of IOCG Deposits*; *PGC Publishing, Adelaide*, v. 4, pp. 553-572.
- Korobeinikov, V.P., Scheglov, A.P., Surkov, V.S. and Isakov, V.M., 1980 - Areal ophiolites of Eastern Tuva and diapiric model for structural developments in mobile belts; *Russian Geology and Geophysics*, no.9, pp. 19-33. (in Russian)
- Krcmarov, R.L. and Stewart, J.I., 1998 - Geology and mineralisation of the Greenmount Cu-Au-Co deposit, southeastern Marimo basin; *Australian Journal of Earth Sciences*, v. 45, p. 463-482.
- Kruger, F.J. 2002. Isotopic constraints on the origin of the Bushveld Complex mag mas in a back-arc environment; *Geochimica et Cosmochimica Acta*, v. 66 (15A), p. A420.
- Lahtinen, R., Hölttä, P., Kontinen, A., Niiranen, T., Nironen, M., Saalman, K. and Sorjonen-Ward, P., 2011 - Tectonic and metallogenic evolution of the Fennoscandian shield: key questions with emphasis on Finland; in Nenonen, K. and Nurmi, P.A., (eds.), *Geoscience for Society, 125th Anniversary Volume, Geological Survey of Finland*, Special Paper 49, pp. 23-33.
- Lahtinen, R., Korja, A. and Nironen, M., 2005 - Palaeoproterozoic tectonic evolution; in Lehtinen, M., Nurmi, P.A. and Rämö, O.T., (eds.), *Precambrian Geology of Finland - Key to the Evolution of the Fennoscandian Shield, Developments in Precambrian geology, Elsevier, Amsterdam*, v. 14, pp. 481-532.
- Lambert, I.B., Drexal, J.F., Donnelly, T.H. and Knutson, J., 1982 - Origin of breccias in the Mount Painter area, South Australia; *Journal of the Geological Society of Australia*, v. 29, pp. 115-125.
- Lancaster Oliveira J., Fanton, J., Almeida, A.J., Leveille, R.A. and Vieira, S., 2000 - Discovery and geology of the Sossego copper-gold deposit, Carajás District, Pará State, Brazil; in 31st International Geology Congress, *Proceedings, International Union of Geological Sciences*, [CD-ROM].
- Lara, P.L. and Godoy, P-B.E., 1998 - Hoja Quebrada Salitrosa, Region de Atacama; *Servicio Nacional de Geología y Minería, Santiago, Chile*, Mapas Geológicos No.4, 1 mapa, escala 1:100 000.
- Large, R.R., 1975 - Zonation of hydrothermal minerals at the Juno Mine, Tennant Creek goldfield, Central Australia. *Economic Geology*, v. 70, pp. 1387-1413.
- Le Messurier, P., Williams, B.T. and Blake, D.H., 1990 - Tennant Creek Inlier - regional geology and mineralisation; in Hughes, F.E., (ed.), *Geology of the Mineral Deposits of Australia and Papua New Guinea*, *The AusIMM, Melbourne*, Monograph 14, v. 1 pp. 829-838.
- Lehtonen, M. I., Airo, M-L., Eilu, P., Hanski, E., Kortelainen, V., Lanne, E., Manninen, T., Rastas, P., Räsänen, J. and Virransalo, P., 1998 - Kittilän vihreäkivialueen geologia. Lapin vulkanitiiprosjektin raportti. English summary: The stratigraphy, petrology and geochemistry of the Kittilä greenstone area, northern Finland. A report of the Lapland Volcanite Project; *Geological Survey of Finland*, Report of Investigation 140, 144p.
- Li, Z.X., Bogdanova, S.V., Collins, A.S., Davidson, A., De Waele, B., Ernst, R.E., Fitzsimons, I.C.W., Fuck, R.A., Gladkochub, D.P., Jacobs, J., Karlstrom, K.E., Lu, S., Natapov, L.M., Pease, V., Pisarevsky, S.A., Thrane, K. and Vernikovskiy, V., 2008 - Assembly, configuration, and break-up history of Rodinia: A synthesis; *Precambrian Research*, v. 160, pp. 179-210.

- Lincoln, J.B., Tellez, C., 1995 - The Andacollo gold project, IV Region, Chile; in Green, S.M., Struhsacker, E., (eds.), *Geology and Ore Deposits of the American Cordillera, Field Trip Guidebook compendium Geological Society of Nevada*, pp. 492-495.
- Lindenmayer, Z.G., 1990 - Salobo sequence, Carajás, Brasil: *Geology, Geochemistry and Metamorphism*; PhD thesis, *University of Ontario, Canada*, 407p.
- Lindenmayer, Z.G., 2003 - Depósito de Cu-Au do Salobo, Serra dos Carajás: Uma revisão; in Ronchi, L.H. and Althoff, F.J., (eds.), *Caracterização e Modelamento de Depósitos Minerais, Editora Unisinos, São Leopoldo*, pp. 69-98. (in Portuguese)
- Lobato, L.M., Figueiredo e Silva, R.C., Rosiere, C.A., Zucchetti, M., Baars, F.J., Pimentel, M., Rios, F.J., Seoane, J.C.S. and Monteiro, A.M., 2005 - Hydrothermal origin for the iron mineralisation, Carajas Province, Para State, Brazil; in *Iron Ore 2005 Conference, Perth, WA, September 19-20, 2005, The AusIMM, Melbourne, Publication Series 8*, pp. 99-110.
- Lobato, L.M., Rosiere, C.A., Figueiredo e Silva, R.C., Zucchetti, M., Baars, F.J., Seoane, J.C.S., Rios, F.J., Pimentel, M., Mendes, G.E. and Monteiro, A.M., 2005a - A mineralização hidrotermal de ferro da Província Mineral de Carajás o Controle estrutural e contexto na evolução metalogenética da província; in Marini, O.J., de Queiroz, E.T. and Ramos B.W., (eds.), *Caracterização de Depósitos Minerais em Distritos Mineiros da Amazônia. Departamento Nacional da Produção Mineral (DNPM). Fundo Setorial Mineral (CT-Mineral/FINEP)/Agência para o Desenvolvimento Tecnológico da Indústria Mineral Brasileira (ADIMB), Brasília, Brazil*, pp. 25-92. (in Portuguese)
- Lobo-Guerrero S., A., 2005 - Pre- and post-Katangan granitoids of the greater Lufilian Arc, geology, geochemistry, geochronology and metallogenic significance; unpublished Ph.D. thesis, Faculty of Science, *University of the Witwatersrand, Johannesburg, South Africa*, 452p.
- Lobo-Guerrero S., A., 2010 - Iron Oxide-Copper-Gold Mineralization in the Greater Lufilian Arc, Africa; in Corriveau, L. and Mumin, H., (Eds.), *Exploring for Iron Oxide Copper-Gold Deposits, Canada and Global Analogues*; Geological Association of Canada, pp. 161-184.
- Lowman, J.P. and Jarvis, G.T., 1996 - Continental collisions in wide aspect ratio and high Rayleigh number two-dimensional mantle convection models; *Journal of Geophysical Research*, v. 101, pp. 25 485-25 497.
- Lustrino, M., 2005a - How the delamination and detachment of lower crust can influence basaltic magmatism; *Earth-Science Reviews*, v. 72, pp. 21-38.
- Lustrino, M., 2005b - Basaltic magmatism influenced by high-pressure basaltic lithologies stored in the upper mantle; <http://www.mantleplumes.org/LowerCrust.html>
- MacCready, T., Goleby, B.R., Goncharov, A., Drummond, B.J. and Lister, G.S., 1998 - A framework of overprinting orogens based on interpretation of the Mt Isa deep seismic transect; *Economic Geology*, v. 93, pp. 1422-1434.
- Mark, G. and de Jong, G. 1998 - Synchronous granitoid emplacement and episodic sodic-calcic alteration in the Cloncurry district; styles, timing and metallogenic significance; in: Baker, T., Rotherham, J., Mark, G. and Williams, P., (eds.), *New Developments the Metallogenic Research, the McArthur, Mt Isa, Cloncurry Minerals Province, Economic Geology Research Unit, James Cook University, Townsville, Extended Abstracts, Contribution no.55*, pp. 81-84.
- Mark, G., 1999 - Petrogenesis of mesoproterozoic K-rich granitoids, southern Mt Angelay igneous complex, Cloncurry district, northwest Queensland; *Australian Journal of Earth Science*, v. 46, pp. 933-949.
- Mark, G., 2001 - Nd isotope and petrogenetic constraints for the origin of the Mount Angelay igneous complex: implications for the origin of intrusions in the Cloncurry district NE Australia; *Precambrian Research*, v. 105, pp. 17-35.
- Mark, G. and Foster, D.R.W., 2000 - Magmatic-hydrothermal albite-actinolite-apatite-rich rocks from the Cloncurry district, NW Queensland, Australia; *Lithos*, v. 51, pp. 223-245.
- Mark, G., Foster, D.R.W., Pollard, P.J., Williams, P.J., Tolman, J., Darvall, M. and Blake, K.L., 2004 - Stable isotope evidence for magmatic fluid input during large-scale Na-Ca alteration in the Cloncurry Fe oxide Cu-Au district, NW Queensland, Australia; *Terra Nova*, v. 16, pp. 54-61.
- Mark, G., Oliver, N.H.S., Williams, P.J., Valenta, R.K. and Crookes, R.A., 2000 - The evolution of the Ernest Henry hydrothermal system; in Porter, T.M., (ed.), *Hydrothermal Iron Oxide Copper-Gold and Related Deposits: A Global Perspective, PGC Publishing, Adelaide*, v. 1, pp. 123-136.
- Mark, G., Oliver, N.H.S. and Carew, M.J., 2006 - Insights into the genesis and diversity of epigenetic Cu-Au mineralisation in the Cloncurry district, Mt Isa Inlier, northwest Queensland; *Australian Journal of Earth Sciences*, v. 53, pp. 109-124.
- Mark, G., Oliver, N. and Williams, P., 2006a - Mineralogical and chemical evolution of the Ernest Henry Fe oxide-Cu-Au ore system, Cloncurry district, northwest Queensland, Australia; *Mineralium Deposita*, v. 40, pp. 769-801.
- Mark, G., Pollard, P.J., Foster, D.R.W., McNaughton, N. and Mustard, R., 2005 - Episodic syn-tectonic magmatism in the Eastern Succession, Mount Isa Block, Australia: implications for the origin, derivation and tectonic setting of potassic 'A-type' magmas; in Blenkinsop, T.G., (ed.), *Final Report, Total Systems Analysis of the Mt Isa Eastern Succession. Predictive Mineral Discovery CRC*, pp. 51-74.
- Mark G., Wilde A.R., Oliver N.H.S. and Williams P.J., 2005a - Predicting alteration patterns in the outflow zones of hydrothermal ore systems: a case study using the "spent" fluids from the Ernest Henry Fe-oxide-Cu-Au deposit; *Journal of Geochemical Exploration*, v. 85, pp. 31-46.
- Mark, G., Williams, P.J., Oliver, N.H.S., Ryan, C.G. and Mernagh, T., 2005b - Fluid inclusion and stable isotope geochemistry of the Ernest Henry iron oxide-copper-gold deposit, Queensland, Australia; in Mao, J. and Bierli, F.P., (eds.), *Mineral Deposit Research: Meeting the Global Challenge, Conference Proceedings, Berlin, Springer, Heidelberg*, pp. 785-788.
- Marschik, R., Leveille, R.A. and Martin, W., 2000 - La Candelaria and the Punta del Cobre district, Chile: Early Cretaceous iron-oxide Cu-Au(-Zn-Ag) mineralisation; in Porter T.M., (ed.), *Hydrothermal Iron Oxide Copper-Gold and Related Deposits: A Global Perspective, PGC Publishing, Adelaide*, v. 1, pp. 163-175.
- Marschik, R. and Fontboté, L., 2001 - The Candelaria-Punta del Cobre iron oxide Cu-Au (-Zn, Ag) deposits, Chile; *Economic Geology*, v. 96, pp. 1799-1826.
- Marschik, R., Chiaradia, M. and Fontboté, L., 2003 - Implications of Pb isotope signatures of rocks and iron oxide Cu-Au ores in the Candelaria-Punta del Cobre district, Chile; *Mineralium Deposita*, v. 38, pp. 900-912.

- Marshall, L.L., Oliver, N.H.S. and Davidson, G.J., 2006 - Carbon and oxygen isotope constraints on fluid sources and fluid-wallrock interaction in regional alteration and iron-oxide-copper-gold mineralisation, eastern Mt Isa Block, Australia; *Mineralium Deposita*, v. 41, pp. 429-452.
- Mathur, R., Marschik, R., Ruiz, J., Munziga, F., Leveille, R.A. and Martin, W., 2002 - Age of mineralization of the Candelaria Fe oxide Cu-Au deposit and the origin of the Chilean Iron Belt, based on Re-Os isotopes; *Economic Geology*, v. 97, pp. 59-71.
- McKenzie, D., 1978 - Some remarks on the development of sedimentary basins; *Earth and Planetary Science Letters*, v. 40, pp. 25-32.
- McInnes, B.I.A., Keays, R.R., Lambert, D.D., Hellstrom, J. and Allwood, J.S., 2008 - Re-Os geochronology and isotope systematics of the Tanami, Tennant Creek and Olympic Dam Cu-Au deposits; *Australian Journal of Earth Sciences*, v. 55, pp. 967-981.
- McLean, R. N., 2001 - The Sin Quyen iron oxide-copper gold-rare earth oxide mineralization of North Vietnam; in Porter T.M., (Ed.), *Hydrothermal Iron Oxide Copper-gold and Related Deposits: A global Perspective*, PGC Publishing, Adelaide, v. 2, pp. 293-301.
- McPhie, J., Kamenetsky, V., Chambefort, I., Ehrig, K. and Green, N., 2010 - The origin of Olympic Dam: a revolutionary new view; Proceedings, Giant Ore Deposits Down-Under, 13th Quadrennial IAGOD Symposium 2010, Adelaide, South Australia, 6-9<sup>th</sup> April, 2009, *International Association on the Genesis of Ore Deposits*, Abstracts CD volume, pp. 76-77.
- Mumin, A.H., Phillips, A., Katsuragi, C.J. and Mumin, A., 2009 - Oblique extension, tectonics and mineral deposition, Great Bear Magmatic Zone, NWT, Canada; in Jackson, V. and Palmer, E., (compilers), 37<sup>th</sup> Annual Yellowknife Geoscience Forum Abstracts, *Northwest Territories Geoscience Office*, Yellowknife, NT, YKGSF Abstracts Volume 2009, p. 45.
- Mumin, A.H., Somarin, A.K., Jones, B., Corriveau, L., Ootes, L. and Camier, J., 2010 - The IOCG-porphry-epithermal continuum of deposit types in the Great Bear Magmatic Zone, Northwest Territories, Canada; in Corriveau, L. and Mumin, A.H., (eds.), *Exploring For Iron Oxide Copper-Gold Deposits: Canada and Global Analogues*; *Geological Association of Canada*, Short Course Notes 20, pp. 59-78.
- Mungall, J.E., 2002 - Roasting the mantle: Slab melting and the genesis of major Au and Au-rich Cu deposits; *Geology*, v. 30, pp. 915-918.
- Mutanen, T., 1997 - Geology and ore petrology of the Akanvaara and Koitelainen mafic layered intrusions and the Keivitsa-Satovaara layered complex, northern Finland; *Geological Survey of Finland*, Bulletin 395, 232p.
- Myers, J.S., Shaw, R.D. & Tyler, I.M., 1996 - Tectonic evolution of Proterozoic Australia; *Tectonics*, v. 15, pp. 1431-1446.
- Nägler, T., 1990 - Sm-Nd, Rb-Sr and common lead isotope geochemistry on fine-grained sediments of the Iberian Massif; Unpublished Ph.D. thesis, *Swiss Federal Institute Technology, Zurich*, 139p.
- Nägler, T.F., Schäfer, H.J. and Gebauer, D., 1995 - Evolution of the western European continental crust: implications from Nd and Pb isotopes in Iberian sediments; *Chemical Geology*, v. 121, pp. 345-357.
- Naqvi, S.M. and Rogers, J.J.W., 1987 - Precambrian Geology of India; *Oxford University Press, New York*, 223p.
- Naslund, H.R., Aguirre, R. and Lledó, H., 2004 - Evidence for the formation of massive magnetite ores by liquid immiscibility IAVCEI 2004, Pucon (Chile), Abstract volume
- Nikulin, V.I., Von der Flaass, G.S. and Baryshev, A.S., 1991 - Explosion-volcanic basaltic ore-forming systems, the Angara iron-ore province; *Geology of Ore Deposits*, no. 3, pp. 26-40. (in Russian)
- Nisbet, B., Cooke, J., Richards, M. and Williams, C., 2000 - Exploration for Iron Oxide Copper Gold Deposits in Zambia and Sweden: Comparison with the Australian Experience; in Porter, T. M., (ed.), *Hydrothermal Iron Oxide Copper-gold and Related Deposits: A Global Perspective*, PGC Publishing, Adelaide, v. 1, pp. 297-308.
- Norris, D.K., 1997 - Geology and mineral and hydrocarbon potential of northern Yukon Territory and northwestern district of Mackenzie; *Geological Survey of Canada*, Bulletin 422, 401p.
- Nutman A.P., 1997. The Greenland sector of the North Atlantic Craton. in de Wit, M.J. and Ashwal, L.D., (eds.), *Greenstone Belts*, Clarendon Press, Oxford, pp. 665-674.
- Nyström, J.O. and Henriquez, F., 1994 - Magmatic features of iron ores of the Kiruna type in Chile and Sweden: ore textures and magnetite geochemistry; *Economic Geology*, v. 89, pp. 820-839.
- Odintsov, M.M., Domyshev, V.G., Strakhov, L.G., Zuev, P.P., Khramtsov, A.G., Shames, P.I., Alexeev, S.P., Andreev, R.Yu., Volkov, A.I., Kanitskaya, S.G. and Malykh, A.V., 1980 - The Angara-Vilyui ore belt in the Siberian Craton; *Nauka Publishing, Novosibirsk*, 109p. (in Russian)
- Ödman, O., 1957 - Beskrivning till Bergrundskarta över Norrbottens Län; Geological Survey of Sweden, Ca. 41, 151 p. (in Swedish with English summary).
- Oliver, N.H.S., 1995 - Hydrothermal history of the Mary Kathleen Fold Belt, Mt Isa Block Queensland; *Australian Journal of Earth Science*, v. 42, pp. 267-279
- Oliver, N.H.S., Dickens, G.R. and Dipple, G.M., 2006 - Oxygen isotope study of infiltration of heated meteoric water to form giant Hamersley iron ores; *Geochimica et Cosmochimica Acta*, v. 70, pp. A457-A457.
- Oliver, N.H.S., Rubenach, M.J., Fu, B., Baker, T., Blenkinsop, T.G., Cleverley, J.S., Marshall, L.J. and Ridd, P.J., 2006a - Granite-related overpressure and volatile release in the mid crust: fluidized breccias from the Cloncurry district, Australia; *Geofluids*, v. 6, pp. 346-358.
- Oliver, N.H.S., Butera, K.M., Rubenach, M.J., Marshall, L.J., Cleverley, J.S., Mark, G., Tullemans, F. and Esser, D., 2008 - The protracted hydrothermal evolution of the Mount Isa Eastern Succession: A review and tectonic implications; *Precambrian Research*, v. 163, pp. 108-130.
- Oliver, N.H.S., Rubenach, M.J., and Predictive Mineral Discovery Cooperative Research Centre, 2009 - Distinguishing basinal- and magmatic-hydrothermal IOCG deposits, Cloncurry District, Northern Australia; in Williams, P.J. et al., (eds.), *Smart Science for Exploration and Mining, Proceedings of the 10<sup>th</sup> Biennial SGA Conference, 17-20 August, 2009, Townsville, Australia*, Extended abstracts, v. 2, pp. 647-649.
- Oreskes, N., Einaudi, M.T. and Hitzman, M.W., 1989 - Tectonic setting of Olympic Dam and relation to other Proterozoic Fe-REE deposits; 28<sup>th</sup> *International Geological Conference, Washington D.C.*, June 1989, Abstracts, v. 2, p. 551.
- Oreskes, N. and Einaudi, M.T., 1992 - Origin of hydrothermal fluids at Olympic Dam; preliminary results from fluid inclusions and stable isotopes; *Economic Geology*, v. 87, pp. 64-90.
- Oyarzun, R., Oyarzún, J., Ménard, J.J. and Lillo, J., 2003 - The Cretaceous iron belt of northern Chile: role of oceanic plates, a superplume event, and a major shear zone; *Mineralium Deposita*, v. 38, pp. 640-646.
- Page, R., 1995 - Unpublished SHRIMP I data; OZCHRON database, *Geoscience Australia*.
- Page, R.W. and Sun, S.-S., 1998 - Aspects of geochronology and crustal evolution in the Eastern Fold Belt Mount Isa Inlier; *Australian Journal of Earth Science*, v. 45, pp. 343-362.

- Page, R.W. and Williams, I.S., 1988 - Age of the Barramundi Orogeny in northern Australia by means of ion microprobe and conventional U-Pb studies. *Precambrian Research*, v. 40/41, pp. 21-36.
- Palacios, M.O., Caldas, V.J. and Vela, V.C., 1992 - Geología de los Cu-adrangulos de Lima, Lurin, Chancay y Chosica; Hojas 25-i, 25-j, 24-i, 24-j; Carta Geológica Nacional, *Instituto Geológico Minero y Metalúrgico, Lima*, Bol. Serie A, no. 43:1, 163 p.
- Peacock, S.M., 1993 - Large-scale hydration of the lithosphere above subducting slabs: *Chemical Geology*, v. 108, pp. 49-59.
- Perkins, C. and Wyborn, L., 1998 - Age of Cu-Au mineralisation, Cloncurry district, Mount Isa inlier, as determined by  $^{40}\text{Ar}/^{39}\text{Ar}$  dating; *Australian Journal of Earth Sciences*, v. 45, p. 233-246.
- Perring, C.S., Pollard, P.J., Dong, G., Nunn, A.J. and Blake, K.L., 2000 - The Lightening Creek sill complex, Cloncurry district, northwest Queensland: a source of fluids for Fe oxide Cu-Au mineralization and sodic-calcic alteration; *Economic Geology*, v. 95, pp.1067-1090.
- Petters, S.W., 1986 - Regional geology of Africa; Lecture Notes in Earth Sciences 40 *Springer-Verlag*, 722p.
- Pichon, R., 1981, Contribution à la étude de la ceinture de fer du Chili. Les gisements de Bandurrias (Prov. d'Atacama) et de Colorados Norte (Provincia de Huasco); Unpublished Ph.D. Thesis, *Université de Paris, Paris*, XI, 326p.
- Pichowiak, S., Buchelt, M. and Damm, K. W., 1990 - Magmatic activity and tectonic setting of the early stages of the Andean cycle in northern Chile; in Kay S.M., Rapela C.W. (eds.), Plutonism from Antarctica to Alaska: *Geological Society of America*, Special Paper 241, pp. 127-144.
- Piranjo, F., 2000 - Ore deposits and mantle plumes; *Kluwer Academic Publishers, Dordrecht, Netherlands*, 560p.
- Piranjo, F., 2009 - Hydrothermal processes and mineral systems; *Springer Science+Business Media*, 1250p
- Pitcher, W.S. and Cobbing, E.J., 1985 - A model for the Coastal batholith; in Pitcher, W.S., Atherton, M.P., Cobbing, E.J. and Beckingsale, R.D., (eds.), Magmatism at a Plate Edge: the Peruvian Andes, *Blackie and Son Ltd., Glasgow*, pp. 19-25.
- Pimentel, M.M., Lindenmayer, Z.G., Laux, J.H., Armstrong, R. and Araújo, J.C., 2003 - Geochronology and Nd geochemistry of the Gameleira Cu-Au deposit, Serra dos Carajás, Brazil: 1.8-1.7 Ga hydrothermal alteration and mineralization; *Journal of South American Earth Sciences*, v. 15, pp. 803-813.
- Plumb, K.A., 1979 - The tectonic evolution of Australia; *Earth Science Reviews*, v. 14, pp. 205-249.
- Pollack, H.N., 1986 - Cratonization and thermal evolution of the mantle: *Earth and Planetary Science Letters*, v. 80, pp. 175-182.
- Pollard, P.J., 2001 - Sodic (-calcic) alteration in Fe oxide-Cu-Au districts: an origin via unmixing of magmatic-derived  $\text{H}_2\text{O}-\text{CO}_2-\text{NaCl} \pm \text{CaCl}_2-\text{KCl}$  fluids; *Mineralium Deposita*, v. 36, pp. 93-100.
- Pollard, P.J., Mark, G. and Mitchell, L.C., 1998 - Geochemistry of post-1540 Ma granites in the Cloncurry District Northwest Queensland. *Economic Geology*, v. 93, pp. 1330-1344.
- Polliand, M., Schaltegger, U., Frank, M. and Fontboté, L., 2005 - Formation of intra-arc volcano-sedimentary basins in the western flank of the central Peruvian Andes during Late Cretaceous oblique subduction field evidence and constraints from U-Pb ages and Hf isotopes; *International Journal of Earth Sciences*, v. 94, pp. 231-242.
- Porada, H. and Berhorst, V., 2000 - Towards a new understanding of the Neoproterozoic - Early Palaeozoic Lufilian and northern Zambezi Belts in Zambia and the Democratic Republic of Congo; *Journal of African Earth Sciences*, v. 30, pp. 727-771.
- Porter, T.M., 2000 - Hydrothermal Iron Oxide Copper-Gold and Related Deposits: A Global Perspective, *PGC Publishing, Adelaide*, v. 1, 350p.
- Porter, T.M., 2002 - Hydrothermal Iron Oxide Copper-Gold and Related Deposits: A Global Perspective, *PGC Publishing, Adelaide*, v. 2, 378p.
- Porter, T.M., 2010 - The Carrapateena iron oxide copper gold deposit, Gawler craton, South Australia: a review; in Porter, T.M., (ed.), Hydrothermal Iron Oxide Copper-Gold and Related Deposits: A Global Perspective - Advances in the Understanding of IOCG Deposits; *PGC Publishing, Adelaide*, v. 3, pp. 191-200. (*this volume*).
- Pratt, T.L., Hauser, E.C. and Nelson, K.D., 1992 - Widespread buried Precambrian layered sequences in the U.S. Mid-continent: evidence for large Proterozoic depositional basins; in The American Association of Petroleum Geologists, v. 76, pp. 1384-1401.
- Proffett, J.M., 2003 - Geology of the Bajo de la Alumbrera porphyry copper-gold deposit, Argentina; *Economic Geology*, v. 98 (8), pp. 1535-1574.
- Quesada, C., 1992 - Evolución tectónica del Macizo Ibérico (una historia de crecimiento por acrecencia sucesiva de terrenos durante el Proterozoico Superior y Paleozoico); in Gutierrez J.C., Saavedra M.J. and Rábano, I., (eds.) *Paleozoico Inferior de Ibero-América*, Junta de Extremadura, pp. 173-192. (*in Spanish*)
- Rainaud, C., Master, S., Armstrong, R.A. and Robb, L.J., 2005 - Geochronology and nature of the Palaeoproterozoic basement in the Central African Copperbelt (Zambia and the Democratic Republic of Congo), with regional implications; *Journal of African Earth Sciences*, v. 42, pp 1-31.
- Ramos, V.A. and Basei, M., 1997 - The basement of Chilenia: an exocitic continental terrane to Gondwana during the Early Paleozoic; in Bradshaw, J.D. and Weaver, S.D., (eds.), Terrane Dynamics - 97, *Department of Geological Sciences, University of Canterbury, Christchurch, New Zealand*, pp. 140-143.
- Ramos, V.A., 2000 - The southern central Andes; in Cordani, U.G., Milani, E.J., Thomaz Filho, A. and Campos, D.A., (eds.), Tectonic Evolution of South America - *Proceedings 31st International Geological Congress, Rio de Janeiro*, pp. 561-604.
- Ramos, V.A., 2004 - Cuyania, an Exotic Block to Gondwana: Review of a Historical Success and the Present Problems; *Gondwana Research*, v. 7, pp. 1009-1026
- Ramos, V.A., 2008 - The Basement of the Central Andes: The Arequipa and Related Terranes; *The Annual Review of Earth and Planetary Sciences*, v. 36, pp 289-324.
- Rapp, R.P. and Watson, E.B., 1995 - Dehydration melting of metabasalt at 8-32 kbar: implications for continental growth and crust-mantle recycling; *Journal of Petrology*, v. 36, pp. 891-931.
- Rastas, P., Huhma, H., Hanski, E., Lehtonen, M.I., Härkönen, I., Kortelainen, V., Mänttari, I. and Paakkola, J., 2001 - U-Pb isotopic studies on the Kittilä greenstone area, Central Lapland, Finland; in Vaasjoki, M., (ed.), Radiometric Age Determinations from Finnish Lapland and Their Bearing on the Timing of Precambrian Volcano-sedimentary Sequences, *Geological Survey of Finland*, Special Paper 33, pp. 95-141.
- Rao, V.V. and Reddy, P.R., 2002 - A Mesoproterozoic supercontinent: evidence from the Indian shield; *Gondwana Research*, v. 5, pp. 63-74.
- Raymond, O.L., Fletcher, I., and McNaughton, N., 2002 - Copper-gold mineral systems in the southeastern Gawler Craton - another Mt Isa Eastern Succession?; in Preiss, V.P., (ed.), Geoscience 2002: Expanding Horizons: 16th Australian Geological Convention, Adelaide, South Australia, *Geological Society of Australia*, Abstracts No. 67, p. 69.

- Reddy, S.M. and Evans, D.A.D., 2009 - Palaeoproterozoic supercontinents and global evolution: correlations from core to atmosphere; *Geological Society, London, Special Publications*, v. 323, pp. 1-23.
- Reeve, J.S., 1990 - The discovery and evaluation of the Olympic Dam deposit; in Glasson, K.R., Rattigan, J.M., Blaikie, A.H. and Woodcock, J.T., (eds.), *Geological Aspects of the Discovery of Important Mineral Deposits in Australia, The Australasian Institute of Mining and Metallurgy, Melbourne*, v. 2, pp. 125-133.
- Reeve, J.S., Cross, K.C., Smith, R.N. and Oreskes, N., 1990 - Olympic Dam copper-uranium-gold-silver deposit; in Hughes, F.E. (ed.), *Geology of the Mineral Deposits of Australia and Papua New Guinea, The Australasian Institute of Mining and Metallurgy, Melbourne, Monograph 14*, pp. 1009-1035.
- Reid, A., Davies, M., Jagodzinski, E., Gregory, C. and Jeffrey, L., 2010 - PACE 2020 - PACE Geochronology; From Airborne Electromagnetic Survey; Geoscientist Assistance Program; *MESA Journal*, v. 57, pp. 9-12.
- Requia, K. and Fontboté, L., 2000 - The Salobo iron oxide copper-gold deposit, Carajás, northern Brazil; in Porter, T.M. (ed.), *Hydrothermal Iron-Oxide Copper-Gold and Related Deposits: A Global Perspective, PGC Publishing, Adelaide*, v. 1, pp. 225-236.
- Requia, K. and Fontboté, L., 2001 - The Salobo iron oxide copper-gold hydrothermal system, Carajás Mineral Province, Brazil; *Geological Society of America, Abstract with Programs*, v. 33, no. 6, p. 2.
- Requia, K., Stein, H., Fontboté, L. and Chiaradia, M., 2003 - Re-Os and Pb-Pb geochronology of the Archean Salobo iron oxide copper-gold deposit, Carajás Mineral Province, northern Brazil; *Mineralium Deposita*, v. 38, pp. 727-738.
- Rey, P.F. and Coltice, N., 2008 - Neoproterozoic lithospheric strengthening and the coupling of Earth's geochemical reservoirs; *Geology*, v. 36; pp. 635-638.
- Reynolds, L.J., 2000 - Geology of the Olympic Dam Cu-U-Au-Ag-REE deposit; in Porter, T.M., (ed.), *Hydrothermal Iron Oxide Copper-gold and Related Deposits: A Global Perspective, PGC Publishing, Adelaide*, v. 1, pp. 93-104.
- Richardson, S.H., Gurney, J.J., Erlank, A.J. and Harris, J.W., 1984 - Origin of diamonds in old enriched mantle; *Nature*, v. 310, pp. 198-202.
- Richards, J.P., Boyce, A.J. and Pringle, M.S., 2001 - Geologic evolution of the Escondida area, northern Chile: a model for spatial and temporal localization of Porphyry Cu Mineralization; *Economic Geology*, v. 96, pp. 271-305.
- Richards, J.P., 2003 - Tectono-magmatic precursors for porphyry Cu-(Mo-Au) deposit formation; *Economic Geology*, v. 98, pp. 1515-1533.
- Richards, J.P., 2005 - Cumulative factors in the generation of giant calc-alkaline porphyry Cu deposits; in Porter, T.M. (ed.), *Super Porphyry Copper and Gold Deposits: A Global Perspective, PGC Publishing, Adelaide*, v. 1, pp. 7-25.
- Rieger, A.A., Marschik, R., Spangenberg, J.E. and Díaz, M., 2009 - Sulphur and lead isotope characteristics of sulphides of the Mantoverde IOCG district, Chile; in Williams, P.J. et al., (eds.), *Smart Science for Exploration and Mining, Proceedings of the 10<sup>th</sup> Biennial SGA Conference, 17-20 August, 2009, Townsville, Australia, Extended abstracts*, v. 2, pp. 653-655.
- Rieger, A.A., Marschik, R. and Díaz, M., 2010 - The Mantoverde district, northern Chile: an example of distal portions of zoned IOCG systems; in Porter, T.M., (ed.), *Hydrothermal Iron Oxide Copper-gold and Related Deposits: A Global Perspective - Advances in the Understanding of IOCG Deposits; PGC Publishing, Adelaide*, v. 3, pp. 273-284. (this volume).
- Rieger, A.A., Marschik, R., Díaz, M., Holz, S., Chiaradia, M., Akker, B. and Spangenberg, J.E., 2010a - The hypogene iron oxide copper-gold mineralization in the Mantoverde district, northern Chile; *Economic Geology*, v. 105, pp. 1271-1299.
- Rigon, J.C., Munaro, P., Santos, L.A., Nascimento, J.A.S. and Barreira, C.F., 2000 - Alvo 118 copper-gold deposit: geology and mineralization, Serra dos Carajás, Pará, Brazil; in 31st International Geological Congress, Rio de Janeiro, *Sociedade Brasileira de Geologia, International Union of Geological Sciences, Abstract Volume*, [CD-ROM].
- Roberts, D.E. and Hudson, G.R.T., 1983 - The Olympic Dam copper-uranium-gold deposit, Roxby Downs, South Australia; *Economic Geology*, v. 78, pp.799-822.
- Rogers, J.J.W. and Santosh, M., 2004 - Continents and supercontinents; *Oxford University Press, Oxford*, 328p.
- Rohs, R.C. and Van Schmus, R.V., 2007 - Isotopic connections between rocks exposed in the St. Francois Mountains and the Arbuckle Mountains, southern Mid-continent, North America; *International Journal of Earth Sciences*, v. 96, pp. 599-611.
- Romeuf, N., Aguirre, L., Carlier, G., Soler, P., Bonhomme, M., Elmi, S. and Salas, G., 1993 - Present knowledge of the Jurassic volcanogenic formations of the southern coastal Perú; *Second International Symposium on Andean Geodynamics (ISAG)*, Oxford, 21-23 September, pp. 437-440.
- Ronchi, L.H., Lindenmayer, Z.G., Araújo, J.C. and Baecker, C.A., 2001 - Assinatura granítica das inclusões flúidas relacionadas ao depósito de Cu-Au de Gameleira, Carajás, PA; in VII Simpósio de Geologia da Amazônia, *Sociedade Brasileira de Geologia, Belém*, [CD-ROM]. (in Portuguese)
- Ronzê, P.C., Soares, A.D.V., Santos, M.G.S.dos. and Barreira, C.F., 2000 - Alemão copper-gold (U-REE) deposit, Carajás, Brazil; in Porter, T.M. (ed.), *Hydrothermal Iron-Oxide Copper-Gold and Related Deposits: A Global Perspective, PGC Publishing, Adelaide*, v. 1, pp. 191-202.
- Rosiere, C.A., Baars, F.J., Seoane, J.C.S., Lobato, L.M., da Silva, L.L., de Souza, S.R.C. and Mendes, G.E., 2006 - Structure and iron mineralisation of the Carajás Province; in *Transactions IMM (incorporating AusIMM Proceedings), Section B, Applied Earth Sciences*, v. 115, pp. 126-133
- Rotherham, J., 1997 - Origin and fluid chemistry of the Starra ironstones and high grade Au-Cu mineralization, Cloncurry district, Mount Isa Inlier, Australia; Unpublished Ph.D. thesis, *James Cook University, Townsville, Australia*, 251 p.
- Rotherham, J.F., 1997 - A metasomatic origin for the iron-oxide Au-Cu Starra orebodies. Eastern fold belt, Mount Isa inlier; *Mineralium Deposita*, v. 32, pp. 205-218.
- Rotherham, J.F., Blake, K.L., Cartwright, I., and Williams, P.J., 1998 - Stable isotope evidence for the origin of the Mesoproterozoic Starra Au-Cu deposit, Cloncurry district, Northwest Queensland; *Economic Geology*, v. 93, pp. 1435-1449.
- Rubenach, M.J., Adshead, N.D., Oliver, N.H.S., Tullemans, F., Esser, D., Stein, H., 2001. The Osborne Cu-Au deposit: geochronology and genesis of mineralization in relation to host albitites and ironstones; in: Williams P.J., (ed.), *A Hydrothermal Odyssey, Economic Geology Research Unit, James Cook University, Townsville, Extended Abstracts*, Contribution no.59, pp. 172- 173.
- Rubenach, M.J., Foster, D.R.W., Evins, P.M., Blake, K.L. and Fanning, C.M., 2008 - Age constraints on the tectonothermal evolution of the Selwyn Zone, Eastern Fold Belt, Mount Isa Inlier; *Precambrian Research*, v. 163, pp. 81-107.

- Rusk, B., Oliver, N.H.S., Brown, A., Lilly, R. and Jungmann, D., 2009 - Barren magnetite breccias in the Cloncurry region, Australia; comparisons to IOCG deposits; in Williams, P.J. *et al.*, (eds.), *Smart Science for Exploration and Mining, Proceedings of the 10<sup>th</sup> Biennial SGA Conference, 17-20 August, 2009, Townsville, Australia*, Extended abstracts, v. 2, pp. 656-658.
- Rusk, B., Oliver, N.H.S., Cleverley, J., Blenkinsop, T.G., Zhang, D., Williams, P.J. and Habermann, P., 2010 - Physical and chemical characteristics of the Ernest Henry iron oxide copper gold deposit, Cloncurry, Qld, Australia; implications for IOCG genesis; in Porter, T.M., (ed.), *Hydrothermal Iron Oxide Copper-Gold and Related Deposits: A Global Perspective - Advances in the Understanding of IOCG Deposits*; *PGC Publishing, Adelaide*, v. 3, pp. 201-218. (*this volume*).
- Sánchez-García, T., Quesada, C., Bellido, F., Dunning, G.R. and González del Tánago, J., 2008 - Two-step magma flooding of the upper crust during rifting: The Early Paleozoic of the Ossa Morena Zone (SW Iberia); *Tectonophysics*, v. 461, pp. 72-90.
- Santos, J.O.S., Hartmann, L.A., Gaudette, H.E., Groves, D.I., McNaughton, N.J. and Fletcher, I.R., 2000 - New understanding of the Amazon craton provinces, based on field work and radiogenic isotope data. *Gondwana Research*, pp. 453-486.
- Schenk, C.J., Viger, R.J. and Anderson, C.P., 1996 - Maps showing geology, oil and gas fields, and geologic provinces of the South America region; *U.S. Geological Survey, Open-File Report 97-470D*, 2 maps, 12p.
- Schott, B. and Schmeling, H., 1998 - Delamination and detachment of a lithospheric root; *Tectonophysics*, v. 296, pp. 225-247.
- Schobbenhaus, C., Campos, D.A., Derze, G.R. and Asmus, H.E., 1995 - Mapa geológico do Brasil e da área oceânico adjacente incluindo depósitos minerais; DNPM (Brasil), scale 1:2 500 000, 1995 edition.
- Schweitzer, J.K., Hatton, C.J. and de Waal, S.A. 1995 - Regional lithochemical stratigraphy of the Rooiberg Group, upper Transvaal Supergroup: A proposed new subdivision; *South African Journal of Geology* v. 98, pp. 245-255
- Seedorff, E., Dilles, J.H., Proffett, J.M. Jr., Einaudi, M.T., Zurcher, L., Stavast, W.J.A., Johnson, D.A. and Barton, M.D., 2005 - Porphyry deposits: Characteristics and origin of hypogene features; in Hedenquist, J.W., Thompson, J.F.H., Goldfarb, R.J. and Richards, J.P. (eds.), *Economic Geology, 100 Anniversary Volume, Society of Economic Geologists*, pp. 251-298.
- Seeger, C.M., 1989 - The Pilot Knob hematite deposit; in Brown, V.M., Kisvarsanyi, E.B. and Hagni, R.D. (eds.), "Olympic Dam-Type" Deposits and Geology of Middle Proterozoic Rocks in the St. Francois Mountains Terrane, Missouri, *Society of Economic Geologists*, Guidebook no. 4, pp. 55-68.
- Seeger, C.M. 2000 - Southeast Missouri iron metallogenic province: characteristics and general chemistry; in Porter, T.M. (ed.), *Hydrothermal Iron-Oxide Copper-Gold and Related Deposits: A Global Perspective*, *PGC Publishing, Adelaide*, v. 1, pp 237-248.
- Selley, D., Broughton, D., Scott, R., Hitzman, M., Bull, S., Large, R., McGoldrick, P., Croaker, M. and Pollington, N., 2005 - A new look at the geology of the Zambian Copperbelt; in Hedenquist, J.W., Thompson, J.F.H., Goldfarb, R.J. and Richards, J.P. (eds.), *Economic Geology, 100 Anniversary Volume, Society of Economic Geologists*, pp. 965-1000.
- Sharma, K.K., 2004 - The Neoproterozoic Malani magmatism of the northwestern Indian shield: implications for crust-building processes; *Proceedings of the Indian Academy of Science (Earth Planetary Sciences)*, v. 113, pp. 795-807.
- Shaw, R.D., Wellman, P., Gunn, P., Whitaker, A.J., Tarlowski, C. and Morse, M., - 1996 - Guide to using the Australian crustal elements map, *Geoscience Australia, Canberra*, Record 1996/30, 99p.
- Shaw, R.D. Wellman, P., Gunn, P., Whitaker, A.J., Tarlowski, C., and Morse, M., 1996, Australian Crustal Elements based on the distribution of geophysical domains; 1:5 000 000 scale map; version 2.4, 2010 revision, ArcGIS dataset, *Geoscience Australia, Canberra*.
- Shervais, J.W., 2006, The significance of subduction-related accretionary complexes in early Earth processes; in Reimold, W.U., and Gibson, R.L., (eds.), *Processes on the Early Earth, Geological Society of America, Special Paper 405*, pp. 173-192.
- Shirey, S.B., Harris, J.W. Richardson, S.H., Fouch, M., James, D.E. Cartigny, P., Deines, P and Viljoen, F., 2003 - Regional patterns in the paragenesis and age of inclusions in diamond, diamond composition, and the lithospheric seismic structure of Southern Africa; *Lithos*, v. 71, pp. 243-258.
- Sillitoe, R.M., 2003 - Iron oxide-copper-gold deposits: an Andean view; *Mineralium Deposita*, v. 38, p. 787-812.
- Silva J.B., Oliveira J.T. and Ribeiro, A., 1990 - South Portuguese Zone, structural outline; in Dallmeyer, R.D. and Martínez García, E., (eds.), *Pre-Mesozoic Geology of Iberia, Springer-Verlag, Berlin-Heidelberg*, pp. 348-362.
- Sims, P.K., Kisvarsanyi, E.B. and Morey, G.B., 1987 - Geology and metallogeny of Archean and Proterozoic basement terranes in the northern midcontinent, U.S.A. - an overview; *U.S. Geological Survey, Bulletin 1951*, 51p.
- Singh, Y.K., De Waele, B., Karmakar, S., Sarkar, S. and Biswal, T.K., 2010 - Tectonic setting of the Balaram-Kui-Surpagla-Kengora granulites of the South Delhi Terrane of the Aravalli Mobile Belt, NW India and its implication on correlation with the East African Orogen in the Gondwana assembly; *Precambrian Research*, v. 183, pp. 669-688.
- Siqueira, J.B. and Costa, J.B.S., 1991 - Evolução geológica do duplex Salobo-Mirim; in III Simpósio de Geologia da Amazônia, Belém, *Sociedade Brasileira de Geologia*, pp. 232-243. (*in Portuguese*)
- Skirrow, R.G., 1993 - The genesis of gold-copper-bismuth deposits, Tennant Creek, Northern Territory; Unpublished Ph.D. thesis, *Australian National University, Canberra, Australia*.
- Skirrow, R.G., 1999 - Proterozoic Cu-Au-Fe mineral systems in Australia: filtering key components in exploration models; in Stanley, C. J. *et al.*, (eds.), *Mineral Deposits. Processes to Processing. Balkema, Rotterdam*, pp. 1361-1364.
- Skirrow, R.G., 2009 - "Hematite-group" IOCG±U ore systems: tectonic settings, hydrothermal characteristics, and Cu-Au and U mineralizing processes; in Corriveau, L. and Mumin, A.H., (eds.), *Exploring for Iron Oxide Copper-Gold Deposits: Canada and Global Analogues, Geological Association of Canada, Short Course Notes, No. 20*, pp. 39-57.
- Skirrow, R.G., Bastrakov, E.N., Barovich, K., Fraser, G.L., Creaser, R., Fanning, M.C., Raymond, O.L. and Davidson, G.J., 2007 - Timing of iron oxide Cu-Au-(U) hydrothermal activity and Nd isotope constraints on metal sources in the Gawler craton, South Australia; *Economic Geology*, v. 102, pp. 1441-1470.
- Skirrow, R.G., Bastrakov, E., Davidson, G., Raymond, O. L. and Heithersay, P., 2002 - The geological framework, distribution and controls of Fe oxide Cu-Au mineralisation in the Gawler craton, South Australia. Part II. Alteration and mineralisation; in Porter, T. M., (ed.), *Hydrothermal Iron Oxide Copper-gold and Related Deposits: A Global Perspective*, *PGC Publishing, Adelaide*, v. 2, pp. 33-47.

- Skirrow, R.G., Fairclough, M.C., Budd, A.R., Lyons, P., Raymond, O., Milligan, P., Bastrakov, E., Fraser, G., Highet, L., Holm, O. and Williams, N., 2006 - Iron oxide Cu-Au (-U) potential map of the Gawler Craton, South Australia (1st Edition), 1:500 000 scale map: *Geoscience Australia*, Canberra.
- Skirrow, R.G. and Walshe, J. L., 2002 - Reduced and oxidised Au-Cu-Bi deposits of the Tennant Creek inlier, Australia: An integrated geologic and chemical model; *Economic Geology*, v. 97, pp. 1167-1202.
- Sleigh, D.W., 2002 - Digesting data to put on weight; in *Exploration in the Shadow of the Headframe: Getting a New Life on Lease*, SMEDG-AIG-ASEG Symposium, North Sydney, 11 October, 2002, The *Australian Institute of Geologists*, Perth, Bulletin 35, 9p.
- Smith, J., 2001 - Summary of Results Joint NTGS-AGSO Age Determination Program, 1999 - 2001; *Northern Territory Geological Survey Record* 2001- 007
- Smith, M. and Wu, C., 2000 - The Geology and Genesis of the Bayan Obo Fe-REE-Nb Deposit: A Review; in Porter, T.M. (ed.), *Hydrothermal Iron-Oxide Copper-Gold and Related Deposits: A Global Perspective*, PGC Publishing, Adelaide, v. 1, pp. 271-281.
- Smith, M., Coppard, J. and Herrington, R., 2010 - The geology of the Rakkurijärvi Cu-prospect, Norrbotten County, Sweden; in Porter, T.M., (ed.), *Hydrothermal Iron Oxide Copper-Gold and Related Deposits: A Global Perspective - Advances in the Understanding of IOCG Deposits*; PGC Publishing, Adelaide, v. 4, pp. 427-440.
- Smith, R.N., 1993 - Olympic Dam: some developments in geological understanding over nearly two decades; The AusIMM Centenary Conference, Adelaide, 30 March - 4 April, 1993, *The Australasian Institute of Mining and Metallurgy*, Melbourne, pp. 113-118.
- Sokolov, G.A. and Grigor'ev, V.M., 1977 - Deposits of Iron; in Smirnov, V.I. (ed.), *Ore Deposits of the USSR* Pitman Publishing, London, v. 1, pp. 7-113.
- Soloviev, S.G., 2010a - Iron oxide ( $\pm$ copper, gold) and associated deposits of the Altai-Sayan Orogenic System, south-western Siberia, Russia; in Porter, T.M., (ed.), *Hydrothermal Iron Oxide Copper-Gold and Related Deposits: A Global Perspective - Advances in the Understanding of IOCG Deposits*; PGC Publishing, Adelaide, v. 4, pp. 475-494.
- Soloviev, S.G., 2010b - Iron oxide copper-gold and related mineralisation of the Siberian Craton, Russia: I - iron oxide deposits in the Angara and Ilim river basins, south-central Siberia; in Porter, T.M., (ed.), *Hydrothermal Iron Oxide Copper-Gold and Related Deposits: A Global Perspective - Advances in the Understanding of IOCG Deposits*; PGC Publishing, Adelaide, v. 4, pp. 495-514.
- Soloviev, S.G., 2010c - Iron oxide copper-gold and related mineralisation of the Siberian Craton, Russia: II - iron oxide, copper, gold and uranium deposits of the Aldan shield, south-eastern Siberia; in Porter, T.M., (ed.), *Hydrothermal Iron Oxide Copper-Gold and Related Deposits: A Global Perspective - Advances in the Understanding of IOCG Deposits*; PGC Publishing, Adelaide, v. 4, pp. 515-535.
- Souza, L.H. and Vieira, E.A.P., 2000 - Salobo 3 Alpha deposit: geology and mineralisation; in Porter, T.M. (ed.), *Hydrothermal Iron-Oxide Copper-Gold and Related Deposits: A Global Perspective*, PGC Publishing, Adelaide, v. 1, pp. 213-224.
- Stewart, K.P., 1994 - High temperature silicic volcanism and the role of mantle magmas in Proterozoic crustal growth: the Gawler Range Volcanic Province; Unpublished PhD thesis, *University of Adelaide*, 220p.
- Stewart, K.P. and Foden, J., 2003 - Mesoproterozoic granites of South Australia; *South Australia Department of Primary Industries and Resources*, Report Book, 2003/15.
- Stolz, A.J. and Morrison, R.S., 1994 - Proterozoic igneous activity in the Tennant Creek region, Northern Territory, Australia, and its relationship to Cu-Au-Bi mineralization; *Mineralium Deposita*, v. 29, pp. 261-274.
- Storey, C.D., Smith, M.P. and Jeffries, T.E., 2007 - In situ LAICP-MS U-Pb dating of metavolcanics in Norrbotten, Sweden: Records of extended geological histories in complex titanite grains; *Chemical Geology*, v. 240, pp. 163-181.
- Stosch, H.G., Romer, R.L., Daliran, F. and Rhede, D., 2011 - Uranium-lead ages of apatite from iron oxide ores of the Bafq District, East-Central Iran; *Mineralium Deposita*, v. 46, pp. 9-21.
- Strakhov, L.G., 1978 - The ore-bearing volcanic apparatus in the Southern Siberian Craton; *Nauka Publishing, Novosibirsk*, 117p. (in Russian)
- Strickland, C.D. and Martyn, J.E., 2002 - The Guelb Moghrein Fe-oxide copper-gold-cobalt deposit and associated mineral occurrences, Mauritania: a geological introduction; in Porter, T.M. (ed.), *Hydrothermal Iron Oxide Copper-Gold and Related Deposits: A Global Perspective*, PGC Publishing, Adelaide, v. 2, pp. 275-291.
- Ta Viet Dung *et al.*, 1975 - The geological report on detailed exploration of the Sin Quyen copper deposit; *General Department of Geology, Hanoi*. [unpublished].
- Tallarico, F.H.B., Figueiredo, B.R., Groves, D.I., Kositcin, N., McNaughton, N.J., Fletcher I.R. and Rego J.L., 2005 - Geology and SHRIMP U-Pb geochronology of the Igarapé Bahia deposit, Carajás copper-gold belt, Brazil: an Archean (2.57 Ga) example of iron-oxide Cu-Au-(U-REE) mineralization; *Economic Geology*, v. 100, pp. 7-28.
- Tatsumi, Y., Hamilton, D.L. and Nesbitt, R.W., 1986 - Chemical characteristics of fluid phase released from a subducted lithosphere and the origin of arc magmas: Evidence from high pressure experiments and natural rocks; *Journal of Volcanology and Geothermal Research*, v. 29, pp. 293-309.
- Tazava, E., 1999 - Mineralização de Au-Cu-( $\pm$ ETR-U) associada às brechas hidrotermais do depósito de Igarapé Bahia, Província Mineral de Carajás, PA; Unpublished MSc. Dissertation, *Departamento de Geologia, Universidade Federal de Ouro Preto, Ouro Preto*, 81p.
- Tazava, E. and Oliveira, C.G., 2000 - The Igarapé Bahia Au-Cu-(REE-U) deposit, Carajás Mineral Province, northern Brazil; in Porter, T.M. (ed.), *Hydrothermal Iron-Oxide Copper-Gold and Related Deposits: A Global Perspective*, PGC Publishing, Adelaide, v. 1, pp. 203-212.
- Teale, G.S., and Fanning, C.M., 2000 - The Portia-North Portia Cu-Au-(Mo) prospect, South Australia: Timing of mineralisation, albitisation and origin of ore fluid; in Porter, T.M., (ed.), *Hydrothermal Iron Oxide Copper-Gold and Related Deposits: A Global Perspective*, PGC Publishing, Adelaide, v. 1, pp. 137-147.
- Teixeira, N.A., Rigon, J.C., Huhn, S.R.B., Vieira, F.M., Nascimento, M.J.A.S., Silva, F.H.F., Aires, B., Freitas, C.O. and Fonseca, E., 2009 - Geological setting of Carajás IOCG deposits; PDAC 2009 presentation, [www.pdac.ca/pdac/conv/2009/pdf/tech-session/ts-teixeira.pdf](http://www.pdac.ca/pdac/conv/2009/pdf/tech-session/ts-teixeira.pdf)
- Thompson, A.B., 1999 - Some time-space relationships for crustal melting and granitic intrusion at various depths; in Castro, A., Fernandez, C. and Vigneresse, J.L., (eds.), *Understanding Granites: Integrated new and Classical Techniques*, *Geological Society of London*, Special Publications, v. 168, pp. 7-25.
- Thorkelson, D.J., 2000 - Geology and mineral occurrences of the Slats Creek, Fairchild Lake and "Dolores Creek" areas, Wernecke Mountains, Yukon Territory; Exploration and Geological Services Division, Yukon Region, *Indian and Northern Affairs Canada*, Bulletin 10, 73p.

- Thorkelson, D.J., Mortensen, J.K., Davidson, G.J., Creaser, R.A., Perez, W.A. and Abbott, J.G., 2001 - Early Mesoproterozoic intrusive breccias in Yukon, Canada: the role of hydrothermal systems in reconstructions of North America and Australia; *Precambrian Research*, v. 111, pp. 31-55.
- Tornos, F. and Chiaradia, M., 2004 - Plumbotectonic evolution of the Ossa Morena zone, Iberian Peninsula: tracing the influence of mantle-crust interaction in ore-forming processes; *Economic Geology*, v. 99, pp. 965-985.
- Tornos, F., Casquet, C. and Relvas, J.M.R.S., 2006 - Transpressional tectonics, lower crust decoupling and intrusion of deep mafic sills: A model for the unusual metallogenesis of SW Iberia; *Ore Geology Reviews*, v. 27, pp. 133-163.
- Tornos, F., Galindo, C., Casquet, C., Rodrigues Pevida, L., Martínez, C., Martínez, E., Velasco, F. and Iriondo, A., 2006 - The Aguablanca Ni-(Cu) sulfide deposit, southwest Spain: geologic and geochemical controls and the relationship with a mid-crustal layered mafic complex; *Mineralium Deposita*, v. 41, pp. 737-769.
- Tornos, F. and Velasco, F., 2009 - Magmatic-hydrothermal Evolution of the IOCG Deposits of Central Chile; in Williams, P.J. et al., (eds.), Smart Science for Exploration and Mining, *Proceedings of the 10<sup>th</sup> Biennial SGA Conference, 17-20 August, 2009, Townsville, Australia*, Extended abstracts, v. 2, pp. 662-664.
- Tornos, F., Velasco, F., Barra, F. and Morata, D., 2010 - The Tropezón Cu-Mo-(Au) deposit, northern Chile: the missing link between IOCG and porphyry copper systems?; *Mineralium Deposita*, v. 45, pp. 313-321.
- Torrealdy, H.I., Hitzman, M.W., Stein, H.J., Markley, R.J., Armstrong, R., Broughton, D., 2000 - Re-Os and U-Pb dating of the vein-hosted mineralization at the Kansanshi Copper deposit, northern Zambia; *Economic Geology*, v. 95, pp. 1165-1170.
- Tuisku, P., 1985 - The origin of scapolite in the Central Lapland schist area, northern Finland, preliminary results; *Geological Survey of Finland*, Bulletin 331, pp. 159-173.
- Twyerould, S.C., 1997 - The geology and genesis of the Ernest Henry Fe-Cu-Au deposit, Northwest Queensland, Australia; Unpublished PhD thesis, *University of Oregon, Eugene*, 494p.
- Ullrich, T.D. and Clark, A.H., 1999 - The Candelaria Cu-Au deposit, III Región, Chile: Paragenesis, geochronology and fluid composition, in Stanley, C.J. et al., (eds.), Mineral Deposits: Processes to Processing; *Balkema, Rotterdam*, pp. 201-204.
- Ulrich, T., Günther, D. and Heinrich, C.A., 2001 - The evolution of a porphyry Cu-Au deposit based on LA-ICP-MS analysis of fluid inclusions: Bajo de la Alumbrera, Argentina; *Economic Geology*, v. 96, pp. 1743-1774.
- Vakhrushev, V.A. and Vorontsov, A.E., 1976 - Mineralogy and geochemistry of the iron ore deposits in southern part of Siberian Craton; *Nauka Publishing, Novosibirsk*, 199p. (in Russian)
- Vakhrushev, V.A., Vorontsov, A.E. and Sapozhnikov, A.N., 1973 - Chalcopyrite-pentlandite-pyrrhotite association in the Korshunovskoe iron deposit; *Transactions (Doklady) of the USSR Science Academy*, v. 212, no. 3, pp. 702-704. (in Russian)
- Vallinayagam, G. and Kumar, N., 2010 - First report of spheroidal rhyolite from Nakora area of Malani Igneous Suite, northwestern peninsular India; *Earth Science India*, v. 3, pp. 97-104.
- Van Schmus, W.R., Bickford, M.E., Sims, P.K., Anderson, R.R., Shearer, C.K. and Treves, S.B., 1993 - Proterozoic geology of the western midcontinent basement, in Van Schmus and 24 others, Chapter 4: Transcontinental Proterozoic Provinces, in Reed, J.C., Jr., Bickford, M.E., Houston, R.S., Link, P.K., Rankin, D.W., Sims, P.K. and Van Schmus, W.R., (eds.), *Precambrian: Conterminous U.S. The Geology of North America, Geological Society of America, Boulder, Colorado*, v. C-2, pp. 239-259.
- Van Schmus, W.R., Bickford, M.E. and Turek, A., 1996 - Proterozoic geology of the east-central Midcontinent basement, in van der Pluijm, B.A. and Catacosinos, P.A., (eds.), *Basement and Basins of Eastern North America, Geological Society of America, Boulder, Colorado*, Special Paper 308, pp. 7-32.
- Vanhanen, E., 2001 - Geology, mineralogy and geochemistry of the Fe-Co-Au-(U) deposits in the Paleoproterozoic Kuusamo Schist Belt, northeastern Finland; *Geological Survey of Finland*, Bulletin 399, 229p.
- Vázquez, F. and Fernández Pompa, F., 1976 - Contribución al conocimiento geológico del SW de España en relación con la prospección de magnetitas; *Memorias del Instituto Geológico y Minero de España*, v. 89, 139p. (in Spanish)
- Velasco, F. and Tornos, F., 2009 - Pegmatite-like Magnetite-Apatite Deposits of Northern Chile: A Place in the Evolution of Immiscible Iron Oxide Melts?; in Williams, P.J. et al., (eds.), Smart Science for Exploration and Mining, *Proceedings of the 10<sup>th</sup> Biennial SGA Conference, 17-20 August, 2009, Townsville, Australia*, Extended abstracts, v. 2, pp. 665-667.
- Vella, L. and Cawood, M., 2006 - Carrapateena: discovery of an Olympic Dam-style deposit; Preview, Australian Society Exploration Geophysicists, Issue 122, pp. 26-29.
- Verwoerd, W.J., 1986 - Mineral deposits associated with carbonatites and alkaline rocks; in Anhaeusser, C.R., and Maske, S., (eds.), Mineral Deposits of Southern Africa. *Geological Society of South Africa, Johannesburg*, v. 2, pp. 2173-2191.
- Vielreicher, N.M., Groves, D.I. and Vielreicher, R.M., 2000 - The Phalaborwa (Palabora) deposit and its potential connection to iron-oxide copper-gold deposits of Olympic Dam type; in Porter, T.M., (ed.), Hydrothermal Iron Oxide Copper-Gold and Related Deposits: A Global Perspective, *PGC Publishing, Adelaide*, v. 1, pp. 321-329.
- Vila, T., Lindsay, N. and Zamora, R., 1996 - Geology of the Mantoverde copper deposit, Northern Chile: a specularite-rich hydrothermal-tectonic breccia related to the Atacama Fault Zone; in Camus, F., Sillitoe, R.H., Petersen, R., (eds.), Andean Copper Deposits, New Discoveries, Mineralization, Styles and Metallogeny, *Society of Economic Geologists, Special Publication 5*, pp. 157-170.
- Villas, R.N. and Santos, M.D., 2001 - Gold deposits of the Carajás Mineral Province: deposit types and metallogenesis; *Mineralium Deposita*, v. 36, pp. 300-331.
- Wada, H., Harayama, S. and Yamaguchi, Y., 2004 - Mafic enclaves densely concentrated in the upper part of a vertically zoned felsic magma chamber: the Kurobegawa granitic pluton, Hida Mountain Range, central Japan; *Geological Society of America, Boulder, Colorado*, Bulletin 116, pp. 788-801.
- Wall, V.J. and Valenta, R.K., 1990 - Ironstone-related gold-copper mineralisation: Tennant Creek and elsewhere; Pacific Rim 90 Congress, Gold Coast, Queensland, *The AusIMM, Melbourne*, Abstracts, pp. 855-864.
- Wanhainen, C. and Martinsson, O., 2010 - The hybrid character of the Aitik deposit, Norrbotten, Sweden: a porphyry Cu-Au-Ag(-Mo) system overprinted by iron-oxide Cu-Au hydrothermal fluids; in Porter, T.M., (ed.), Hydrothermal Iron Oxide Copper-Gold and Related Deposits: A Global Perspective - Advances in the Understanding of IOCG Deposits; *PGC Publishing, Adelaide*, v. 4, pp. 415-426.
- Weihed, P. and Eilu, P., 2005 - Fennoscandian Shield - Proterozoic VMS deposits; *Ore Geology Reviews*, v. 27, pp. 324-325.
- Wedekind, M. R., 1990 - Geology and chemistry of the Warrego Au-Cu-Bi Mine, Tennant Creek, N.T. Australia; Unpublished Ph.D. thesis, *University of Tasmania, Hobart*.

- Wedekind, M.R., Large, R.R. and Williams, B.T., 1989 - Controls on high-grade gold mineralization at Tennant Creek, Northern Territory, Australia; *Economic Geology*, Monograph 6, pp. 168-179.
- Wedekind, M.R. and Love, R.J., 1990 - Warrego gold-copper-bismuth deposit; in Hughes, F.E. (ed.), *Geology of the Mineral Deposits of Australia and Papua New Guinea*, *The AusIMM, Melbourne*, Monograph 14, v. 1, pp. 839-843.
- Wilde, S.A., Valley, J.W., Peck, W.H. and Graham, C.M., 2001 - Evidence from detrital zircons for the existence of continental crust and oceans on the Earth 4.4 Gyr ago; *Nature*, v. 409, pp. 175-178.
- Williams, H., Hoffman, P.H., Lewry, J.F., Monger, J.W.H. and Rivers, T., 1991 - Anatomy of North America: thematic geologic portrayals of the continents; *Tectonophysics*, v. 187, pp. 117-134.
- Williams, P.J., Guoyi Dong, Ryan, C.G., Pollard, P.J., Rotherham, J.F., Mernagh, T.P. and Chapman, L.H., 2001 - Geochemistry of high salinity fluid inclusions from the Starra (Fe)-Cu-Au deposit, Cloncurry district, Queensland; *Economic Geology*, v. 96, pp. 875-883.
- Williams, P.J., Barton, M.D., Johnson, D.A., Fontboté, L., de Haller, A., Mark, G., Oliver, N.H.S. and Marschik, R., 2005 - Iron oxide-copper-gold deposits: Geology, space-time distribution, and possible modes of origin; in Hedenquist, J.W., Thompson, J.F.H., Goldfarb, R.J. and Richards, J.P. (eds.), *Economic Geology*, 100 Anniversary Volume, *Society of Economic Geologists*, pp. 371-405.
- Williams, P.J. and Pollard, P.J., 2001 - Australian Proterozoic Iron Oxide-Cu-Au Deposits: An Overview with New Metallogenic and Exploration Data from the Cloncurry District, Northwest Queensland; *Exploration and Mining Geology*, v. 10, pp. 191-213.
- Williams, P.J. and Pollard, P.J., 2003 - Australian Proterozoic iron oxide Cu-Au deposits: An overview with new metallogenic and exploration data from the Cloncurry district, northwest Queensland; *Exploration and Mining Geology*, v. 10, pp. 191-213.
- Williams, P.J., Kendrick, M.A. and Xavier, R.P., 2010 - Sources of ore fluid components in IOCG deposits; in Porter, T.M., (ed.), *Hydrothermal Iron Oxide Copper-Gold and Related Deposits: A Global Perspective - Advances in the Understanding of IOCG Deposits*; *PGC Publishing, Adelaide*, v. 3, pp. 107-116. (*this volume*).
- Wilson, J., Ferré, E.C. and Lespinasse, P. (2000) - Repeated tabular injection of high-level alkaline granites in the eastern Bushveld, South Africa; *Journal of the Geological Society of London*, v. 157, pp. 1077-1088.
- Wood, J.A., 1999 - Origin of the Solar System; in Beatty, J.K., Petersen, C.C. and Chaikin, A., (eds.), *The Solar System*, Cambridge University Press, 4<sup>th</sup> edition, 425p.
- Wyborn, L.A.I., 1998 - Younger ca. 1500 Ma granites of the Williams and Narku Batholiths, Cloncurry district, eastern Mt Isa Inlier: geochemistry, origin, metallogenic significance and exploration indicators; *Australian Journal of Earth Science*, v. 45, pp. 397-411.
- Wyborn, L.A.I., Page, R.W. and McCulloch, M.T., 1988 - Petrology, geochronology, and isotope geochemistry of the post-1820 Ma granites of the Mt Isa Inlier: mechanisms for the generation of Proterozoic anorogenic granites. The early to middle Proterozoic of Australia; in Wyborn, L.A.I. and Etheridge, M.A., (eds.), *Precambrian Research*, v. 40/41, pp. 509-541.
- Xavier, R.P., Monteiro, L.V.S., Souza Filho, C.R., Torresi, I., Carvalho, E.R., Dreher, A.M., Wiedenbeck, M., Trumbull, R.B., Pestilho, A.L.S. and Moreto, C.P.N., 2010 - The iron oxide copper-gold deposits of the Carajás Mineral Province, Brazil: an updated and critical review; in Porter, T.M., (ed.), *Hydrothermal Iron Oxide Copper-Gold and Related Deposits: A Global Perspective - Advances in the Understanding of IOCG Deposits*; *PGC Publishing, Adelaide*, v. 3, pp. 285-306. (*this volume*).
- Wu, J.C., 2007 - The Mineral Industry of Vietnam; USGS 2005 Minerals Yearbook, minerals.usgs.gov/minerals/pubs/country/2005/vmmyb05.pdf
- Youles, I.P., 1984 - The Olympic Dam copper-uranium-gold deposit, Roxby Downs, South Australia - a comment; *Economic Geology*, v. 79, pp. 1941-1944.
- Zang, W., 2003 - Maitland, Special map sheet, South Australia, 1:250 000 Series, Sheet SI53-12 and portion SI153-16, Second edition. *South Australian Geological Survey, Adelaide*, Geological Atlas 1:250 000 Series.
- Zhao, G., Cawood, P.A., Wilde, S.A. and Sun, M., 2002 - Review of global 2.1-1.8 Ga orogens: implications for a pre-Rodinia supercontinent; *Earth-Science Reviews*, v. 59, pp. 125-162.
- Zentilli, M., 1974 - Geological evolution and metallogenetic relationships in the Andes of northern Chile between 26° and 29° S; Unpublished Ph.D. thesis, *Queen's University, Kingston, Ontario*, 394p.
- Zhao, G., Sun, M., Wilde, S.A. and Li, S.Z., 2004 - A Paleo-Mesoproterozoic supercontinent: assembly, growth and breakup; *Earth-Science Reviews*, v. 67, pp. 91-123.
- Zuchetti, M., 2007 - Rochas máfi cas do Grupo Grão Pará e sua relação com a mineralização de ferro dos depósitos N4 E N5, Carajás, PA; Ph.D. thesis, Universidade Federal de Minas Gerais, 165p. (*in Portuguese*)
- Zuchetti, M., Lobato, L.M. and Hagemann, S.G., 2007 - Hydrothermal alteration of basalts that host the giant Northern Range Carajás iron ore deposits, Brazil [ext. abs.], *Society for Geology Applied to Mineral Deposits Meeting, 9<sup>th</sup> SGA, Dublin, Ireland*, Proceedings, v. 2, pp. 1231-1234.